



Welcome to the
14th Annual Meeting of the
SRC/Sematech
Engineering Research Center for
Environmentally Benign Semiconductor
Manufacturing

February 17-19, 2010

SRC/Sematech Engineering Research Center for Environmentally Benign Semiconductor Manufacturing

ERC Members and Participants

Founded in 1996 by NSF & SRC; now co-sponsored by Sematech and SRC

Founding Universities

- U Arizona
- U California – Berkeley
- MIT
- Stanford

Other University members

- Arizona State U (1998 -)
- Columbia (2006 - 2009)
- Cornell (1998 -)
- Georgia Inst. of Tech. (2009 -)
- U Maryland (1999-2003)
- U Massachusetts (2006 - 2009)
- U North Carolina (2009 -)
- Purdue (2003 - 2008)
- U Texas - Dallas (2009 -)
- Tufts (2005 - 2008)
- U Washington (2008-)
- U Wisconsin (2009-)

11 Current member universities
28 Current PI/Co-PIs
36 Current graduate students

Cumulative Data:

241 PhD and MS
205 Undergraduates (reported)
13 Academic disciplines

> 80% joining SC industry & suppliers; mostly by ERC members

Partnership in Funding

- SRC (core)
- Sematech/ISMI (core)
- Other industrial members
- Customized projects
- Cost sharing by participating universities
- Grants from Federal and State agencies
- Gifts and donations
 - Three endowments
 - Fellowships
 - Unrestricted industry gifts

Others

SRC
(core)

Sematech
(core)

Success in creating research leverage for S/C industry

Current ERC Research Projects

- **Two types of projects:**
 - **11 new core projects** (started in 2009, mainly funded by the core SRC/Sematech contract; cost shared by other ERC funds)
 - **8 customized projects** (non-core funding)
 - **6 extended projects** (completed in mid-2009)
- **Core projects were selected through RFP process, proposals, and review/selection by a panel appointed by Sematech and SRC.**
- **Customized projects are added throughout the year. Review and selection procedures are set by the ERC and the sponsors.**

New Core Project in (2009 – 2012 Cycle)

- **Development of Quantitative Structure-Activity Relationship for Prediction of Biological Effects of Nanoparticles Associated with Semiconductor Industries**
PIs: Yongsheng Chen (Georgia Inst. of Technology), Trevor Thornton, Jonathan Posner (Arizona State U)
- **Environmental Safety and Health (ESH) Impacts of Emerging Nanoparticles and Byproducts from Semiconductor Manufacturing**
PIs: Jim Field, Reyes Sierra, Scott Boitano, Farhang Shadman (U of Arizona); Buddy Ratner (U of Washington)
- **Low-ESH-impact Gate Stack Fabrication by Selective Surface Chemistry**
PI: Anthony Muscat (U of Arizona)
- **Predicting, Testing, and Neutralizing Nanoparticle Toxicity**
PIs: Steven Nielsen, Rockford Draper, Paul Pantano, Inga Musselman, Gregg Dierkmann, (U of Texas- Dallas); Ara Philipossian (U of Arizona)

New Core Project in (2009 – 2012 Cycle)

- **Lowering the Environmental Impact of High-k and Metal Gate-Stack Surface Preparation Processes**

PIs: Yoshio Nishi (Stanford); Srini Raghavan, Farhang Shadman (U of Arizona); Bert Vermeire (Arizona State U)

- **Sugar-Based Photoacid Generators (Sweet PAGs): Environmentally Friendly Materials for Next Generation Photolithography**

PIs: Christopher Ober (Cornell); Reyes Sierra (U of Arizona)

- **Carbon Dioxide Compatible Additives: Design, Synthesis, and Application of an Environmentally Friendly Development Process to Next Generation Lithography**

PIs: Christopher Ober (Cornell); Juan de Pablo (U of Wisconsin)

- **Fundamentals of Advanced Planarization: Pad Micro-Texture, Pad Conditioning, Slurry Flow, and Retaining Ring Geometry**

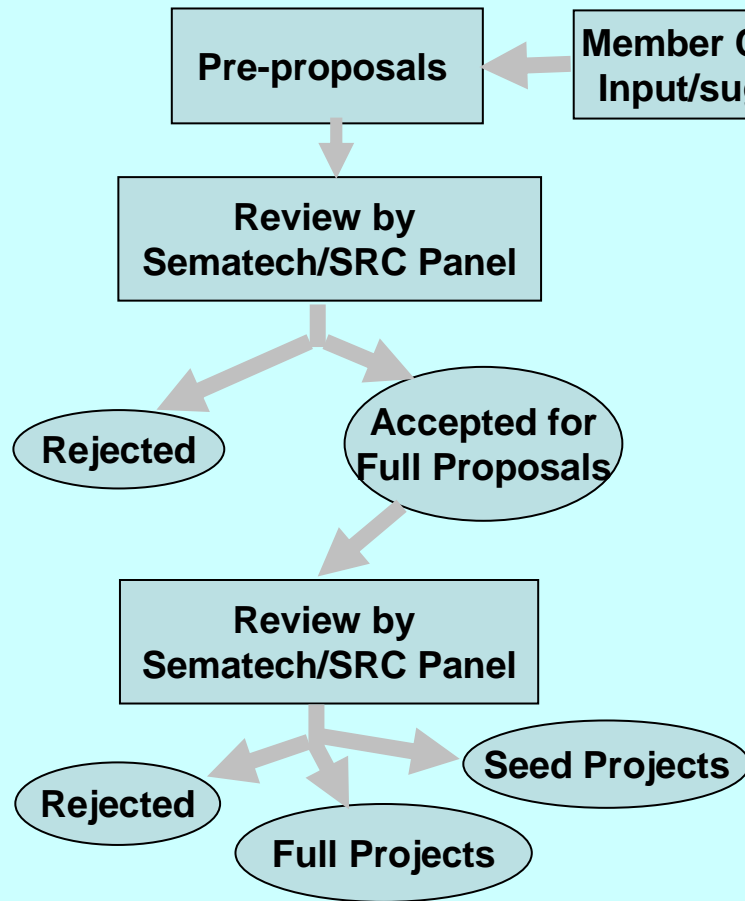
PIs: Ara Philipossian (U of Arizona); Duane Boning (MIT)

New Core Project in (2009 – 2012 Cycle)

- **High-Dose Implant Resist Stripping (HDIS): Alternatives to ASH/Strip Method**
PI: Srini Raghavan (U of Arizona)
- **Improvement of ESH Impact of Back-End-of-Line (BEOL) Cleaning Formulations Using Ionic Liquids to Replace Traditional Solvents**
PI: Srini Raghavan (U of Arizona)
- **Computational Models and High-Throughput Cellular-Based Toxicity Assays for Predictive Nanotoxicology**
PIs: Alex Tropsha, Russell Mumper (U of North Carolina)

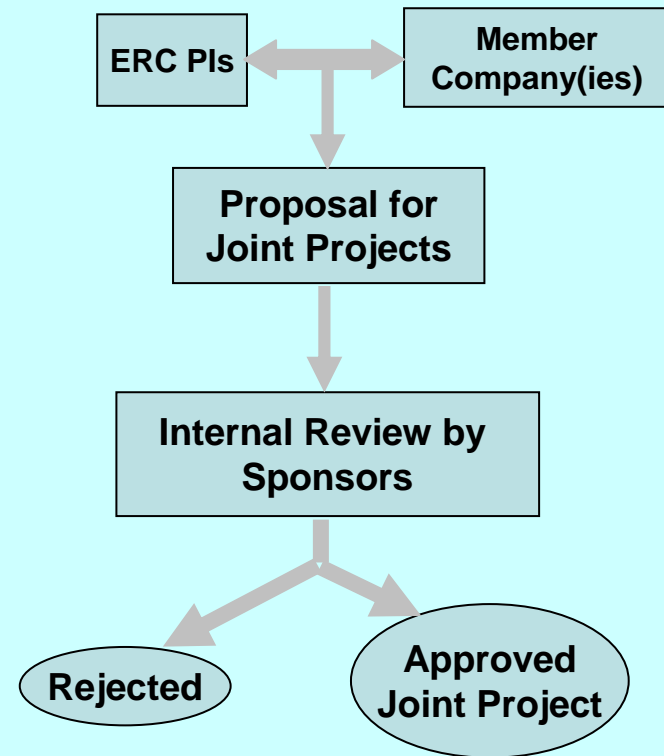
New Projects Selection

Core Projects (funded by Sematech/SRC)



Planning cycle: 3 years
11 new projects selected for 2009-2012
1-2 seed projects every year

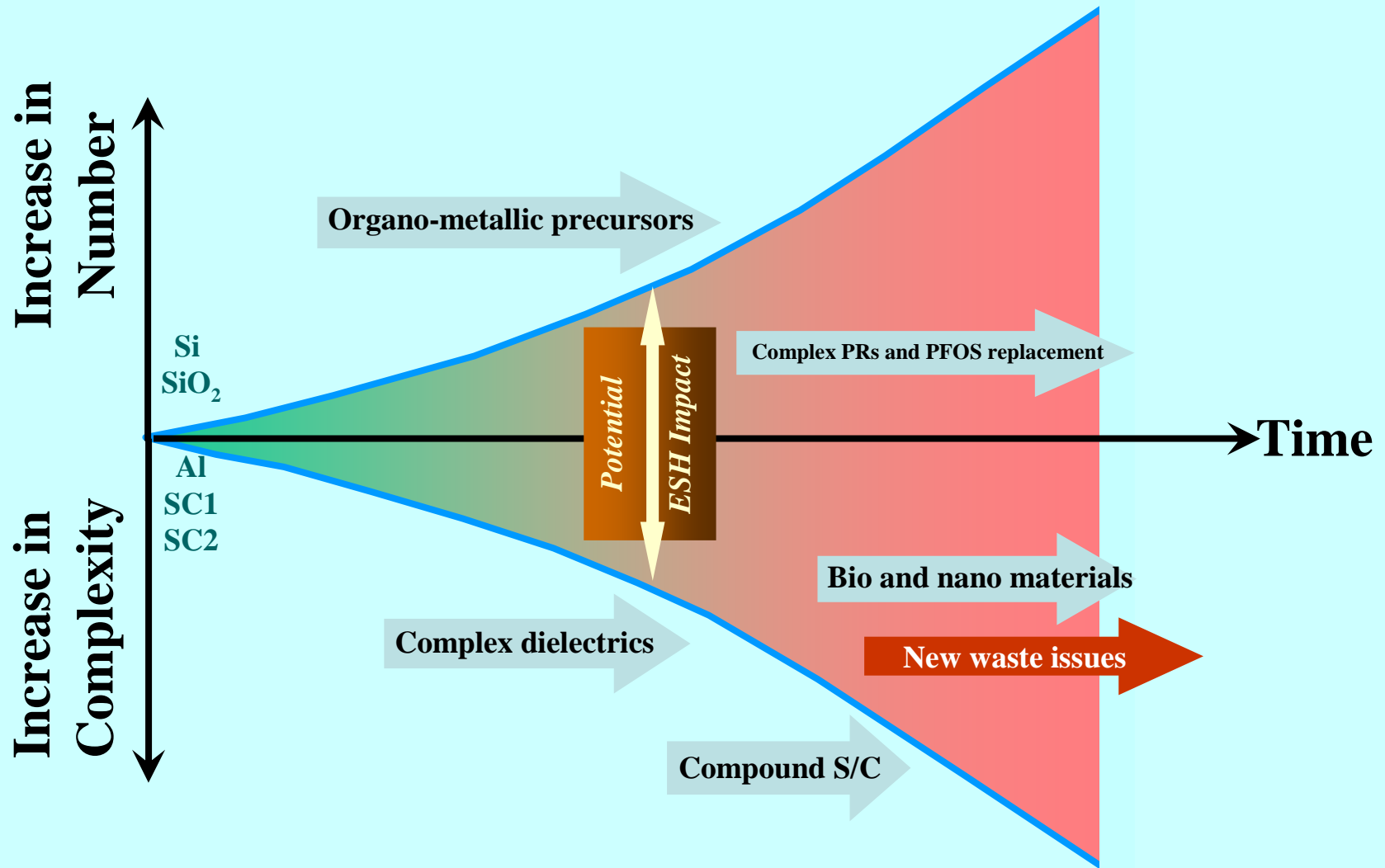
Customized Projects (funded by one or a group of member companies)



Start time and duration: flexible and customized

SRC/Sematech Engineering Research Center for Environmentally Benign Semiconductor Manufacturing

Increasing Role of ESH in SC Manufacturing

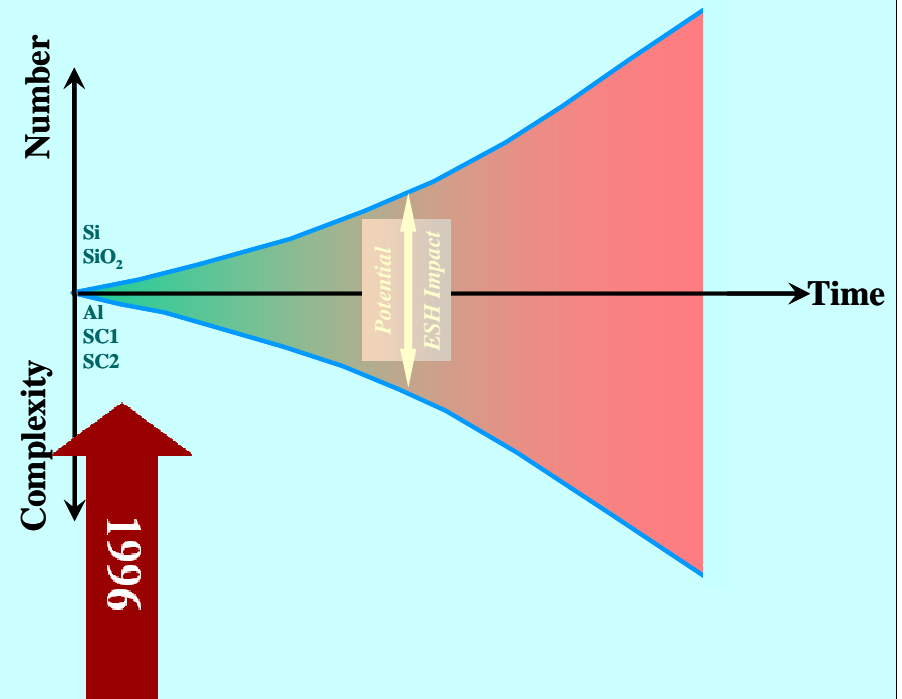


Evolution of ESH Scope and Application

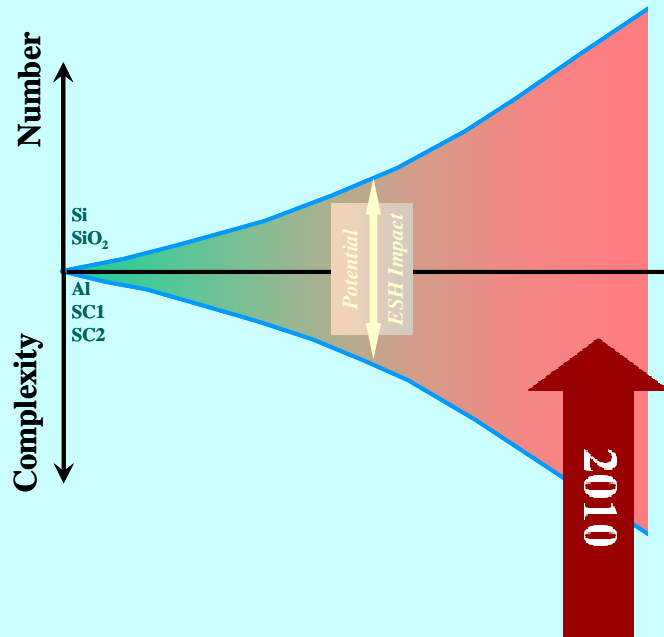
ESH Frontiers and Scope in 1996

- Reduced PFC usage and emission
- Dilute chemistry
- Wastewater treatment and reuse
- Water use reduction (batch tools)
- Abatement of potential VOCs and HAPs
- Lowering energy use in facilities (pumping and ventilation)
- Concern about lead and a few other compounds

Ownership: Facilities Group in a Fab



Evolution of ESH Scope and Application



ESH frontiers and scope in 2010

- ESH aspect of nano particles and new materials
- ESH in high-volume nano-manufacturing
- Low-energy processes
- Surface prep of new materials/nano-structures
- Energy recovery and reuse
- New patterning and etch materials
- Wafers size and single-wafer tools
- Planarization of new material
- Additive processing and selective deposition

Ownership: Shared and Integrated in Process

New Technology ↔ New ESH Developments

Customized Program on:
High-Volume Nano-Manufacturing (HVnM)
Co-sponsored by Intel and ERC

- **Lowering Slurry Use and Waste in CMP Processes: Investigation of the Relationship between Planarization & Pad Surface Micro-Topography; *Philipossian***
- **Lowering Waste in CMP Processes: Retaining Ring and Conditioner Interactions; *Philipossian***
- **Contamination Control in Gas Distribution Systems of Semiconductor Fabs; *Shadman***
- **Develop an AFM-Based Methodology to Optimize APM Composition for Removing Particles from Surfaces; *Raghavan***
- **Integrated Electrochemical Treatment of CMP Waste Streams for Water Reclaim and Conservation; *Baygents, Farrell***

New Initiative in Energy Use Reduction

White Papers and Pre-Proposals

- **Electro-Deposition of Semiconducting Silicon Films**
Dominic Gervasio (Chemical and Environmental Engineering, UA)
- **Efficiency Standards for Facilities Components: Pumps, Chillers, and Fans**
David Dornfeld (Mechanical Engineering, UC Berkeley)
- **Metamaterial-Inspired Nanoscale-Engineered Thermo-Electrics for Efficient Heat Harvesting in Semiconductor Devices**
Krishna Muralidharan (Material Science and Engineering, UA)
- **Low-Energy Amorphous Silicon Processing: Femtosecond-Processed Hydrogenated Amorphous Silicon**
Charles Falco (Optical Sciences - Physics, UA)
- **Thermo-Economic Analysis of Selected Wet Cleaning Processes**
Manish Keswani (Material Science and Engineering, UA)
- **Improved Energy Efficiency in Buildings**
Steven Leeb (Electrical Engineering, MIT)

Environmental Safety and Health (ESH) Impacts of Emerging Nanoparticles and Byproducts from Semiconductor Manufacturing

Tasks 425.023 and 425.024

Research Team

PIs:

- **Jim A Field, Dept. Chemical and Environmental Engineering, UA**
- **Scott Boitano, Dept. of Physiology & Arizona Respiratory Center, UA**
- **Buddy Ratner, University of Washington Engineered Biomaterials Center, UWEB**
- **Reyes Sierra, Dept. Chemical and Environmental Engineering, UA**
- **Farhang Shadman, Dept. Chemical and Environmental Engineering, UA**

Graduate Students:

- **Isabel Barbero: PhD candidate, Chemical and Environmental Engineering, UA**
- **Rosa Daneshvar: PhD candidate, Chemical Engineering, UW**
- **Cara L Sherwood: PhD candidate, Cell Biology and Anatomy, UA**
- **Hao Wang: PhD candidate, Chemical and Environmental Engineering, UA**

Other Researchers:

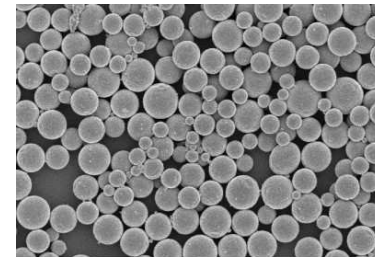
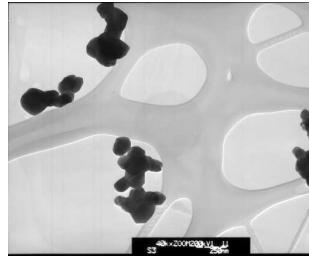
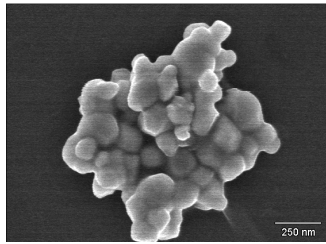
- **Antonia Luna, Postdoctoral Fellow, Chemical and Environmental Engineering, UA**
- **Citlali Garcia, Postdoctoral Fellow, , Chemical and Environmental Engineering, UA**
- **Angel Cobo, Exchange MS Student, Chemical and Environmental Engineering, UA**
- **Jacky Yao, Research Scientist, Chemical and Environmental Engineering, UA**

Cost Share (other than core ERC funding):

- **\$80k from UA Water Sustainability Program**

Overall Objectives

- **Characterize toxicity of current and emerging nanoparticles (NP) & NP byproducts**



- **Develop new rapid methodologies for assessing and predicting toxicity**



ESH Metrics and Impact

1. *Reduction in the use or replacement of ESH-problematic materials*

Data on toxicity of nanoparticles can assist in selecting materials in the semiconductor industry which are candidates for replacement or use reduction.

2. *Reduction in emission of ESH-problematic material to environment*

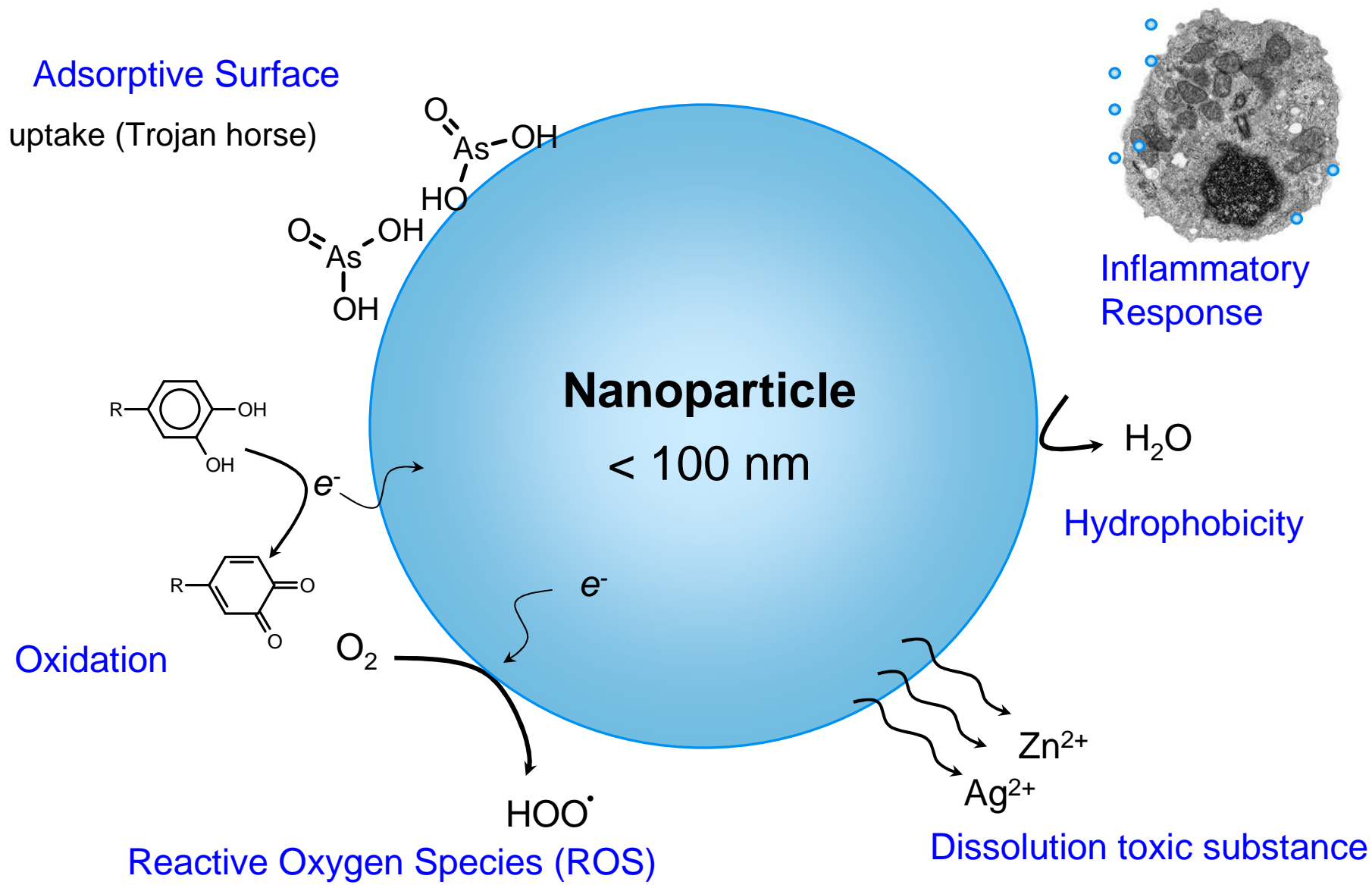
The knowledge gained can be utilized to modify the manufacture of nanoparticles so that they have a lowered toxicity and thus a lowered environmental impact.

Toxicity Assessment and Prediction

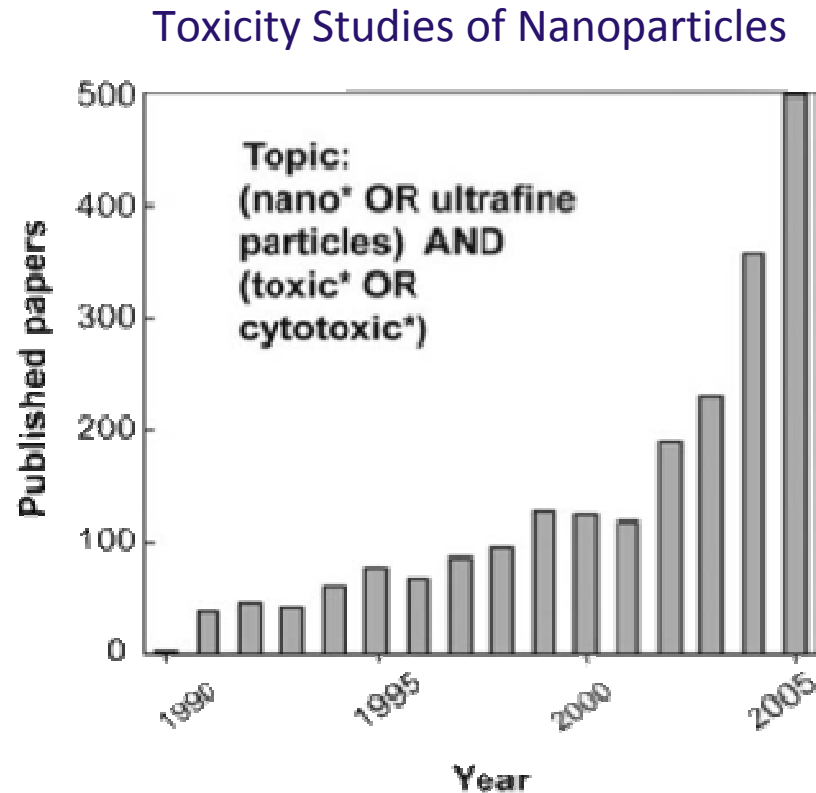
Objectives

- **Establish role for reactive oxygen species (ROS) and/or oxidative stress as a potential marker for NP toxicity assessment**
- **Develop predictable models of toxicity based on physico-chemical properties elucidated by advanced surface analysis techniques**
- **Validate toxicity assessments and predictions with organ skin cultures (and advanced lung cultures)**

Introduction: Toxicity Mechanisms



Introduction: Toxicity Studies



Some parameters suggested as responsible for toxicity of nanoparticles:

1. Size
2. Dose
3. Aspect Ratio
4. Composition
5. Crystalline Structure
6. Morphology
7. Concentration
8. Surface Area
9. Surface Energy

Graph borrowed from: Buzza, C; Pacheco, I. I.; Robbie, K. Nano materials and nanoparticles: Sources and toxicity. *BioInterphases*. 2007, 2, MR17-MR71

SRC/Sematech Engineering Research Center for Environmentally Benign Semiconductor Manufacturing

Materials

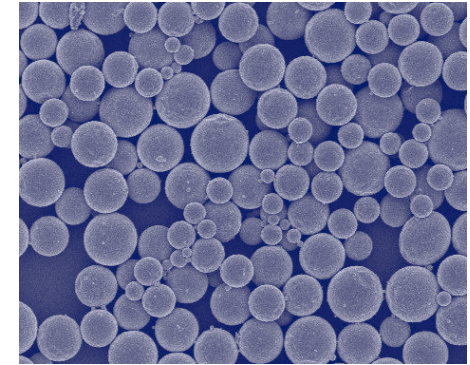
- Nanoparticles

Hafnium Oxide (HfO_2), immersion lithography

Silica Oxide (SiO_2), CMP

Ceria Oxide (CeO_2), CMP

Others (Al_2O_3 , carbon and germanium- nanotubes, quantum dots *etc*)



- Biological targets

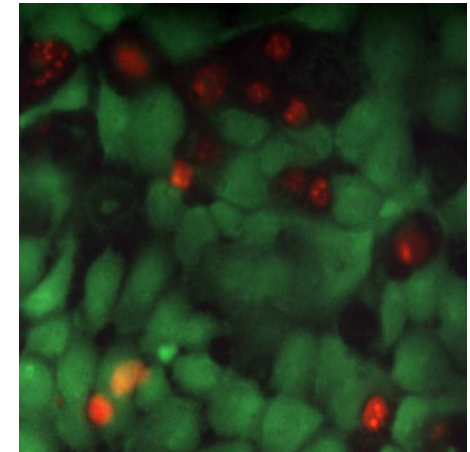
Human skin cell line (HaCat)

Human lung epithelial cell line (16HBE14o-)

Bacterium (*Vibrio fischeri*) Microtox test

Yeast (*Saccharomyces cerevisiae*) O_2 uptake test

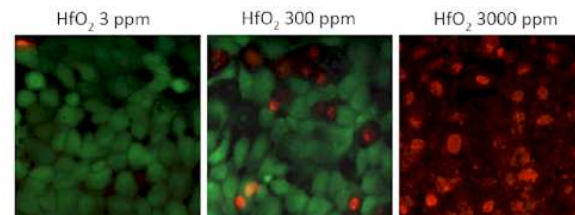
Others (methanogens, human foreskin rafted organ culture, *etc*)



Methods

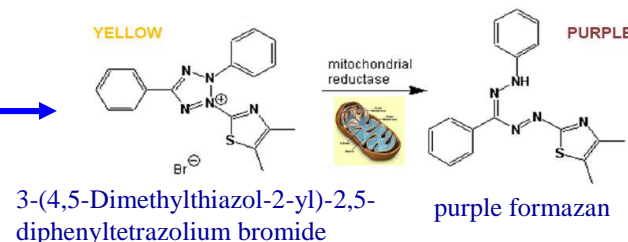
- Main Toxicity Tests Utilized

Live/Dead Assay with HaCat Skin Cell Line (HaCat)



Live: calcein AM) Dead: ethidium homodimer-1

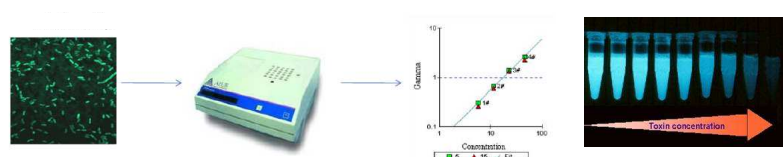
Mitochondrial Toxicity test (MTT) (ureter cells)



Yeast O₂ uptake test

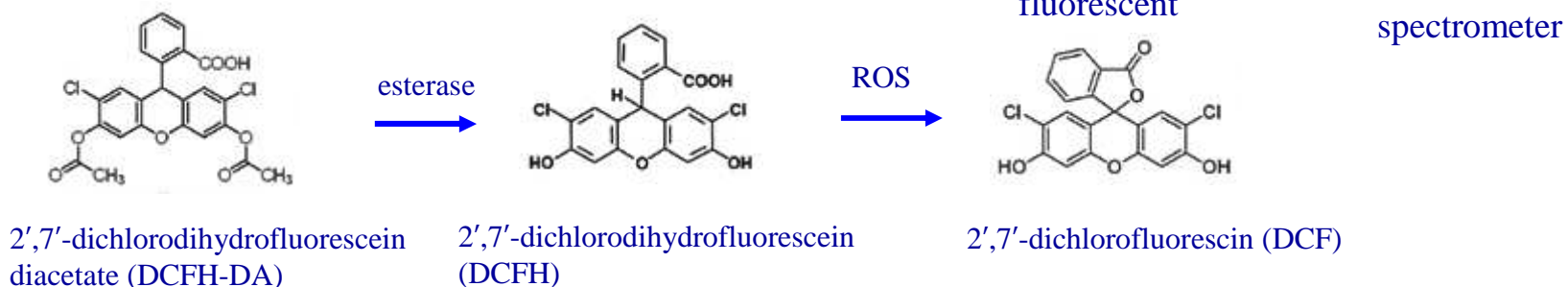
Microtox (*Vibrio fischeri*)

Methanogenic Activity



- Chemical: Reactive Oxygen Species (ROS) Production

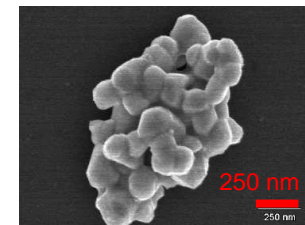
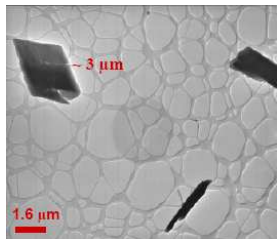
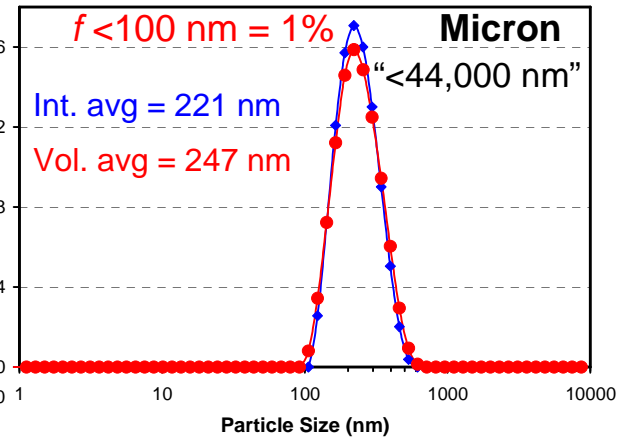
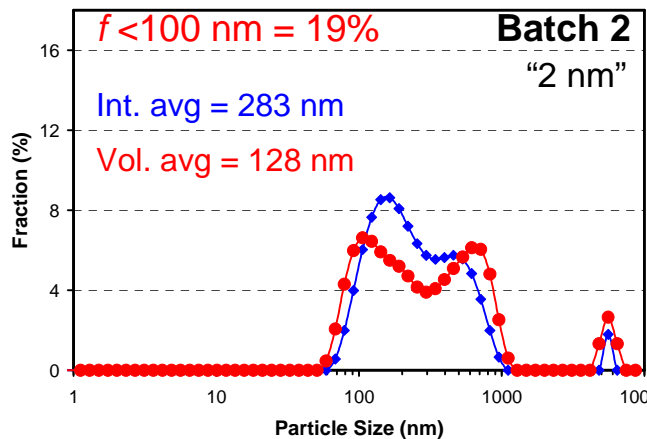
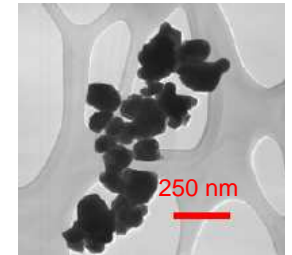
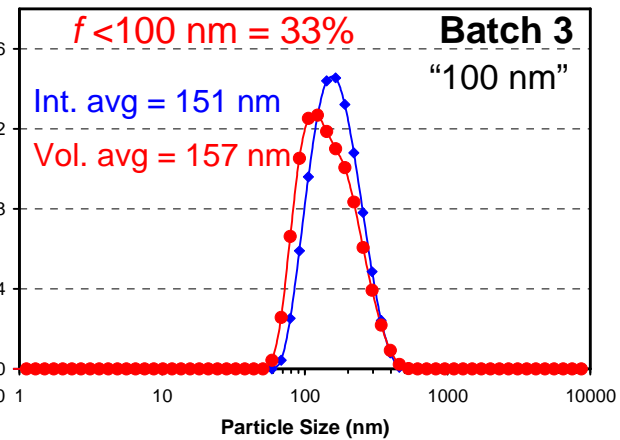
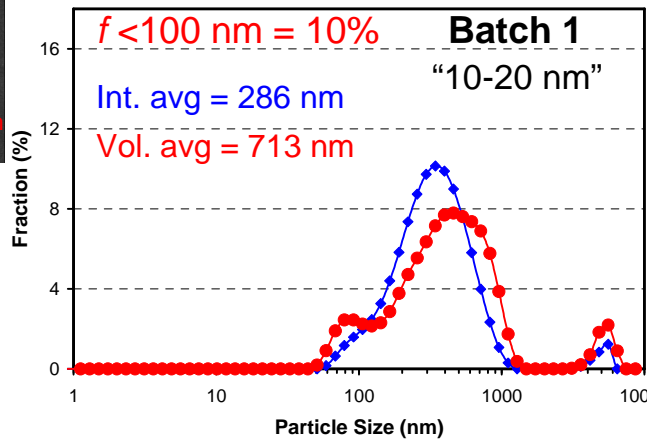
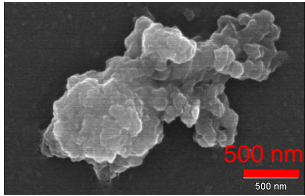
Detection of fluorescent ROS-sensitive dye



Results on HfO₂

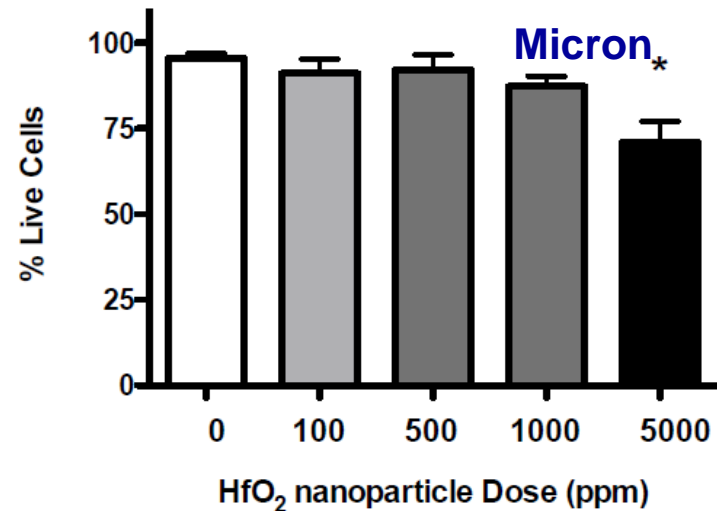
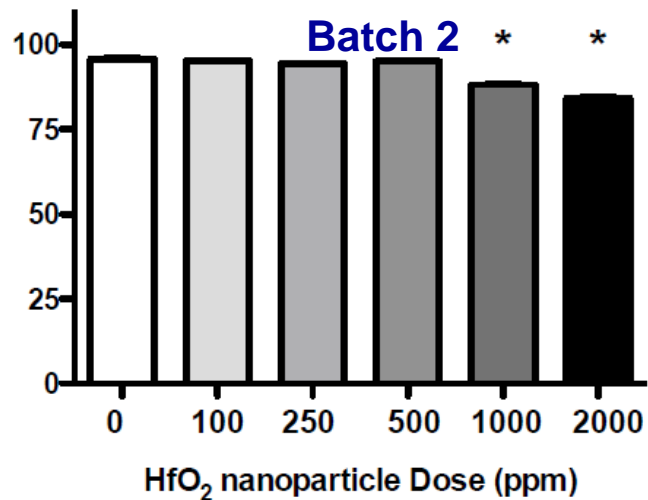
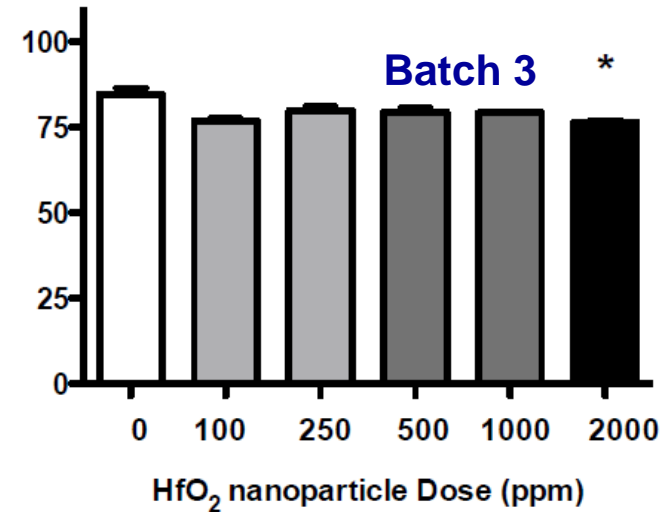
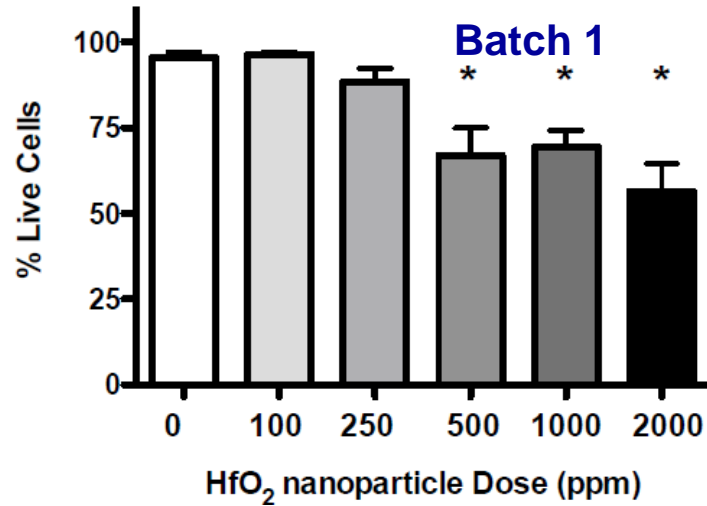
Four distinct batches of hafnium oxide tested

(dispersions measured at pH 4 – 5)



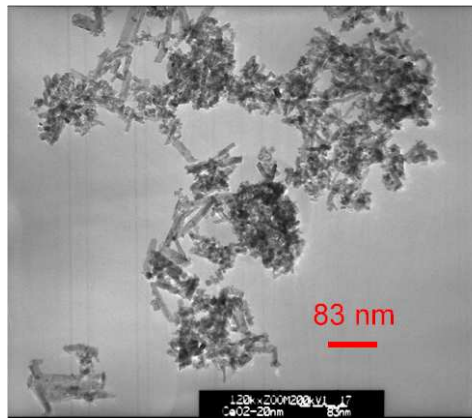
Results on HfO₂

Example Toxicity Results: Live/Dead test (HaCat skin cells)

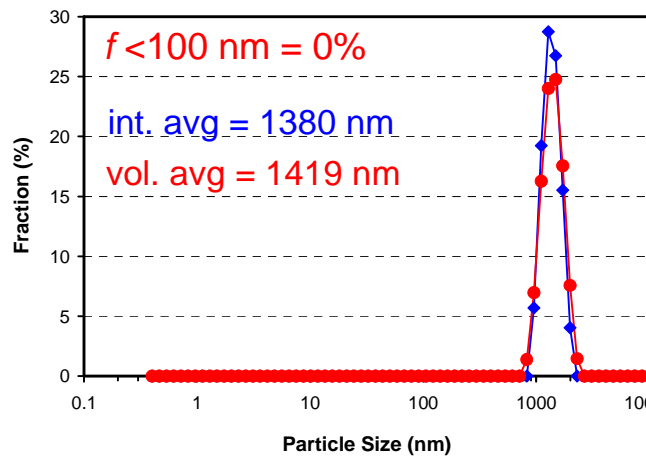


Results on CeO₂

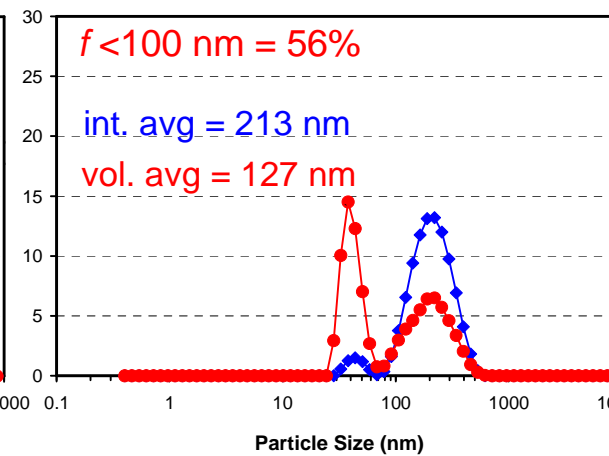
Cerium oxide (MTI, "20 nm") in Suspension at pH 7



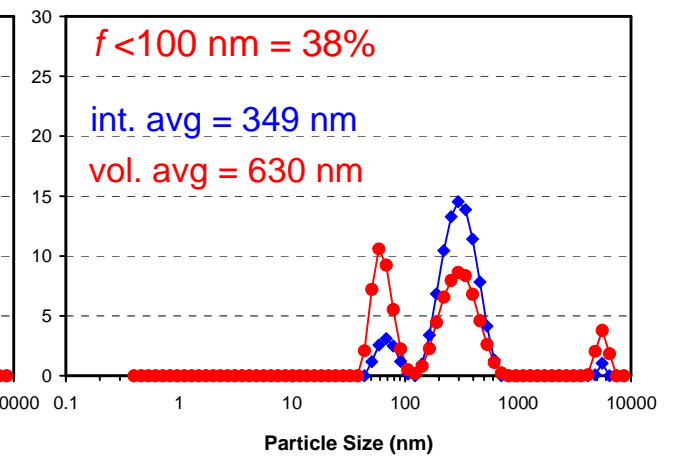
MQ water pH7



MQ water pH7 + Dispex

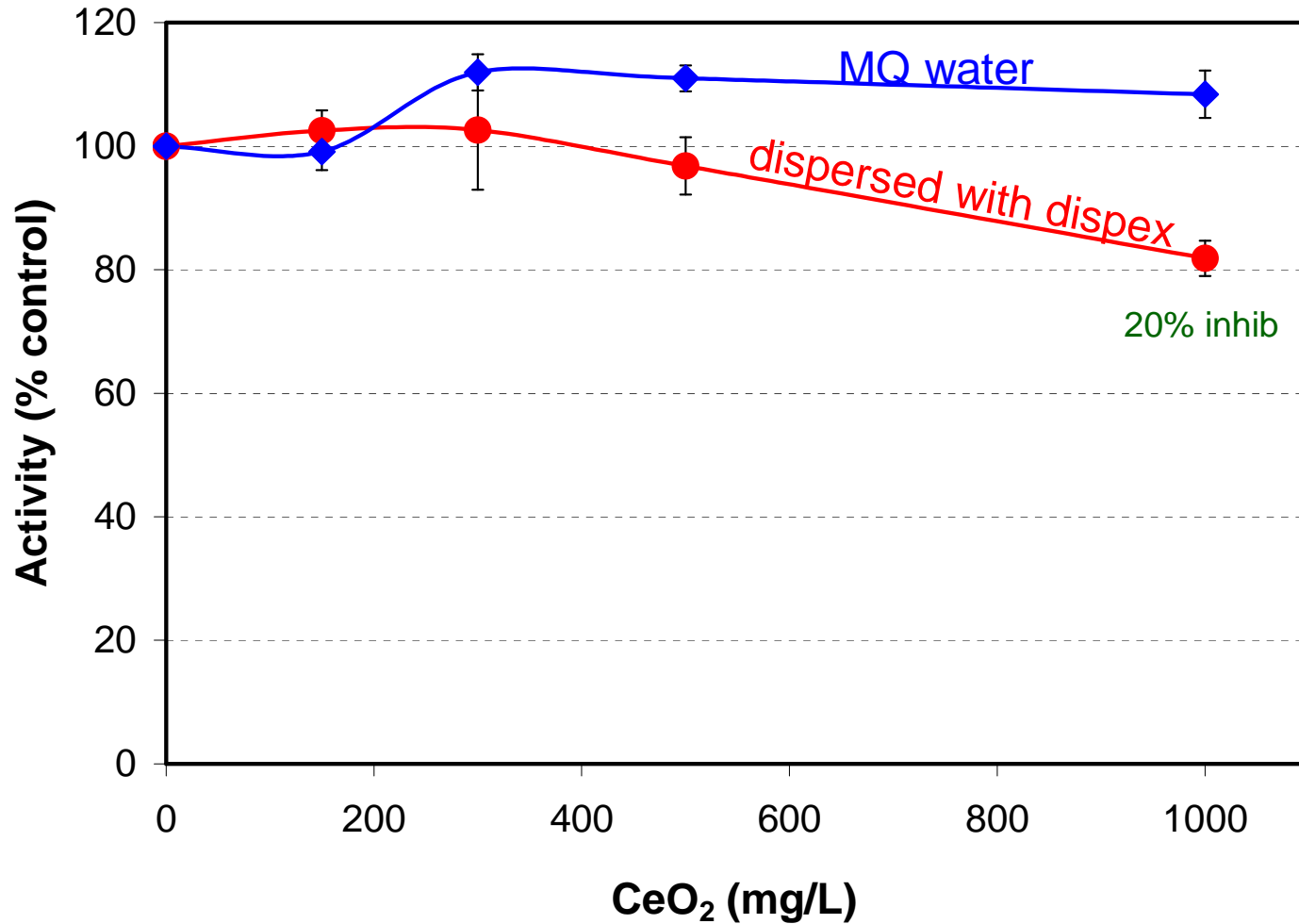


Microtox med. + Dispex



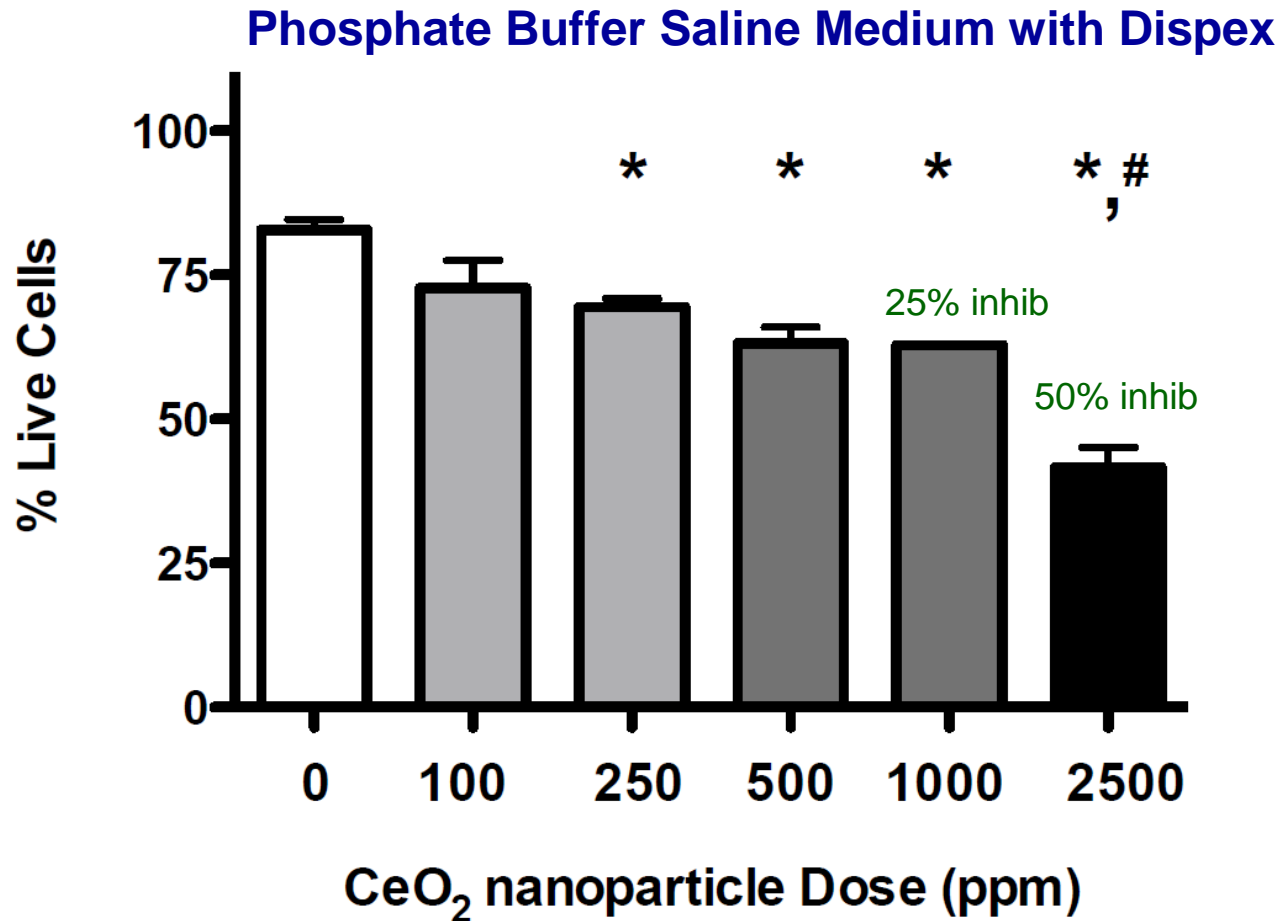
Results on CeO₂

Cerium oxide (MTI, "20 nm"). Example Microtox Test



Results on CeO₂

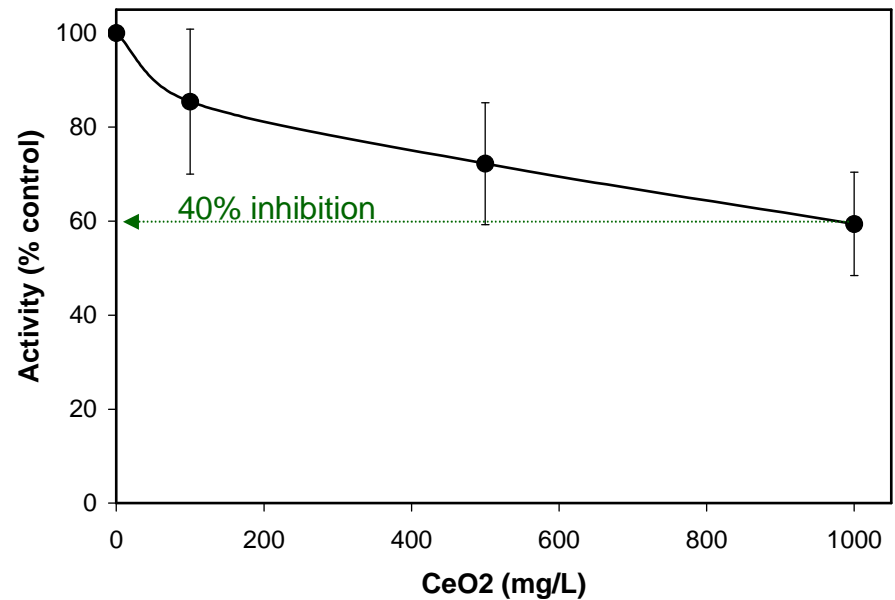
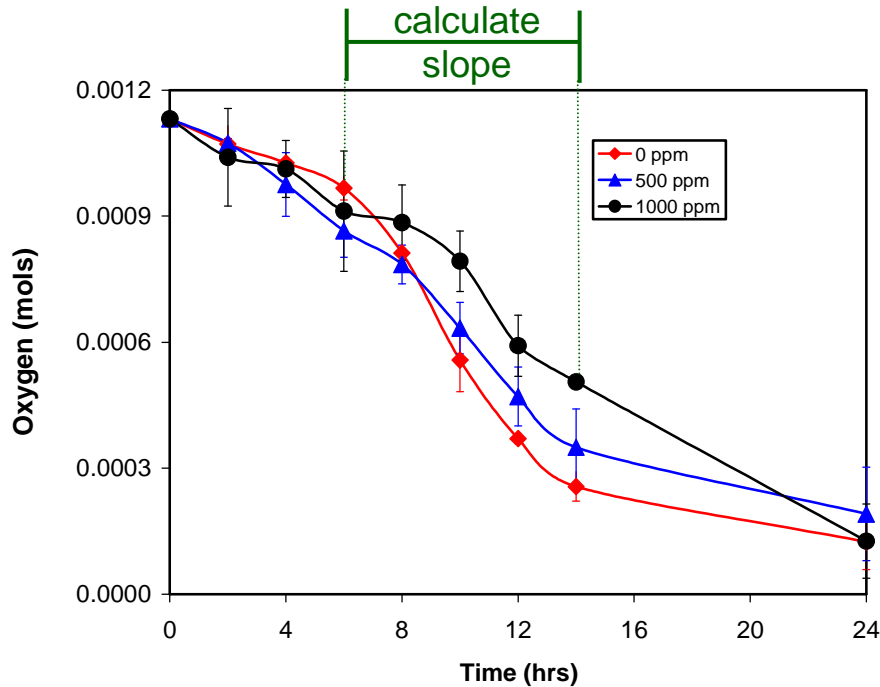
Cerium oxide (MTI, “20 nm”). Example Live/Dead with Dispex



Results on CeO₂

- O₂ uptake assay with yeast cells

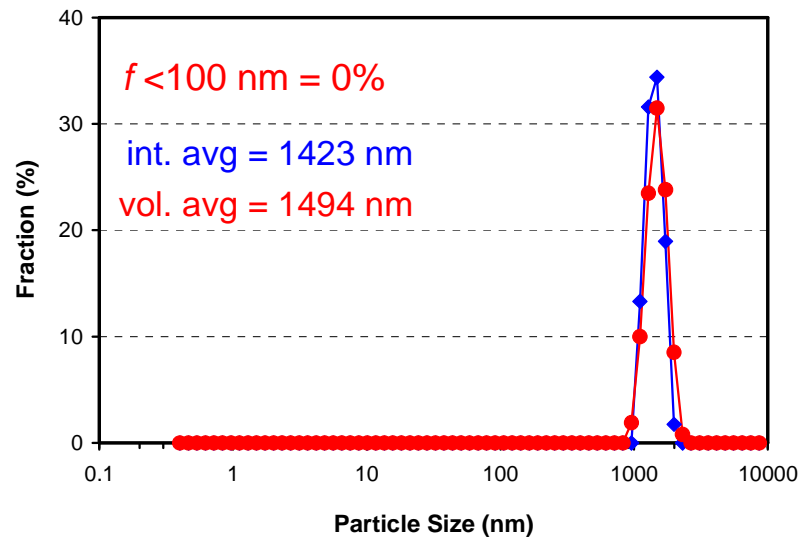
Inhibition of Yeast (*Saccharomyces cerevisiae*) Respiration by CeO₂ with Dispex



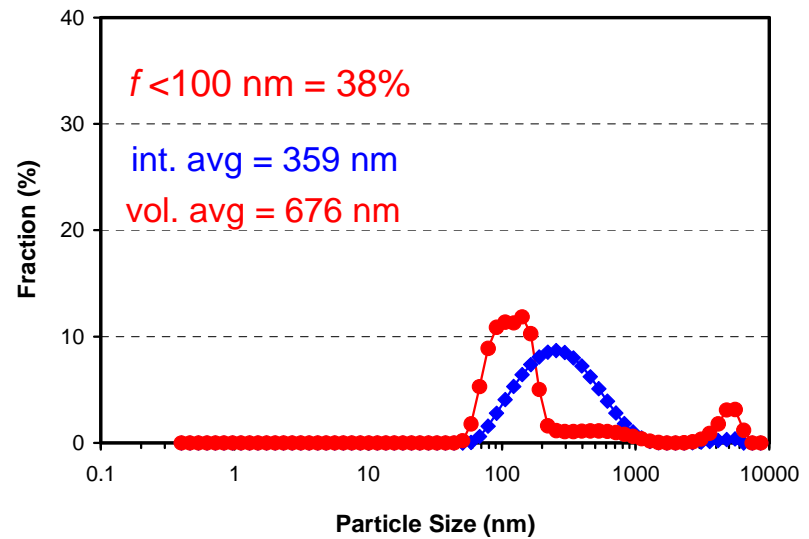
Results on Mn₂O₃

Manganese Oxide (SSNano, “40-60 nm”)

MQ water pH7

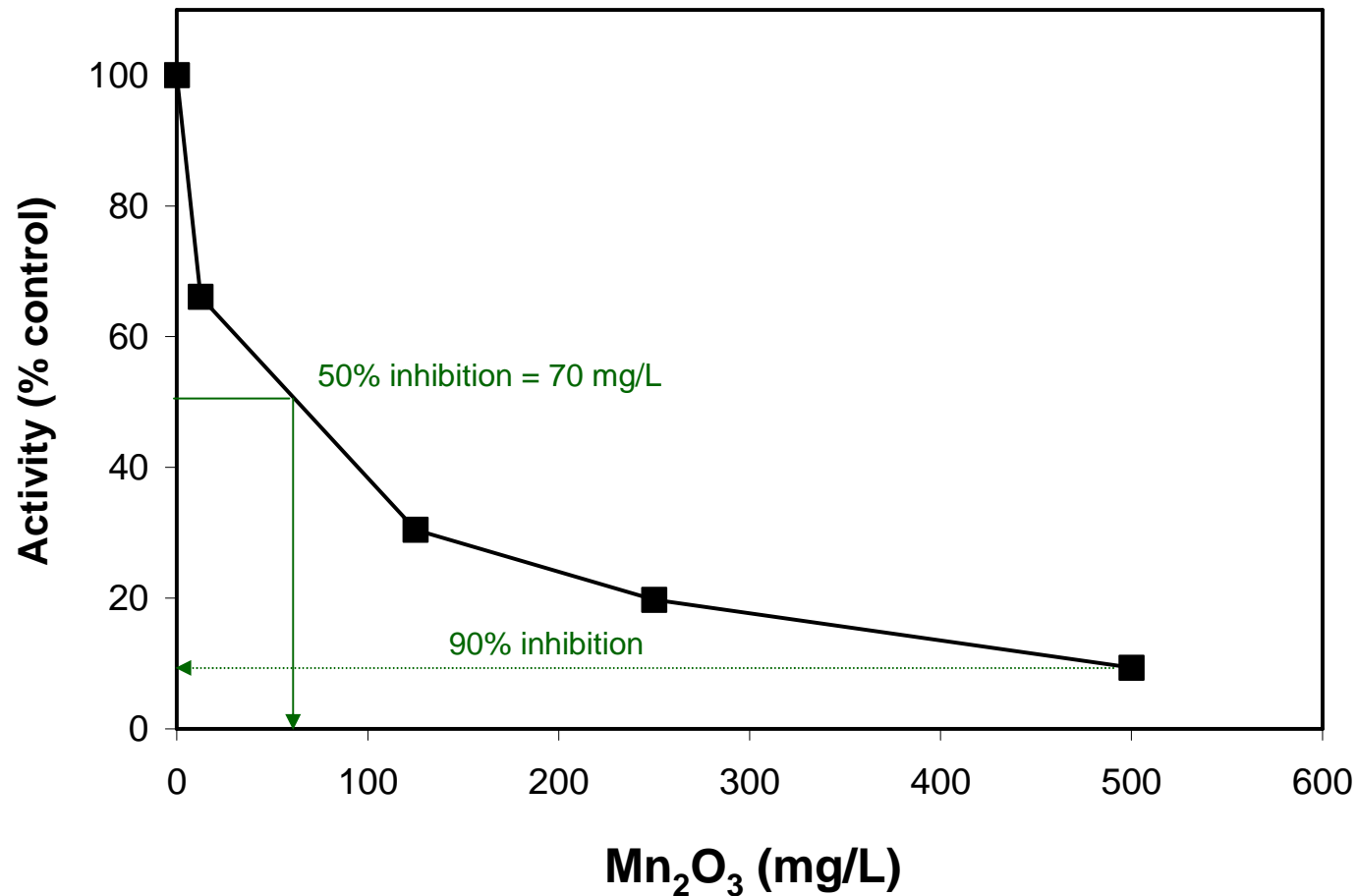


MQ water pH7 + Displex



Results on Mn₂O₃

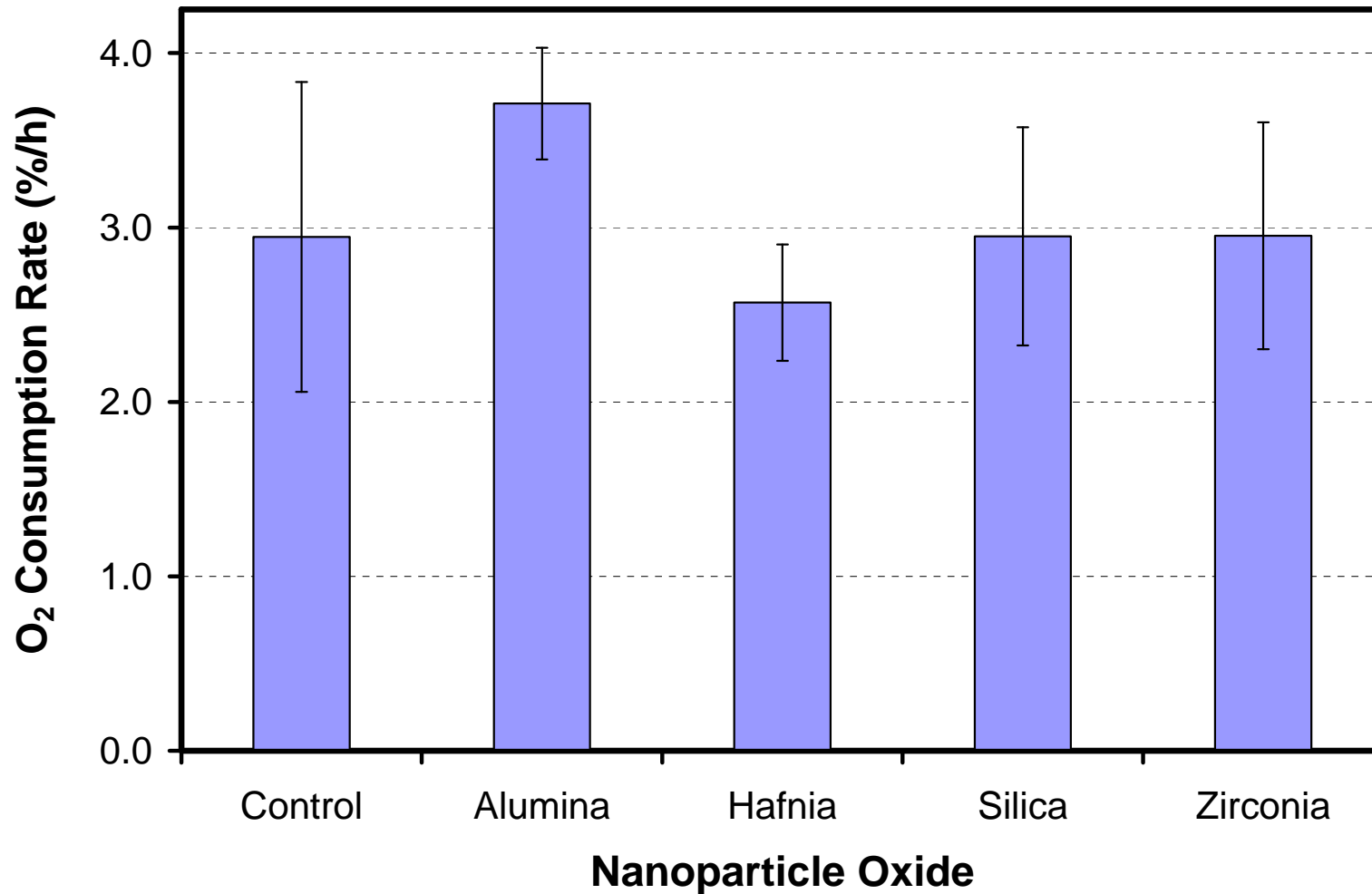
Manganese Oxide (SSNano, “40-60 nm”). Example Microtox with Dispex



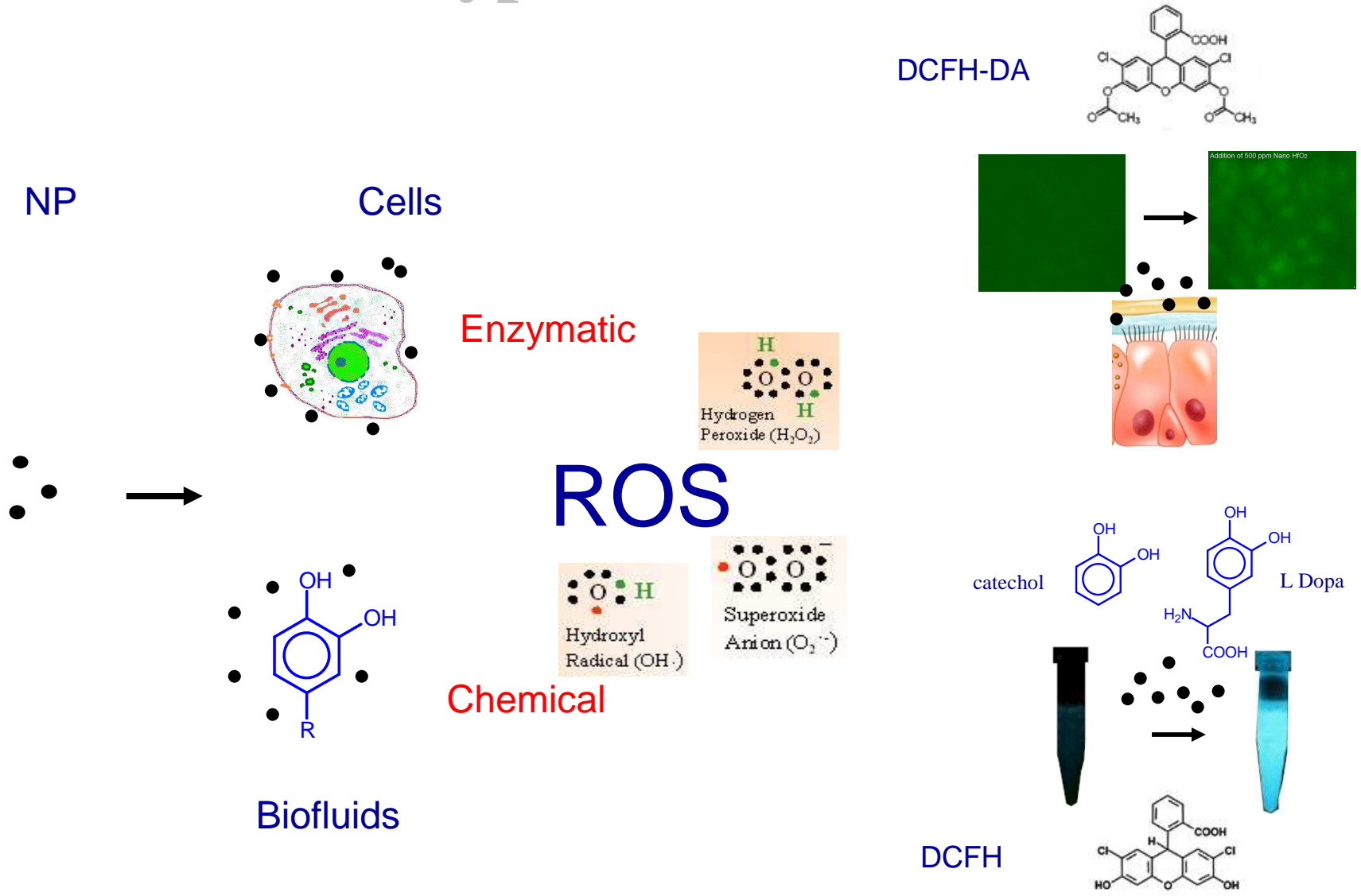
Results on Various Nanoparticle Oxides

O₂ uptake assay with yeast cells

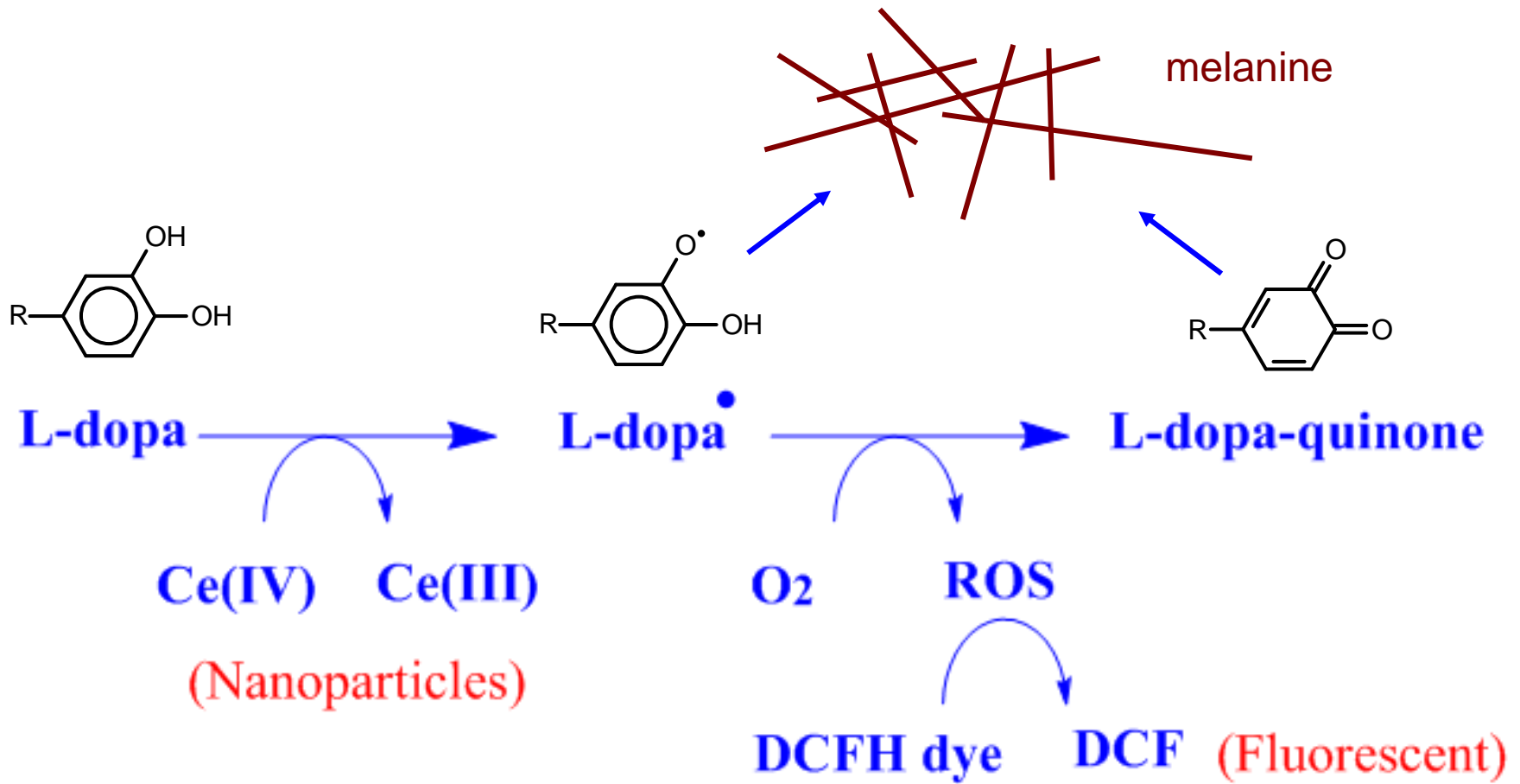
1000 mg/L nanoparticle oxide with Dispex



Hypothesis ROS

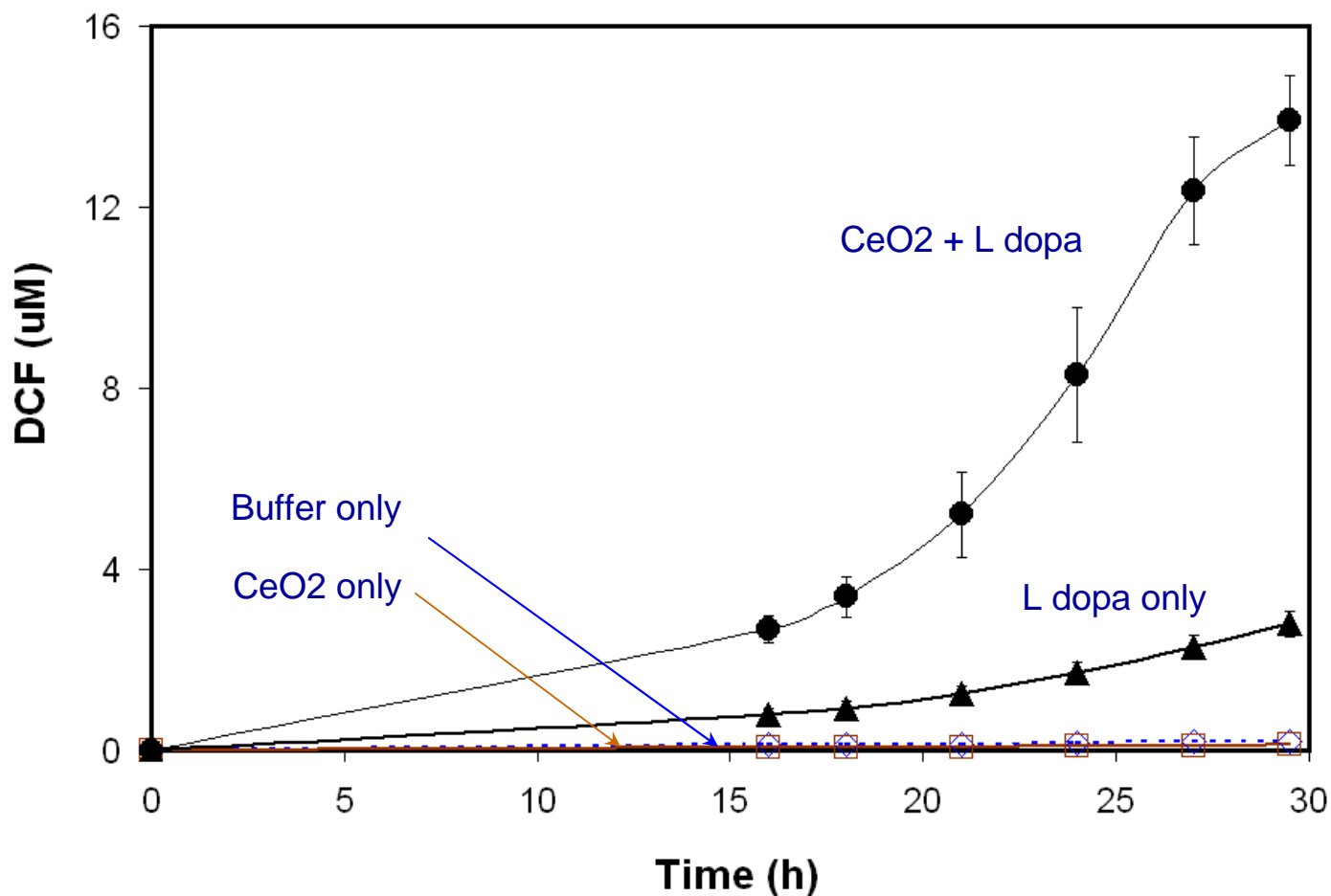


Hypothesis ROS



Chemical Production ROS

CeO₂ (MTI, “20 nm”)



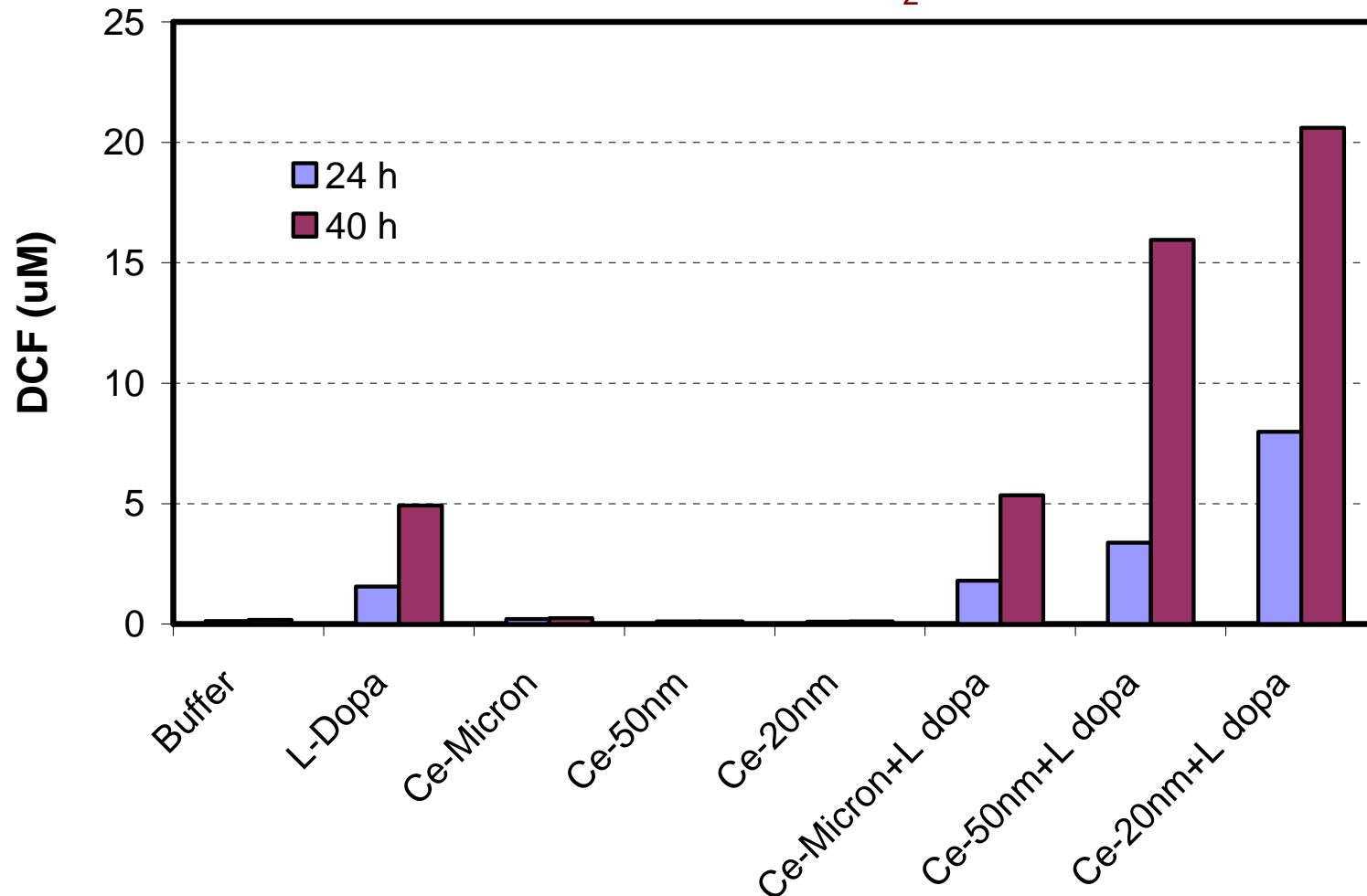
The results indicate that the oxidation of L dopa by CeO₂ NP produces ROS.

Direct reaction of CeO₂ with dissolved oxygen or the dye does not produce ROS or dye oxidation

Chemical Production ROS

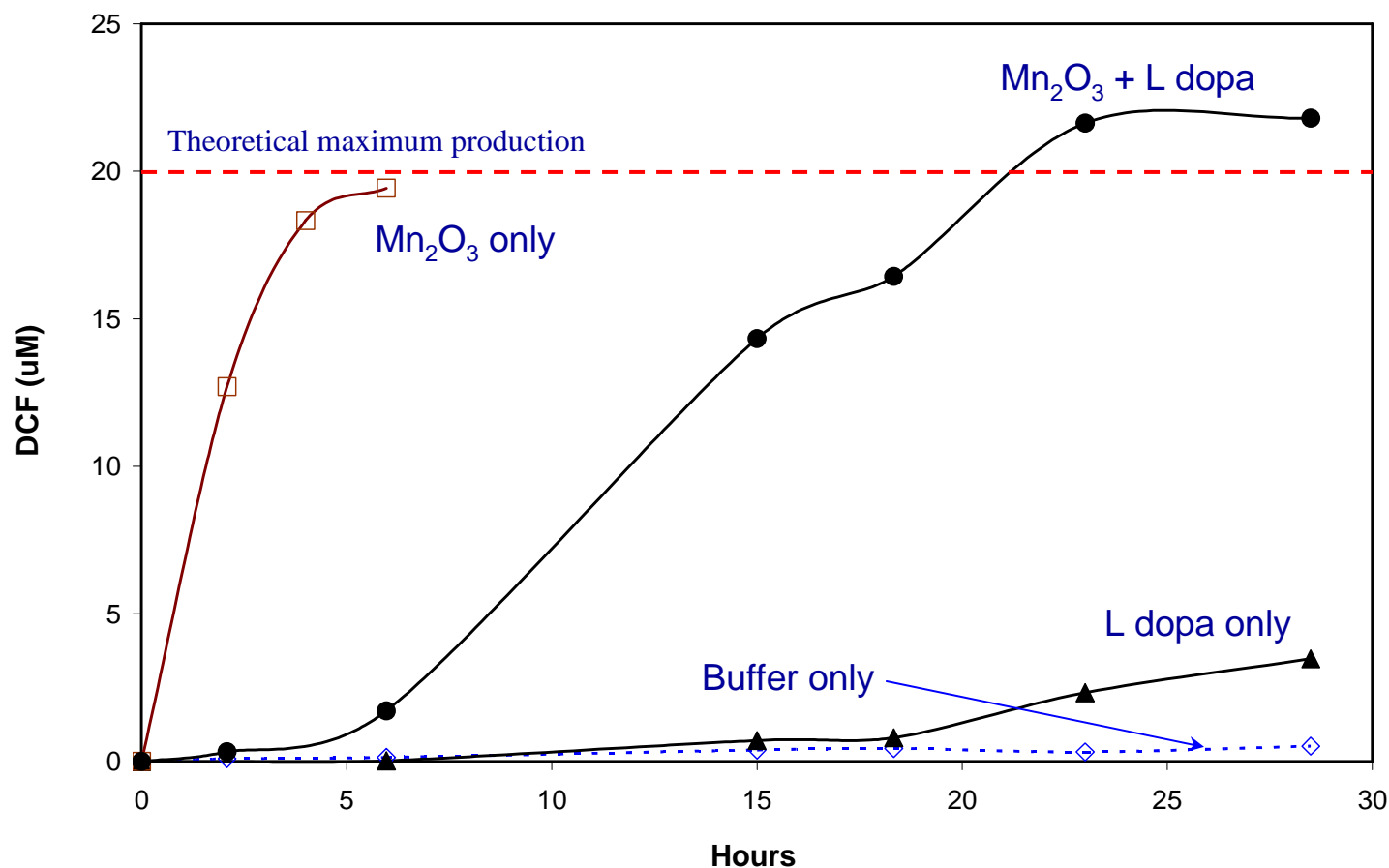
CeO₂ (MTI, “20 nm” vs Sigma “50 nm” vs Micron sized)

Effect of Different CeO₂ Sources



Chemical Production ROS

Mn_2O_3 (SSNano “40-60 nm”).

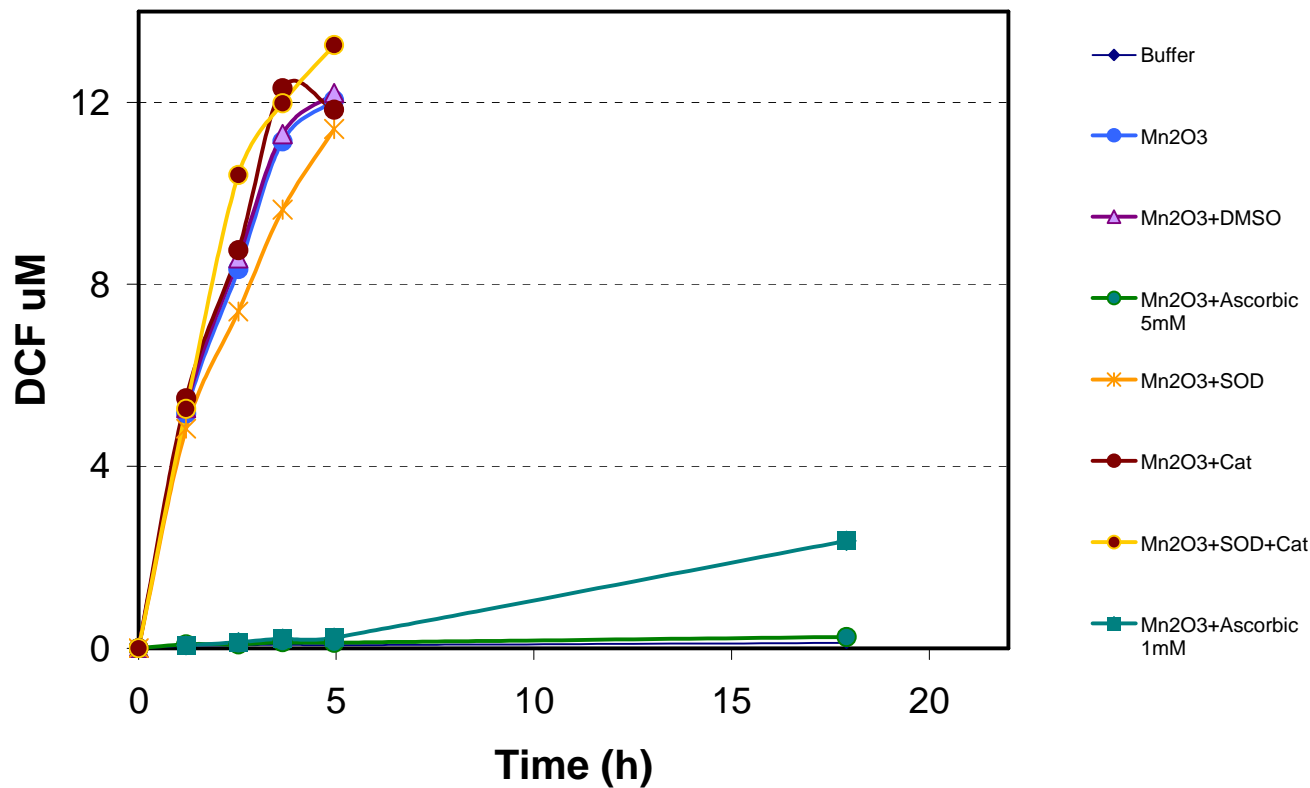


Results indicate that the interaction of Mn_2O_3 NP with water, dissolved oxygen and/or the dye causes the formation of ROS or direct dye oxidation.

L dopa inhibits the dye oxidation by Mn_2O_3 indicating competitive oxidation

Chemical Production ROS

Mn_2O_3 (SSNano “40-60 nm”).
Effect of Different ROS Inhibitors



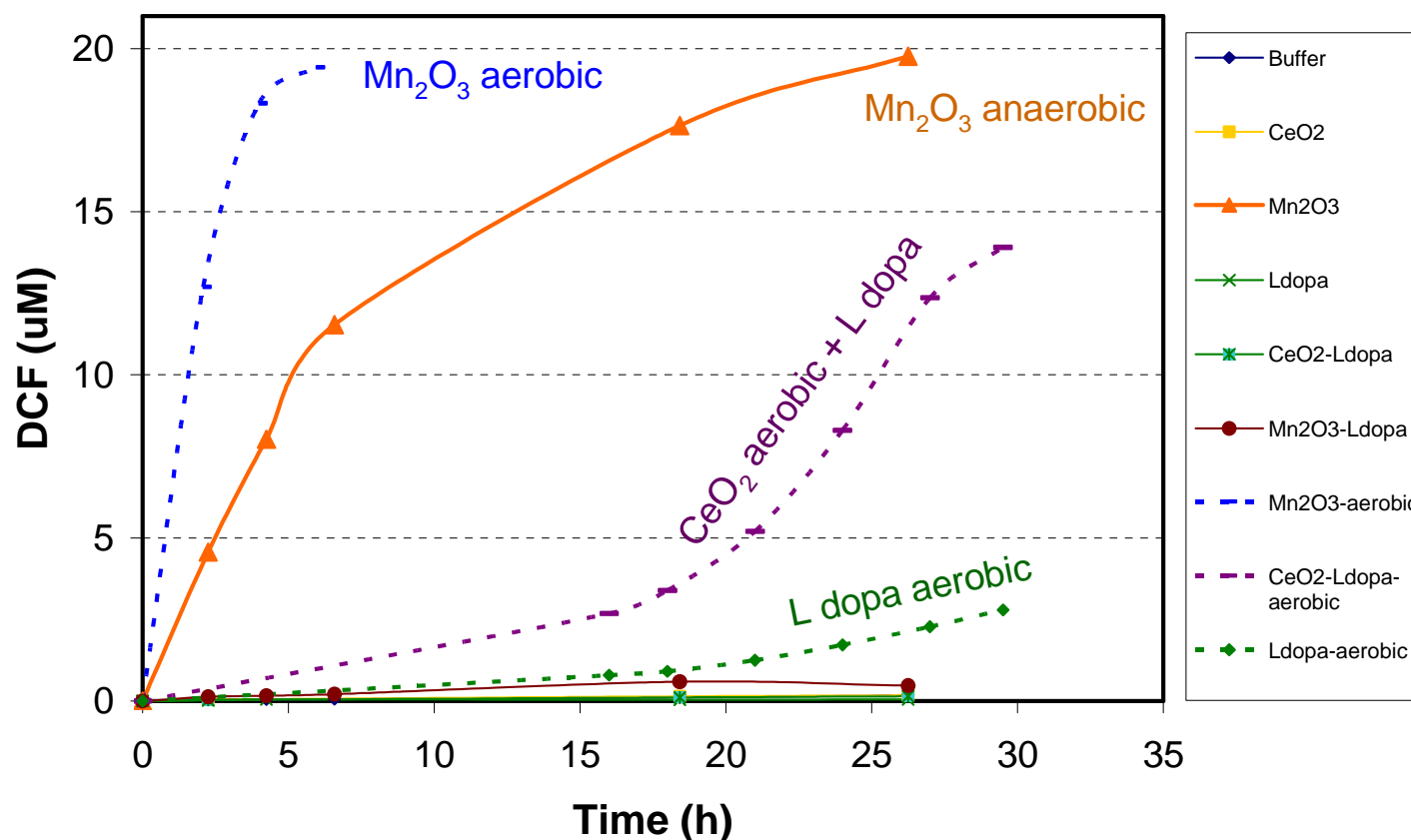
Results indicate that ROS inhibitors are ineffective in stopping the reaction of dye fluorescence by Mn_2O_3

Only the general antioxidant ascorbic acid is effective

Chemical Production ROS

Mn_2O_3 (SSNano “40-60 nm”).

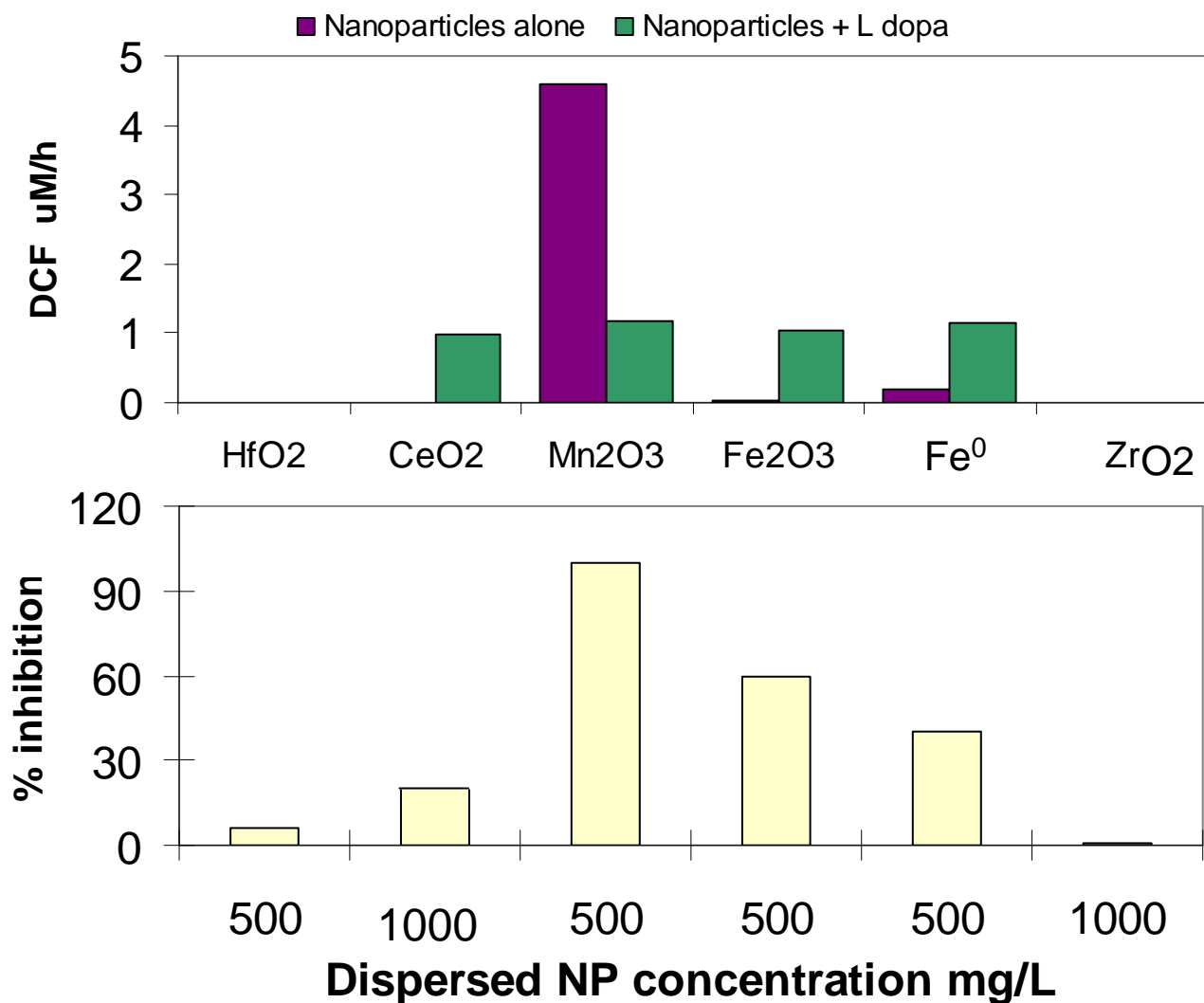
Effect of Anaerobic Incubation



Results indicate that the reaction of dye fluorescence by Mn_2O_3 is mostly a direct reaction not involving O_2

The reaction of dye fluorescence with CeO_2 and Ldopa involves O_2

Correspondence Oxidative Stress Versus Inhibition



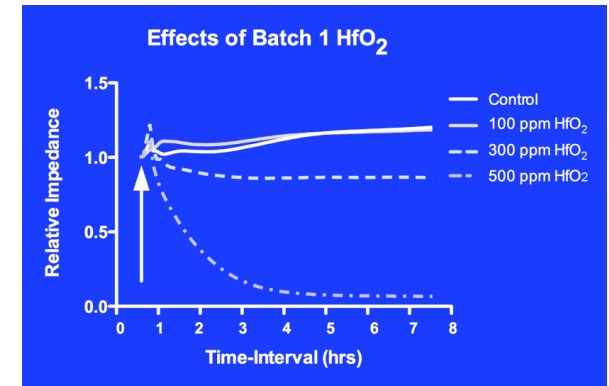
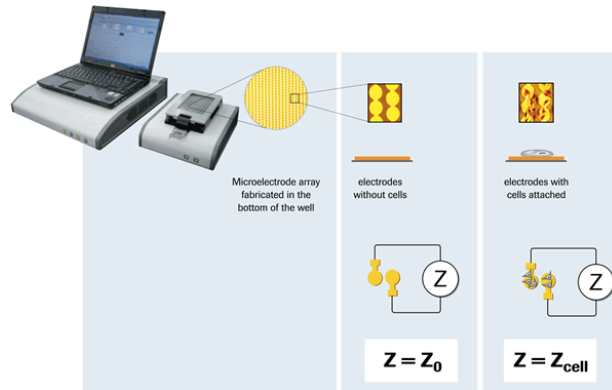
ROS assay

Microtox

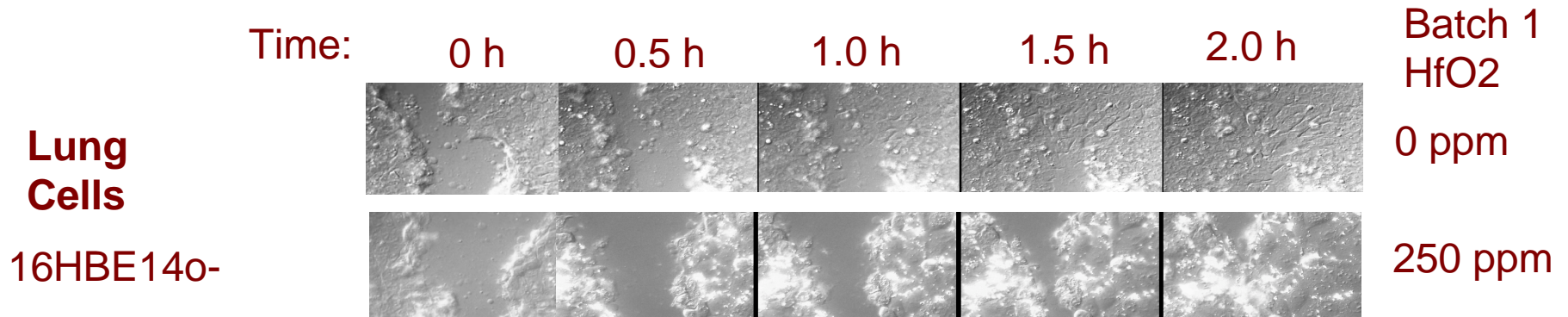
Development New Techniques

New dye-free techniques that are less prone to interferences

- xCELLigence based on measuring impedance



- Wound healing assay, based on time to close scrape wound



Preliminary Conclusions

- **Semiconductor NP oxides (HfO₂, ZrO₂, CeO₂, Al₂O₃, and SiO₂) mild to no toxicity.**

Higher Toxicity of Batch 1 HfO₂ may be due to chemical contamination (from synthesis)

	L/D	Microtox	Methanog	Yeast
	50% death	50% inhib	50% inhib	50% inhib
	----- mg/L -----			
HfO₂ [*]	>2000	3000	>2500	>1000 ^{**}
CeO₂	2500 ^{**}	>1000 ^{**} (18%)	>1000	>1000 ^{**} (40%)
ZrO₂		>1000 ^{**}		>1000 ^{**}
Al₂O₃		>1000 ^{**}		>1000 ^{**}
SiO₂		>1000 ^{**}		>1000 ^{**}

^{*}batch3 ^{**}with dispersant

Preliminary Conclusions

- Some NPs cause oxidative stress via chemical reactions

CeO₂ reacts with polyhydroxy phenols and O₂ enhancing ROS production

Mn₂O₃ causes direct chemical oxidation fluorescent dye (and potentially also cell components)

- NPs oxidizing fluorescent dye directly most toxic.
Chemical ROS production or oxidative dye reaction indicative of NP toxicity

Mn₂O₃ 50% IC microtox = 70 mg/L

Fe₂O₃ 50% IC microtox ≈ 500 mg/L

Fe⁰ 50% IC microtox ≅ 500 mg/L

Industrial Interactions and Technology Transfer

- **ISMI-Sematech (Steve Trammell, Laurie Beu)**
- **AMD (Reed Content)**
- **IBM (Arthur T. Fong)**
- **Intel (Steve W. Brown, Paul Zimmerman, Mansour Moinpour)**

Future Plans

Next Year Plans

- Fractionation of CeO₂ for toxicity study size fractions
- Biochemical indicators of oxidative stress
- Complete development of new non-dye based techniques
- Study effect surface contaminants on Toxicity

Long-Term Plans

- Rapid screening protocols of for assessing NP toxicity
- Toxicity to organ models

Publications, Presentations

- Brownbag presentation: Nanoparticle Interaction with Biological Wastewater Treatment Processes, Water Sustainability Program, Phoenix, Arizona Jan 20th, 2010 at Arizona Cooperative Extension
- Sierra-Alvarez, R. 2009. Toxicity characterization of HfO₂ nanoparticles. SRC/Sematech Engineering Research Center for Environmentally Benign Semiconductor Manufacturing Teleseminar Series. August 6.
- Boitano, S. 2009. Measuring cytotoxicity of nanoparticles in human cells. SRC/Sematech Engineering Research Center for Environmentally Benign Semiconductor Manufacturing Teleseminar Series. Sept. 17.
- Ratner, B. 2009. Static SIMS: A Powerful Tool to Investigate Nanoparticles and Biology. SRC/Sematech Engineering Research Center for Environmentally Benign Semiconductor Manufacturing Teleseminar Series. May 14.

Nanoparticle Toxicology

Surface Physical Characterization

Hypothesis: The size of nanoparticles makes them more adsorptive to external chemicals, and these surface molecules lead to the observed toxic effects

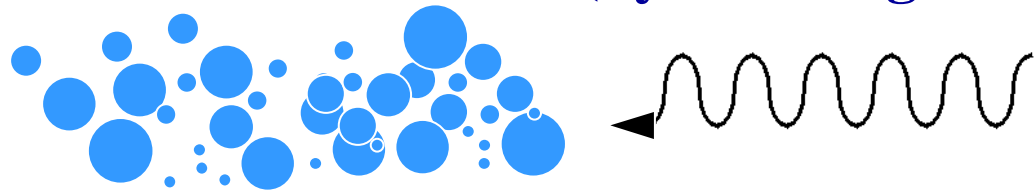
Principal Investigators:

- Buddy Ratner, University of Washington Engineered Biomaterials Center, UWEB
- Jim A Field, Dept. Chemical and Environmental Engineering, UA
- Scott Boitano, Dept. of Physiology & Arizona Respiratory Center, UA
- Reyes Sierra, Dept. Chemical and Environmental Engineering, UA
- Farhang Shadman, Dept. Chemical and Environmental Engineering, UA



Surface Physical Characterization

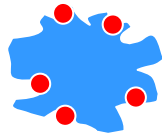
- Particle size distribution (dynamic light scattering)



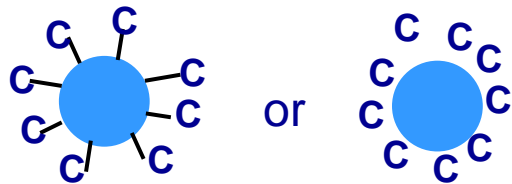
- Specific area (area/volume or area/mass of NP)



- Active site density; site energetics

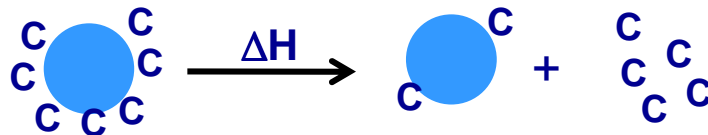


- Physical adsorption vs chemical adsorption



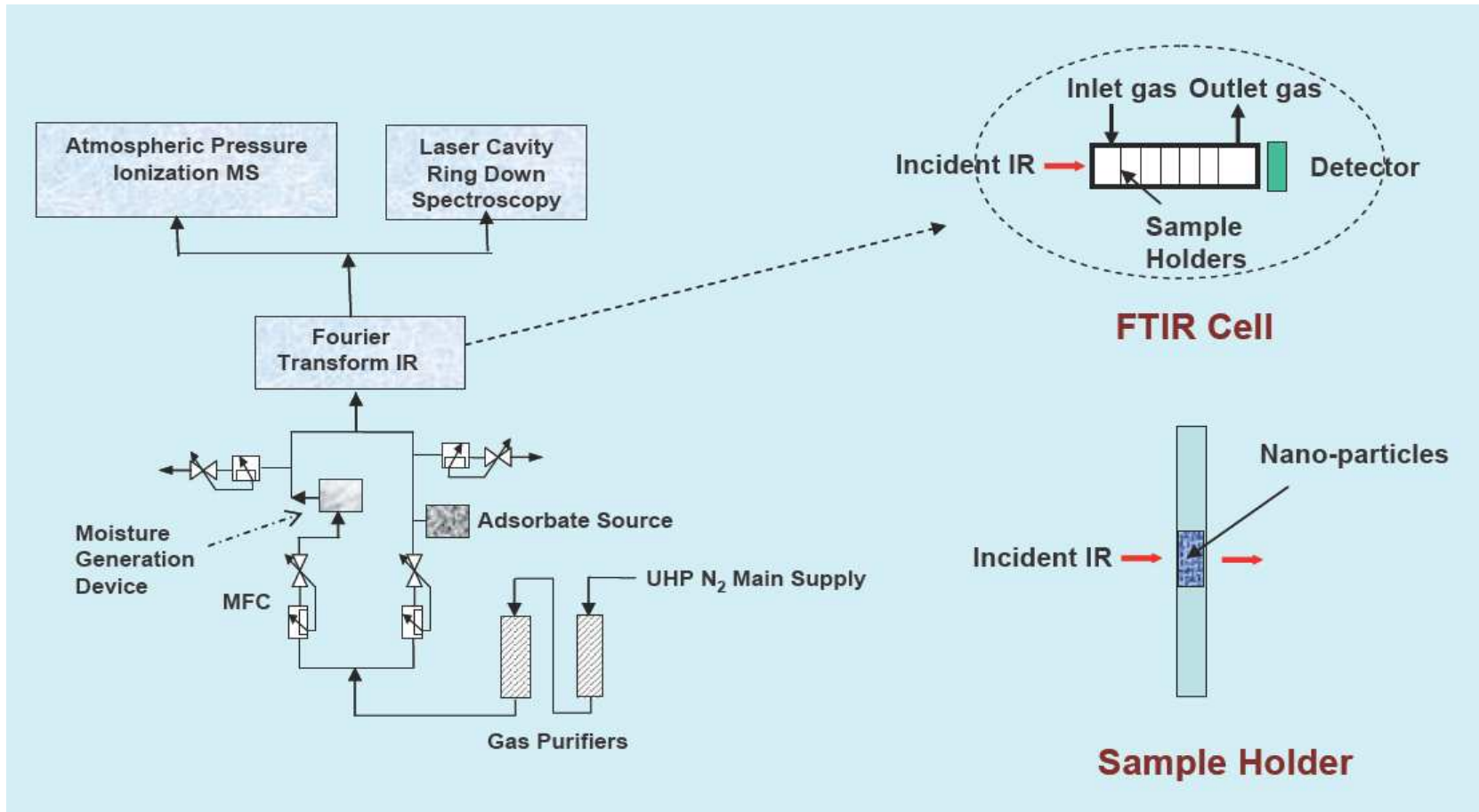
What is at the particle surface and how is it bound?

- Retention of contaminants

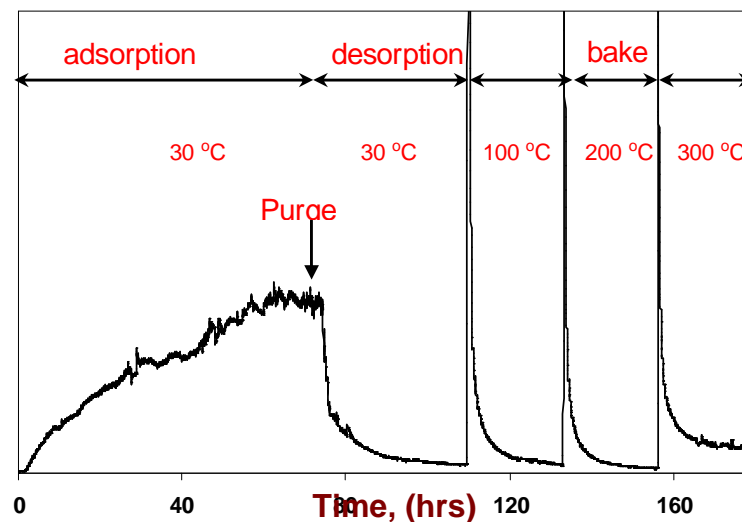
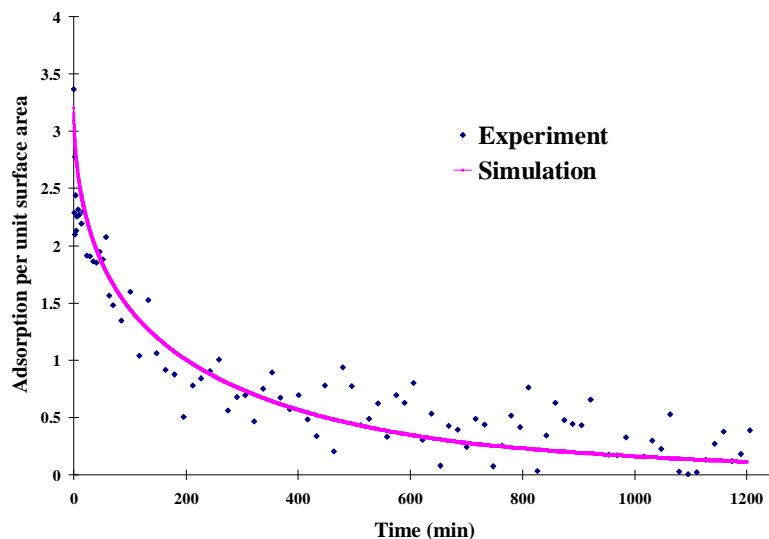


FTIR-MS-LCRDS Characterization

Objective: determine surface ability to concentrate and retain bulk contaminants. Key parameters are specific area, active site density, and surface energetics for selective adsorption



Experimental Method & Typical Results

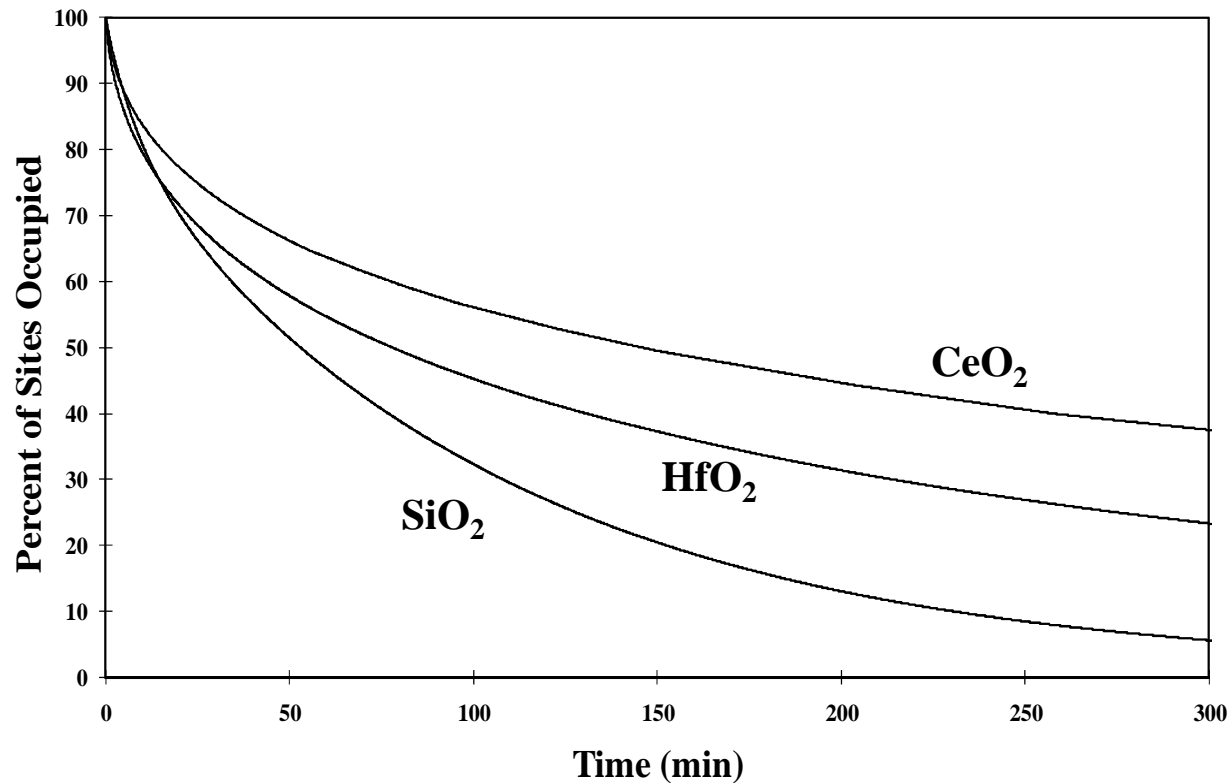


- **Physical adsorption of inert adsorbent (similar to BET isotherm) for area measurement**
- **Chemical adsorption of reactive adsorbent for measuring site density**

- **Temperature-Programmed Interaction (TPI) for measuring site energetics**

Comparison of Surface Activity of Different NP Materials

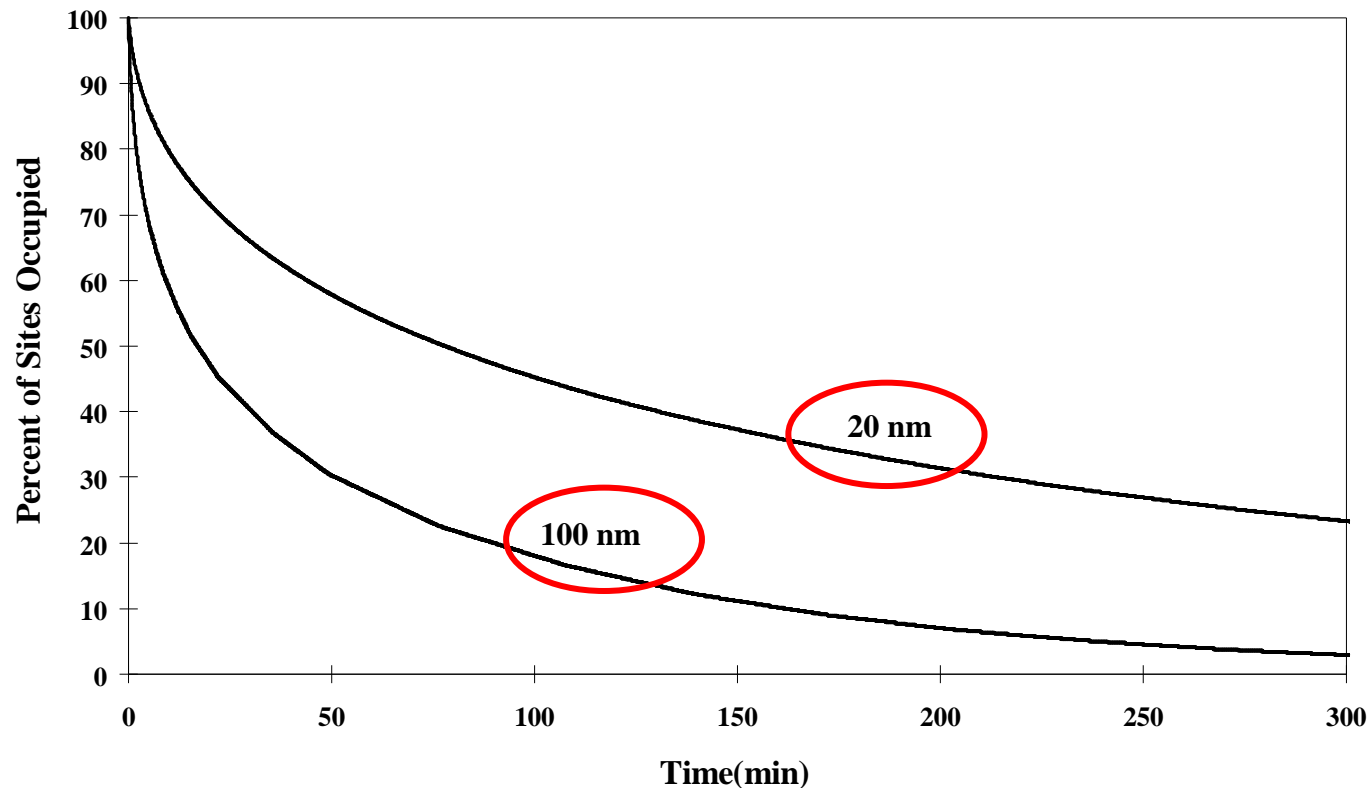
Experimental data using moisture adsorption on 20 nm NPs



Contamination retention is compound dependent: highest for CeO₂ and lowest for SiO₂; adsorption on CeO₂ seems to be strong chemisorption

NPs Retention of Contaminants

Dynamics of Moisture Desorption



Contamination retention of NPs is dependent on NP batch

Note: particle sizes are as reported by the manufacturer – the absolute numbers have been found to be unreliable

Surface Characterization Summary

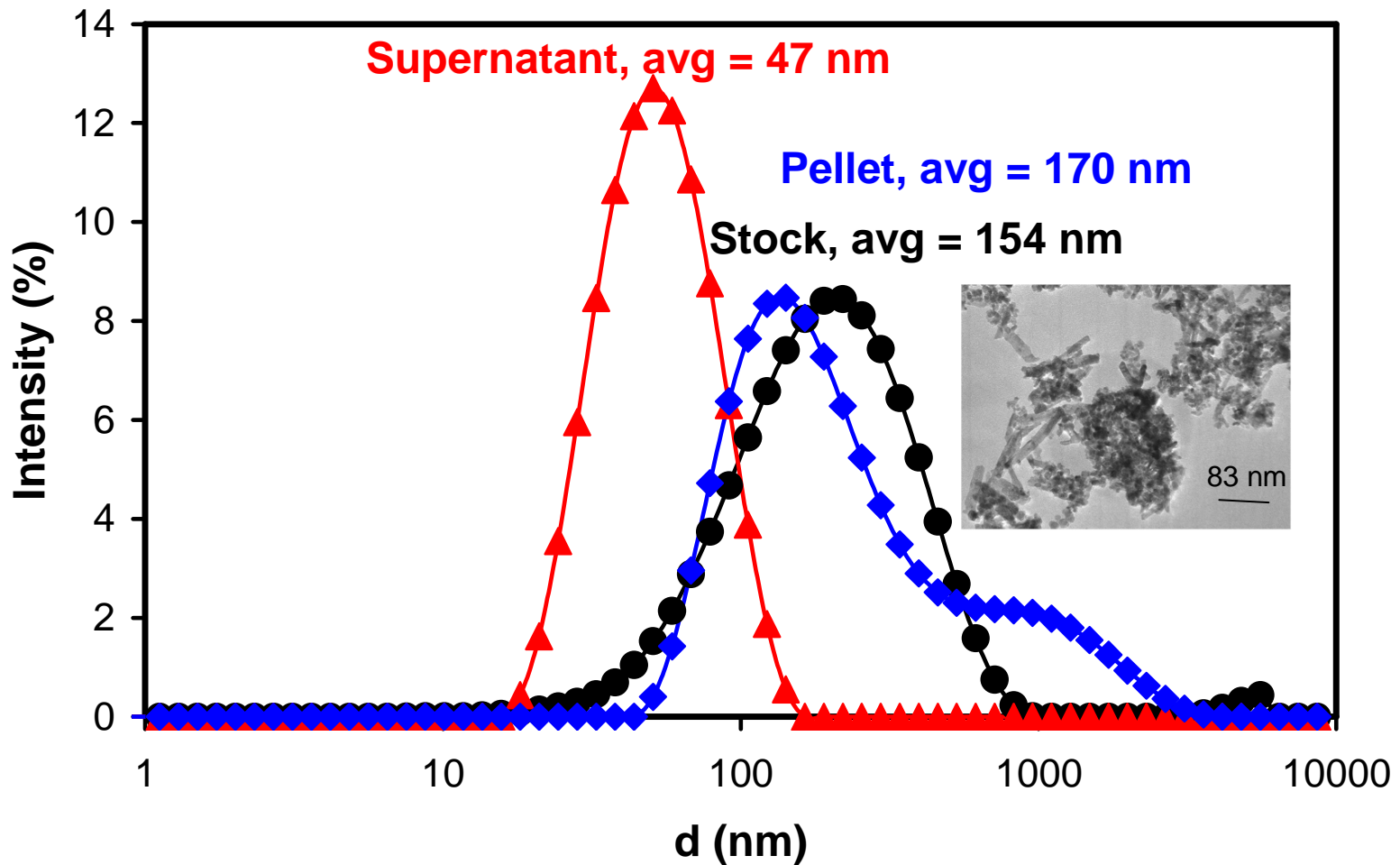
	Particle Size	Adsorption Rate Coeff.	Desorption Rate Coeff.	Active Site Density	Adsorption Capacity
	d_p (nm)	k_a ($\text{cm}^3 \text{ mol}^{-1} \text{ s}^{-1}$)	k_d (s^{-1})	S_0 (mol/cm^2)	C_{s0} (mol/cm^2)
HfO₂	20	3.30E+08	2.4	7.00E-10	6.56E-10
HfO₂	100	8.00E+08	0.8	2.50E-10	2.48E-10
SiO₂	20	5.30E+08	360	2.00E-08	2.74E-09
CeO₂	20	3.00E+08	1	8.75E-10	8.49E-10

- Different batches of HfO₂ particles adsorbed contaminants differently (*higher activation energy*)
- Some particles have higher *capacity* for adsorption and retention of secondary contaminants

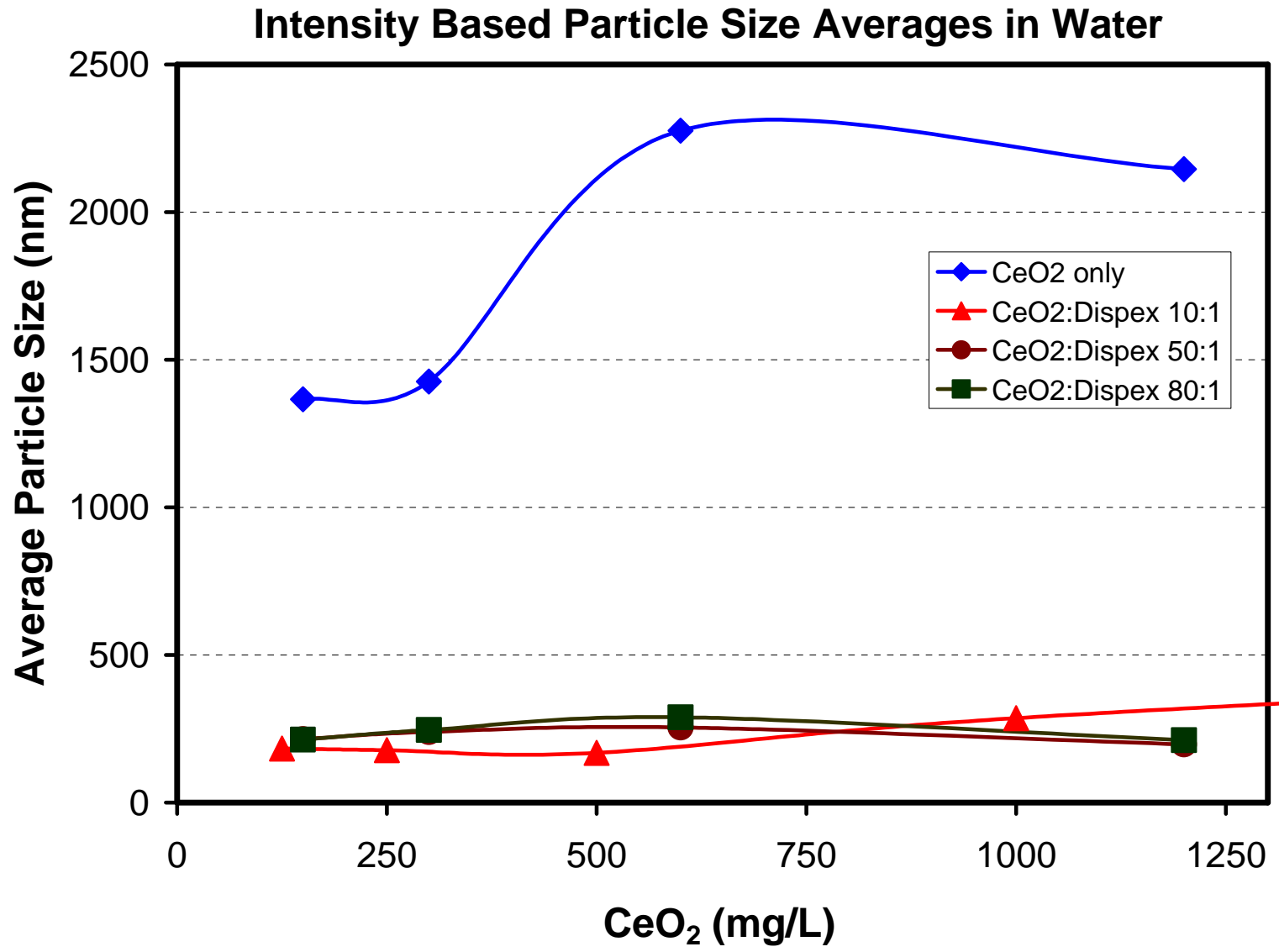
Note: particle sizes are as reported by the manufacturer – the absolute numbers have been found to be unreliable

Fractionation of CeO₂ by Centrifugation

Fractioning CeO₂ 2g/L Eppendorf Centrifuge 4500 rpm



Role of Surfactant Conc. on CeO₂ NP Size



Surface Chemical Characterization

University of Washington has a strong campus resource facility permitting state-of-the-art nanoparticle surface analysis. Instrumentation available includes:

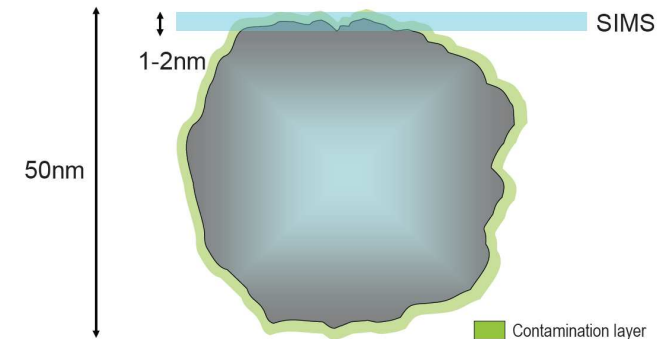
- Electron spectroscopy for chemical analysis (ESCA)
- Secondary ion mass spectrometry (SIMS)
- Surface plasmon resonance (SPR)
- Atomic force microscopy (AFM)
- Sum Frequency Generation (SFG)
- Attenuated Total Reflectance IR (ATR-IR)

Secondary Ion Mass Spectrometry (SIMS)

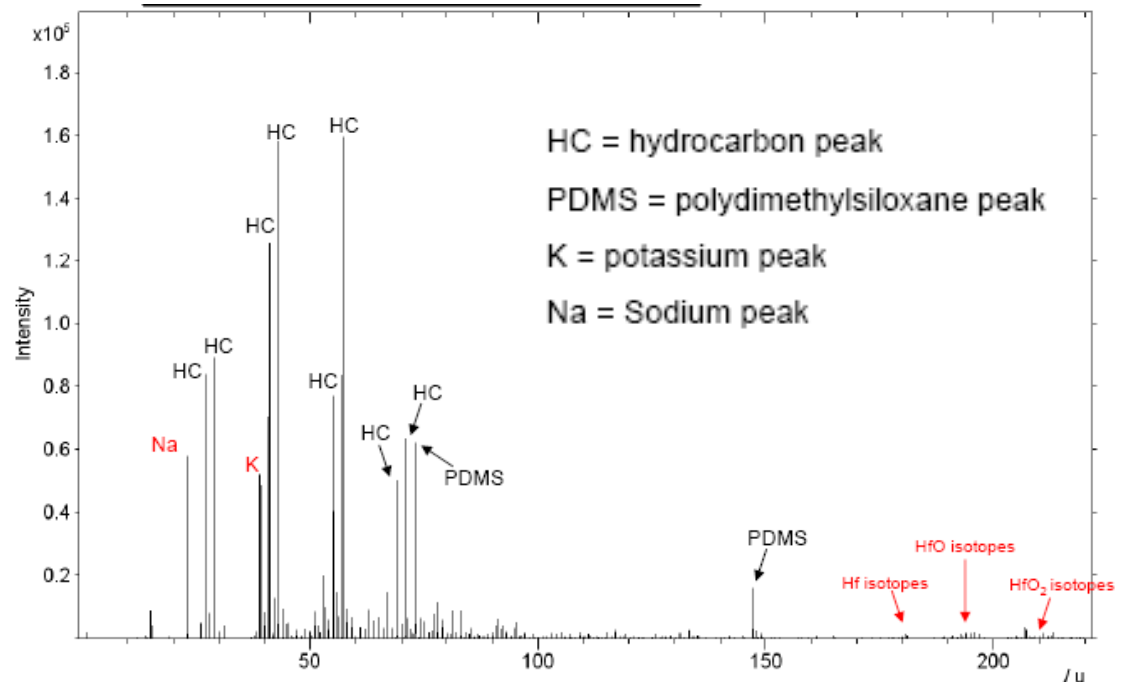
Time-of-flight (ToF) SIMS; Static SIMS



- Probably the most information-rich of the modern surface analysis methods
- Various organic/inorganic contaminants detected on the surface of NPs



- Positive and negative spectra can be used to identify impurities including metals from fabrication or organics from unidentified sources



Nanoparticle Impurities – ToF SIMS

Positive Spectra Impurities

mass	ID	Ref Micron	NP1 20 nm	NP2 1-2 nm	NP3 100 nm
27	Al	+	+		+
28	CH ₂ N	+	++		++
30	CH ₄ N	+	+		+
40	Ca	++			+
45	C ₂ H ₅ O	++		++	+
46	C ₂ H ₆ O	+		+	+
52	C ₃ H ₂ N		+		+
55	Fe	+			+
58	Ni		+		
78	C ₂ H ₆ O ₃		+		
90	Zr	++	+		+
118	C ₅ H ₁₂ NO ₂	+		+	+
135	C ₉ H ₁₁ O	++		++	+
161	C ₁₁ H ₁₃ O	++		+++	+

Note: particle sizes are as reported by the manufacturer – the absolute numbers have been found to be unreliable

“+” represents presence of listed fragment. “++” and “+++” are used to indicate relative amounts of listed fragments within row and cannot be used to compare rows one to another.

Nanoparticle Impurities – ToF SIMS

Negative Spectra Impurities

mass	ID	Ref Micron	NP1 20 nm	NP2 1-2 nm	NP3 100 nm
19	F	+++	+	++	++
26	CN	+	++		+
31	P		+		
35	Cl	+++	+	+	++
47	PO	+	++		
51	CIO	+			
59	C ₂ H ₃ O ₂	+		++	
78	C ₃ H ₇ OF		+		
78.96	PO ₃		+		
78.92	⁷⁹ Br	+	++		
81	⁸¹ Br	+	++		
104	C ₃ H ₈ N ₂ O ₂		+		
127	I	+			
205	C ₁₃ H ₁₉ NO			+	

Note: particle sizes are as reported by the manufacturer – the absolute numbers have been found to be unreliable

“+” represents presence of listed fragment. “++” and “+++” are used to indicate relative amounts of listed fragments within row and cannot be used to compare rows one to another.

SRC/Sematech Engineering Research Center for Environmentally Benign Semiconductor Manufacturing

Surface Characterization

Summary/Preliminary Conclusions

SIMS Analysis

Impurity	Ref Micro	NP1 20 nm	NP2 1-2 nm	NP3 100 nm
Light Organics (<100 MW)	+	+	+	+
Heavy Organics (>100 MW)			+	
Silicon	+		+	
Chlorine	+	+		+
Bromine		+		
Rare Earth Metals	+	+	+	

Note: particle sizes are as reported by the manufacturer – the absolute numbers have been found to be unreliable

University of Washington surface
characterization is now expanding its efforts to:

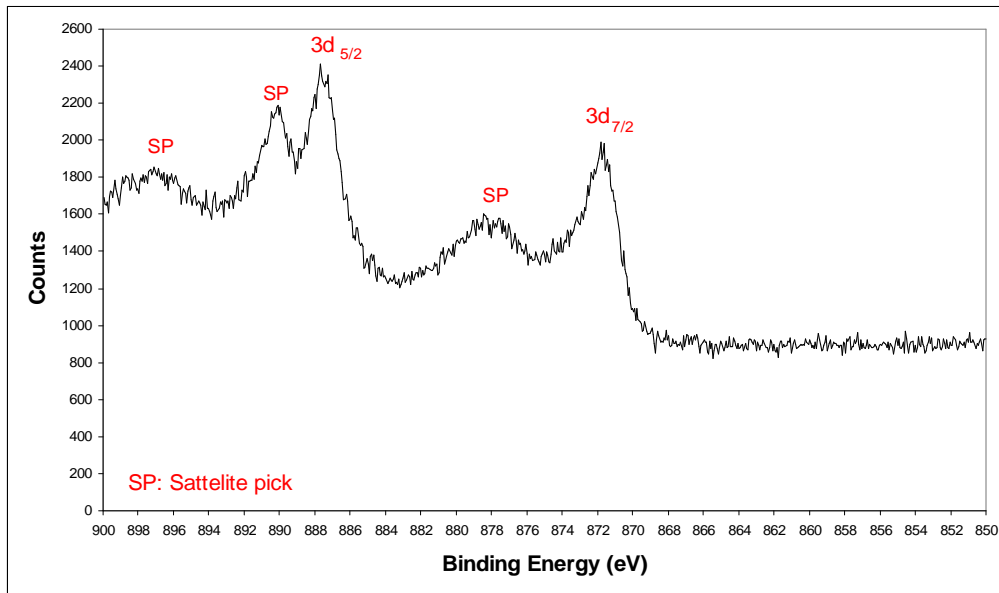
Cerium

Silica

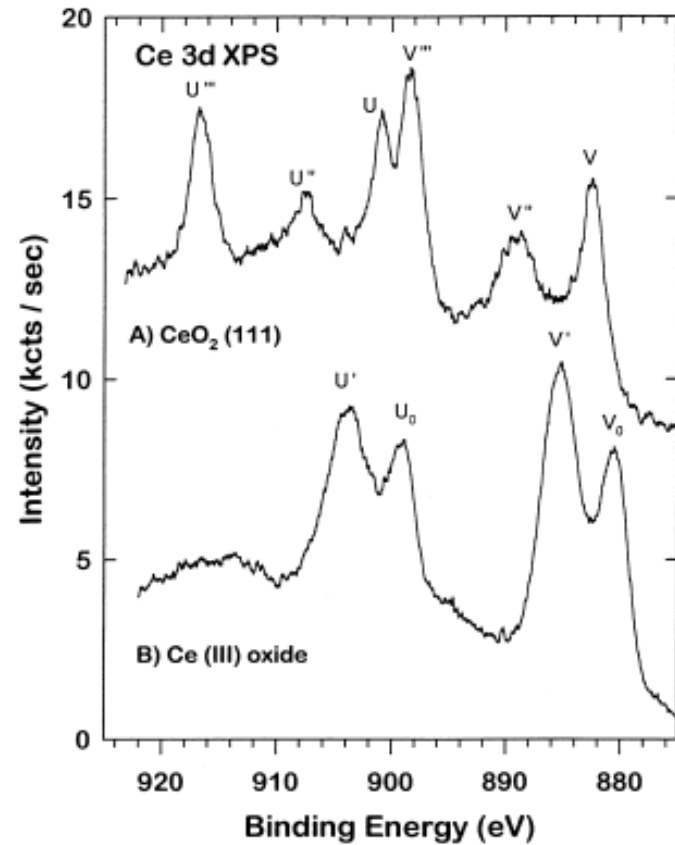
Titanium

*Nanoparticles relevant to the interests of the
semiconductor industry*

CeO₂ core level XPS spectra comparison



High resolution XPS spectra of catechol treated CeO₂

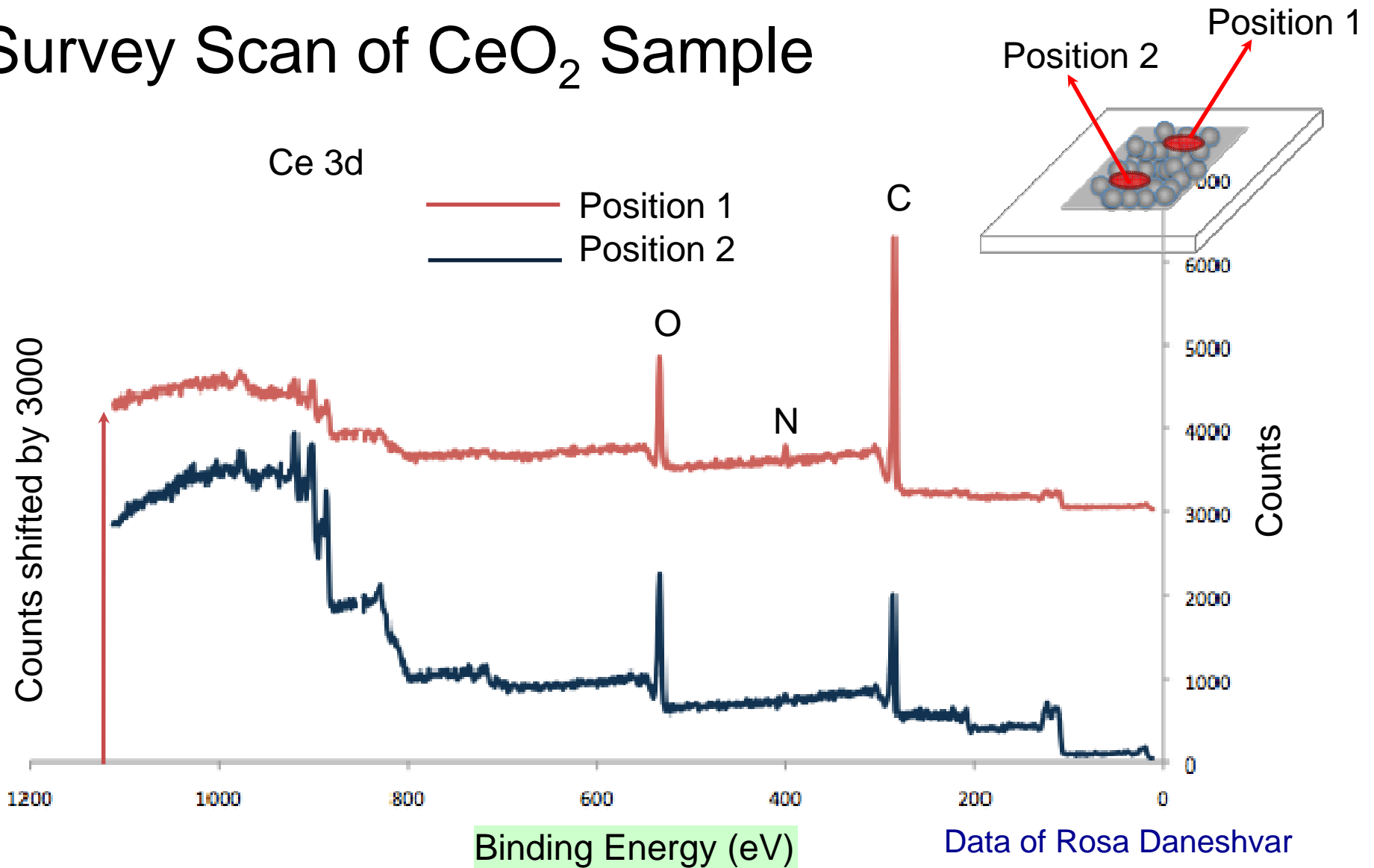


Ce 3d core level photoemission

spectra from (A) CeO₂ (111), (B) Ce (III)

* D.R. Mullins, S.H. Overbury, D. R. Huntley. Surface Science 409 (1998) 307-319.

Survey Scan of CeO₂ Sample



C, O, N, Ce are present on the surface of the sample; Contamination is not homogenous

SRC/Sematech Engineering Research Center for Environmentally Benign Semiconductor Manufacturing

Development of Quantitative Structure-Activity Relationship for Prediction of Biological Effects of Nanoparticles Associated with Semiconductor Industries *(Task Number: 425.025)*

PIs:

- **Yongsheng Chen, Environmental Engineering, Georgia Institute of Technology (GIT)**

Graduate Students:

- **Wen Zhang: PhD student, Environmental Engineering, GIT**
- **Steven Klein: PhD student, Mechanical engineering, ASU**

Other Researchers:

- **Trevor J. Thornton, Electric Engineering, ASU**
- **Jonathan Posner, Mechanical Engineering, ASU**

Cost Share (other than core ERC funding):

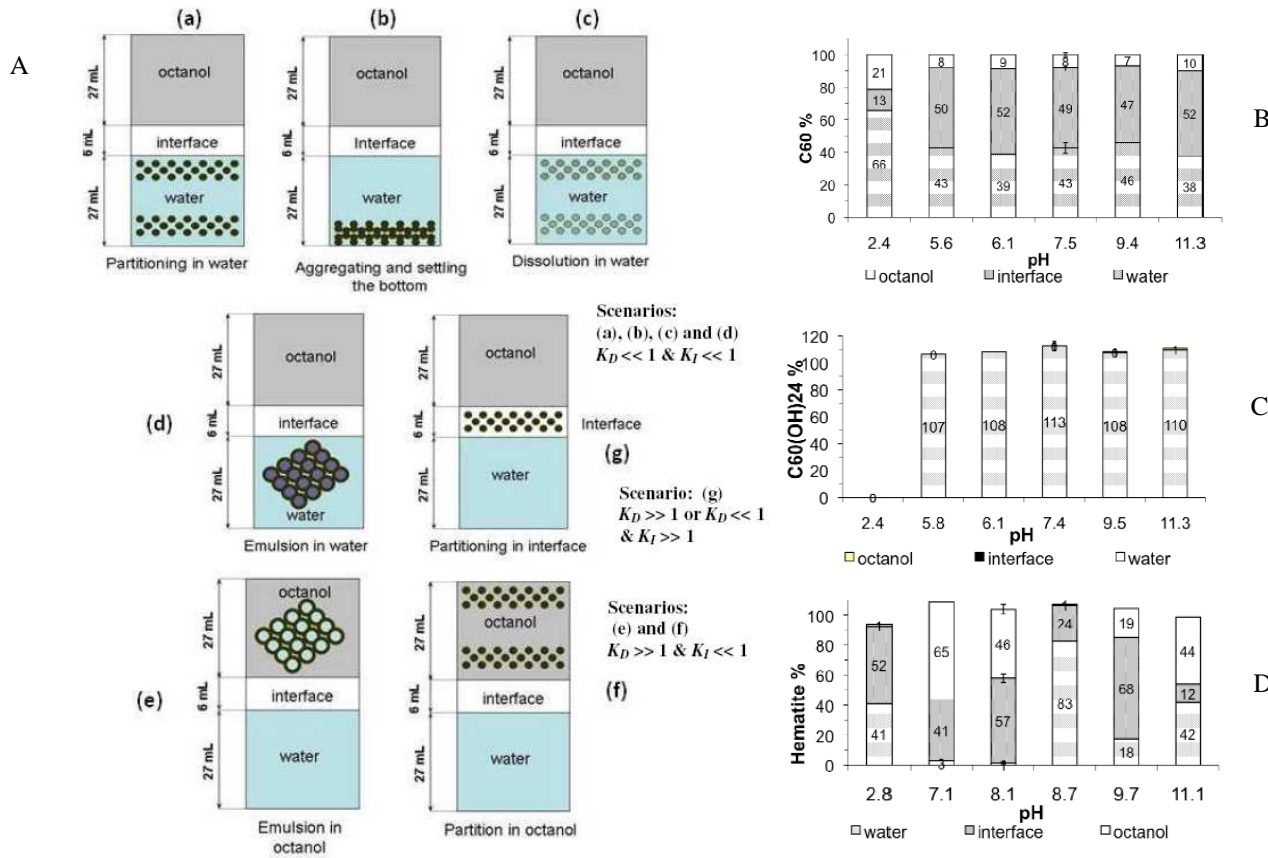
- **\$25 k start-up fund from ASU**
- **\$152k funds from GIT for AFM and other lab instrument purchase**

Objectives

Develop a quantitative structure-activity relationships (QSARs) model for prediction of the biological effects of engineered nanoparticles (NPs) associated with semiconductor industries. To pursue this goal, our approach mainly includes:

- Development of new surrogate descriptors (relative to those for conventional contaminants) for NPs and Methodology development of experimental measurement.**
- Correlation of the descriptors with their environmental behaviors and impact.**

Bias of traditional descriptors for NPs: study of octanol-water partitioning coefficients (K_{ow})

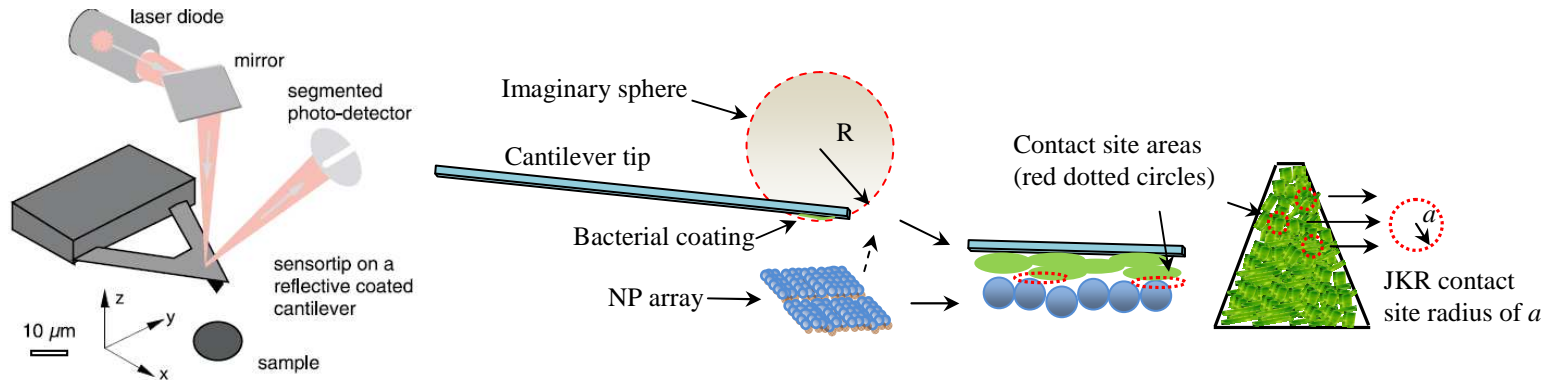


Findings: NPs display complex partitioning scenarios (into the octanol phase, water phase, and interface), and pH/ionic strength/presence of natural organic matter all can alter the partitioning state due to uncontrollable mechanisms (e.g., aggregation/dissociation leads to size differences under a wide range of pH or ionic strengths).

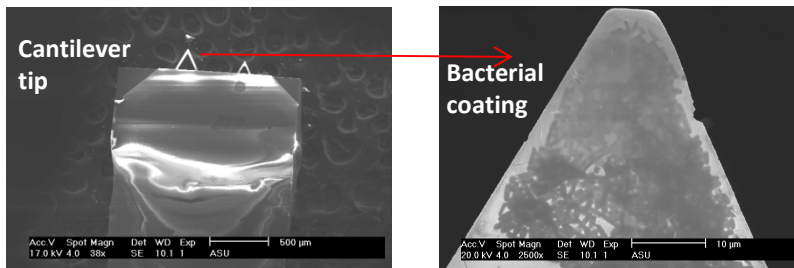
A: Boundary partitioning scenarios (a~g) of nanoparticles in the octanol and aqueous phases and the interface. B: Partitioning of n-C₆₀, C: n-C₆₀(OH)₂₄ D: hematite nanoparticles in the interface, octanol, and aqueous phases at different pH values in the presence of 1 mM NaHCO₃ buffer.

Method and materials: New descriptor development

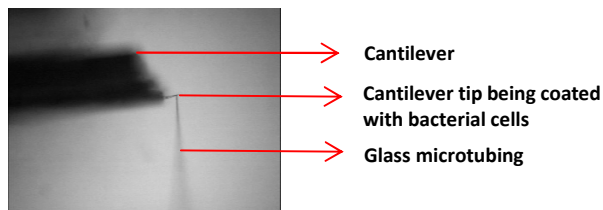
1. Adhesion force measurement with AFM



Demonstrations of adhesion force measurement with AFM and determination of contact area with JKR model. Cantilever probe coated with bacterial cells is approaching to NP array and the contact surface of the probe is assumed to be a part of the surface on the imaginary sphere (R). Multiple contact sites (indicated by the red circles) between bacteria and NPs add up to a total contact site area of πa^2 .

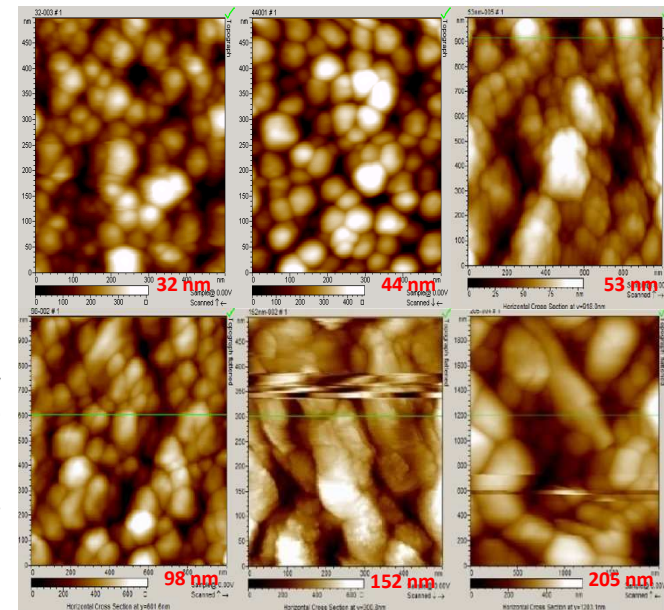


Coating process with micromanipulator



Images of NP array achieved by tapping mode AFM:

NP array composed of NPs (different sizes were determined by Malvern Zetasizer)

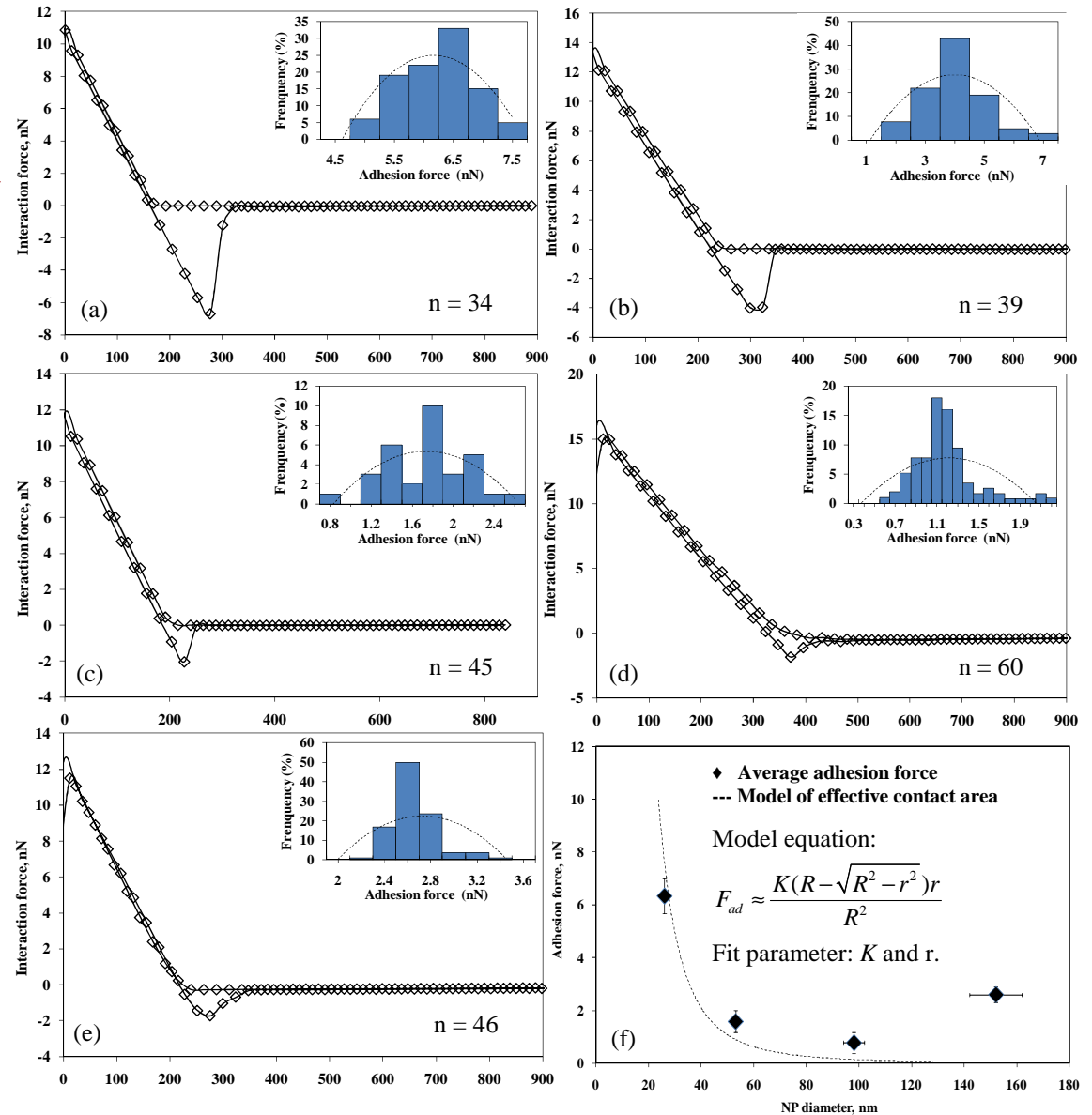


Results and discussion:

1.1 Size effect on Adhesion force between *E. coli* cells and hematite NPs

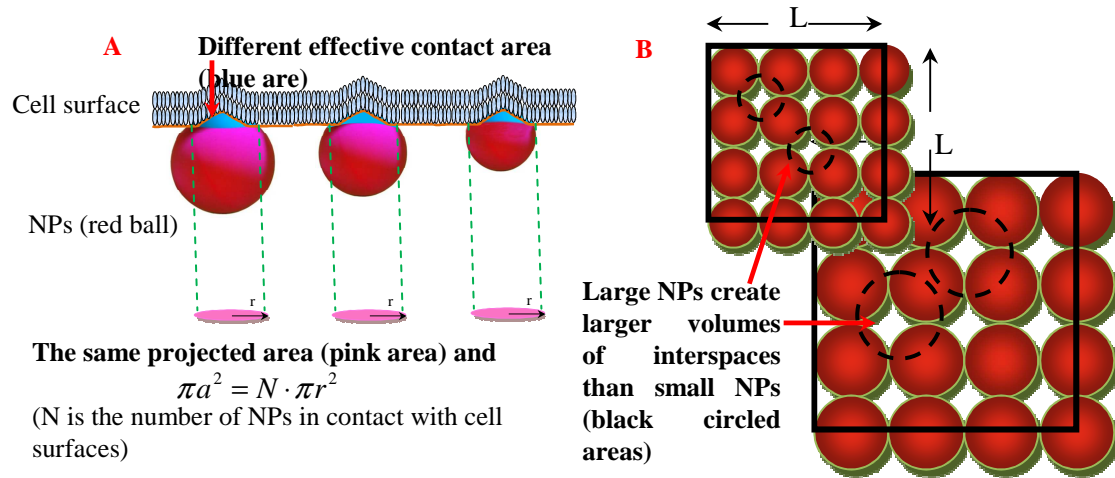
Representative interaction force-distance curves for different sizes of NP array probed by *E. coli* cells. (a) 26 nm. (b) 44 nm. (c) 53 nm. (d) 98 nm. (e) 152 nm. (f) Average adhesion force for different sizes of NPs (horizontal error bars indicate standard deviation of particle diameter and vertical error bars indicate standard deviation of adhesion force). n is the number of force measurements for each sample.

Significance: Adhesion forces between *E. coli* cells and hematite NPs decreased as particle size increased as Figure 3 showed and our model of the effective contact area fitted the trend.



Results and discussion:

1.2 Modeling Size effect on Adhesion force and validation

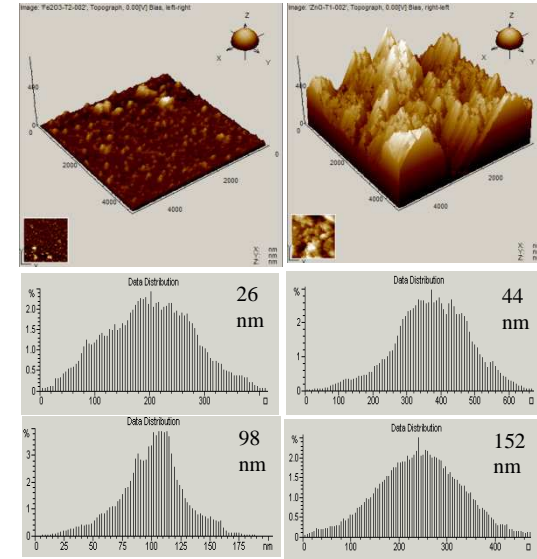


Schematics of modeling the size effect of NPs on adhesion force.

Brief introduction to our proposed model of effective contact area used for explaining the size effect on adhesion force:

$$\left. \begin{aligned}
 F_{ad} &\propto \int_0^{R-\sqrt{R^2-r^2}} 2\pi \sqrt{R^2 - (\sqrt{R^2-r^2} + x)^2} dx \\
 V &= N \times [(2R)^3 - (4\pi R^3/3)]/2 = L \times (4-2\pi/3)R^2 \\
 F_{ad} &\propto 1/V
 \end{aligned} \right\} F_{ad} = K \int_0^{R-\sqrt{R^2-r^2}} \frac{\sqrt{R^2 - (\sqrt{R^2-r^2} + x)^2}}{R^2} dx \approx \frac{K(R-\sqrt{R^2-r^2})r}{R^2} \Rightarrow F_{ad} \propto \frac{Kr}{R}$$

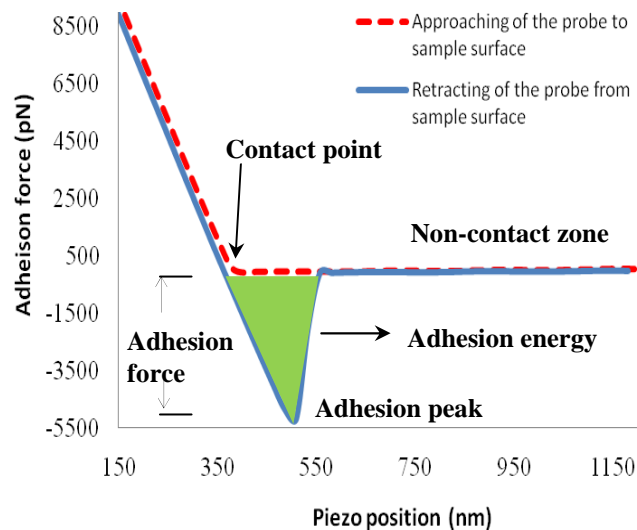
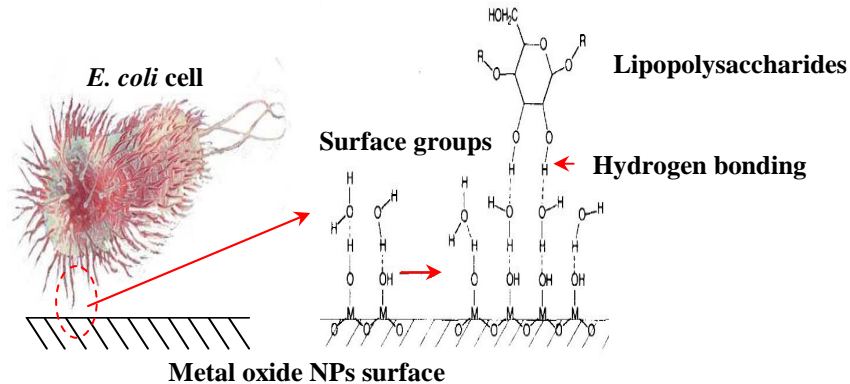
Validations were made between *E. coli* cells and Al₂O₃ NPs, and between Caco-2 cells (human intestinal cells) and hematite NPs. For detailed information, refer to our manuscript.



Surface topography and surface height distribution

Results and discussion:

1.3 Hydrogen bond estimation with force-distance curve and its support of our model of size effect



Adhesion energy and hydrogen bond calculation

Adhesion energy and hydrogen bond number

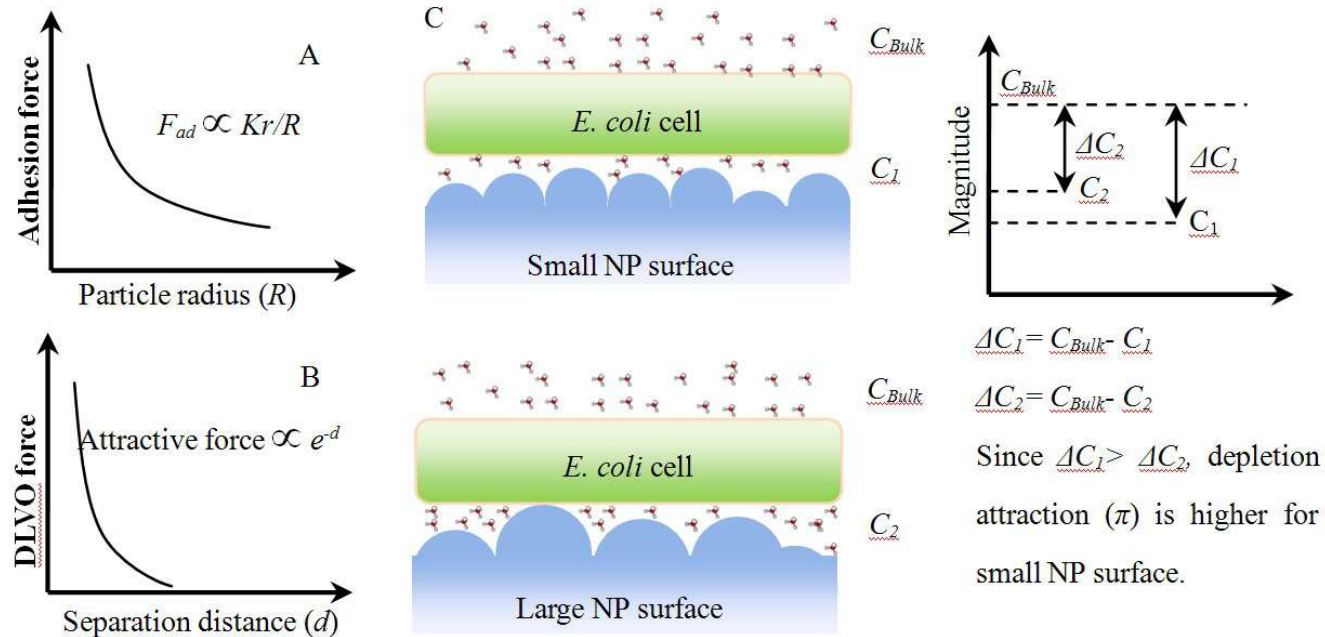
NP diameter (nm)	Adhesion energy (J)	Hydrogen bond number on contact site area
Hematite NPs	23	$(8.5 \pm 1.7) \times 10^4$
	42	$(7.7 \pm 2.2) \times 10^4$
	53	$(1.0 \pm 2.6) \times 10^4$
	98	$(3.7 \pm 2.0) \times 10^3$
	150	$(3.6 \pm 1.2) \times 10^3$
Al ₂ O ₃ NPs	25*	$(6.5 \pm 1.7) \times 10^4$
	30-40*	$(3.2 \pm 1.7) \times 10^4$
	40-80*	$(1.2 \pm 1.7) \times 10^4$
	100-120*	$(7.3 \pm 1.7) \times 10^3$

The surface of an *E. coli* cell (average cell surface area is $6 \times 10^{-12} \text{ m}^2$) contains about 3.5×10^6 LPS molecules that can form hydrogen bonds with a mineral oxide surface. The contact site area between hematite NP array and *E. coli* cells is about 6359 nm^2 ($=\pi \cdot 45^2$, estimated by JKR model). Thus, the average number of hydrogen bonds formed is 3709 ($=6359 \times 10^{-18} \text{ m}^2 \times 3.5 \times 10^6 / 6 \times 10^{-12} \text{ m}^2$).

Implications: NP arrays of small NPs may have a much higher contact area than large NPs.

Results and discussion:

1.4 Other mechanisms involved in adhesion that may explain the size effect

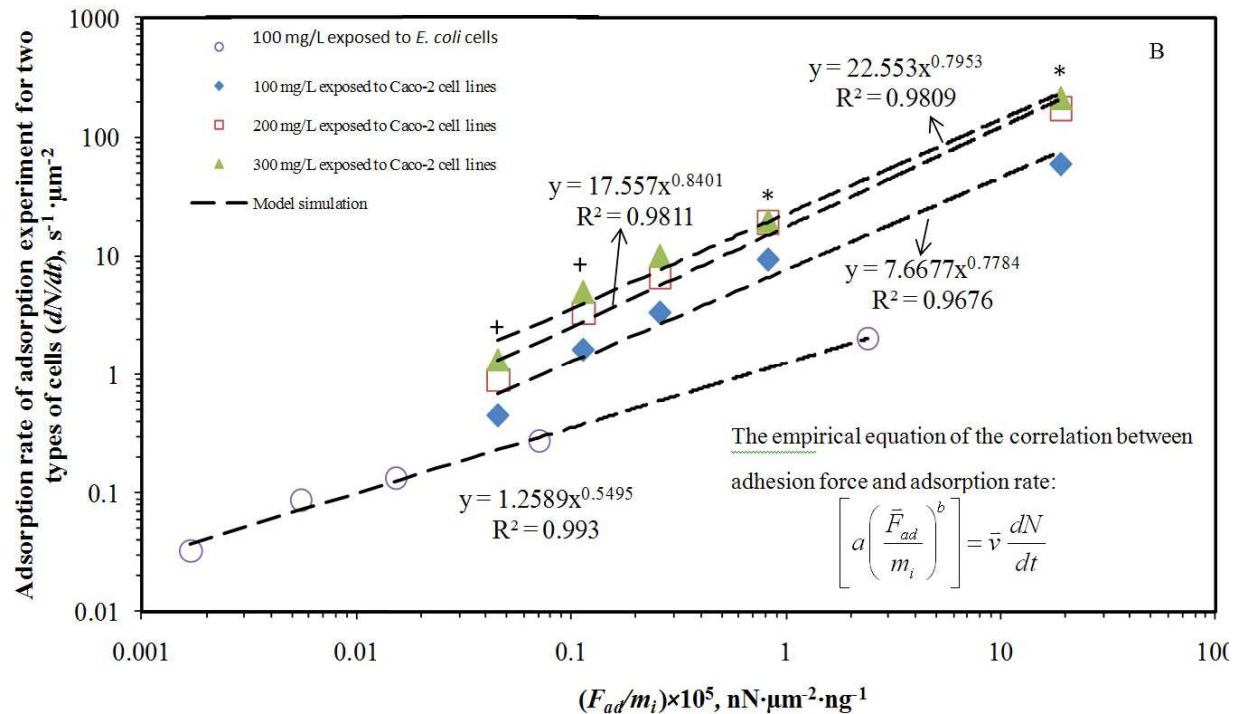


Representation of potential mechanism of size effect on adhesion force. A. Relationship between adhesion force (F_{ad}) and particle radius (R). B. Exponential decay of DLVO forces with distance. C. Depletion attraction (potentially different for cell surface interacting with different sizes of NPs).

Implication: a combined effect of three potential mechanisms were proposed to account for the size effect on adhesion force between NPs and cell surfaces, including the effective contact area, topographical effects on interfacial energy, and depletion attraction.

Results and discussion:

1.5 Correlation between adhesion force and adsorption rate of NPs toward cell surfaces

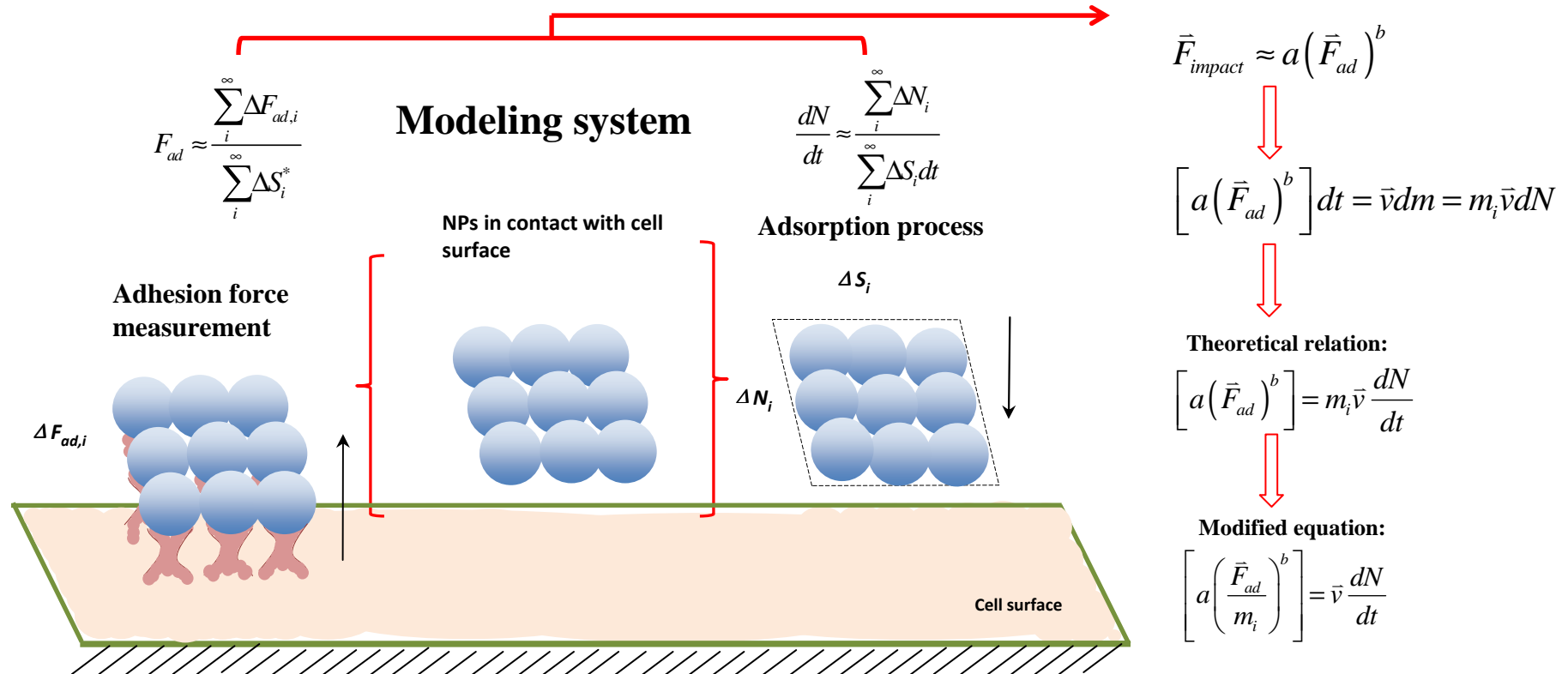


Comparison of the model simulation (dotted line) and experimental data. Symbols (* and +) indicate a significant difference ($p < 0.05$) between the groups of three points marked by (+) and those groups marked by (*).

Significance: an important interconnection between adhesion force and adsorption rate of NPs onto the cell surface was established and the theoretical relationship can be derived mathematically from the conceptual model in the next slide.

Results and discussion:

1.5 Correlation between adhesion force and adsorption rate of NPs toward cell surfaces

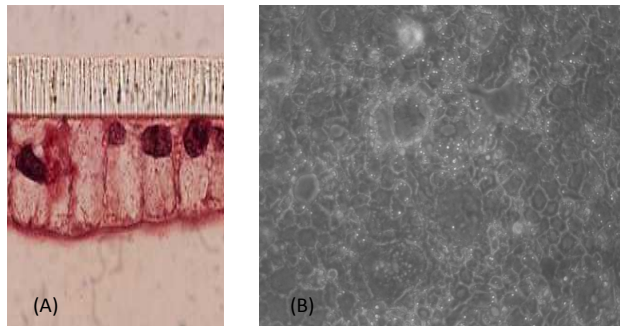


Conceptual model of the relation between adhesion force and adsorption rate (dN/dt).

This model was derived based on the impulse-momentum theorem and the relationship between the impact force and the resulted adhesion force. The above theoretical relationship between adhesion force and adsorption rate has the following parameters: m_i is the mass of a single NP; v is the approach speed of the cantilever tip toward the cells; a and b is the fit parameters.

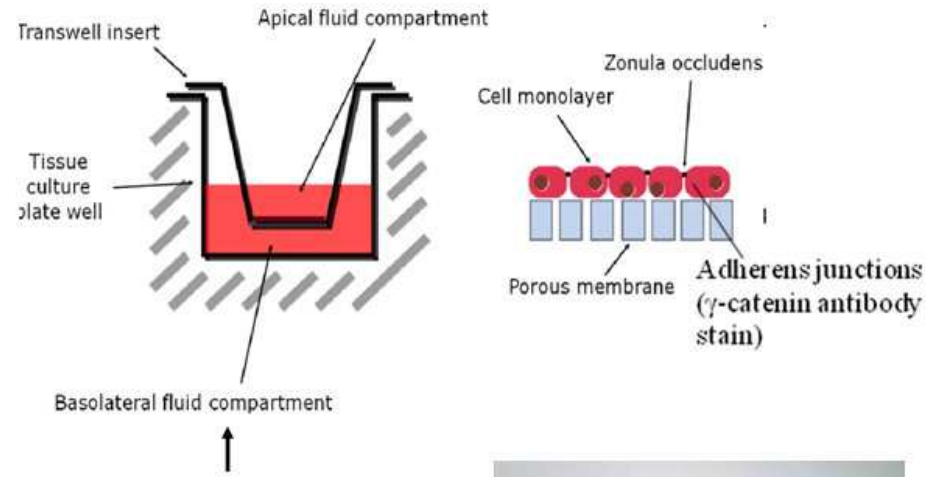
Method and materials:

2. Cytotoxicity of hematite NPs on Caco-2 cells: size effect



Microscopic images and structures of Caco-2 cells. (a): Side view of the cell lines; (b): phase contrast image for Caco-2 cell lines. The bottom drawing indicates the surface structure (microvilli) of the cell line.

Cytotoxicity was shown by junctional disruption of the cell lines and quantified with transepithelial electrical resistance (TEER). Cell penetration of NPs was visualized by confocal imaging.



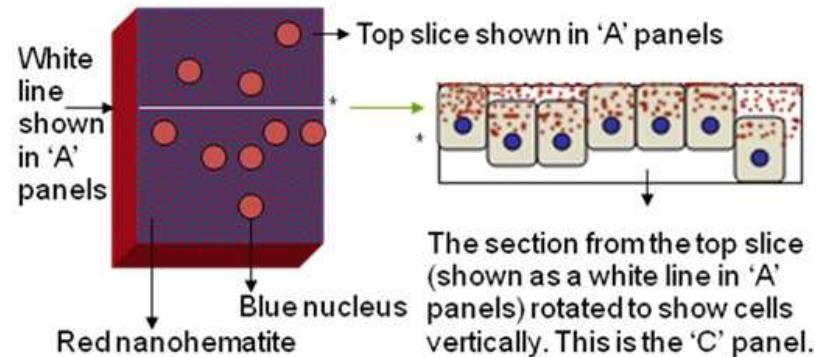
The first step: cell lines growth on the semi-porous membranes;

The second step: measure TEER after the exposure to NPs;

The third step: Imaging of cell structures with confocal microscopy at different profiles

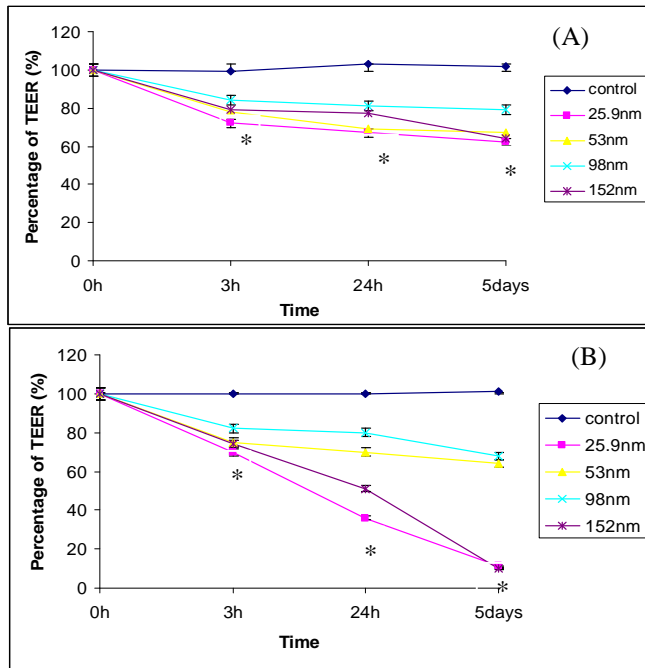


Z-Series stack

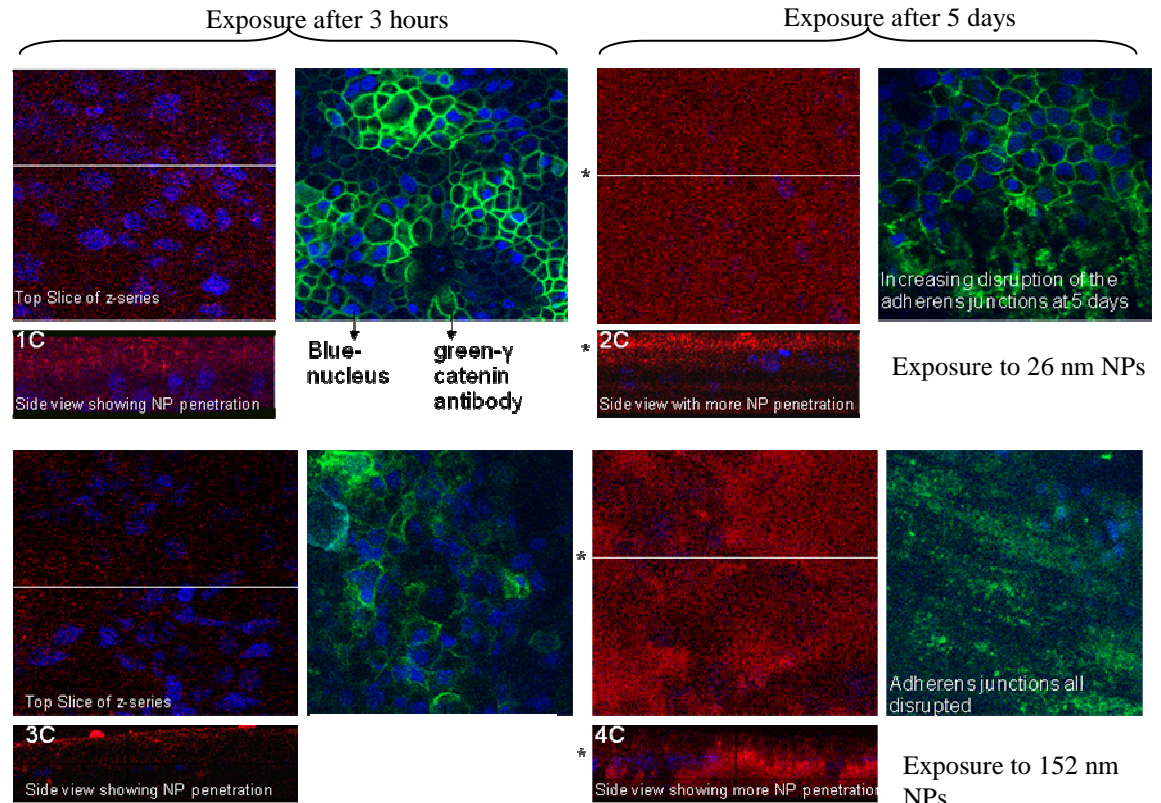


Schematics of cytotoxicity experiments with Caco-2 cells through TEER test and confocal microscopy

Results and discussion: TEER changes and junctional disruption induced by the exposure to NPs



Caco-2 epithelial cells treated with 100 mg/L (A) and 300 mg/L (B) of various sizes of hematite NPs. Error bars represent mean \pm SD (n=3), some of them may be obscured by the data marker; * = $p < 0.002$ when compared to Control (Caco-2 cells without any added hematite NPs).



Representative confocal images of junctional changes of Caco-2 cells exposed to 26 nm and 152 nm hematite NPs. The important panels to consider are 3C and 4C. In these panels the red is the hematite NPs and blue color is the nucleus of a Caco-2 cell (refer to the picture of the cell in slide 2). The 3 panels show the penetration of NPs into cells at the specific time point and concentration tested. The nucleus for Caco-2 cells is toward the lower half of a cell, so NPs above the nucleus means NPs are inside the cell.

Future Plans

Next Year Plans

- Cell penetration of NPs and the governing factors
- Interactions between various NPs and representative human proteins such as biotinylated bovine serum albumin(biotin-BSA)
- The effects of environmental parameters (e.g., pH) on the interactions of NPs with

Long-Term Plans

- Build robust QSAR models based on fundamental data of adhesion force and its predicting impact on cells
- Provide information for manufacturing environmental benign NPs for industries.

Low ESH-impact Gate Stack Fabrication by Selective Surface Chemistry

Project 425.026

Shawn Miller and Anthony Muscat
Department of Chemical and Environmental Engineering
University of Arizona, Tucson, AZ 85721



ERC Review Meeting
Feb 18-19, 2010
Tucson, AZ

Industrial partners:
Sematech
ASM

SRC/Sematech Engineering Research Center for Environmentally Benign Semiconductor Manufacturing

Low ESH-impact Gate Stack Fabrication **by Selective Surface Chemistry**

(Task Number: 425.026)

PI:

- **Anthony Muscat, Chemical and Environmental Engineering, UA**

Graduate Students:

- **Shawn Miller, MS candidate, Optical Science and Engineering, UA**

Cost Share (other than core ERC funding):

- **ASM**

Industrial Interactions and Technology Transfer

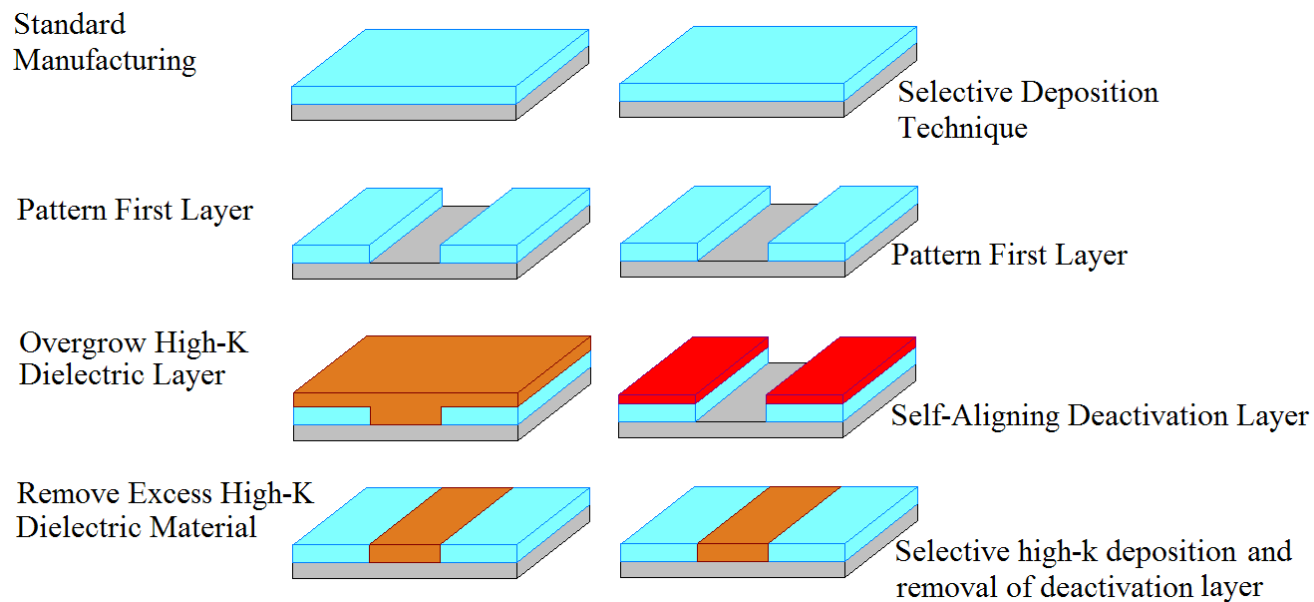
- **Biweekly project updates to ASM**

Mentors

- **Joel M. Barnett, SEMATECH**
- **Willy Rachmady, Intel**

Objectives

- **Simplify multistep subtractive processing used in microelectronic device manufacturing**
 - Develop new processes that can be integrated into current devices flows
 - Minimize water, energy, chemical, and materials consumption
 - Reduce costs
- **Focus on high-k gate stack testbed**
 - Fabricate low defect high-k/semiconductor interfaces



ESH Metrics and Impact: Cost Reduction

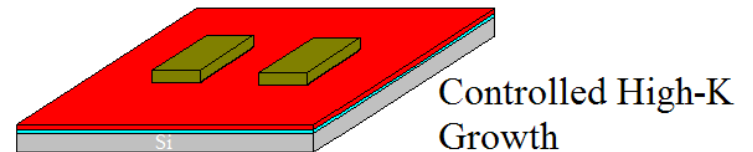
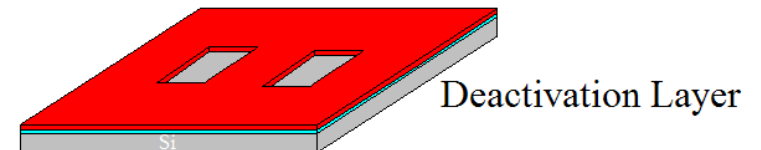
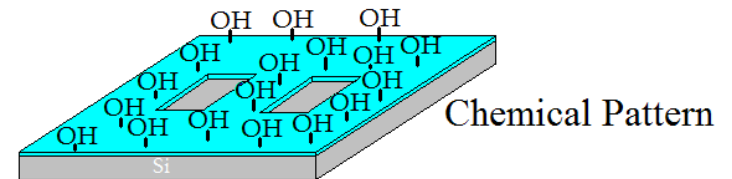
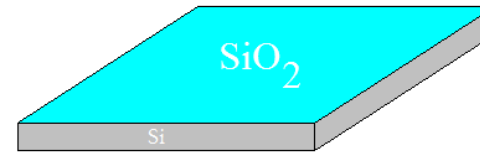
- Integration of selective deposition processes into current front end process flow could reduce ~16% of the processing costs
 - Calculation based on Sematech cost model
 - Eliminate eight processing steps from the gate module
 - Tool depreciation, tool maintenance, direct personnel, indirect personnel, direct space, indirect space, direct material, and indirect material were included
 - Energy, waste disposal, and addition of two selective deposition steps were not included
- There is potential for greater ESH benefit due to minimized cost of raw materials and waste generated

Novelty

- Develop industrially feasible processes to activate and deactivate surfaces
 - Significantly lower time scale
 - Extend to metal and semiconductor surfaces
- Integrate selective deposition steps at carefully chosen points in the CMOS process flow
 - Realize ESH and technical performance gains
- Quantify costs associated with selective deposition steps to refine industry models
 - Account for energy and waste disposal
 - More accurate prediction of the cost model

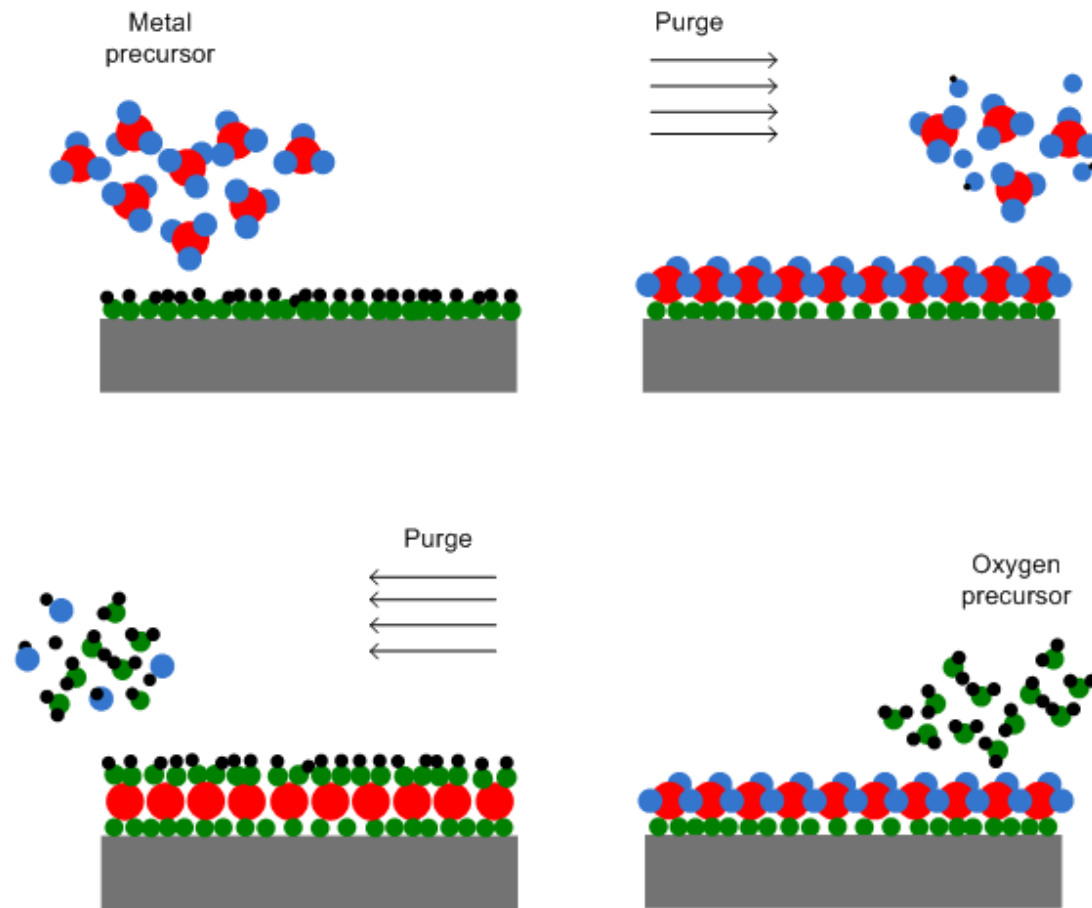
Methods and Approach

- Grow high-k films on semiconductors by activation and deactivation of surface sites
- Activation
 - Utilize surface chemistries to activate substrates for high-k film growth
 - Halogen, amine terminations
- Deactivation
 - Hydrophobic self assembled monolayer (SAM)
 - Prevents adsorption of H_2O
 - Prevents reaction of metal precursor
- Model systems
 - Si, Ge, and III-V substrates
 - High-k films by atomic layer deposition (ALD)
 - Al_2O_3
 - TiO_2



Atomic Layer Deposition of High-k Films

- Break overall reaction into two half reactions and run one at a time to achieve self-limiting growth
 - Surfaces exposed to sequential pulses of metal and oxygen precursors to deposit oxide

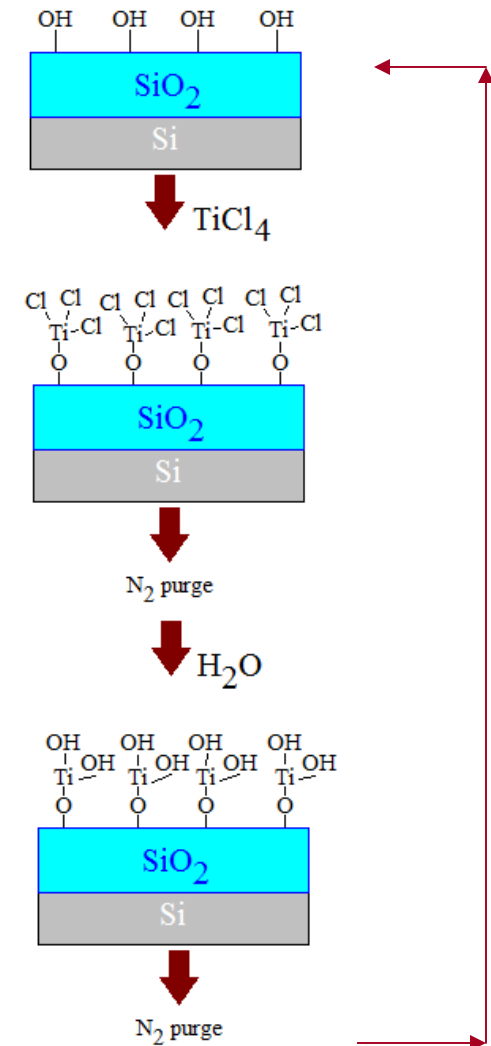


ALD Reaction Mechanism

- Factors governing the selective deposition of high-k film
 - Surface conditioning
 - Precursor selection
 - Deposition conditions
- Hydroxylated surface promotes high-k growth on Si
- Two half reaction in TiO_2 deposition

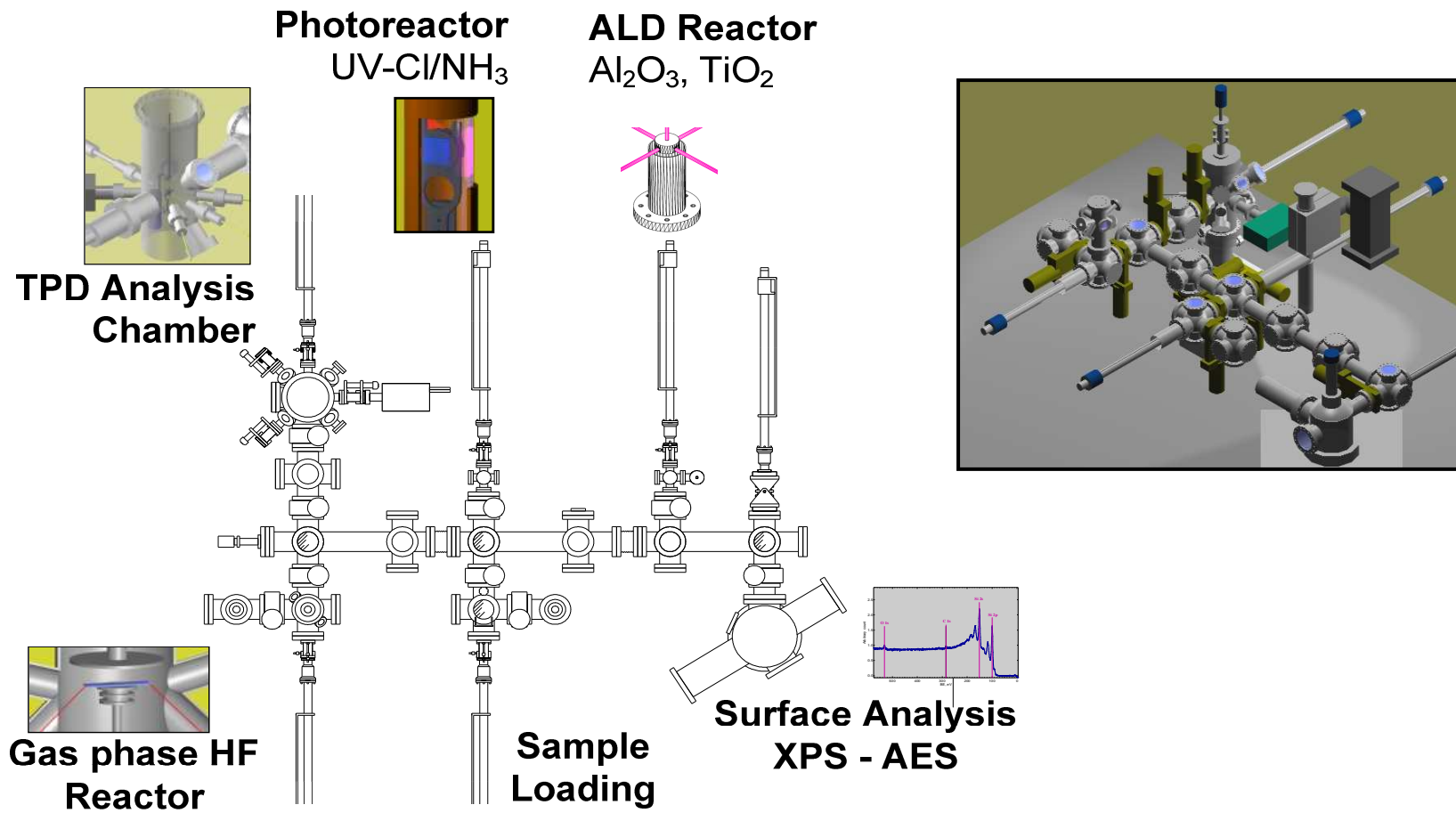
$$\text{TiCl}_{4(g)} + \text{-OH} \rightarrow \text{-O-TiCl}_3 + \text{HCl}_{(g)}$$

$$2 \text{H}_2\text{O}_{(g)} + \text{-O-TiCl}_3 \rightarrow \text{-O-Ti-OH} + 3 \text{HCl}_{(g)}$$
- Deposition mechanism using TiCl_4 precursor could be used as a model for HfCl_4 precursor



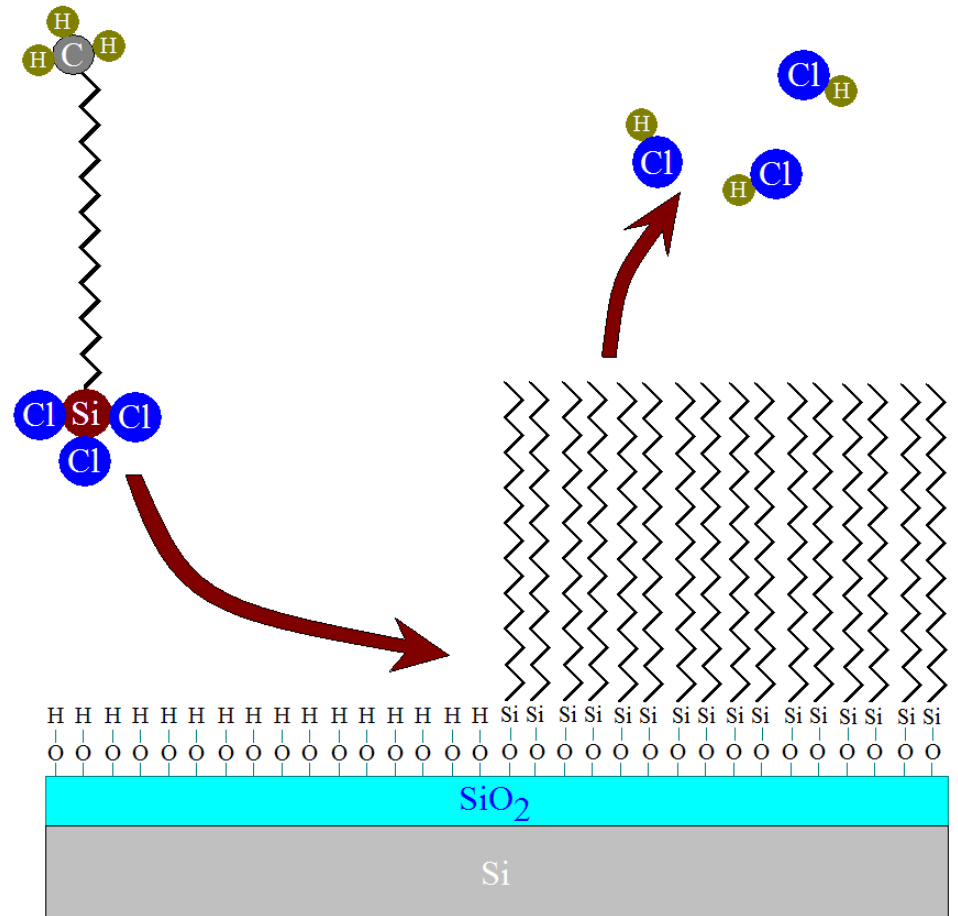
Clustered Reactor Apparatus

- In situ cleaning, high-k deposition, and surface analysis enables studies of surfaces without atmospheric contamination
 - Important for highly reactive substrate such as III-V materials



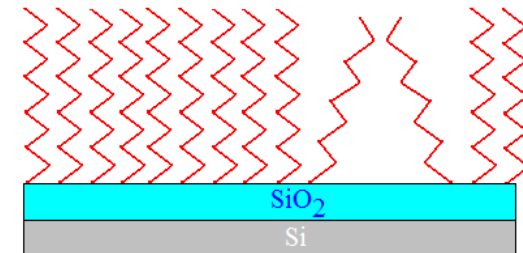
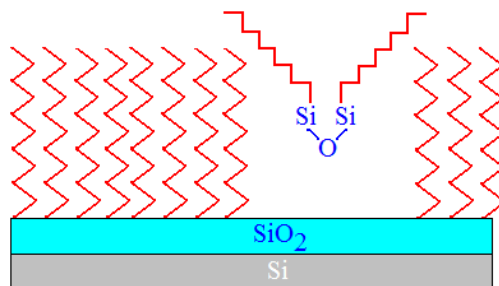
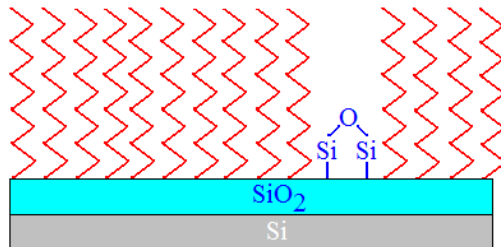
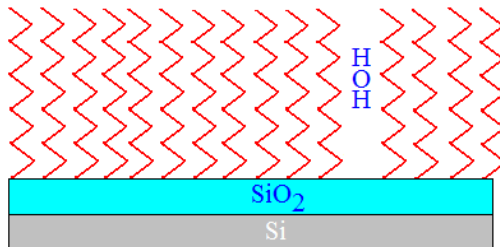
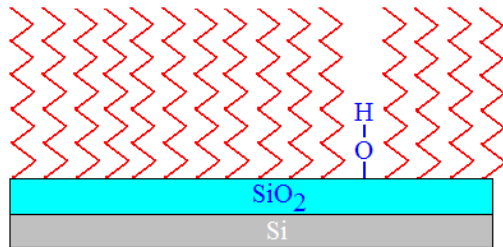
Deactivation using SAM Chemicals

- Octadecyltrichlorosilane
 - OTS
 - $C_{18}H_{37}Cl_3Si$
 - Molecular length 26Å
- OTS SAM layer
 - Formed on piranha etched SiO_2 ¹⁻⁷
 - 48hrs in 10mM OTS in toluene^{2-4,6}
 - 26Å Thickness¹⁻⁶
 - 110° water contact angle¹⁻⁶
 - Deactivates for 50 ALD cycles of $HfCl_4$ or $Hf[N(CH_3)_2]_4$ and H_2O ²⁻⁵
 - Longer deactivation for larger metal precursors such as $CH_3C_5H_4Pt(CH_3)_3$ or $Ir(acac)_3$ ^{2,7}



- 1) J. Hong, D. Porter, R. Sreenivasan, P. McIntyre, S. Bent. *Langmuir*, 23, 1160-1165, (2007)
- 2) X. Jiang, S. Bent. *Journal of the Electrochemical Society*, 154 (12), D648-D656, (2007)
- 3) X. Jiang, R. Chen, S. Bent. *Surface & Coatings Technology*, 201, 799-8807, (2007)
- 4) R. Chen, H. Kim, P. McIntyre, D. Porter, S. Bent. *Applied Physics Letters*, 86, 191910, (2005)
- 5) R. Chen, H. Kim, P. McIntyre, S. Bent. *Chem. Mater.*, 17, 536-544, (2005)
- 6) Park, J. Doub, T. Gougousi, G. Parsons. *Applied Physics Letters*, 86, 051903, (2005)
- 7) E. Färm, M. Kemell, M. Ritala, M. Leskelä. *Chem. Vap. Deposition*, 12, 415-417, (2006)

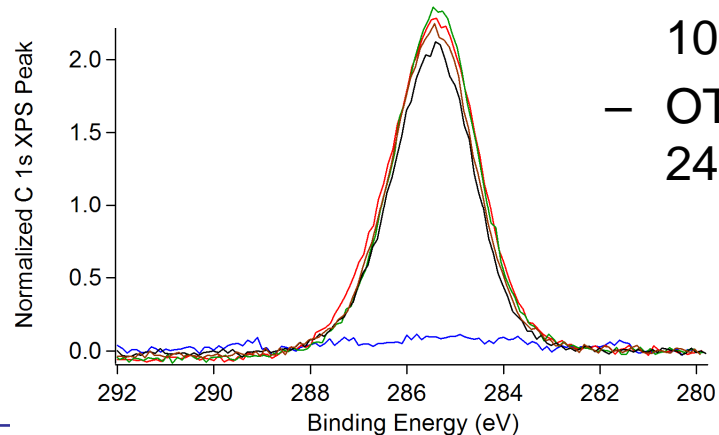
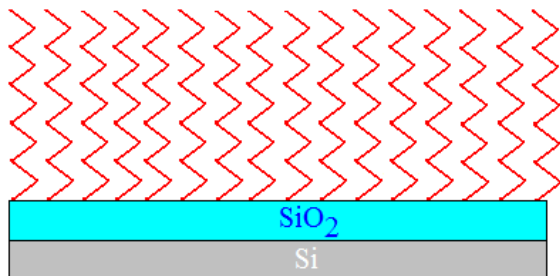
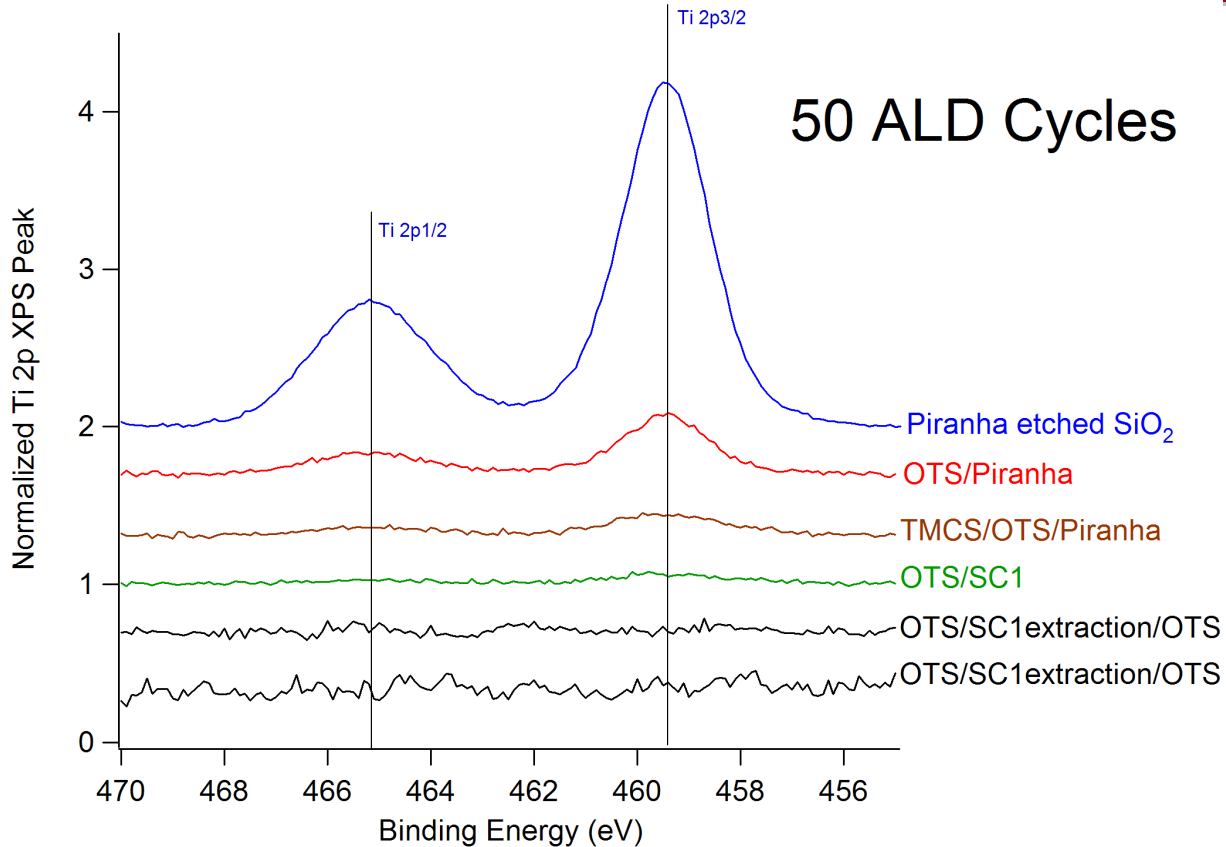
SAM Formation and Defects



- Unblocked hydroxyl group
 - Difficult to fill in even with small SAM molecules
- Trapped water in SAM
 - ALD water pulse doesn't stick in SAM
- Open Si-O-Si bond
 - Better (more complete chemical oxidation)
 - Nitric acid etch and SC1 cleaning
- Polymerized SAM molecules laying down on surface
 - Cleaning and re-exposing surface to SAM
- Open grain boundaries between SAM islands

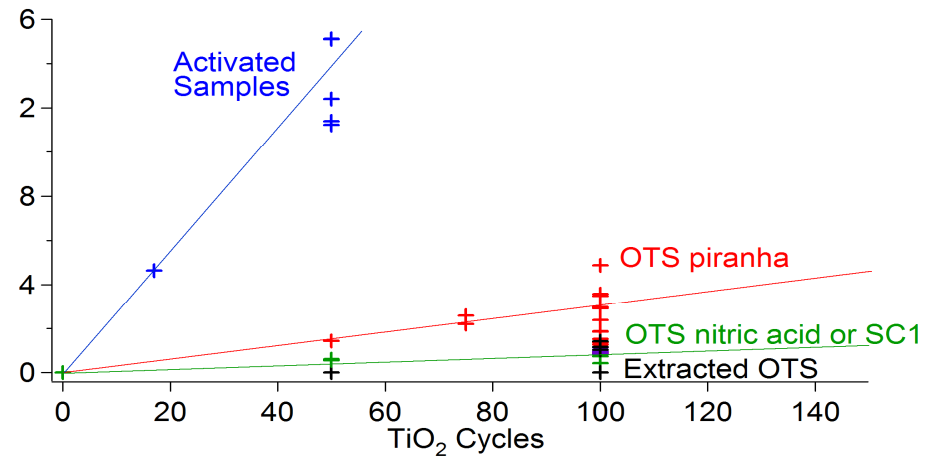
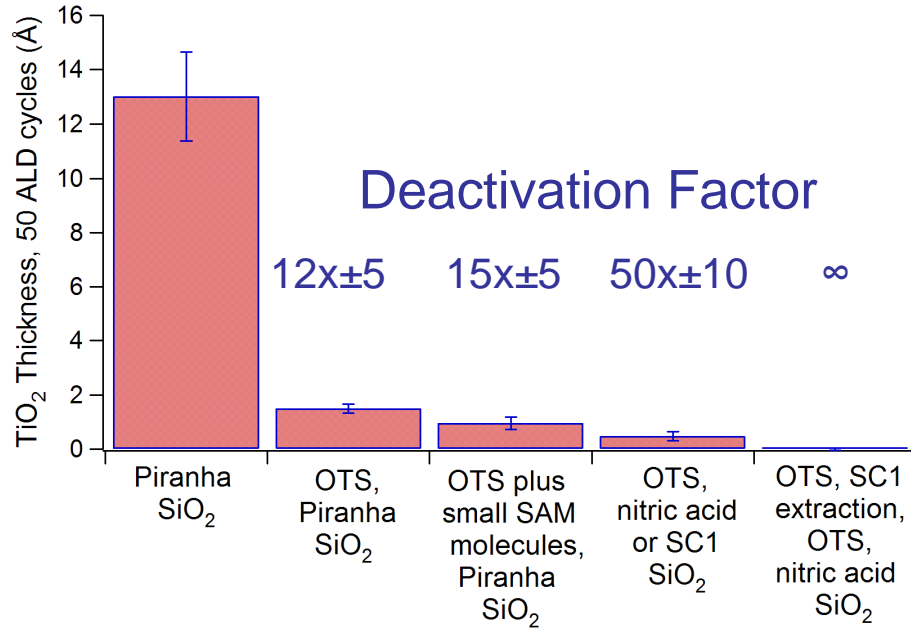
XPS Peak Analysis

50 ALD Cycles



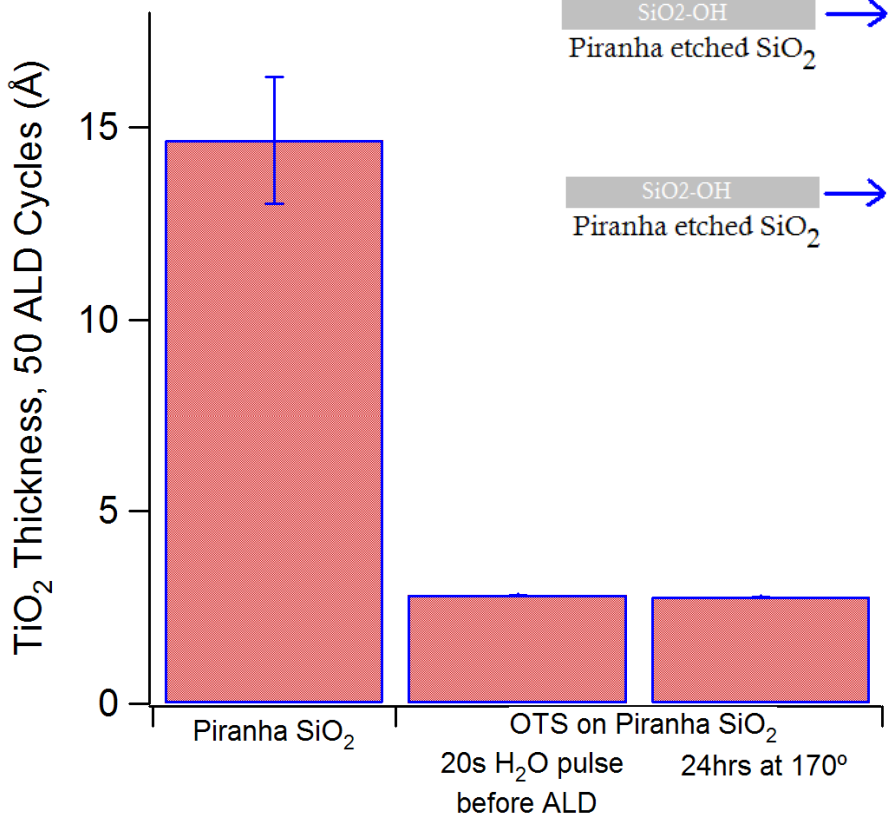
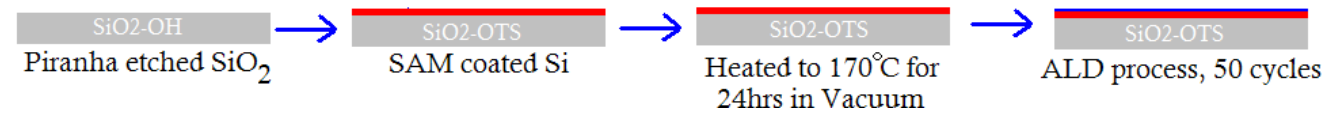
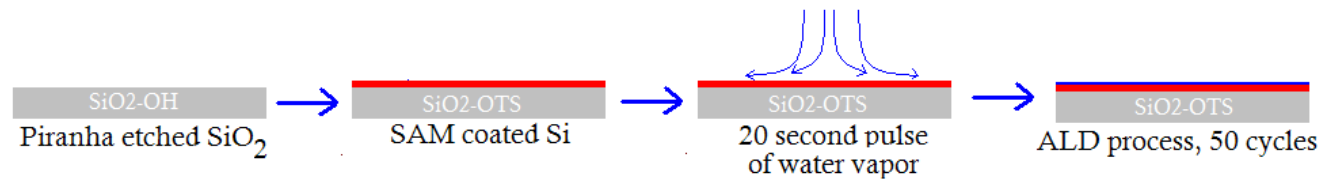
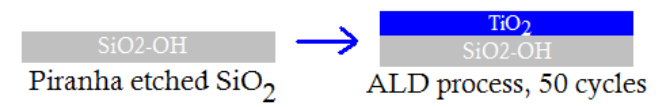
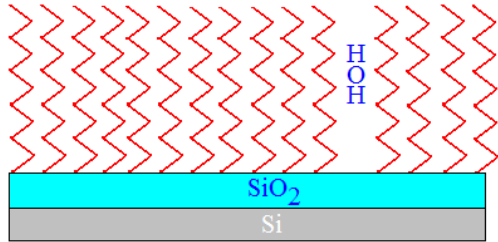
- Relative Thickness determined by calibrating normalized peak area to ellipsometry measurements of activated samples
- No deposition for extracted samples
 - OTS exposed 24hrs
 - SC1 cleaned 10min
 - OTS exposed 24hrs

Surface Deactivation: Results



- Deactivated TiO₂ growth for up to 100 cycles
 - Level of defects varies with sample preparation methods
- Potential SAM defects
 - Unblocked hydroxyl groups
 - Exposed Si-O bridges
 - Polymerized SAM molecules on surface
 - Water in/on SAM

Surface Deactivation: Effect of Water



- SAM is equally stable to subsequent water pulses during an ALD process
 - No change in Ti due to additional 20 second water pulse before ALD
 - TiCl₄ is the nucleating precursor

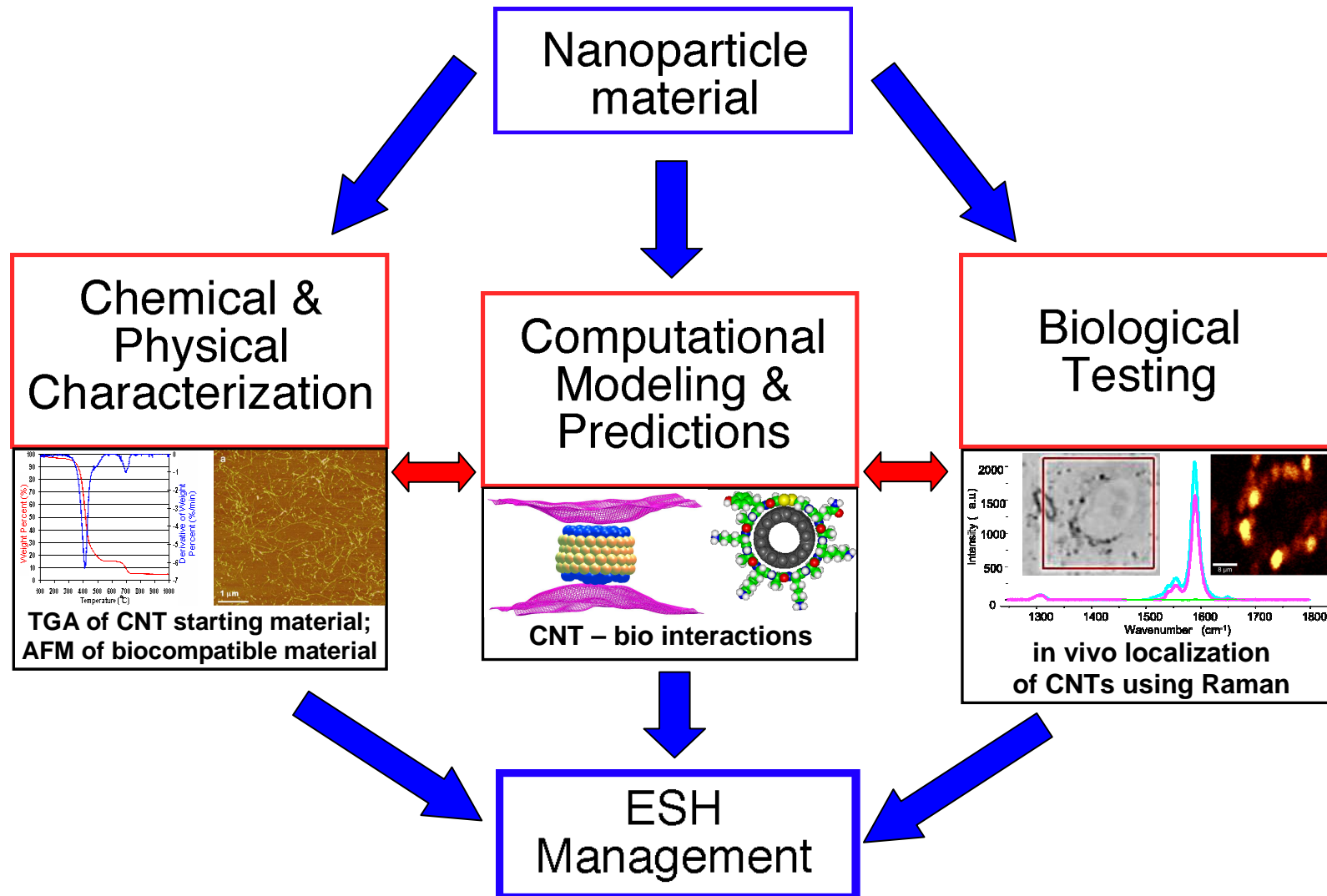
Conclusions

- Extended deactivation for double the number of ALD cycles previously shown in the literature for dielectric surfaces
 - TiCl_4 is also a more reactive precursor than HfCl_4
- Improvements made in forming effective SAM in liquid phase
 - Using smaller SAM molecules like TMCS or TMDS helps fill in any gaps in the OTS SAM
 - Growing the SAM on nitric acid etched and SC1 cleaned samples eliminates many of the defects found in SAM formed on piranha etch samples
 - Extracting polymerized SAM molecules from surface then re-exposing surface to fresh SAM solution yields deactivation for at least 50 cycles
- SAM layer is stable during the ALD water pulse process
 - TiCl_4 is the nucleating precursor

Future Work

- Shorten liquid phase time scale using extraction processes
- Develop an industrially viable method for vapor phase delivery of SAM molecules
 - Pulse and purge both water and SAM molecules as opposed to sealing vapor in a reactor for extended time
 - Extend extraction process to vapor phase SAMs
- Investigate vapor phase ozone and gas phase HF/vapor treatment to increase and control hydroxylation of oxide surfaces
- Characterize SAM layers
 - Thermal stability for deactivation
 - Durability for large numbers of ALD cycles
 - Chemical bonding between SAMs and surface
 - Degradation and repair of SAMs layers
- Investigate selective deposition method on III-V semiconductor surfaces

Predicting, Testing, and Neutralizing Nanoparticle Toxicity





Task Title: (Task Number: 425.027)

Predicting, Testing, and Neutralizing Nanoparticle Toxicity

The University of Texas at Dallas: Department of Chemistry, Department of Biology, and the Alan G. MacDiarmid NanoTech Institute; University of Arizona

PIs:

- **Steven O. Nielsen (PI)**
- **Rockford K. Draper (co-PI)**
- **Inga H. Musselman (co-PI)**
- **Paul Pantano (co-PI)**
- **Gregg R. Dieckmann (co-PI)**
- **Ara Philipossian (co-PI)**

Graduate Students:

- **Chi-cheng Chiu (poster presentation):** PhD candidate (100% funded)
- **David K. Bushdiecker:** PhD candidate (Not funded)

Undergraduate Students:

- **Laura Lockwood, Kyle Bruner, Nancy Jacobsen, and Prashant Raghavendran**

Other Researchers:

- **Ruhung Wang (poster presentation):** Research Associate
- **Bob Helms**

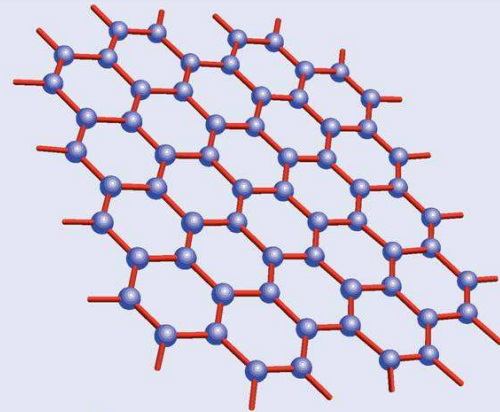
Year 1 Deliverables & Objectives



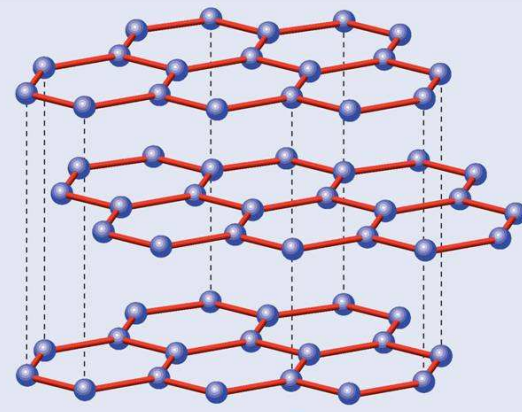
- Obtain and validate data on the characterization, fate, and toxicity (tested in model mammalian cells) of single-walled carbon nanotube (SWNT) nanoparticles.

Allotropes of carbon

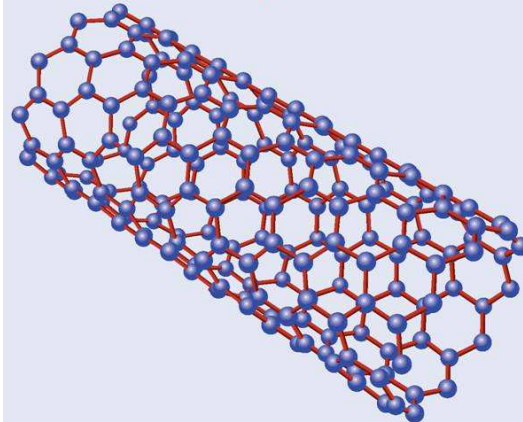
graphene



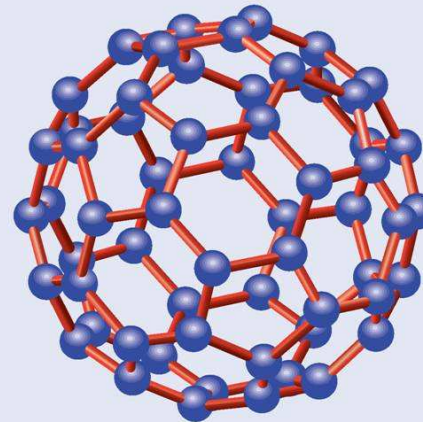
graphite



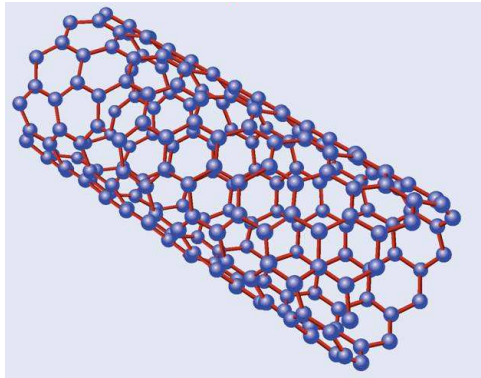
nanotube
(SWNT)



C₆₀



identification or prediction of inherent material ESH properties and any process by-products



carbon nanotube



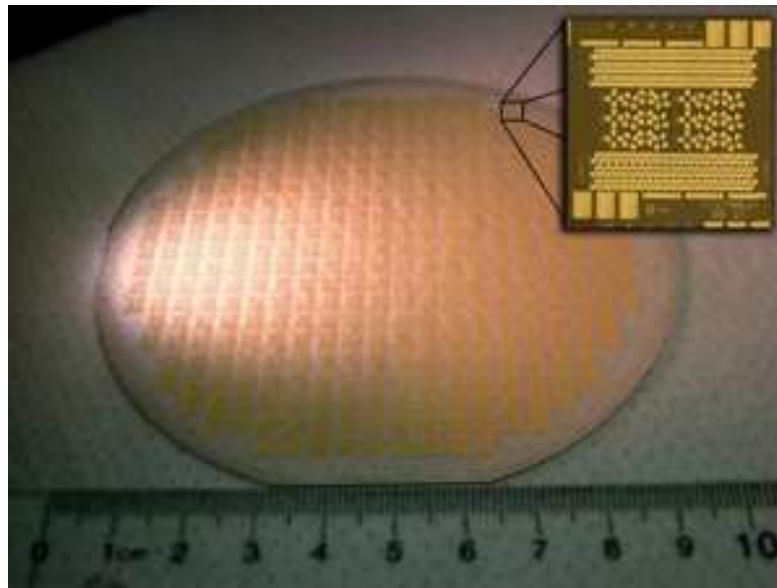
**National
Nanomanufacturing
Network**
Volume 2 Issue 11 - December 2009

**Carbon Nanotube Thin Film
Transistors – Ready for
Prime Time?**

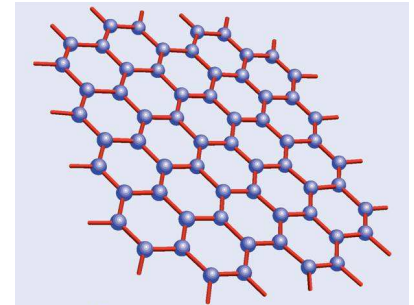


Tuesday, February 2, 2010

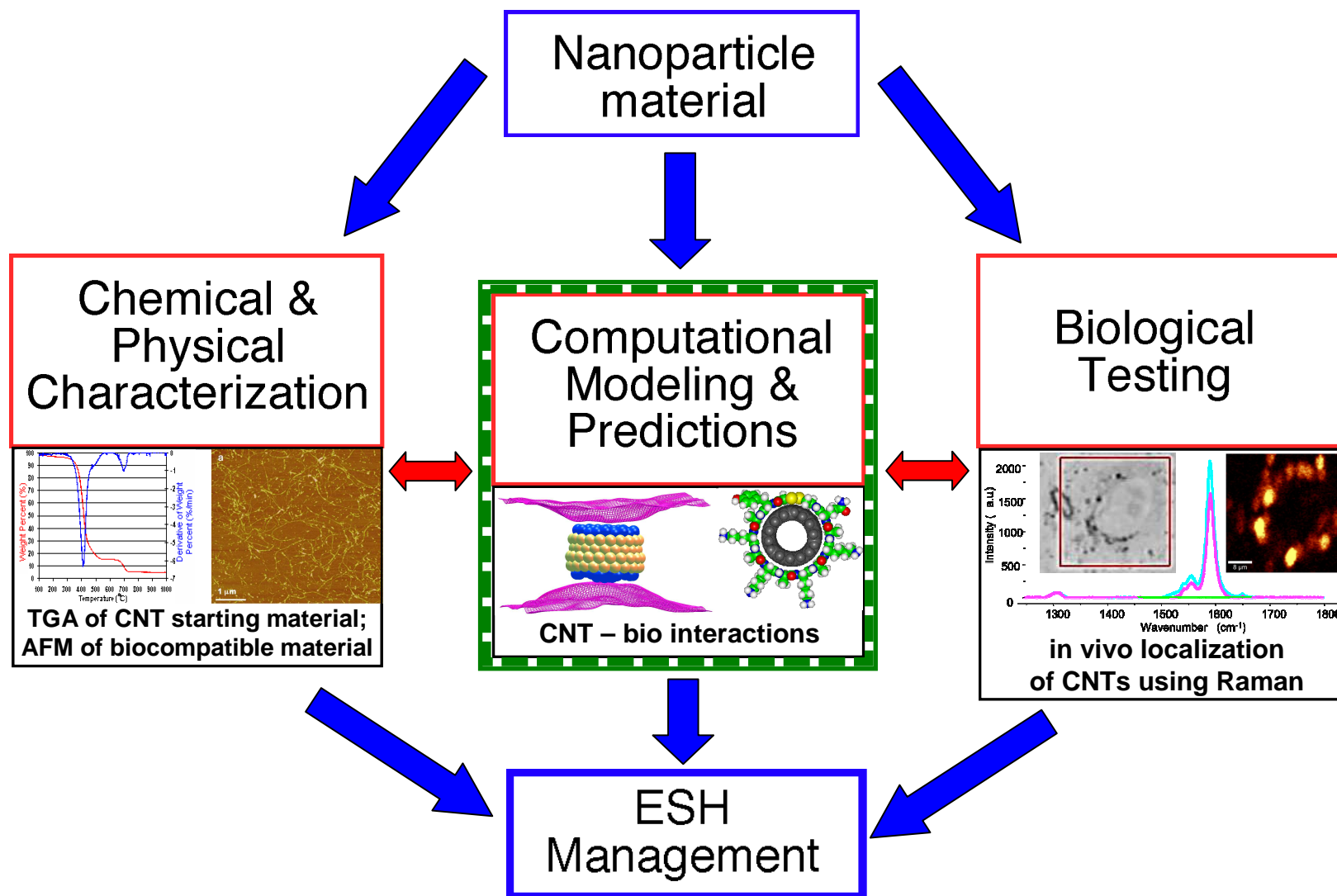
**A 100 mm graphene wafer:
a key milestone in the
development of graphene for
next generation high
frequency electronic devices.**



graphene

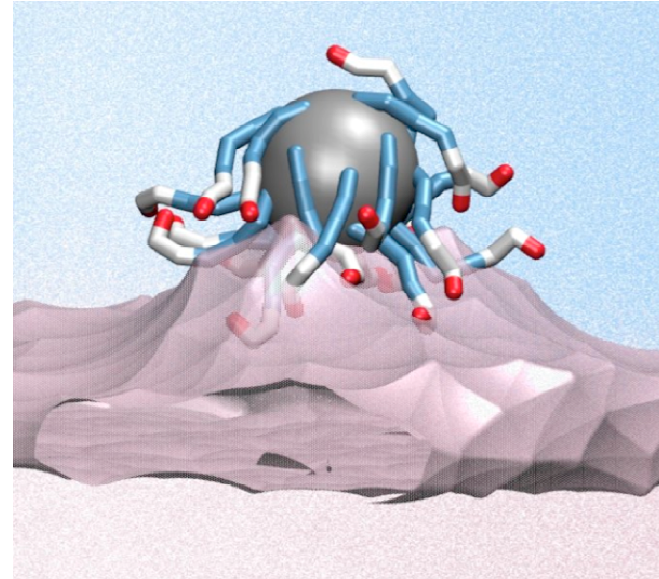


Predicting, Testing, and Neutralizing Nanoparticle Toxicity



Molecular Simulation

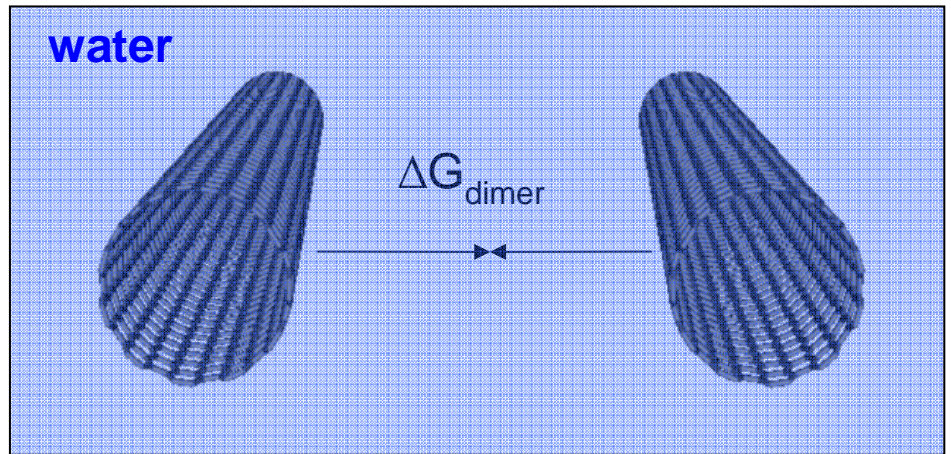
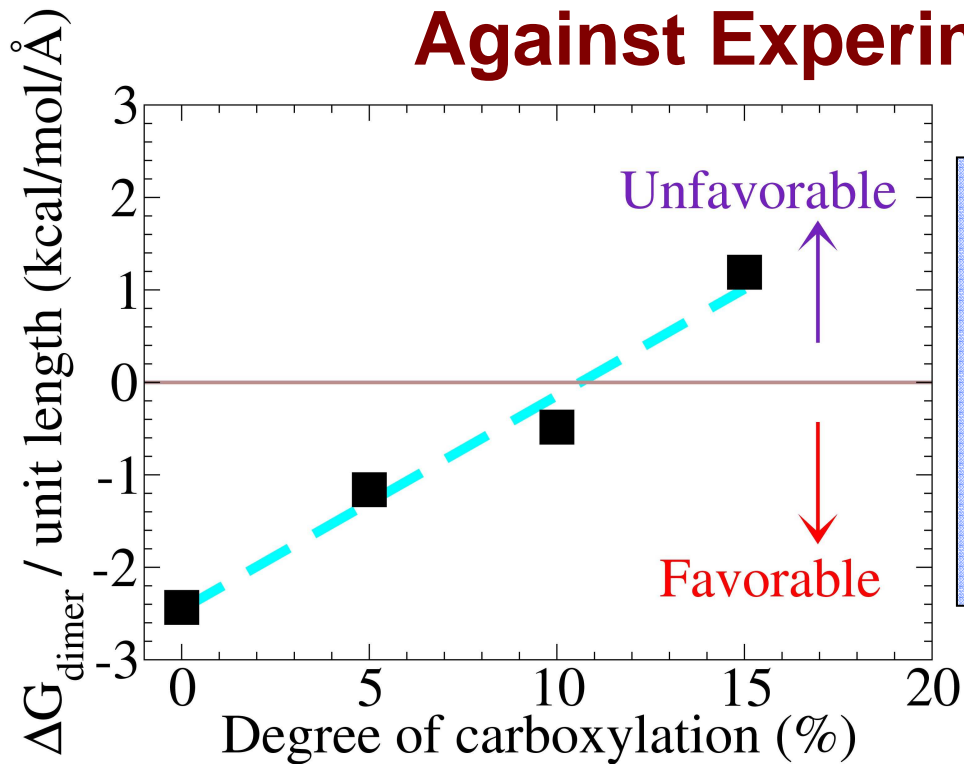
- gain deeper understanding of molecular scale interactions
- make predictions
- validate experimental findings



To be toxic, carbon allotropes must interact with biological molecules or living cells

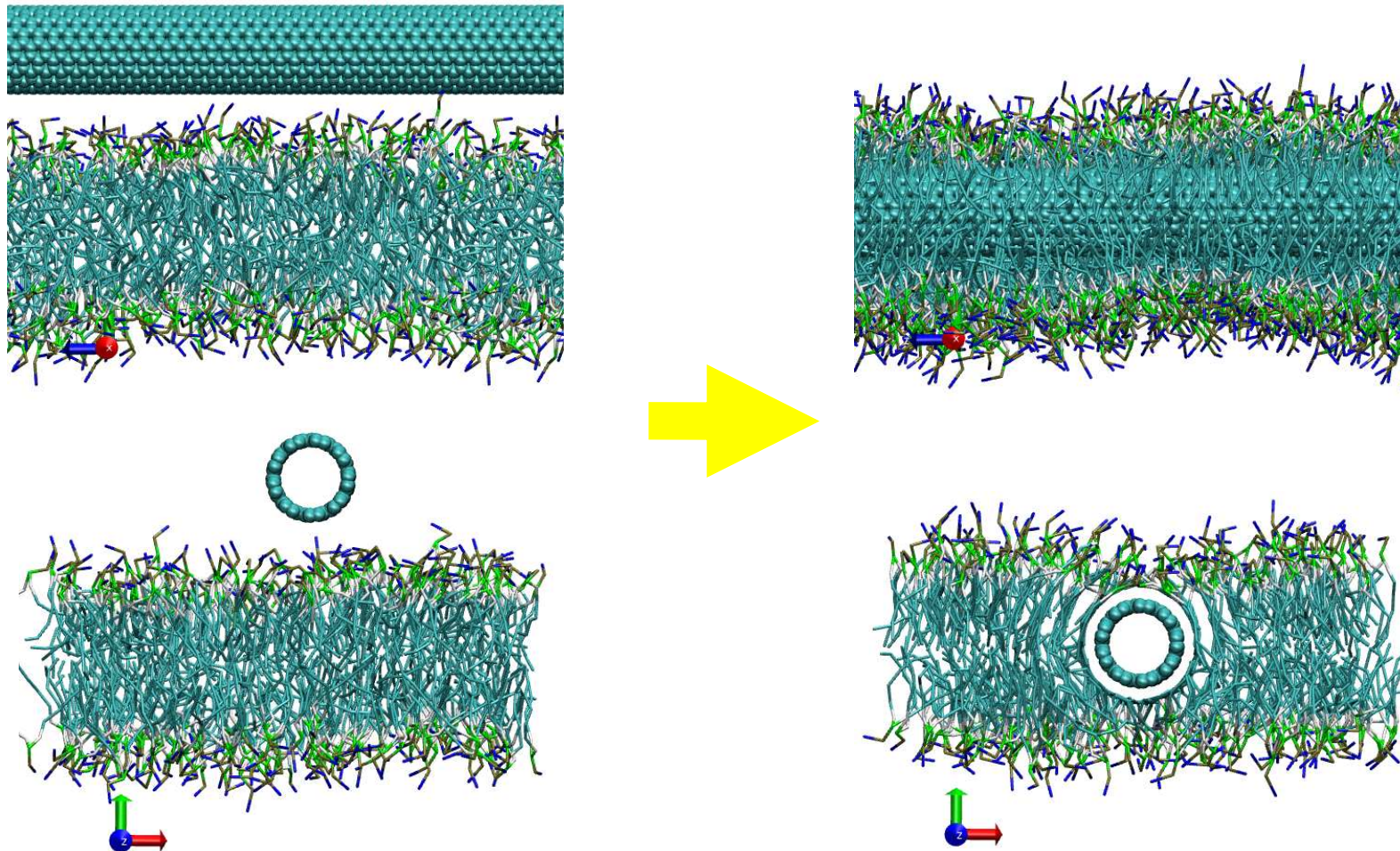
- **We developed a simulation model for this study**

Carboxylated (acid-functionalized) SWNTs: Validation of Molecular Simulation Results Against Experimental Data



- SWNT dimerization free energy in water computed from molecular simulation as a function of SWNT % carboxylation
- $\Delta G_{\text{dimer}} < 0$ indicates that SWNTs will bundle (tangled ropes) in water
- $\Delta G_{\text{dimer}} > 0$ indicates that SWNTs will disperse individually in water
- Crossover %carboxylation agrees with our experimental data: P. Bajaj, M.S. Thesis, The University of Texas at Dallas, Richardson, TX, 2008

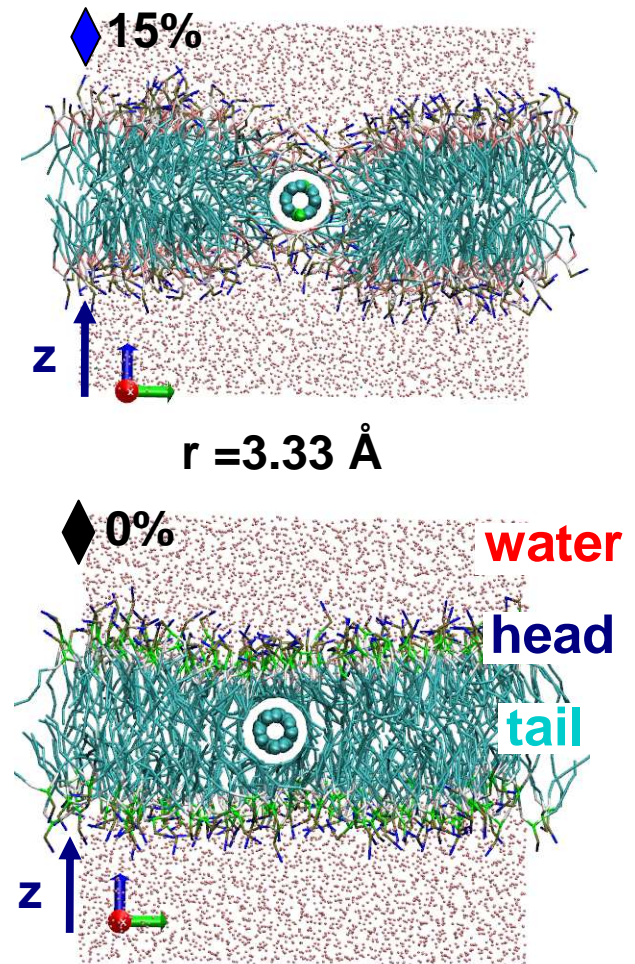
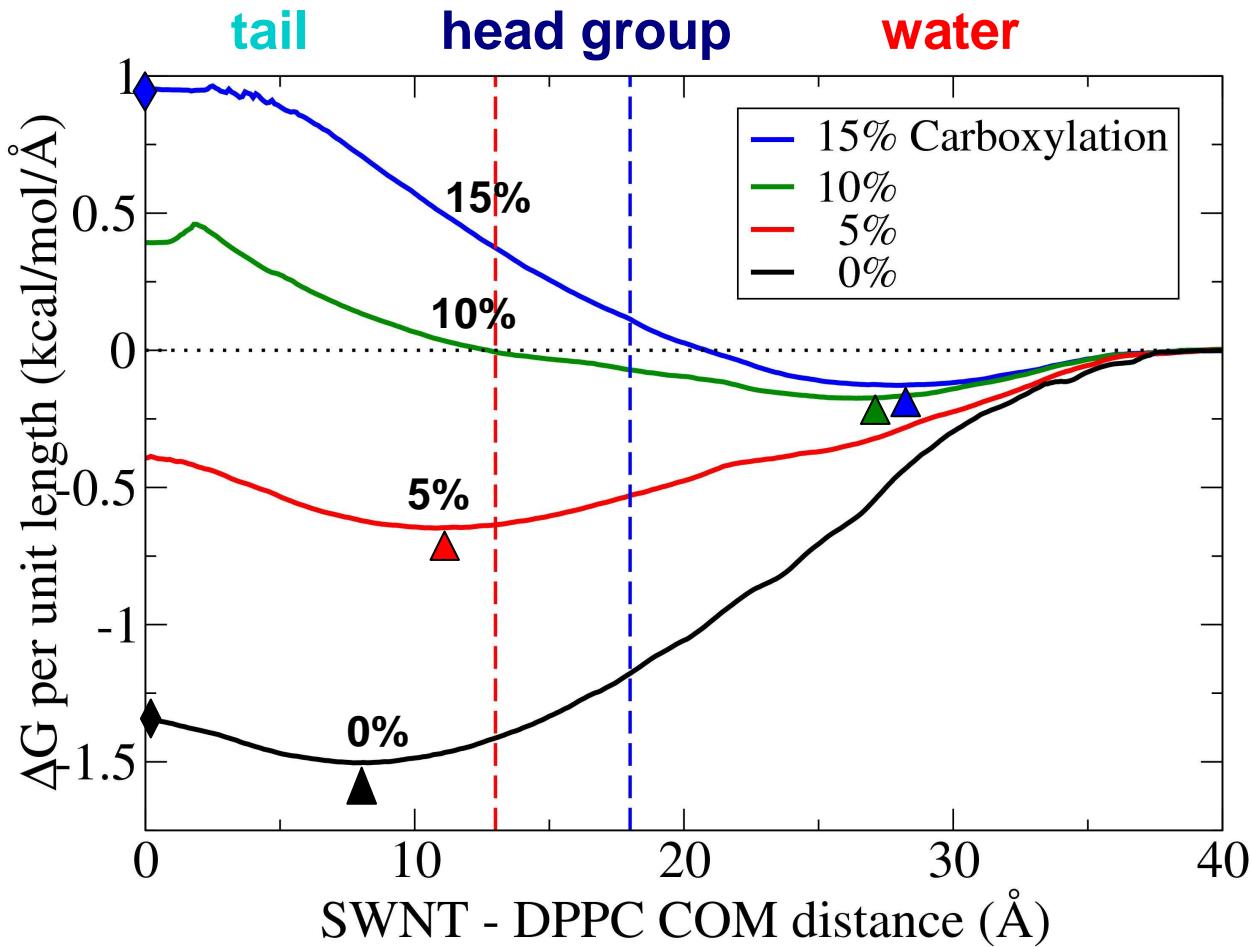
SWNT Interacting with Lipid Bilayer Membrane



- 15 Å diameter pristine SWNT
- 10 ns simulation

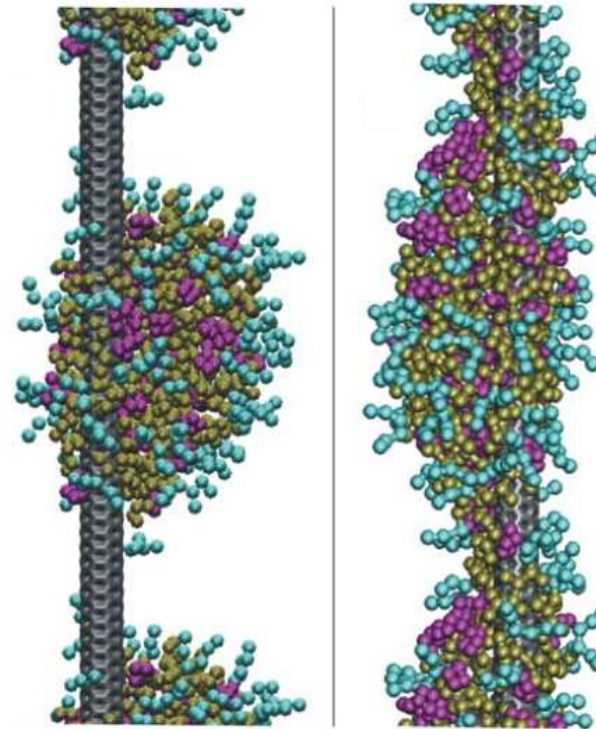
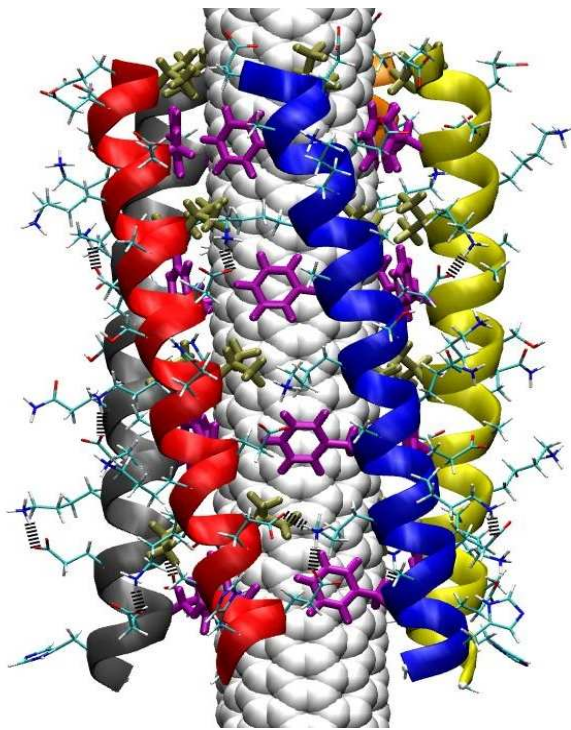
SWNT/Lipid Bilayer Membrane

- Pristine SWNTs spontaneously diffuse into bilayer membrane
- Above 10% carboxylation, it is no longer favorable for SWNTs to penetrate the bilayer membrane.



Molecular Simulation Outlook

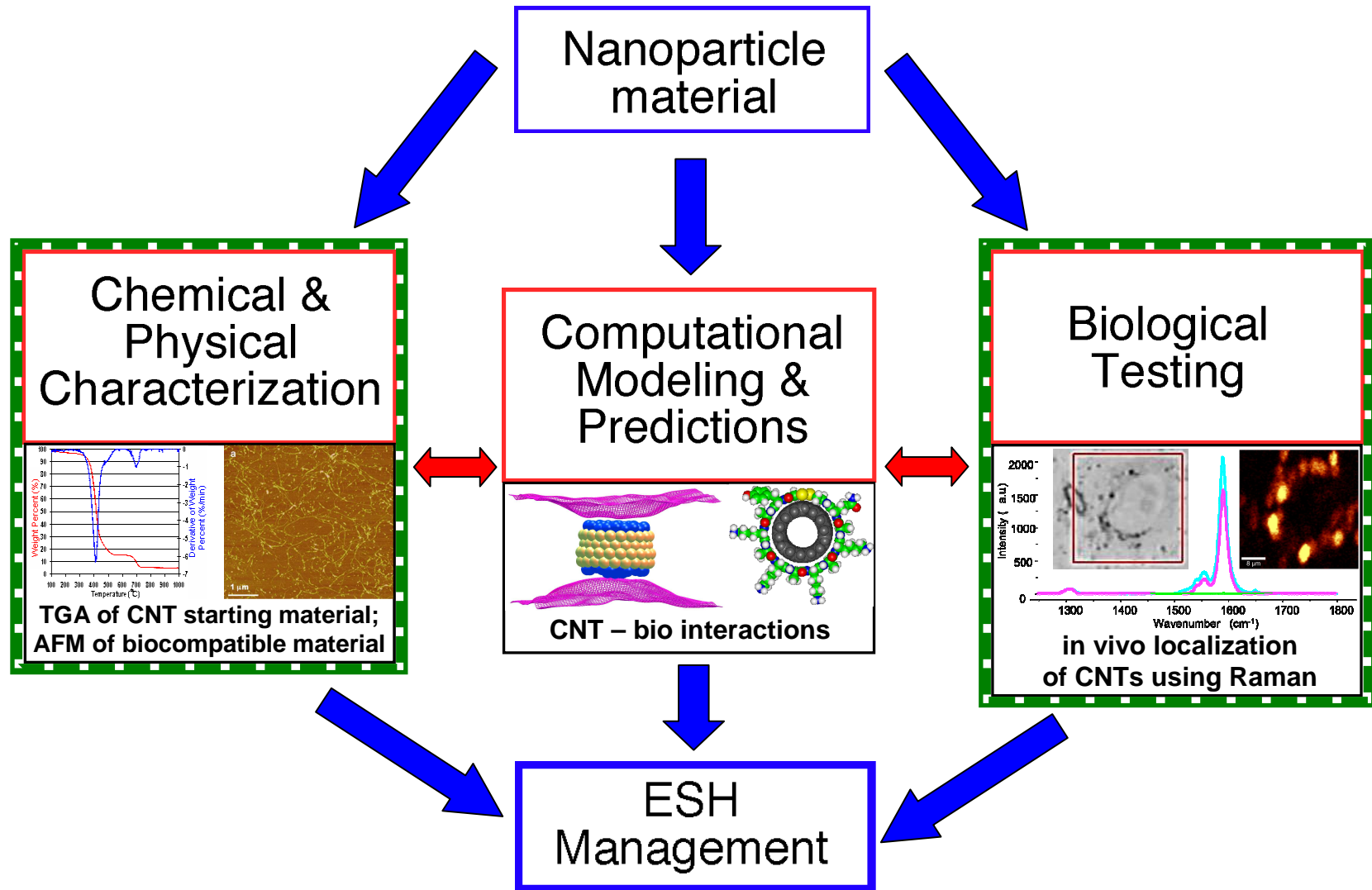
- SWNTs that interact with cells are typically coated with adsorbed proteins
- Protein coat may or may not desorb when SWNTs encounter cell membrane
- We have experience modeling protein coated SWNTs and will examine their interaction with cell membranes in our future work



Chiu *et al.* Journal of Physical Chemistry B 2008, 112, 16326

Chiu *et al.* Biopolymers: Peptide Science 2009, 92, 156

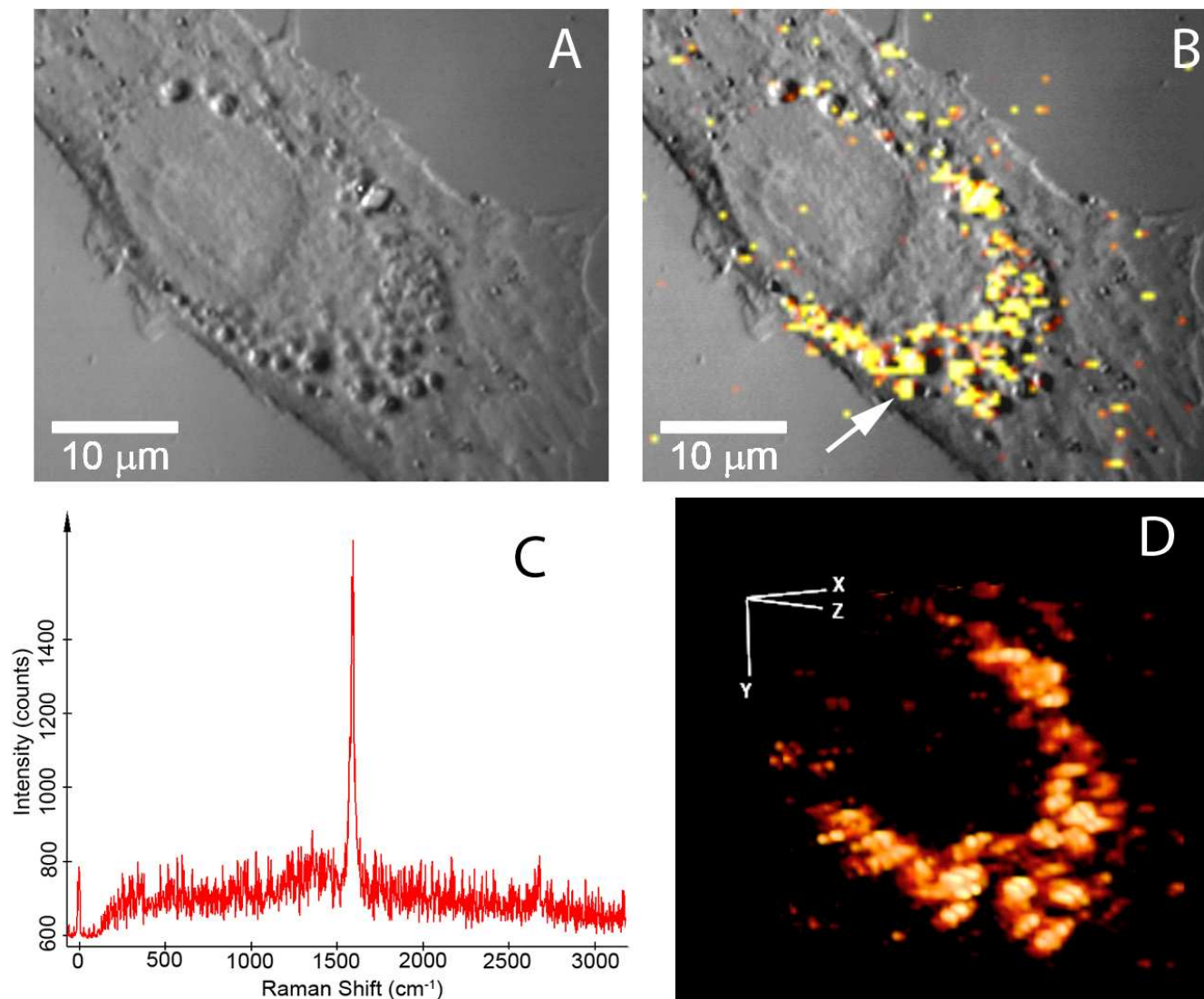
Predicting, Testing, and Neutralizing Nanoparticle Toxicity



Overview: Nanoparticle Characterization and Biological Testing

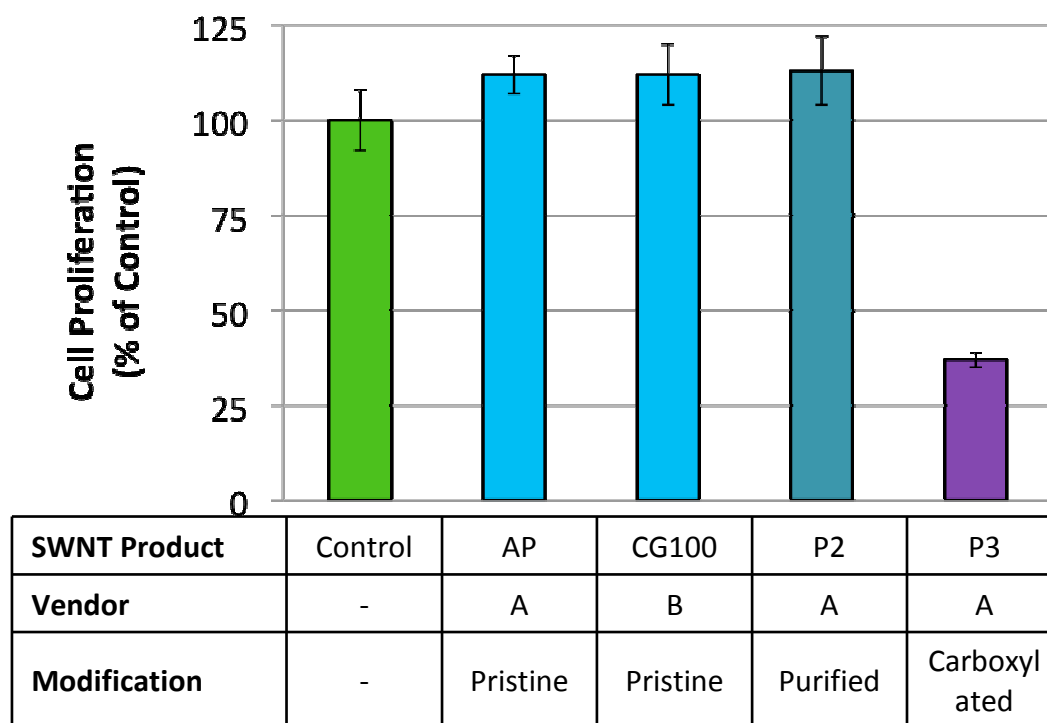
- **Interaction of SWNTs with mammalian cells.**
- **Toxicity of pristine and carboxylated SWNTs with mammalian cells.**
Carboxylated SWNT preparation was unexpectedly toxic
- **Further characterization, purification, and toxicity testing of carboxylated SWNTs.**
- **Interactions of graphene oxide with mammalian cells and toxicity testing.**

SWNTs Inside Mammalian Cells



in vitro Cytotoxicity Comparison of Various Commercial SWNT Products

- Cultured NRK cells were incubated with 100 µg/ml various SWNT dispersions for 3 days.
- Toxicity of a SWNT product was assessed by comparing the number of cells after 3 days with untreated control cells.



Only the carboxylated SWNT commercial product was cytotoxic.

Separation of the Toxic Components from Carboxylated SWNTs Product

Step 1:

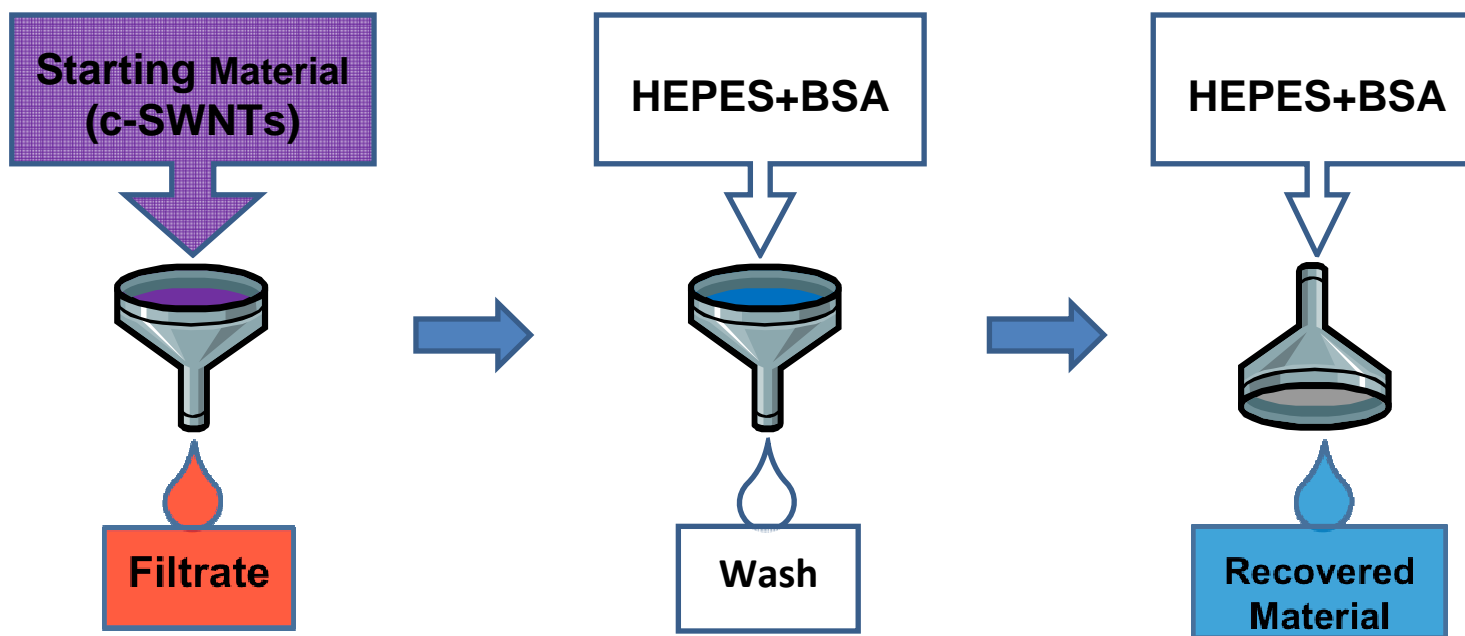
Filter 5 mL diluted P3 dispersion (in HEPES+BSA solution) through a 0.22 μm membrane and collect the Filtrate.

Step 2:

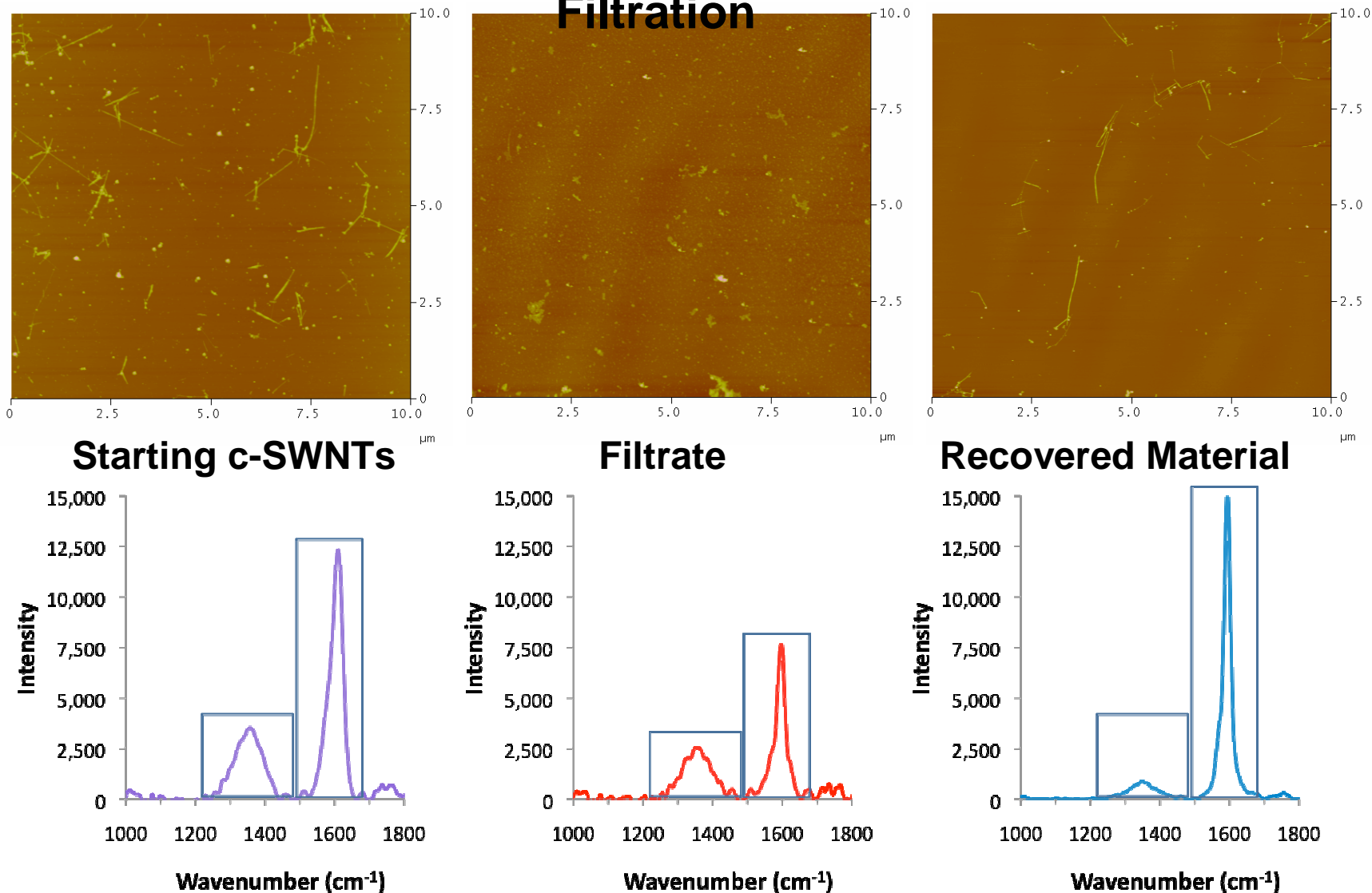
Pass 5 mL HEPES+BSA solution through the same membrane and collect the Wash.

Step 3:

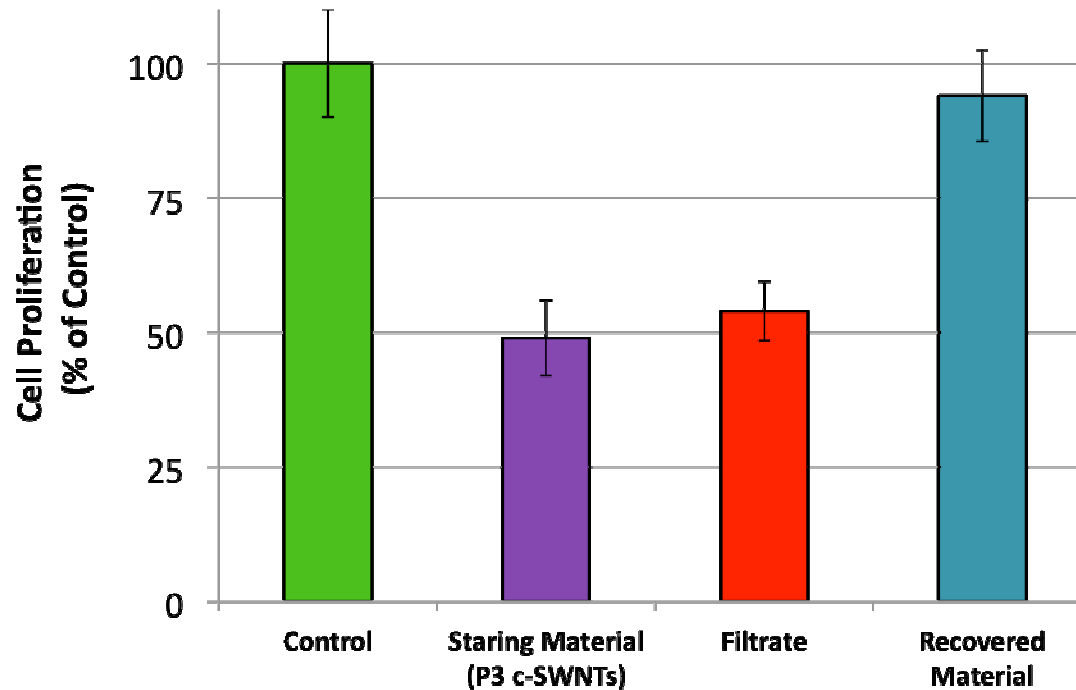
Extract material retained on the membrane with 2 mL HEPES +BSA solution, termed Recovered Material.



AFM and Raman Analysis of C-SWNT Material after Filtration



Filtration-Purified Carboxylated SWNTs are Not Cytotoxic



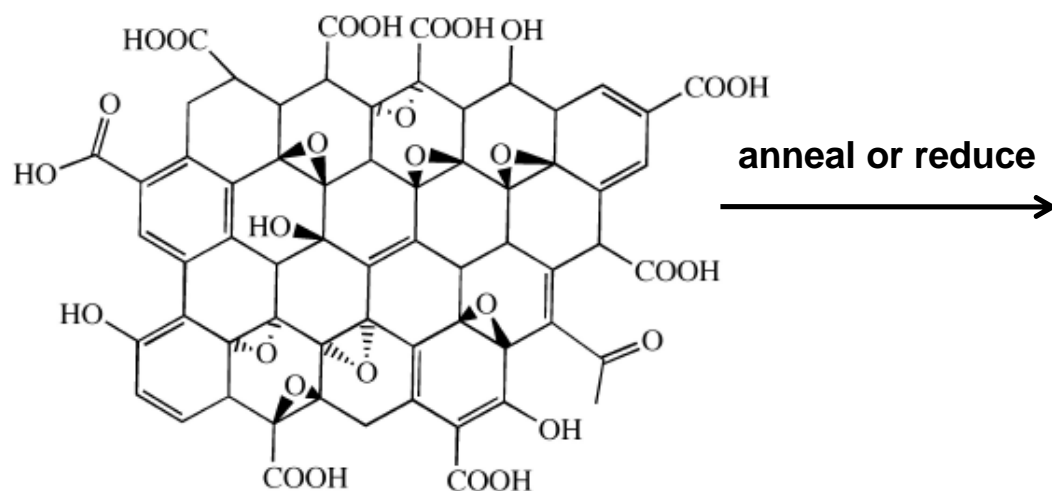
Cells incubated 3 days with material, then cell numbers measured

Conclusions:

- The tested commercially purchased carboxylated SWNTs appear to contain amorphous carbon fragments.
- The toxic activity and amorphous carbon material are removed by filtration.
- The carboxylated SWNTs recovered show little toxicity. This is more consistent with predictions of simulation studies. Detoxified carboxylated SWNTs can be used for various applications with reduced cytotoxic ESH complications.

Graphene Oxide and Graphene

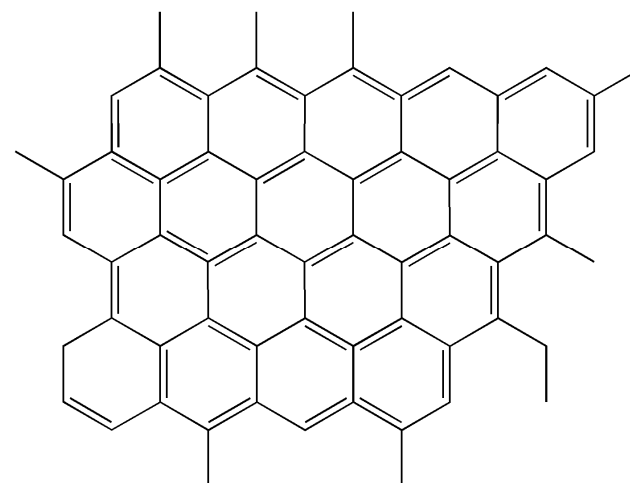
graphene oxide



anneal or reduce

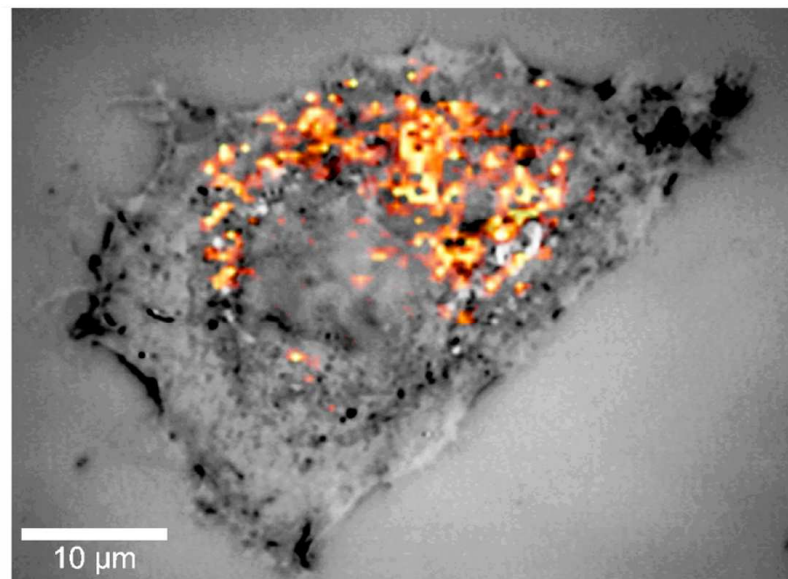
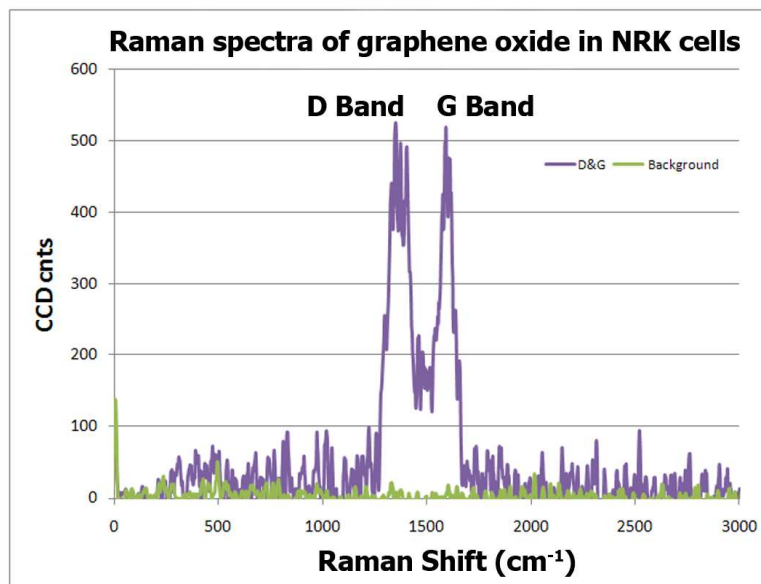
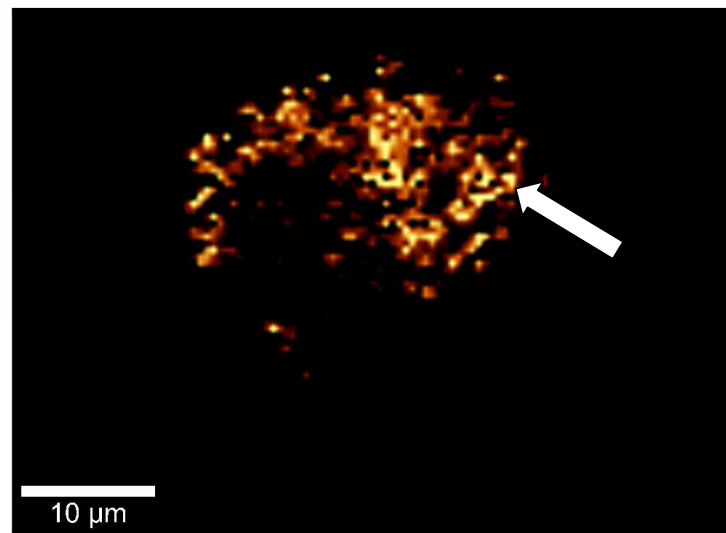
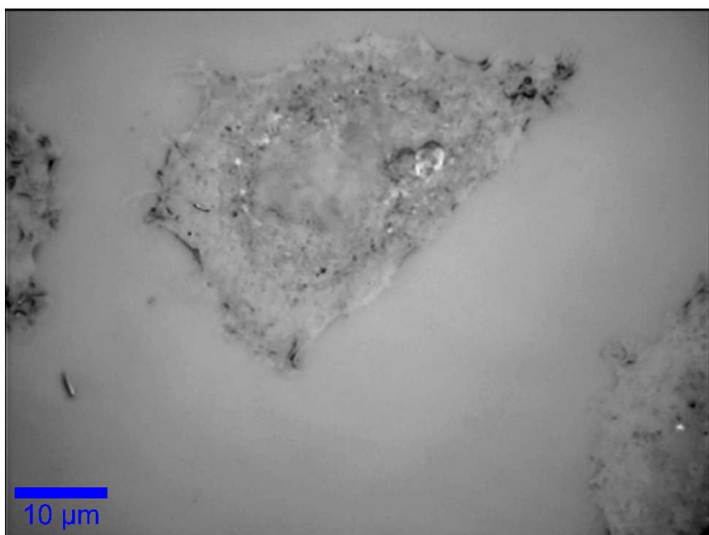


graphene



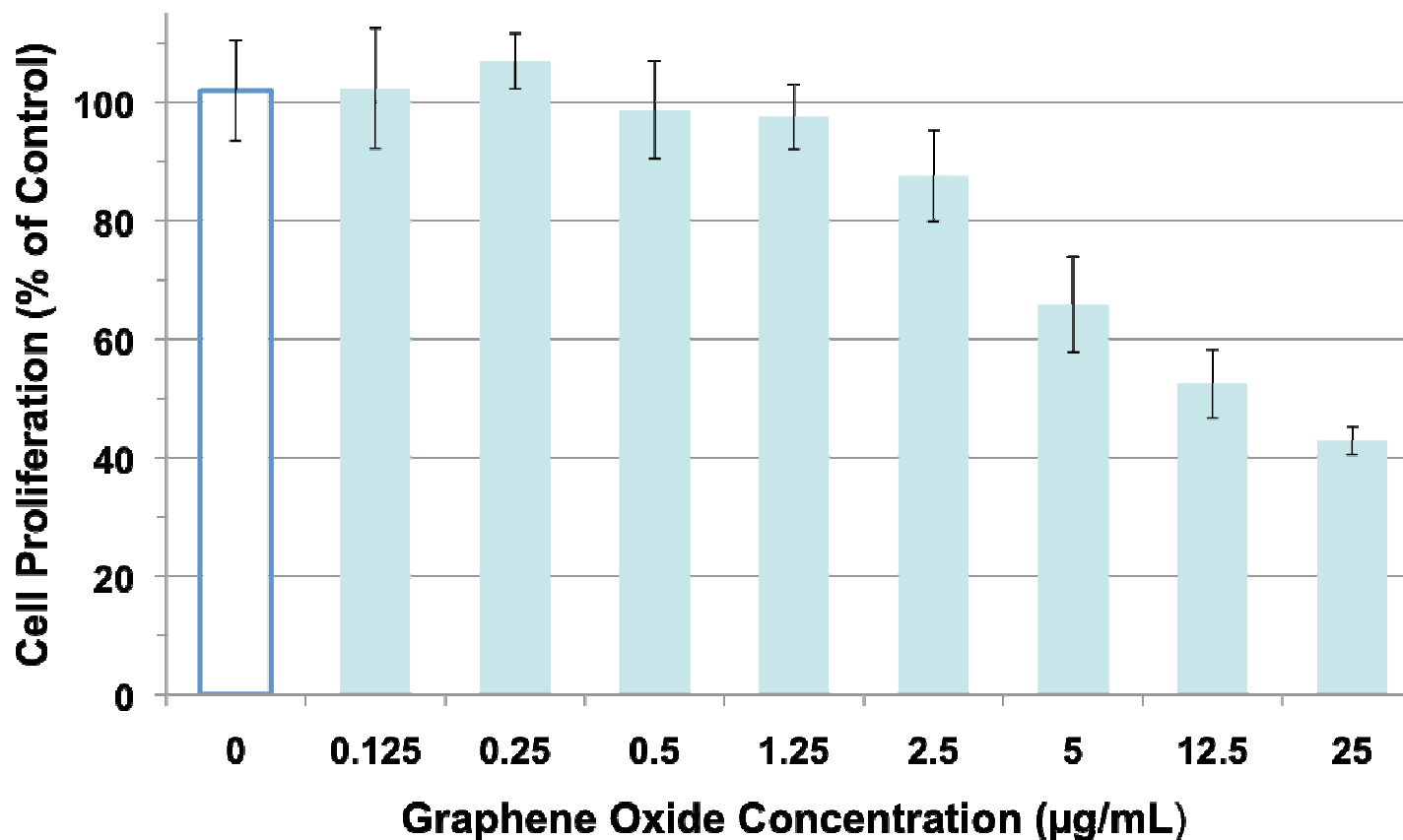
Idealized structure of graphene oxide. Adapted from
C. E. Hamilton, PhD Thesis, Rice University, (2009)

The Interaction of Graphene Oxide with Mammalian Cells



Graphene Oxide Preparations Reduce Cell Proliferation

Cell Proliferation as a Function of Graphene Oxide Concentration



Future Plans

- **Continue work on correlating the results of modeling studies with experimental validation of nanoparticle toxicity and characterization.**
- **Prepare SWNTs that contain different levels of carboxylation and assess the effect of carboxylation on toxicity.**
- **Identify the toxic material in the carboxylated SWNT preparations to determine whether it is a form of amorphous carbon.**
- **Continue work with graphene oxide and identify the toxic material in the preparation.**
- **Based on information obtained, rationally design ways to address ESH issues related to use of SWNTs & graphene oxide.**

Industrial Interactions and Technology Transfer

- **Industrial interaction with Marc Heyns, IMEC.**
 - **Analysis of pads used for CMP of CNT's**
- **Industrial interaction with Don Hooper, Intel.**
 - **ESH of CMP slurries**
- **Industrial interaction with Mario Bolanos-Avila, TI.**
 - **ESH of packaging**

Presentations

- **ERC Teleseminar, April 16, 2009: “Challenges in Assessing the Potential Cytotoxicity of Carbon Nanotubes” by P. Pantano**
- **ERC Teleseminar, Nov. 12, 2009: “Computer Simulations of the Interaction between Carbon Based Nanoparticles and Biological Systems” by C.-c. Chiu**
- **AIST (Japan) seminar, 2009: “Nanoparticles from a soft matter viewpoint” by S. Nielsen**
- **UT Arlington and TCU seminars, 2009: “Accurately Assessing the Potential Toxicity of Carbon Nanotubes and the Use of Carbon Nanotubes as Cancer Theranostic Agents” by P. Pantano**
- **UTD Institute for Innovation & Entrepreneurship: organized Conference on “Nanomedicine: Enterprise and Society”, Jan 22, 2010**

Publications

- **Draper, R.K.; Wang, R.; Mikoryak, C.; Chen, E.; Li, S. and Pantano, P. “Gel electrophoresis method to measure the concentration of single-walled carbon nanotubes extracted from biological tissue”. *Anal. Chem.* 81: 2944-2952 (2009).**
- **Katari, S.C.; Wallack, M.; Hubenschmidt, M.; Pantano, P. and Garner, H.R. “Fabrication and evaluation of a near-infrared hyperspectral imaging system”, *J. Microscopy* 236: 11-17 (2009).**
- **Marches, R.; Chakravarty, P.; Bajaj, P.; Musselman, I.H.; Pantano, P.; Draper, R.K. and Vitetta, E.S. “Specific thermal ablation of tumor cells using a monoclonal antibody covalently coupled to a single-walled carbon nanotube”, *Int. J. Cancer* 125: 2970-2977 (2009).**

Lowering the Environmental Impact of High-k and Metal Gate-Stack Surface Preparation Processes

(Task Number: 425.028)

PIs:

- **Yoshio Nishi, Electrical Engineering, Stanford University**
- **Srini Raghavan, Materials Science and Engineering, University of Arizona**
- **Bert Vermeire, Electrical Engineering, Arizona State University**
- **Farhang Shadman, Chemical Engineering, University of Arizona**

Graduate Students:

- **Gaurav Thareja, Electrical Engineering, Stanford University**
- **Kedar Dhane, Chemical Engineering, University of Arizona**
- **Davoud Zamani, Chemical Engineering, University of Arizona**
- **Shweta Agrawal, Chemical Engineering, University of Arizona**
- **Xu Zhang, Electrical Engineering, Arizona State University**

Research Scientists:

- **Jun Yan, Chemical Engineering, University of Arizona**
- **Junseok Chae, Electrical Engineering, Arizona State University**

Cost Share (other than core ERC funding):

- **\$50k from Stanford CIS**

SRC/SEMATECH Engineering Research Center for Environmentally Benign Semiconductor Manufacturing

Objectives

- **Development of non-fluoride based etch chemistries for hafnium based high-k materials**
- **Elimination of galvanic corrosion between metal gate and polysilicon during wet etching**
- **Significant reduction of water and energy (hot water) usage during rinse**
- **Determination of chemical and electrical characterization methodology for surface preparation of high k dielectric films.**
- **Validation of low resource-usage processes using Metal - high-k device fabrication and electrical characterization**

ESH Metrics and Impact

- **Reduction in the usage of HF and HCl; development of environmentally friendly, non-fluoride based etch chemistries for hafnium-based high-k materials**
- **Significant reduction in water usage during rinse**
- **Significant reduction in energy (hot water) usage during rinse**
- **Reduction of rinse time leading to increase in throughput and decrease in resource usage**

Subtask 1: Environmentally Friendly Chemical Systems for Patterning Silicates and Hafnium Oxide

BACKGROUND

- **In the formation of high k- metal gate structures by the “gate first” process, etching of high k material after ‘P-metal’ removal to prepare the surface for ‘N- metal’ deposition is required. Additionally, selective etching of high k material with respect to SiO₂ is also needed**
- **Currently used chemical system for etching Hf based high-k materials is dilute HF containing HCl; however, these high k materials become very difficult to etch when subjected to a thermal treatment**
- **HF based systems appear to induce galvanic corrosion of polysilicon, which is in contact with metal gate materials; reducing the oxygen level of HF has been recommended to reduce corrosion**

Materials and Experimental Procedures

- Materials

300 mm ALD HfO₂ wafers:

- Provided by ASM
- Film Thickness: ~ 230 Å

300 mm ALD HfSi_{0.74}O_{3.42}

wafers:

- Provided by ASM
- Film Thickness: ~ 240 Å

- Experimental Procedures:

- Wafer was cleaved into 2 x 3 cm pieces for testing
- Cleaned by IPA, rinsed with DI water and dried by N₂
- Etch rate determined from thickness measurements made by spectroscopic ellipsometer (J. A. Woollam Co.) at 5 different locations
- Heat treatment and reduction tests were conducted in a tube furnace;
50% N₂ and 50% H₂ gas mixture was used for reduction tests
- Dilute HF was used for baseline etch rate measurements; ammonium hydroxide was tested as an alternate etchant

Baseline Etch Tests on ALD HfO₂ in Dilute HF Solutions

HF concentration (%)	Temperature (°C)	N ₂ atmosphere / Time (min)	ER _{HfO₂} (Å/min)	Selectivity ER _{HfO₂} :ER _{SiO₂}
0.01	25	No	1.5	4.8 : 1
0.1	25	No	4.1	2.2 : 1
1	25	No	27.6	0.5 : 1
0.1	350	Yes / 1 hr	2.2	1.2 : 1
1	350	Yes / 1 hr	30.1	0.5 : 1
1	600	Yes / 15 min	No etching	-

- **Better etch selectivity of HfO₂ (with respect to SiO₂) at low concentrations of HF---trend in line with literature data for MOCVD HfO₂**
- **Heat treatment at 600 ° C makes HfO₂ very difficult to dissolve in HF**

Wet Etching of ALD HfSi_xO_y in Dilute HF Solutions

HF concentration (%)	Temperature (°C)	Reduced in 50%H ₂ /50%N ₂	ER _{HfSi_xO_y} (Å/min)	Selectivity ER _{HfSi_xO_y} :ER _{SiO₂}
0.01	25	No	2.2	7.1 : 1
0.1	25	No	23.2	12.6 : 1
1	25	No	328.4	5.3 : 1
0.1	400	No	23.8	12.9:1
0.1	400	Yes	22.8	12.4:1

- **Hafnium silicate etches at a higher rate than HfO₂ in dilute HF solutions**
- **Heat treatment in hydrogen does no affect the etch rate of hafnium silicate significantly**

Alternative Etch Chemistries for Hafnium Oxide and Silicate

- Literature data indicates that dissolution of metal silicates such as copper silicates is possible in ammoniacal solutions with a pre-reduction treatment in H_2/N_2 or CO/CO_2
- First set of experiments carried out on hafnium oxide and silicate films exposed to $50\%H_2/50\%N_2$ at different temperatures for different duration
- Films subsequently immersed in ammonium hydroxide solutions

Feasibility of Etching of HfO₂ and HfSi_xO_y in Ammonical Solutions Using a Pre-reduction Treatment

Reduction Temperature (°C)	400	200	100
Reduction Time (hr)	0.5	1	3
pH of Ammonium Hydroxide	9.95	13.8	
Time in Ammonium Hydroxide (hr)	1	21	
Etch Rate (HfO ₂ and HfSi _{0.74} O _{3.42})	insignificant		

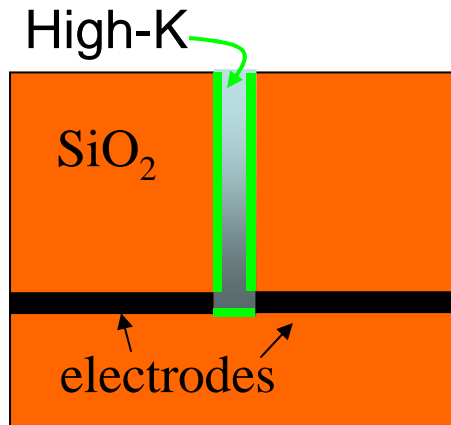
Pre-reduction in H₂/N₂ mixture appears to be ineffective in making HfO₂ and HfSi_{0.74}O_{3.42} soluble in ammoniacal solutions.

Subtask 2: Low-Water and Low-Energy New Rinse and Drying Recipes and Methodologies

BACKGROUND

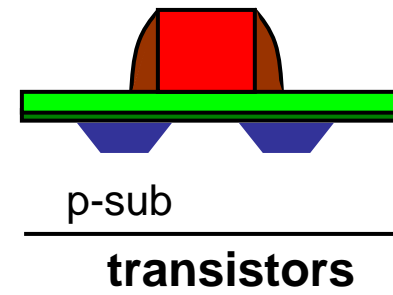
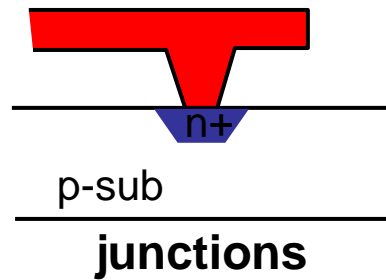
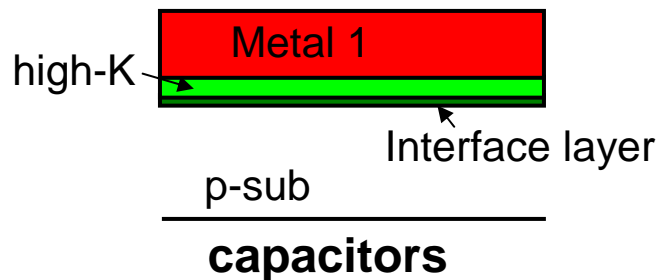
- **Formation of high-k metal gate structures requires cleaning of fine geometries containing materials not traditionally used by the semiconductor industry. Wet etching must be quenched at the appropriate time**
- **More single wafer tools are used for cleaning, rinsing and drying because of better yield. Optimization of cycle time is critical for throughput and reduced resource usage**
- **Elucidating rate-limiting mechanisms to make possible multi-stage, resource-efficient recipes requires in-situ and real-time measurements and accurate simulation capabilities**
- **Validation of low resource-usage processes for high-volume manufacturing using electrical test structures**

Test Structures for Experimental Work



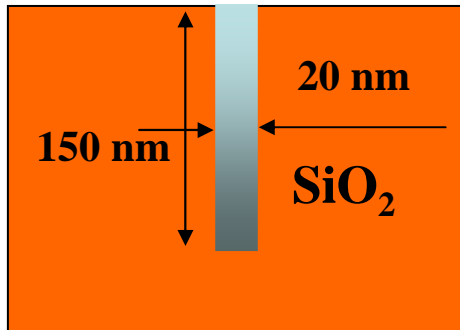
AC impedance of high aspect ratio feature to determine cleaning and drying kinetic parameters in-situ

Quartz Crystal Microbalance to determine etch rates and adsorption/desorption rates

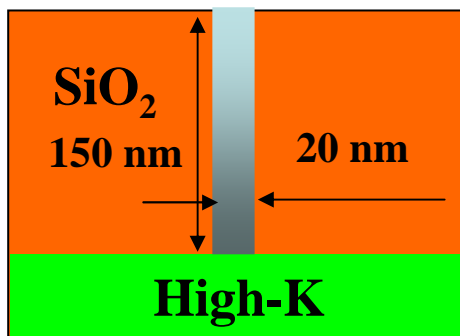


Electrical test structures (capacitors, junctions, transistors) to evaluate impact of new recipes on performance

Rinsing/Cleaning of Heterogeneous Nano- Structures



Conventional Structure



Structure with high-k

The introduction of high-k dielectric makes the surface structure heterogeneous. Rinse must clean both surfaces

A newly developed spin-rinse model was used to parametrically study the heterogeneous structure rinse.

Multi-component transport equations :

$$\frac{\partial C_i}{\partial t} = \nabla \cdot (D_i \nabla C_i + z_i F \mu_i C_i \nabla \phi)$$

Surface adsorption and desorption:

$$\frac{\partial C_S}{\partial t} = k_a C_b (S_0 - C_S) - k_d C_S$$

Poisson equation: $\nabla^2 \phi = -\frac{\rho}{\epsilon}$

Nomenclature

C_i = Liquid Concentration

D_i = Diffusivity

C_s = Surface Concentration

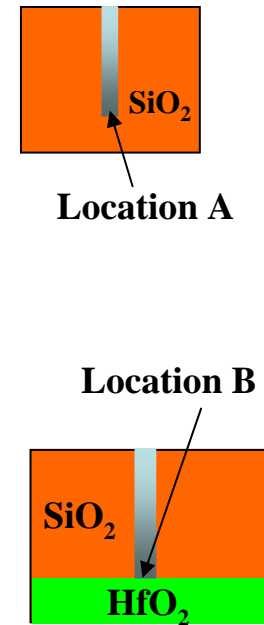
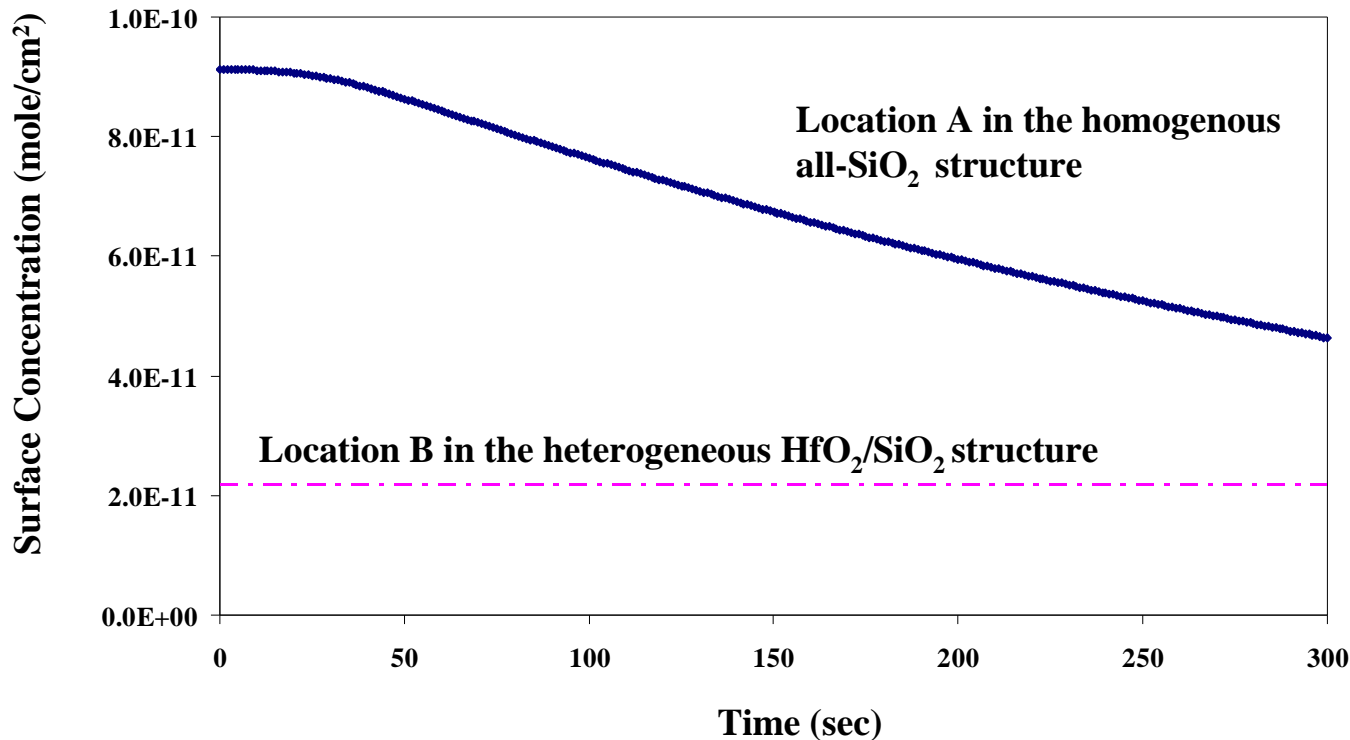
S_0 = Maximum sites available

k_a = Adsorption coefficient

k_d = Desorption coefficient

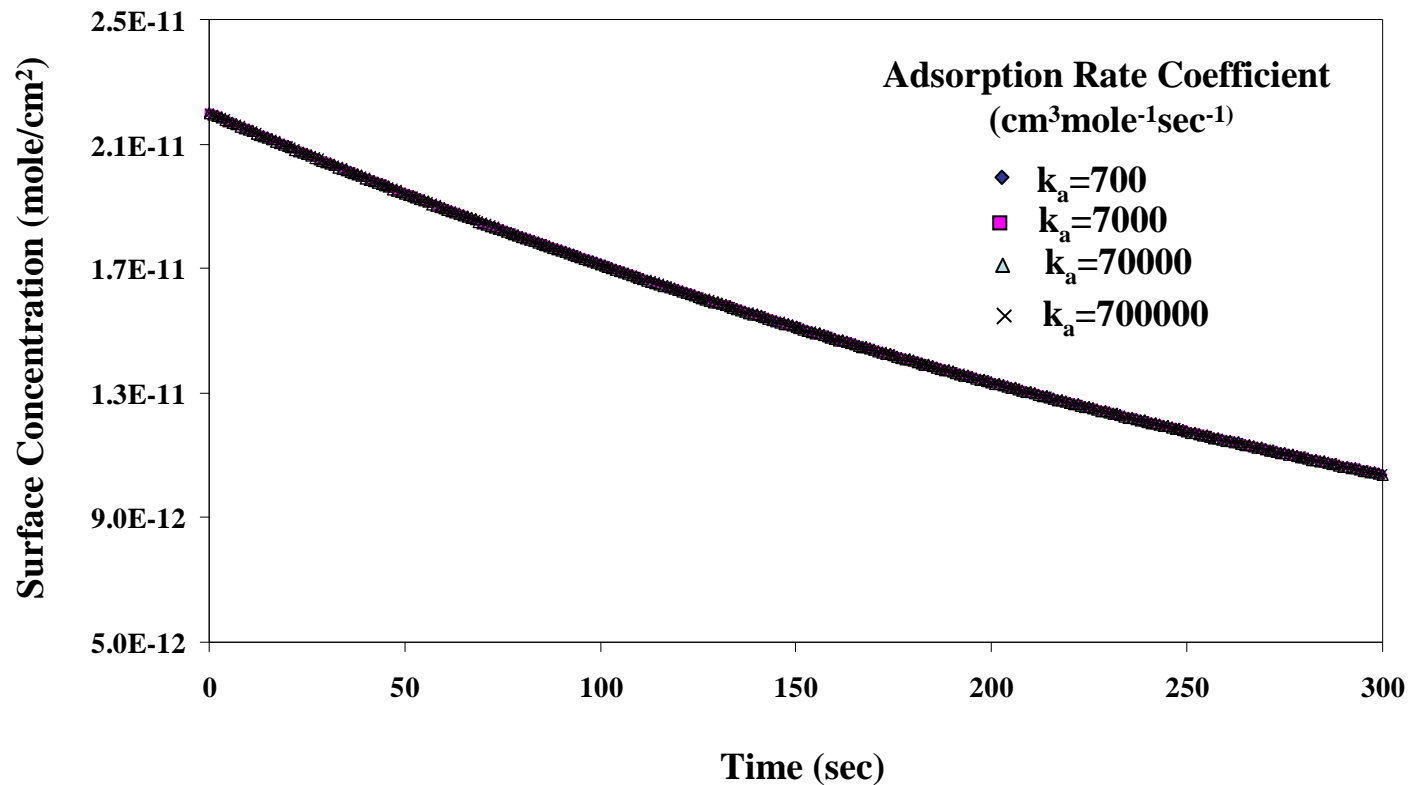
Φ = Electrostatic Potential

Challenges in Rinsing of Nano-Structures that Include HfO₂



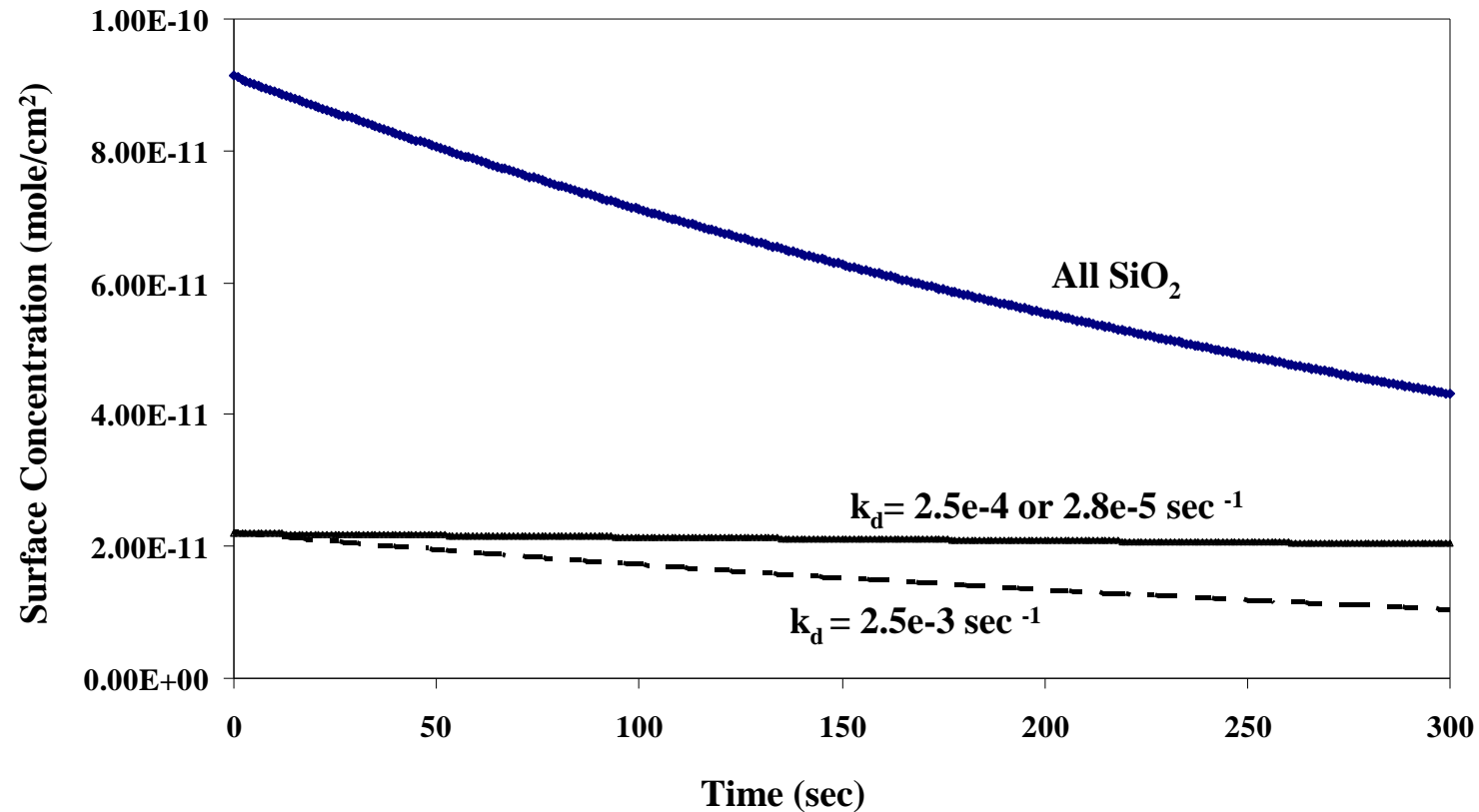
- HfO₂ has lower surface adsorption capacity compared to SiO₂. However, the sites are more energetic and adsorb contaminants more strongly (difficult to clean).
- Current rinse recipes for SiO₂ need to be modified in applications involving heterogeneous structures with Hf-based high-k dielectrics.

Impact of Adsorption Rate on the Cleaning of High-k Dielectric Nano-Structures



Adsorption of contaminants on various dielectrics appears to be thermodynamically favorable; it readily takes place as long as surface is not saturated.

Impact of Desorption Rate on the Cleaning of High-k Dielectric Nano-Structures



The desorption dynamics play a key role in the cleaning of various high-k dielectrics (bottleneck and rate limiting in the overall process)

Electrical Tests Structures

- **Ge as a performance booster and sample novel material**
 - **High electron/hole mobility**
 - **High process compatibility**
 - **Low temperature process**
 - **Possible V_{dd} scaling for reduced power dissipation**

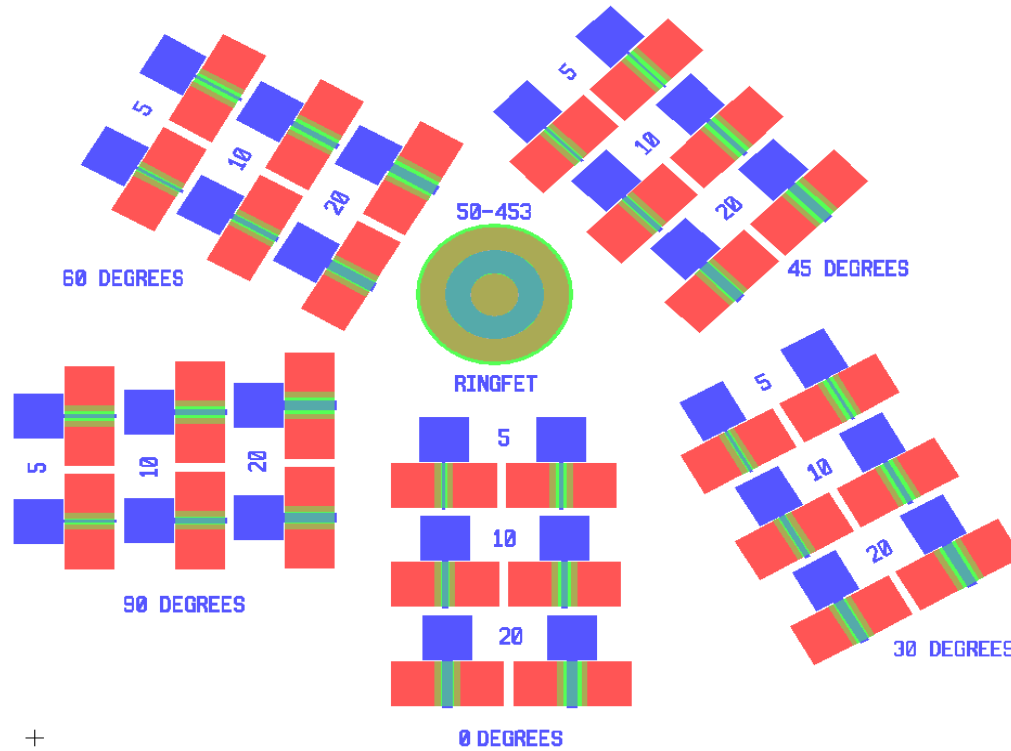
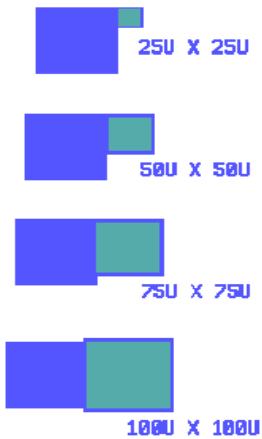
	Si	Ge
Electron m (cm ² /Vs)	1600	3900
Hole m (cm ² /Vs)	430	1900
Band gap (eV, 300K)	1.12	0.66
Dielectric constant	11.9	16
Melting point (°C)	1415	937

- **Key challenges: Interface property of Ge MOS gate stack**
 - **GeO₂ is regarded as a promising interface gate dielectrics***
 - **Since GeO₂ decomposition/GeO evaporation temperature is very low (430°C), low temperature oxidation is needed with high density of oxidant source**

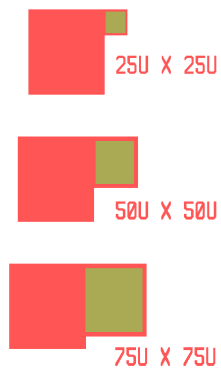
**D. Kuzum, IEDM2007, T. Takahashi, IEDM2007, Y. Nakakita, IEDM2008*

MOSFET Photolithography Mask Design

MOS CAPACITOR

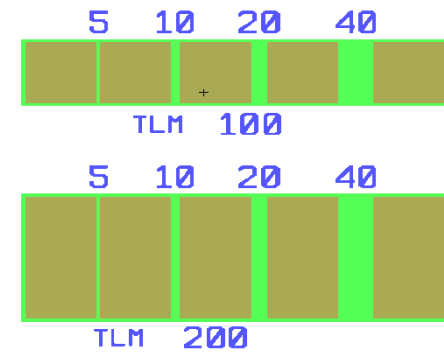
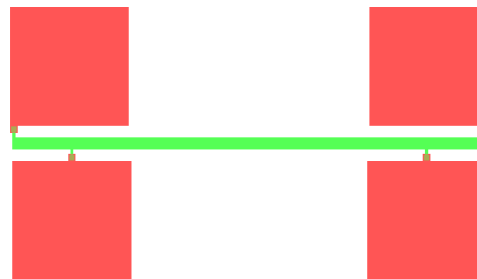


P-N JUNCTION DIODE



+

FOUR POINT PROBE

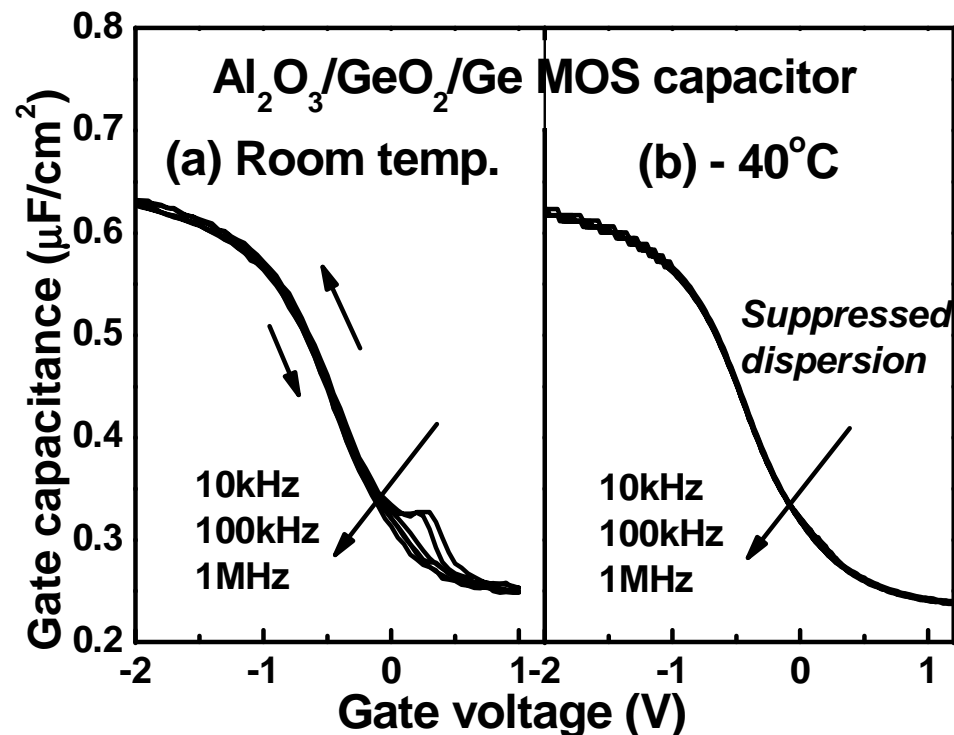


Experiments: Baseline of Cleaning Process using Capacitor Test Structures

- **Sample preparation**
 - (100) and (111) Ge surface was cleaned by PRS100 organic remover and by HCl/HF
 - Surface was oxidized by Slot-Plane-Antennal (SPA) radical oxidation system
 - Thermal oxidation was also done as a reference
- **Electrical property**
 - 5nm ALD Al_2O_3 was deposited on GeO_2/Ge
 - Sputtered Al metal pad
 - 400°C FGA anneal
 - XPS was used to identify surface chemical property
 - Synchrotron radiation photoemission spectroscopy (SRPES) was used for band offset measurement

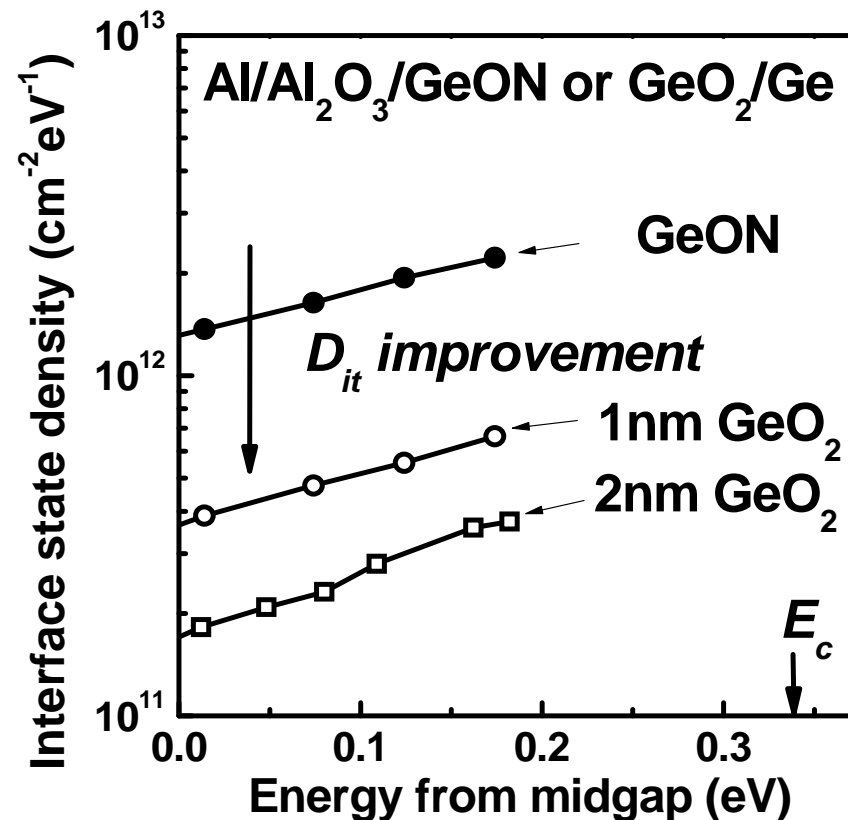
Electrical Properties of GeO₂/Ge Interface

- Al/Al₂O₃/GeO₂/Ge MOS capacitor:
 - 350°C ALD Al₂O₃ deposition + 400°C FGA anneal
 - Very small hysteresis and frequency dispersion
 - Low temperature measurement suppresses frequency dispersion due to minority carrier response



Interface State Density (D_{it}) of GeO_2/Ge

- Comparison between GeON and GeO_2 using capacitor structures
 - D_{it} was measured by conductance method
 - Significant improvement from GeON
 - Achieved $D_{it} = 1.4 \times 10^{11} \text{ cm}^{-2} \text{ eV}^{-1}$ at midgap



Summary

- **Conducted baseline etch tests on ALD HfO₂ and HfSi_xO_y in dilute HF**
- **Investigated the feasibility of etching the materials in ammonium hydroxide solutions after a pre-reduction treatment in H₂/N₂ gas mixtures**
- **Determined the rinse process parameters that are needed and will be used in developing reliable and robust low-water rinse recipes for cleaning of heterogeneous nano-structures**
- **Benchmarked high-k process with electrical characterization using new electrical test structures**

Industrial Interactions and Technology Transfer

- **Collaborative interactions with Initiative for Nanoscale Materials and Processes, INMP, at Stanford which is supported by 7 semiconductor and semiconductor equipment manufacturing companies.**
- **Interactions with ASM (Eric Shero and Eric Liu) for preparation of high-k test samples**

Future Plans

Next Year Plans

- **Pre-reduction of High-k wafers in CO/CO₂ mixtures to improve etching**
- **Use of complexing and chelating agents such as EDTA, and disulfonic acids in ammoniacal solutions to enhance dissolution**
- **Development of methodology and recipes for efficient rinsing and drying of heterogeneous structures using both process simulation and experimental measurements**
- **Ge P/N-MOSFET fabrication and electrical characterization
carrier mobility analysis – substrate orientation and channel anisotropy**
- **Electrical testing methodology applied for comparison of etch and clean/rinse/dry of high-k dielectric using new high aspect ratio features**

Publications, Presentations, and Recognitions/Awards

- Masaharu Kobayashi, Gaurav Thareja, Masato Ishibashi, Yun Sun, Peter Griffin, Jim McVittie, Piero Pianetta, Krishna Saraswat, Yoshio Nishi, “Radical oxidation of germanium for interface gate dielectric GeO₂ formation in metal-insulator-semiconductor gate stack,” *Journal of Applied Physics*, 106, 104117, 2009.
- X. Zhang, J. Yan, B. Vermeire, F. Shadman, J. Chae, “Passive wireless monitoring of wafer cleanliness during rinsing of semiconductor wafers,” *IEEE Sensors* (accepted).

“Sweet” PAGs: Environmentally Friendly Materials for Next Generation Lithography

(Task Number: 425.029)

PIs:

- Christopher K. Ober, Materials Science and Engineering, Cornell University
- Reyes Sierra, Chemical and Environmental Engineering, UA

Graduate Students:

- Lila Otero, PhD candidate, Chemical & Environmental Engineering, UA

Undergraduate Students:

- Lily Milner, Chemical & Environmental Engineering, UA

Other Researchers:

- Youngjin Cho, Postdoctoral Fellow, Materials Science & Eng., Cornell University
- Wenjie Sun, Postdoctoral Fellow, Chemical & Environmental Engineering, UA

Cost Share (other than core ERC funding):

- Intel support for laser spike annealing; \$100k (Jing Sha moved to this project)

SRC/SEMATECH Engineering Research Center for Environmentally Benign Semiconductor Manufacturing

Objectives

- **Develop PFOS-free and environmentally friendly PAGs with superior imaging performance. The novel PAGs will be based on biological units such as sugars and cholic acids for chemically amplified resist application**
- **Identify modeling tools to predict the environmental fate of novel PAGs.**

ESH Metrics and Impact

1. *Reduction in the use or replacement of ESH-problematic materials*

Complete replacement of perfluorooctanesulfonate (PFOS) structures including metal salts and photoacid generators in photoresist formulations

2. *Reduction in emission of ESH-problematic material to environment*

Develop new PAGs that can be readily disposed of in ESH friendly manner

3. *Reduction in the use of natural resources (water and energy)*

Prepare new PAGs using simple, energy reduced chemistry in high yields and purity to reduce water use and the use of organic solvents.

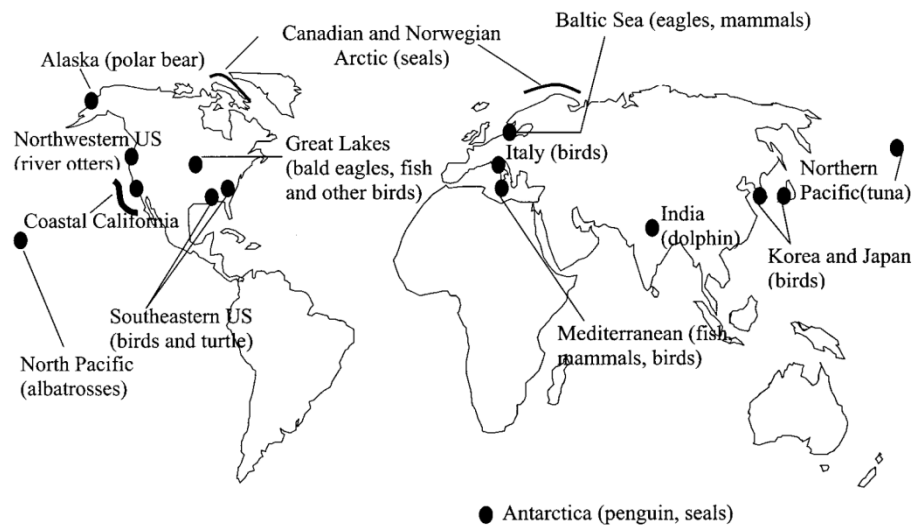
4. *Reduction in the use of chemicals*

By preparing new PAGs using simple chemistry in high yields and purity, we reduce the use of fluorinated chemicals.

Bioaccumulation of PFOS

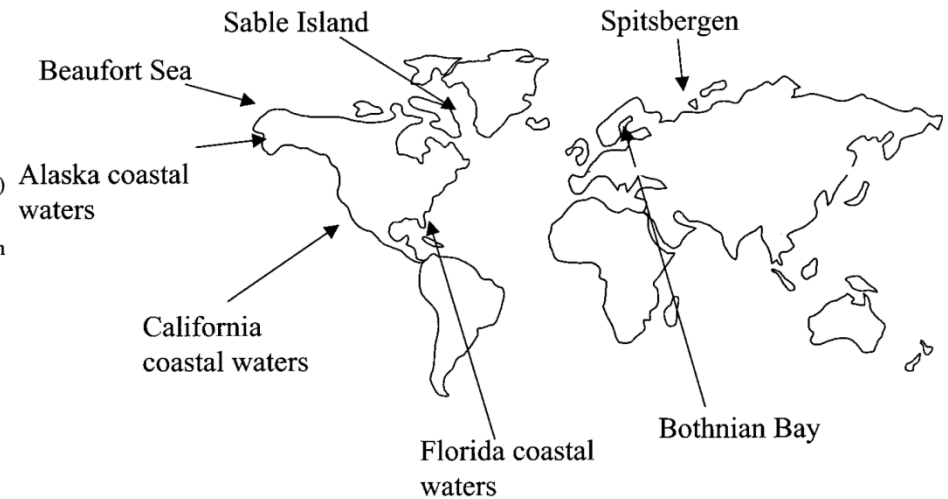
➤ PFOS and PFOS-related materials are potentially environmentally hazardous

Global Distribution of PFOS in Wildlife



Environ. Sci. Technol. 2001, 35, 1339.

Accumulation of PFOS in Marine Mammals



Environ. Sci. Technol. 2001, 35, 1593.

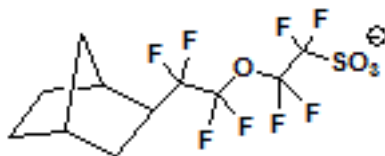
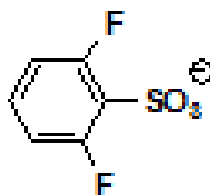
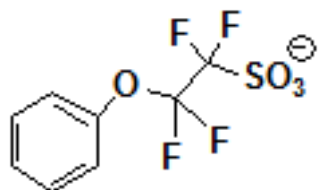
The EPA proposed a significant new use rule (SNUR) for PFOS in 2000

Next Generation PAGs – environmentally friendly, no bioaccumulation

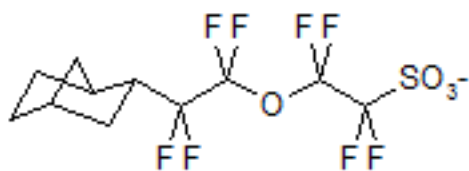
SRC/SEMATECH Engineering Research Center for Environmentally Benign Semiconductor Manufacturing

Prior Non-PFOS PAG Anions

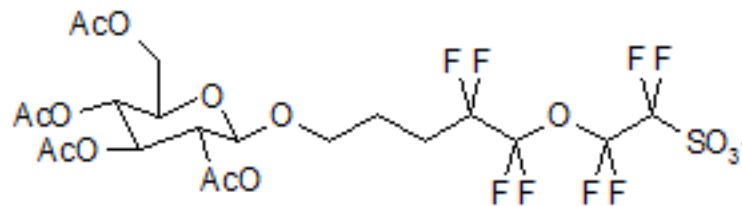
Selected examples:



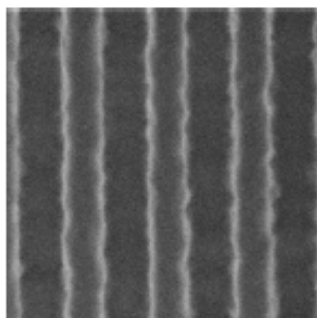
Evaluation of Lithographic Performance



NBPFEES (NB)



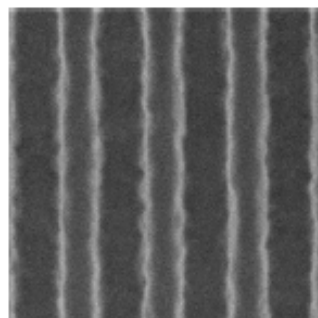
Sweet PAG (Sweet)



TPS-NB

90.8nm @ 23.8mJ/cm²

LER: 5.8±0.4



TPS-Sweet

92.2nm @ 27.3mJ/cm²

LER: 6.5±0.4

PAG	Esize@Ta rget	MEF	EL by +/- 10% of target CD
TPS-NB	25.48	3.18	12.94
Sweet PAG	49.78	3.20	12.90

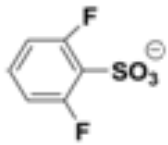
MEF (Mask Error Factor. The lower, the better)

EL (Exposure latitude. The higher, the better)

Collaboration with Rohm & Haas

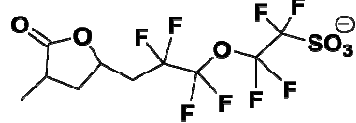
Environmental Compatibility of New Non-PFOS PAG Anions

Selected examples:



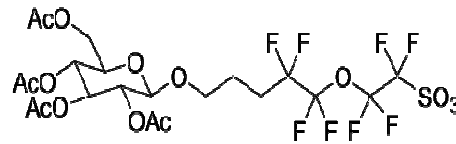
1st generation

(Aromatic structure)



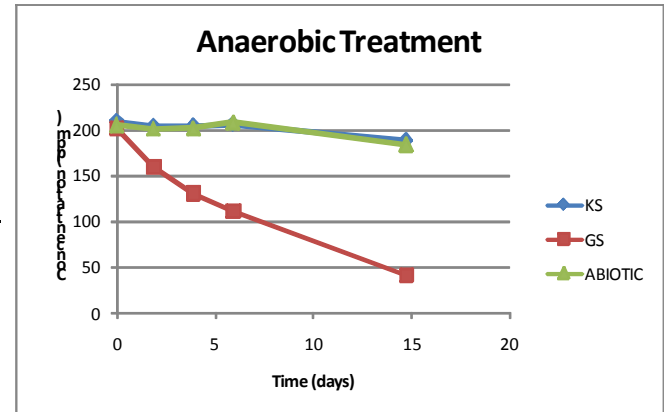
2nd generation

(Aliphatic structure)



3rd generation

(Sugar structure)

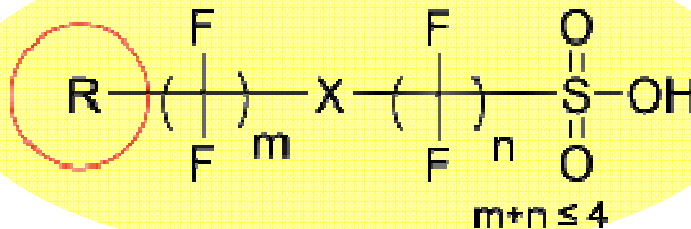


Degradation for 2nd generation PAG in anaerobic batch bioassays. (KS) Abiotic sterilized control; (GS) complete treatment with active sludge; (ABIOTIC) sterile, non-inoculated control.

- **1st Generation Non-PFOS PAGs:** Low toxicity and low bioaccumulation potential but relatively persistent to microbial degradation.
- **2nd Generation Non-PFOS PAGs:** Preliminary results show that replacing the phenyl group with a UV-transparent alicyclic moiety increases the susceptibility of the PAG compound to biodegradation.
- **3rd Generation Non-PFOS PAGs:** Replacing with sugar and natural groups is expected to increase biodegradation.

Molecular Design of New PAGs: PFOS-free salts

1st & 2nd
Generation



3rd Generation

Polar	Hydrophilic	Aromatic	Linear
Nonpolar	Hydrophobic	Aliphatic	branch ring

Sugar based
"Sweet" PAG

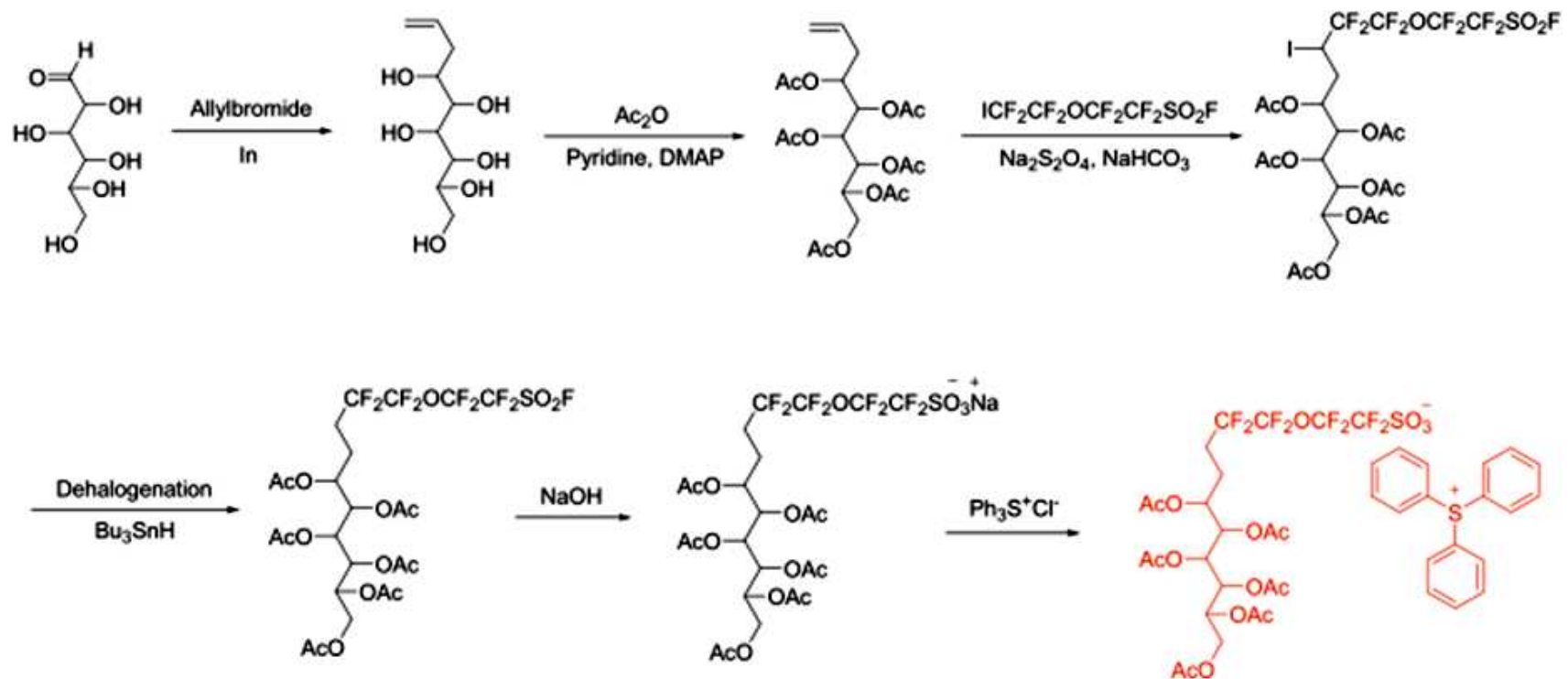
Natural molecules
based
Biocompatible/
Biodegradable PAG

Practical synthetic chemistry considerations:

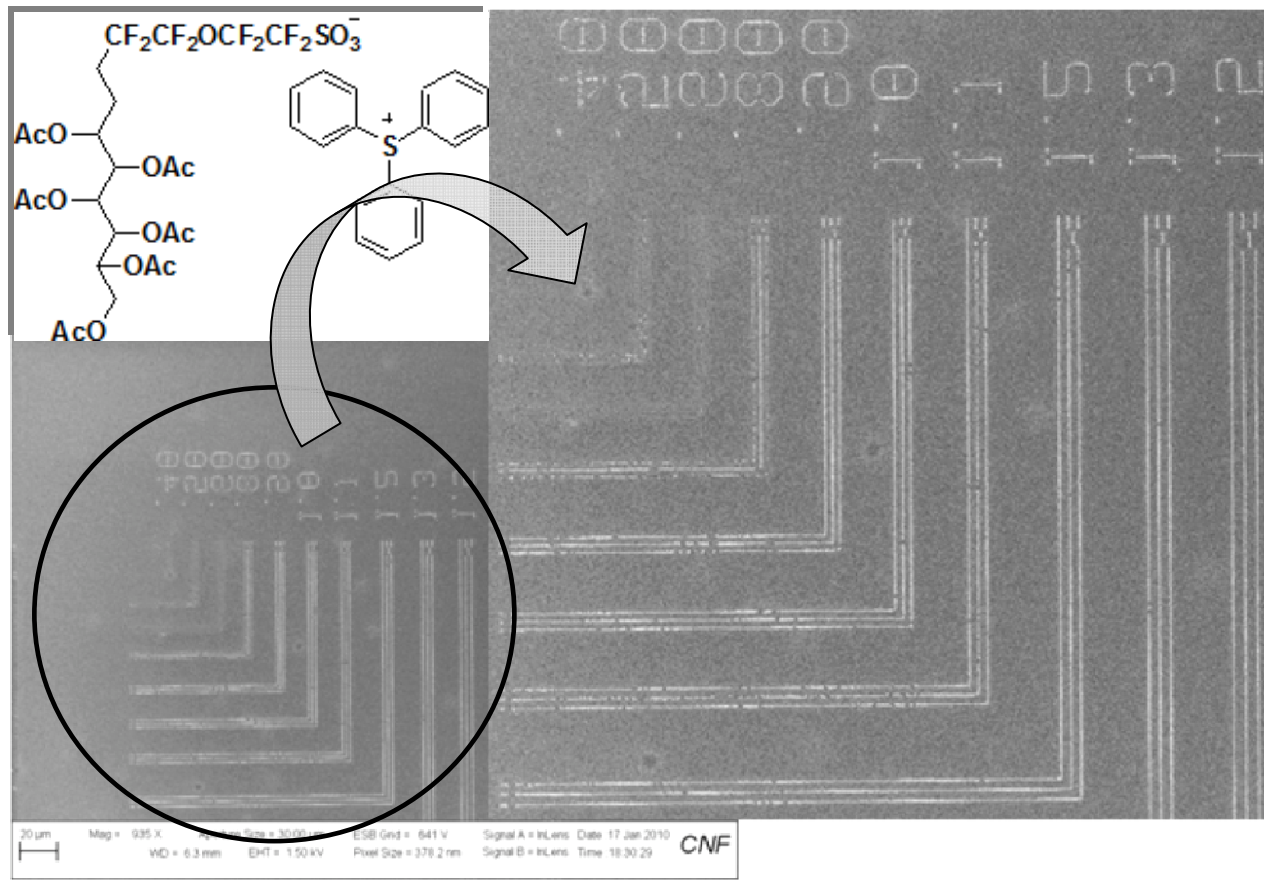
- Simple chemistry — low cost & less time
- Efficient reactions — high yield & high purity

Synthesis of linear type “Sweet” PAG

➤ Synthetic scheme:



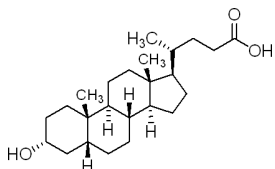
Evaluation of Lithographic Performance



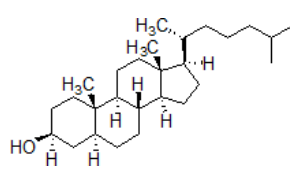
SEM images of resist films of ESCAP blended separately with linear type Sweet PAG.

Synthesis of “Biocompatible” PAGs

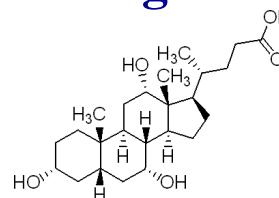
➤ New PAGs based on Steroids and their analogs:



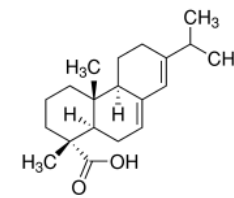
Lithocholic acid



Dihydrocholesterol

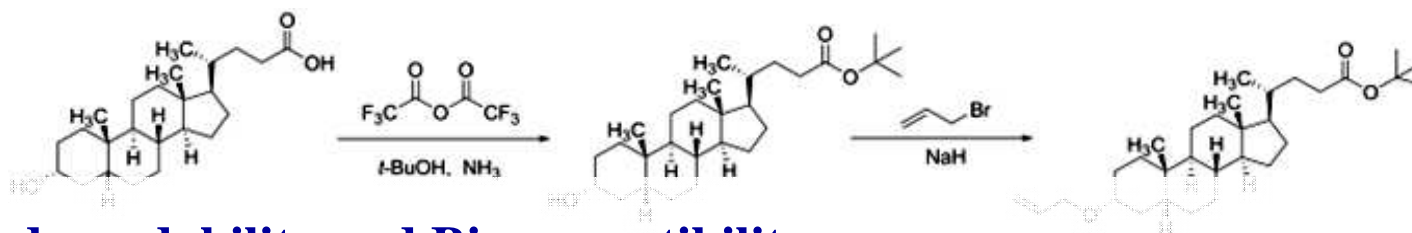


Cholic acid



Abietic acid (Pine resin acid)

➤ Synthetic scheme:



- Biodegradability and Biocompatibility

- Miscibility with 193 nm MG resists

- Cholic acid, Lithocholic acid and Abietic acid (Pine resin acid)

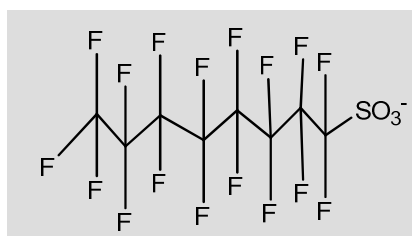


Future Plans

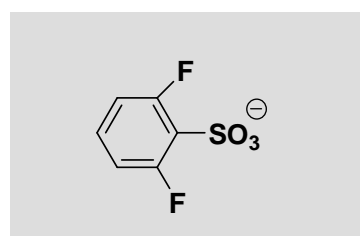
Next Year's Plans

- **Prepare next generation PAGs (4 or more compounds) based on biomolecules**
- **Reduce synthetic steps and use more environmentally friendly chemicals**
- **Evaluate the lithographic performance of new PAGs**

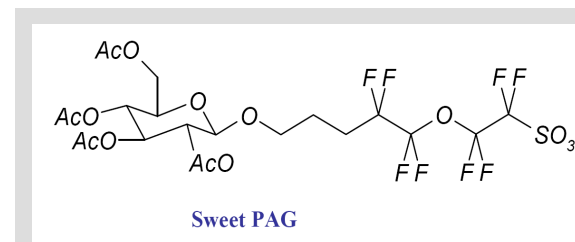
Environmental Compatibility of New Non-PFOS PAGs



PFOS
(Perfluoroalkyl sulfonate)



1st generation PAGs
(Aromatic structure)



2nd and 3rd generation PAGs
(Aliphatic structure)

Biodegradability	NO	NO	YES
Chemical Degradation	NO	YES	YES
Aquatic Toxicity	LOW	LOW	???
Bioaccumulation	YES	NO	NO

Chemical Degradation of New Generation PAGs

Advanced Oxidation: Fenton's Reaction (Fe(II)/H₂O₂)

Fenton's reaction



PAG + radicals → Oxidized products

Non-PFOS PAG compounds were effectively degraded by advanced oxidation using the Fenton's reaction

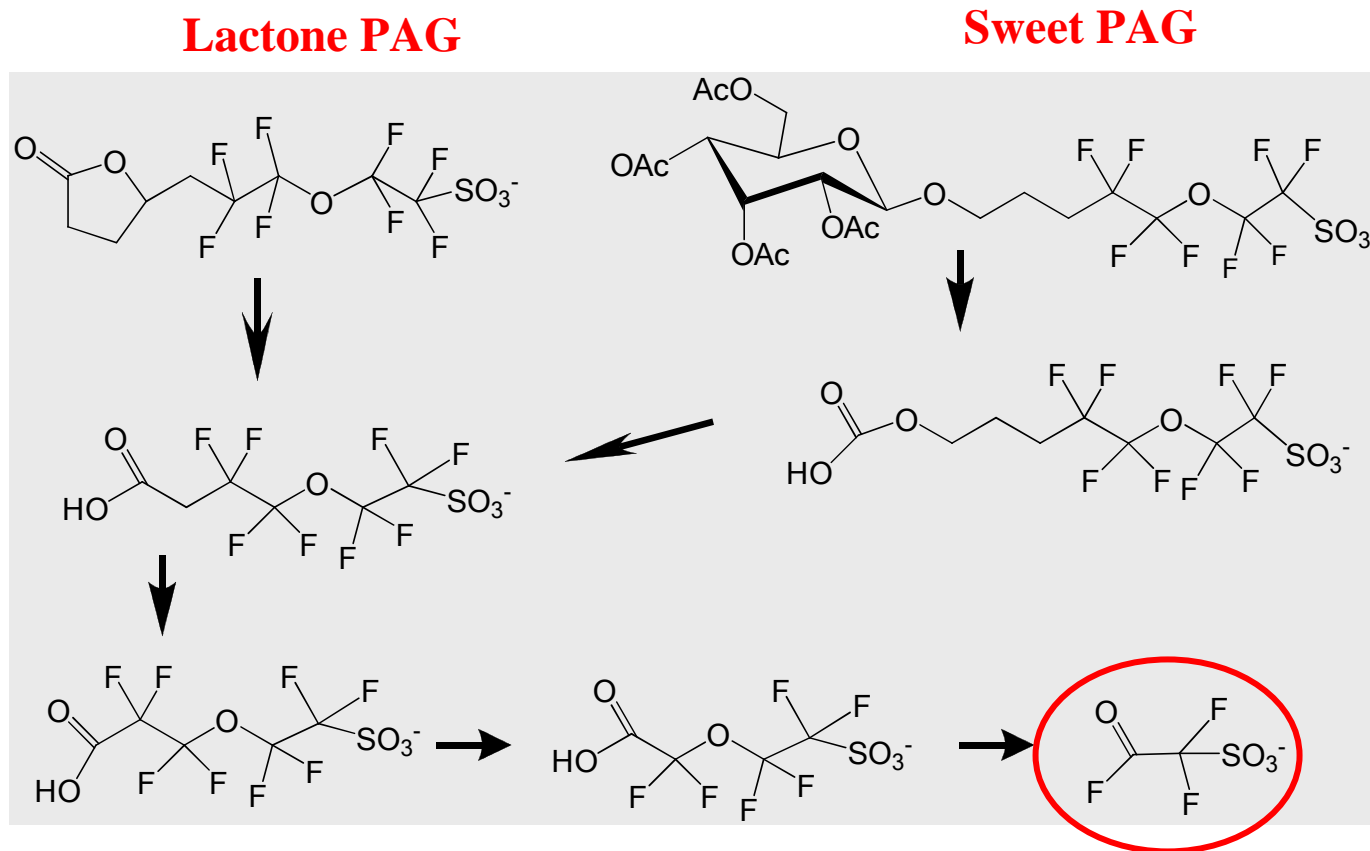
Perfluorinated PAGs such as PFOS and PFBS were resistant to attack.

PAG Compound	Compound Removed (%)	Fluoride Released (%)
1st Generation PAGs		
SF1	100	94.1
SF2	100	3.9
PF1	100	41.9
SF3	ND	0.3
SF4	ND	0.8
2nd Generation PAGs		
Sweet PAG	100	5.7
Lactone PAG	100	8.7
Reference PAGs		
PFOS	0.8	0.6
PFBS	0.5	0.4

ND= Not determined

Chemical Degradation of New Generation PAGs

Advanced Oxidation: Fenton's Reaction ($\text{Fe(II)/H}_2\text{O}_2$)



Proposed degradation mechanism based on mass spectrometry (MS) data

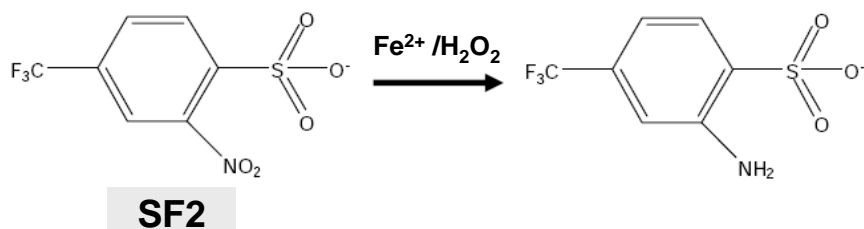
Chemical Degradation of New Generation PAGs

Reductive Treatment with Zero-Valent Iron

Redox degradation by ZVI



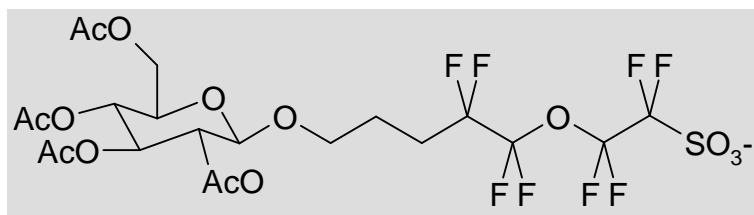
Reductive treatment with ZVI was not effective in removing non-PFOS PAG compounds.



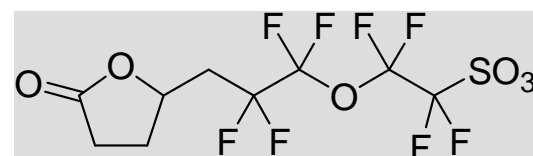
PAG Compound	Compound Removed (%)	Fluoride Released (%)
1st Generation PAGs		
SF1	11	7.1
SF2	100	2.8
PF1	11	2.0
SF3	ND	1.8
SF4	ND	0.8
2nd Generation PAGs		
Sweet PAG	1	5.7
Lactone PAG	1	8.7
Reference PAGs		
PFOS	0	0.1
PFBS	0	0.4

ND= Not determined

Microbial Degradation of New Generation PAGs



Sweet PAG (Sweet)

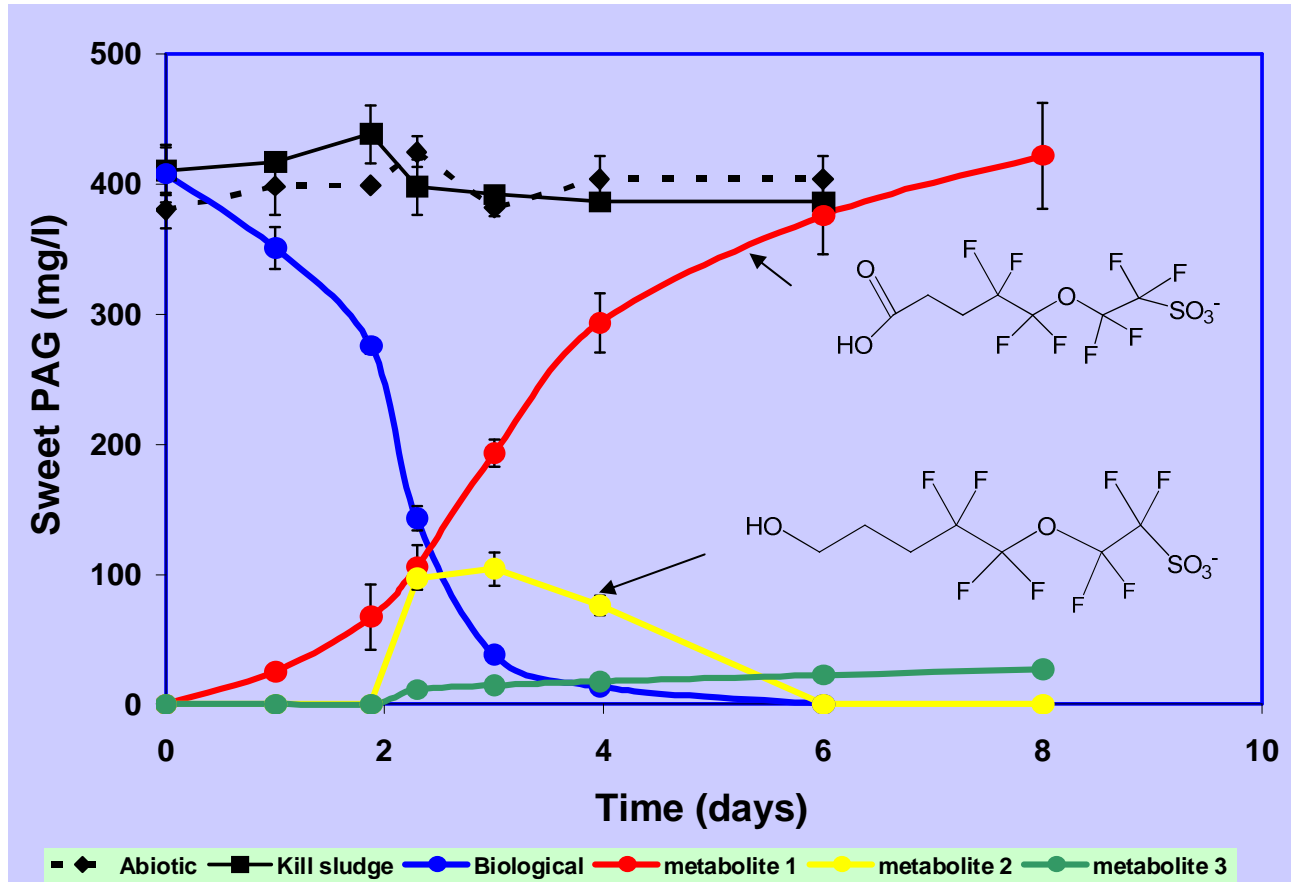


Lactone

Compounds	Aerobic Degradation	Anaerobic Degradation
Sweet PAG	YES	YES
Lactone PAG	YES	??
PFOS	NO	0
PFBS	NO	0

Biomolecule-based PAGs are degraded by microorganisms in activated sludge

Microbial Degradation of New Generation PAGs



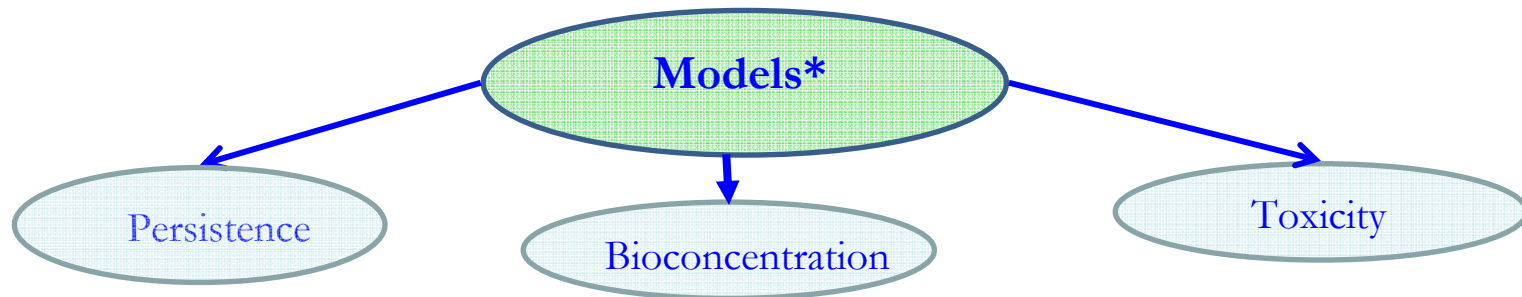
The "Sweet PAG" is readily degradable by aerobic bacteria in activated sludge.

Conclusions

The newly developed, biomolecule-based PAGs present significant ESH advantages compared to PFOS-based PAGs. They are readily degraded by microorganisms and by chemical oxidation (Fenton's reagent ($\text{H}_2\text{O}_2/\text{Fe}(\text{II})$)).

Future Work

- Evaluation of key environmental properties of the novel PAGs.
- Evaluate the treatability of novel PAGs in conventional wastewater treatment.
- Strategies to increase (bio)degradability: Biodegradation testing of structurally-related compounds modified with selected functionalities.
- Testing the validity of selected computer models to predict the (bio)degradation potential and other compound properties determining the environmental fate of PAGs.



e.g. EPA PBT Profiler, UM-BBD (University of Minnesota Biocatalysis/Biodegradation Database)
CATABOL

Industrial Interactions and Technology Transfer

- **Collaboration with Rohm & Haas Electronic Materials for photolithography tests of Sweet PAG concluded**
- **Samples provided to Orthogonal, Inc. – a small startup**
- **Performance at 193 nm and EUV evaluated with the assistance of International Sematech**
- **Ongoing interactions with Intel on LER issues**

Task Deliverables

- **Report on the completion of testing of new PFOS-free photoacid generators for 193 nm and EUV performance (Dec 06)**
 - *completed*
- **Report on the assessment of the environmental compatibility of new PFOS-free photoacid generators. (Dec 07)**
 - *completed*
- **Report on the completion of testing to determine the removal of PFOS-free photoacid generators by biological and physico-chemical treatment methods. (May 08)**
 - *completed*
- **Report on new PFOS-free PAGs with improved performance and improved environmental impact. (Mar 09)**
 - *completed*

Publications, Presentations, and Recognitions/Awards

Publications

- Yi Y., Ayothi R., Wang Y., Li M., Barclay G., Sierra-Alvarez R., Ober C. K. “Sulfonium Salts of Alicyclic Group Functionalized Semifluorinated Alkyl Ether Sulfonates As Photoacid Generators” *Chem. Mater.* 2009, 21, 4037.
- Jing Sha, Byungki Jung, Michael O. Thompson, and Christopher K. Ober, “Submillisecond post-exposure bake of chemically amplified resists by CO2 laser spike annealing”, *J. Vac. Sci. Technol. B*, 27(6), 3020-3024 (2009)
- Ayothi R., Yi Y., Cao H. B., Wang Y., Putna S., Ober C. K. “Arylonium Photoacid Generators Containing Environmentally Compatible Aryloxyperfluoroalkanesulfonate Groups” *Chem. Mater.* 2007, 19, 1434.
- Ober C. K., Yi Y., Ayothi R. “Photoacid generator compounds and compositions” *PCT Application* WO2007124092, April 2007.

Presentations

- Gutenberg Research Prize Award Address, University of Mainz, Mainz, Germany, August 24, 2009. “High Resolution Lithography and the Orthogonal Processing of Organic Semiconductors”, invited talk.
- CMM Workshop on Flexible Electronics, Traditions at the Glen, Johnson City, NY 13790. “Orthogonal Processing - a new strategy for patterning organic electronics”, invited talk.
- European Polymer Federation Meeting, Graz, Austria, July 12 – 17, 2009. “Self-assembly and directed assembly: Tools for Current Challenges in Nanofabrication”, plenary talk.
- 2009 Lithography Workshop, Coeur d’Alene, Idaho, June 20-July 2, 2009. “Molecular glass resists developed in unconventional solvents”, invited talk.
- Frontiers of Characterization and Metrology for Nanoelectronics, College of Nanoscale Science and Engineering, The University at Albany, Albany, NY, May 11-15, 2009. “The challenges posed to metrology by new approaches to advanced patterning”, invited talk – given by E. Schwartz.

Recognitions/Awards

- 2009 Gutenberg Research Awards for C. K. Ober
- 2009 Fellow of the American Chemical Society for C. K. Ober

Students on Task 425.029

- Graduated Students and Current Affiliation
 - Nelson Felix, AZ Microelectronics, Dec 2007
 - Victor Pham, JSR Microelectronics, May 2004
 - Victor Gamez, CH2M Hill, May 2009
- Internships (Task and related students)
 - Katy Bosworth, IBM
 - Evan Schwartz, Intel
 - Anuja de Silva, IBM
 - Jing Sha, NIST

Supercritical Carbon Dioxide Compatible Additives: Design, Synthesis, and Application of an Environmentally Friendly Development Process to Next Generation Lithography (Task Number: 425.030/425.031)

PI:

- Christopher K. Ober, Materials Science and Engineering, Cornell University

Collaborator:

- Juan de Pablo, Chemical and Biological Engineering, University of Wisconsin-Madison

Graduate Student:

- C. Ouyang: PhD candidate, Materials Science and Engineering, Cornell University
- G. N. Toepperwein, PhD candidate, Chemical Engineering, University of Wisconsin



SRC/SEMATECH Engineering Research Center for Environmentally Benign Semiconductor Manufacturing



Objectives

- **To demonstrate high-resolution patterning capabilities and scCO₂ development of molecular glass resists based on environmentally benign cores**
- **To synthesize and characterize fluorinated quaternary ammonium salts (QAS) as CO₂ compatible additives to develop conventional photoresists in scCO₂**
- **To demonstrate environmentally benign development of conventional photoresists using scCO₂ and silicone fluids using silicon-containing additives**

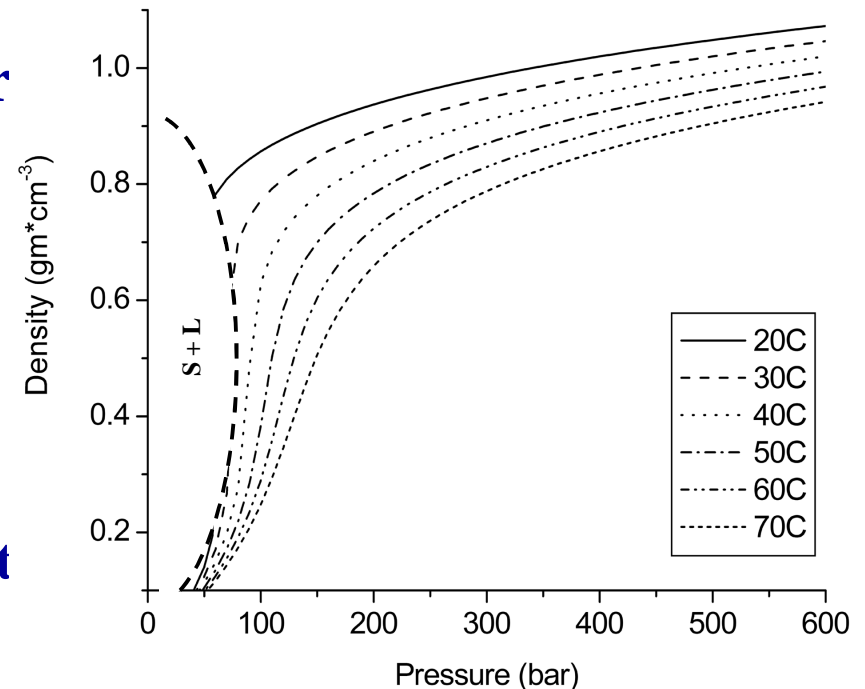
ESH Metrics and Impact

	Usage Reduction			Emmision Reduction			
Goals/Possibilities	Energy	Water	Chemicals	PFCs	VOCs	HAPs	Other
Reduce organic solvents used in processing materials	No energy used to purify and treat water	Eliminate need for water usage	Up to 100% reduction of organic solvents used	N/A	Minimal use of organic solvents	Up to 100% reduction of HAPs	N/A
Reduce processing time / temperature	Reduce anneal process costs	N/A	N/A	N/A	N/A	N/A	N/A
Additive processing	N/A	N/A	Eliminate waste of costly material	N/A	Minimal use of organic solvents	N/A	N/A

Why a Non-Aqueous Developer Solvent?

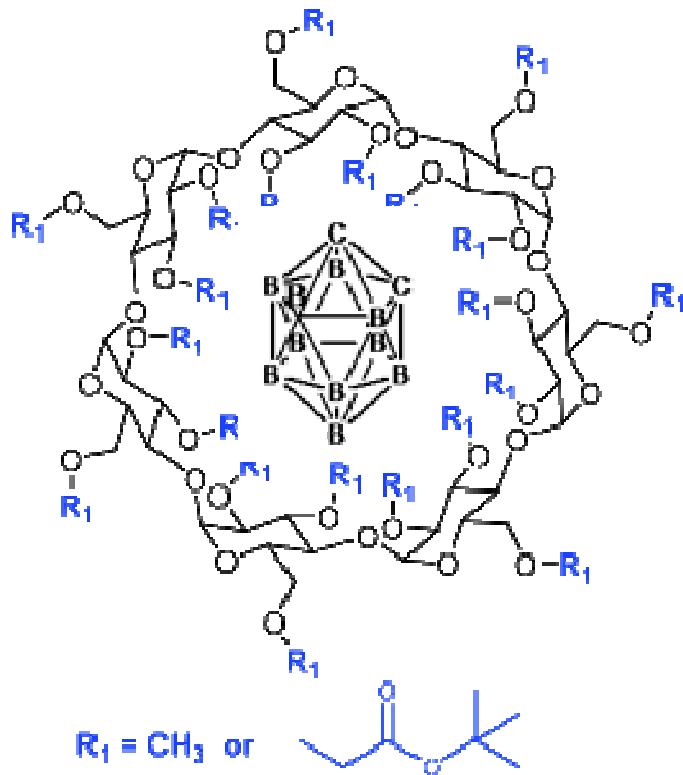
Environmental and Performance Advantages of scCO₂

- **Environmentally friendly, zero VOC solvent**
- **Highly tunable solvating power**
 - $\rho(T,P)$
 - Leaves no residue
 - Clean separations
- **One-phase fluid**
 - Zero surface tension
 - Transport, viscosity between that of liquid and gas
- **Nonpolar, inert character**
- **Potential to reduce LER and eliminate pattern collapse**

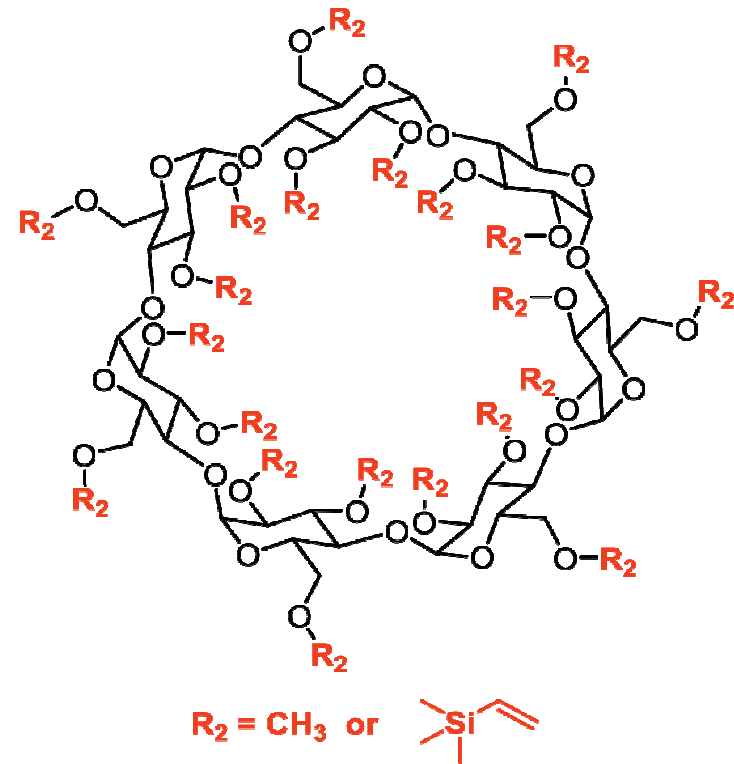


Molecular Glass Resists with Alicyclic Cores

Environmental friendliness and scCO₂ solubility



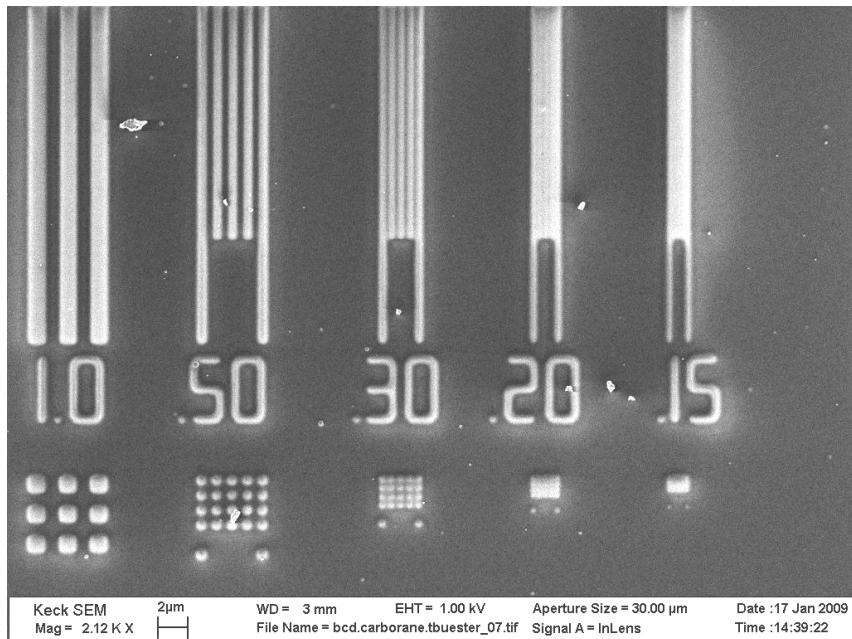
Cyclodextrin-carborane complex



Vinyl silane cyclodextrin

Cyclodextrins are good hosts for inclusion complexes and have potential as molecular resists to hold functional moieties on their periphery

Electron Beam Patterning and scCO₂ Development of Cyclodextrin Resists

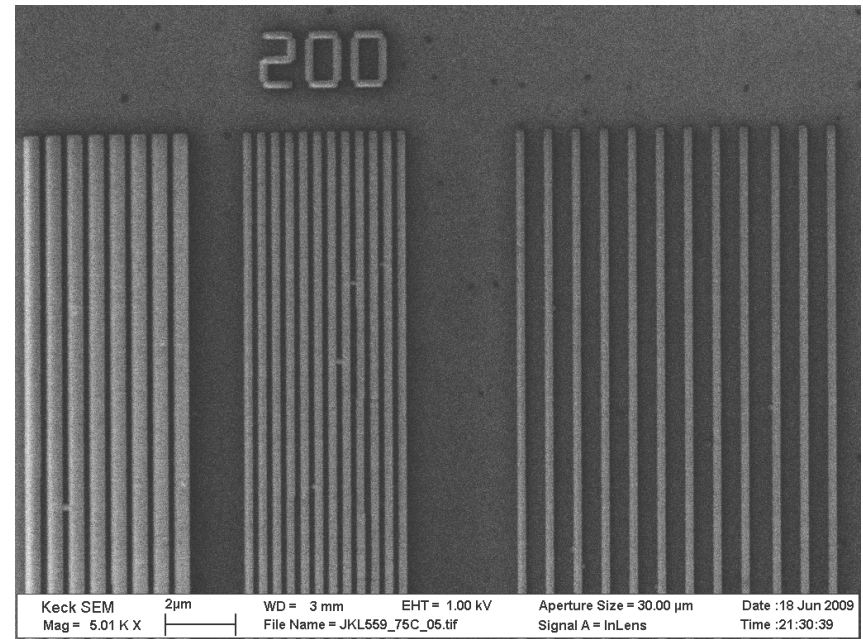


Cyclodextrin-Carborane complex

E-beam dose = $\mu\text{C}/\text{cm}^2$

PEB: 115 °C, 60 sec

scCO₂: 5000 psi, 5 min



Vinyl silane cyclodextrin

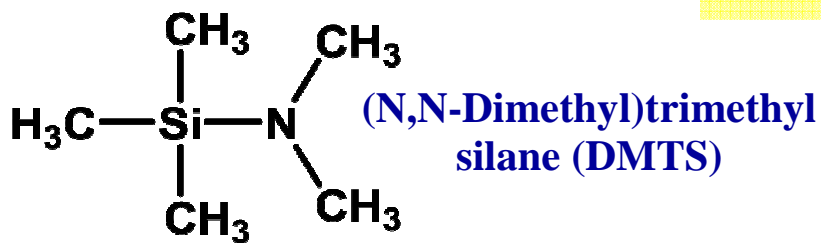
E-beam dose = 44 $\mu\text{C}/\text{cm}^2$

PEB: 75 °C, 60 sec

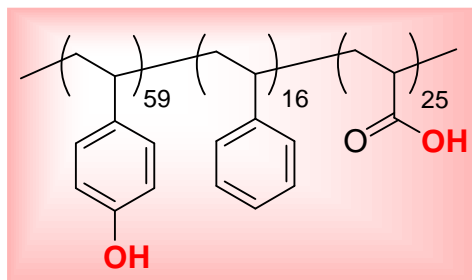
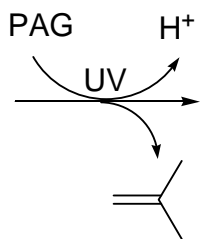
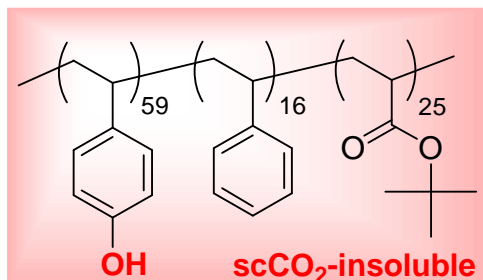
scCO₂: 2000 psi, 2 min

Additives for scCO₂ to Develop Conventional Resists

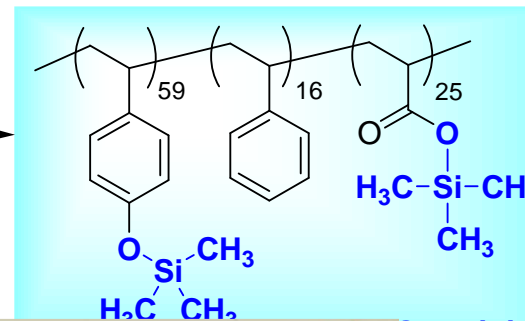
• Silicon-containing Additive



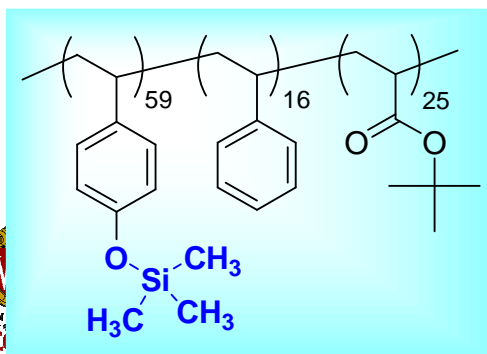
UV exposure



DMTS

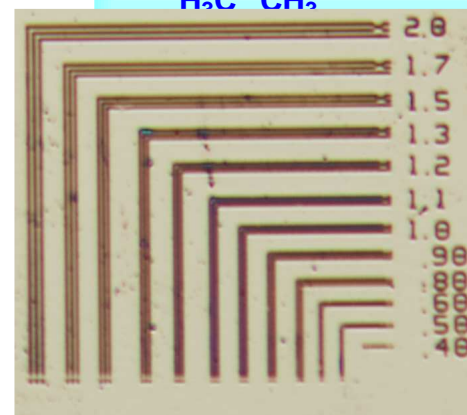


DMTS Development

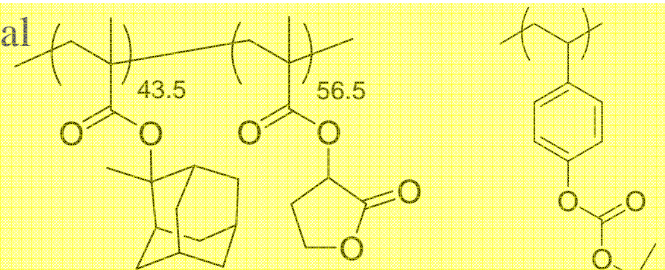


-According to resist materials and lithographic conditions, both positive and negative-tone imaging is possible

Negative image



Other conventional resists tested



PMAMA-co-GBLMA from Mitsubishi Rayon America (PMAMA-co-GBLMA)

PBOCST

Development

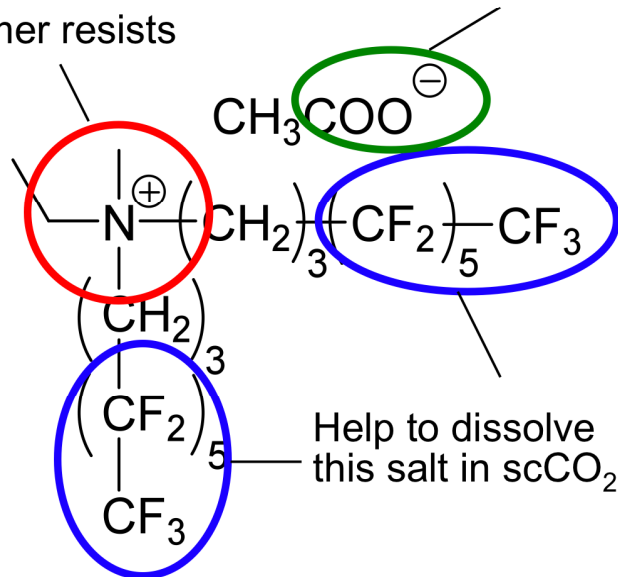
Quaternary Ammonium Salts (QAS)

scCO₂ Compatible Additives:

Fluorinated Quaternary Ammonium Salts (QAS)

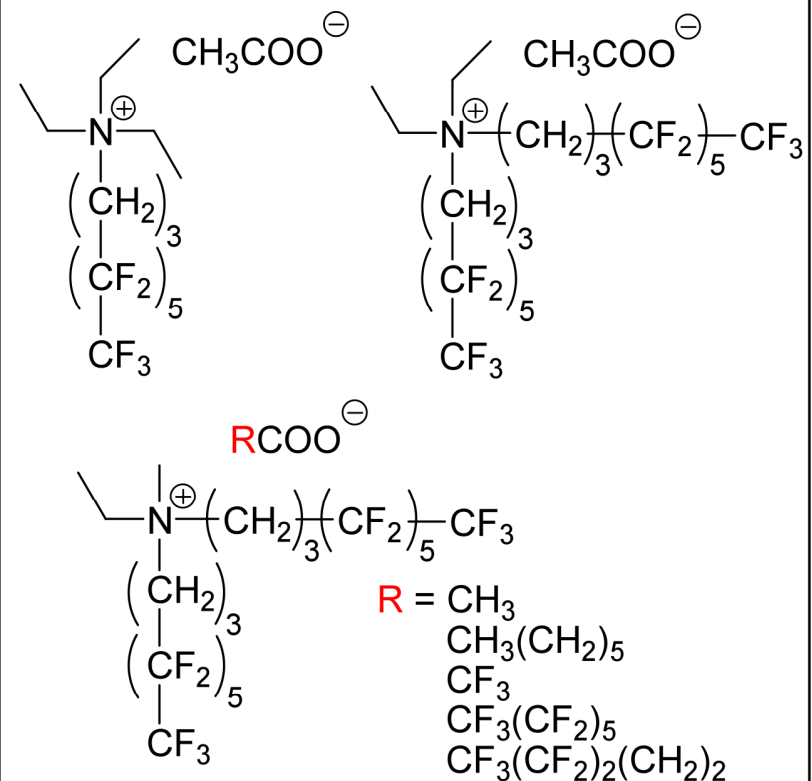
High affinity to phenolate and/or carboxylate moieties in polymer resists

Deprotonate from OH and/or COOH in polymer resists



Some of the fluorinated ammonium salts form **Micelle** in scCO₂.

Examples of fluorinated QAS



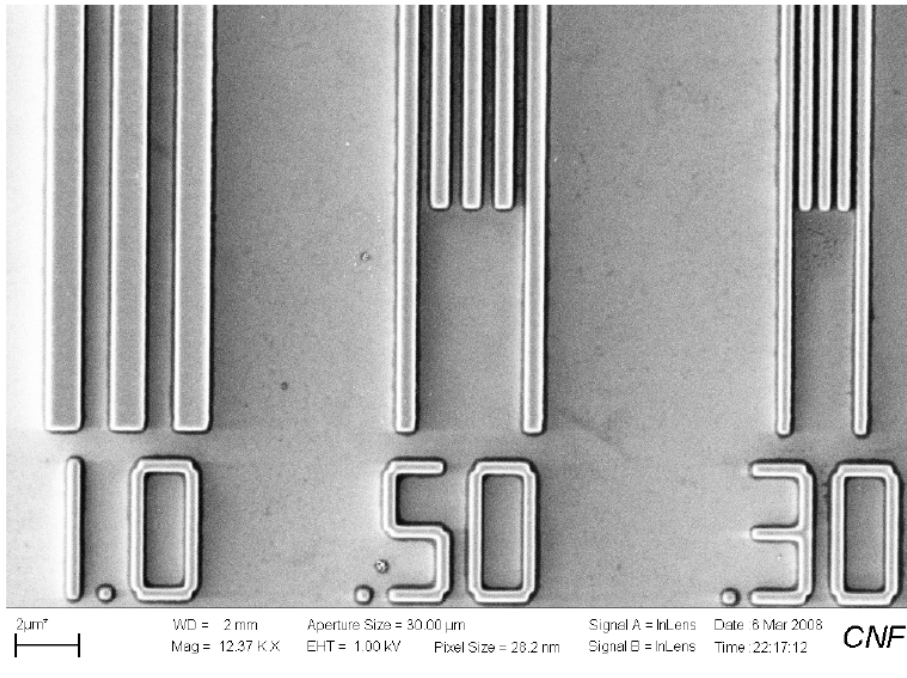
Initial Dissolution Results of Resists with QAS

QAS	Resist	Unexposed	Exposed	note
$ \begin{array}{c} \text{CH}_3\text{COO}^\ominus \\ \\ \text{---N}^\oplus\text{---}(\text{CH}_2)_3\text{---}(\text{CF}_2)_5\text{---CF}_3 \\ \\ (\text{CH}_2)_3 \\ \\ (\text{CF}_2)_5 \\ \\ \text{CF}_3 \end{array} $ <p>QAS-4 (1.25 mM)</p>	PBOCST	Dissolution (40 nm/min)	Slow dissolution (1-4 nm/min)	<i>Negative tone resist</i>
	ESCAP (Du Pont)	Dissolution (25 nm/min)	No dissolution	<i>Negative tone resist</i>
	PMAMA-co- GBLMA (Mitsubishi Rayon)	No dissolution	No dissolution	
	EUV-P568 (TOK)	Dissolution (15 nm/min)	Slow dissolution (1-2 nm/min)	<i>Negative tone resist</i>
$ \begin{array}{c} \text{CF}_3\text{CF}_2\text{COO}^\ominus \\ \\ \text{---N}^\oplus\text{---}(\text{CH}_2)_3\text{---}(\text{CF}_2)_5\text{---CF}_3 \\ \\ (\text{CH}_2)_3 \\ \\ (\text{CF}_2)_5 \\ \\ \text{CF}_3 \end{array} $ <p>QAS-7 (1.25 mM)</p>	PBOCST	No dissolution	No dissolution	
	ESCAP (Du Pont)	No dissolution	No dissolution	
	PMAMA-co- GBLMA (Mitsubishi Rayon)	No dissolution	No dissolution	
	EUV-P568 (TOK)	Dissolution (45 nm/min)	Slow dissolution (<1 nm/min)	<i>Negative tone resist</i>

Exposed by UV lamp (254 nm, 24 mC/cm²), developed in scCO₂ at 50°C and 5000 psi.

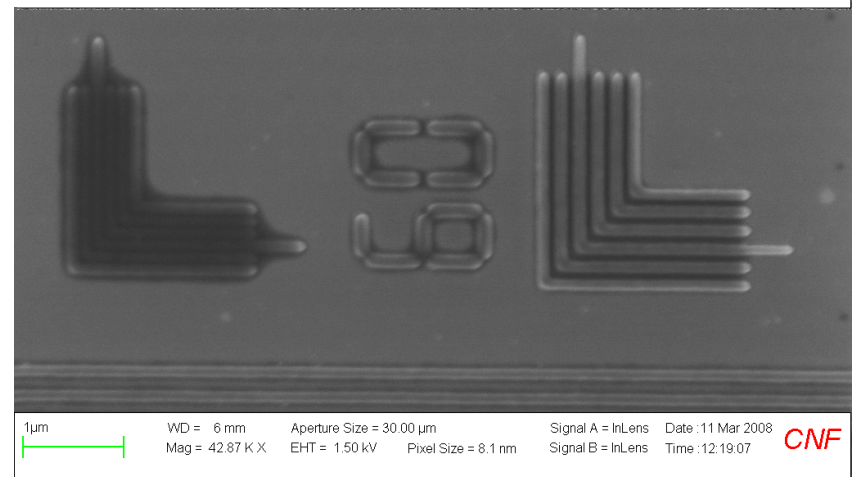
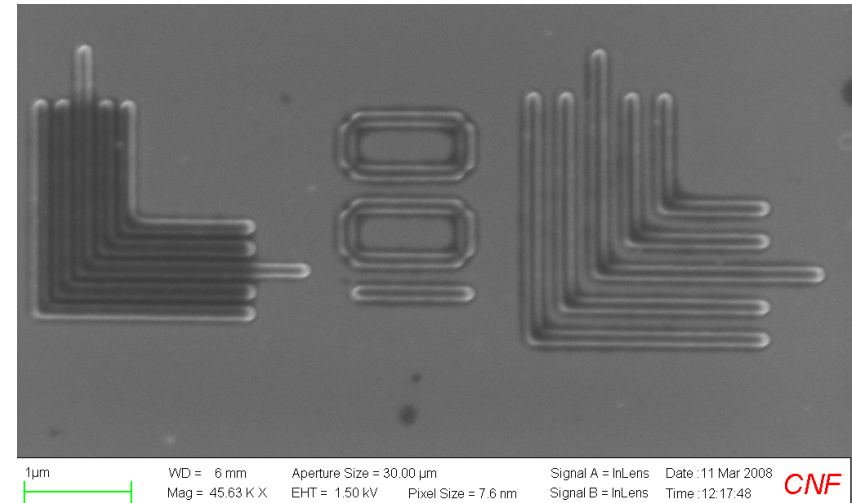
Electron Beam Patterning

Development test of EB-patterned TOK resist (EUV-P568) with QAS-4 or QAS-7



Dose: 107 $\mu\text{C}/\text{cm}^2$, QAS-4 (1.25 mM), dev. for 60 min at 50°C, 5000 psi, flow 30 min

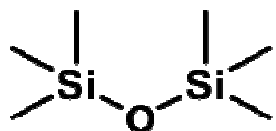
Negative tone patterns with sub-100 nm feature sizes were obtained.



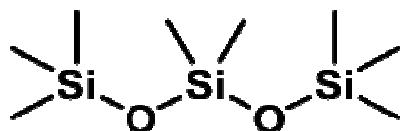
Dose: 20 $\mu\text{C}/\text{cm}^2$, QAS-7 (1.25 mM), dev. for 60 min at 50°C, 5000 psi, flow 30 min

Silicone Fluids-Linear Methyl Siloxanes

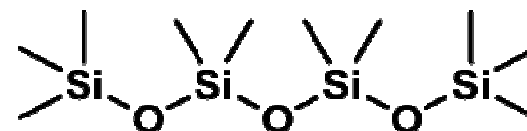
- **Low in toxicity**
 - **Environmentally friendly**
 - **VOC exempt**
- **Contribute little to global warming**
- **Non-ozone depleting**
 - **replacement for Ozone Depleting Substances**
- **Low surface tension**
 - **potential to eliminate patterns collapse**
- **Can be recycled**
 - **degrade to naturally occurring chemical species**



Hexamethyldisiloxane



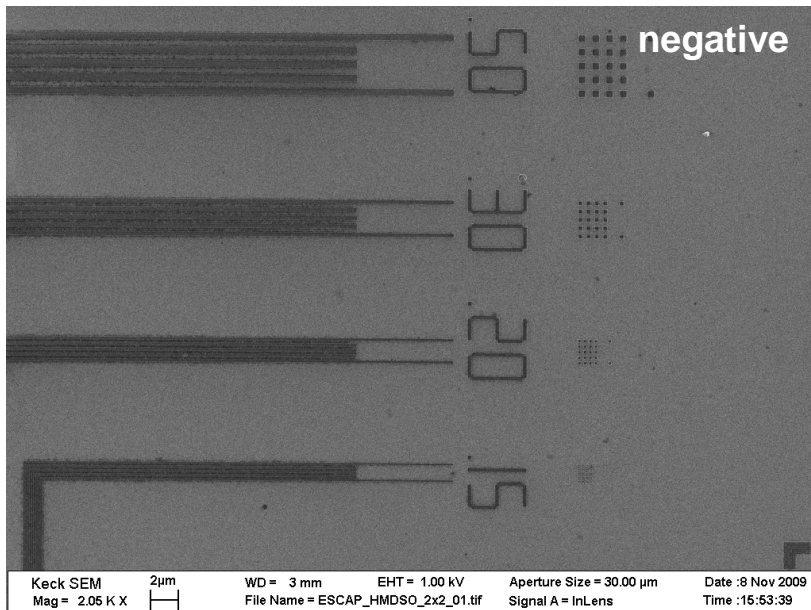
Octamethyltrisiloxane



Decamethyltetrasiloxane

D. E. Williams, ACS Symposium Series, 2000, 767, 244-257.

Electron Beam Patterning and Silicone Fluid Development of Conventional Photoresists



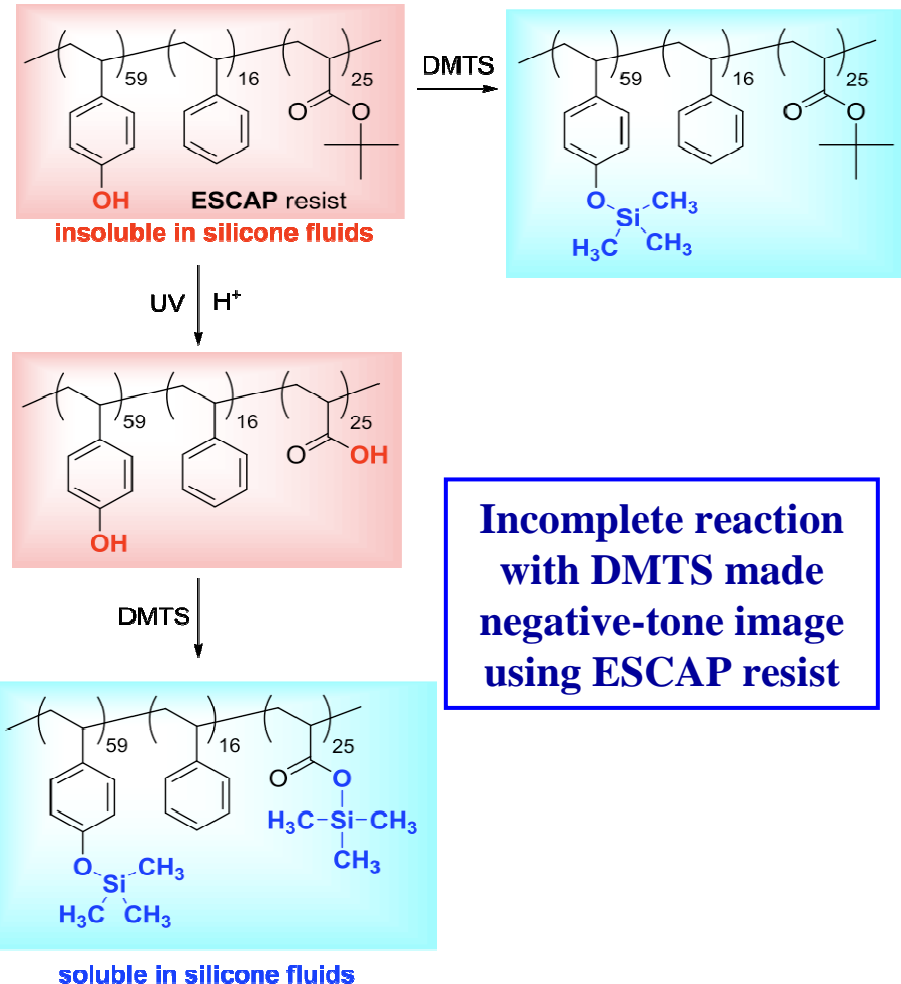
Photoresist: ESCAP

Chemical modifier: DMTS

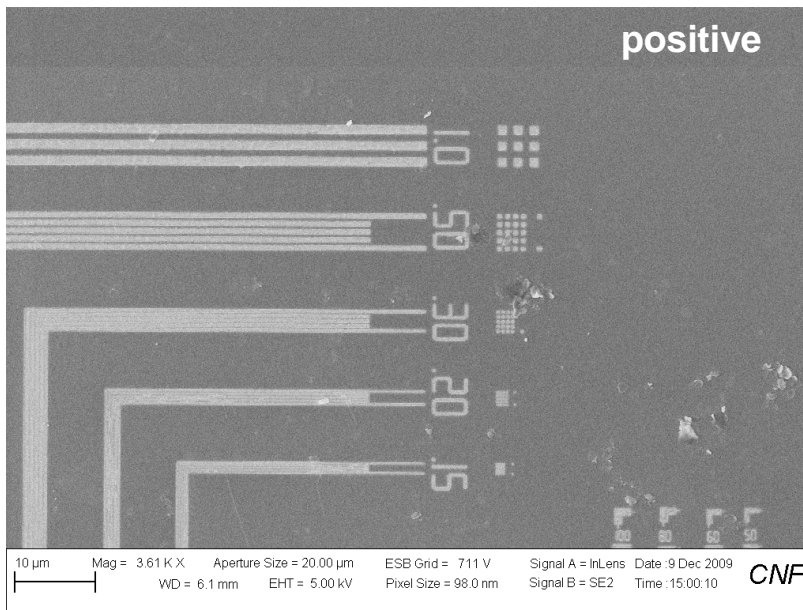
Solvent: Hexamethyldisiloxane

E-beam dose = $\mu\text{C}/\text{cm}^2$

PEB: 115 °C, 60 sec



Electron Beam Patterning and Silicone Fluid Development of Conventional Photoresists



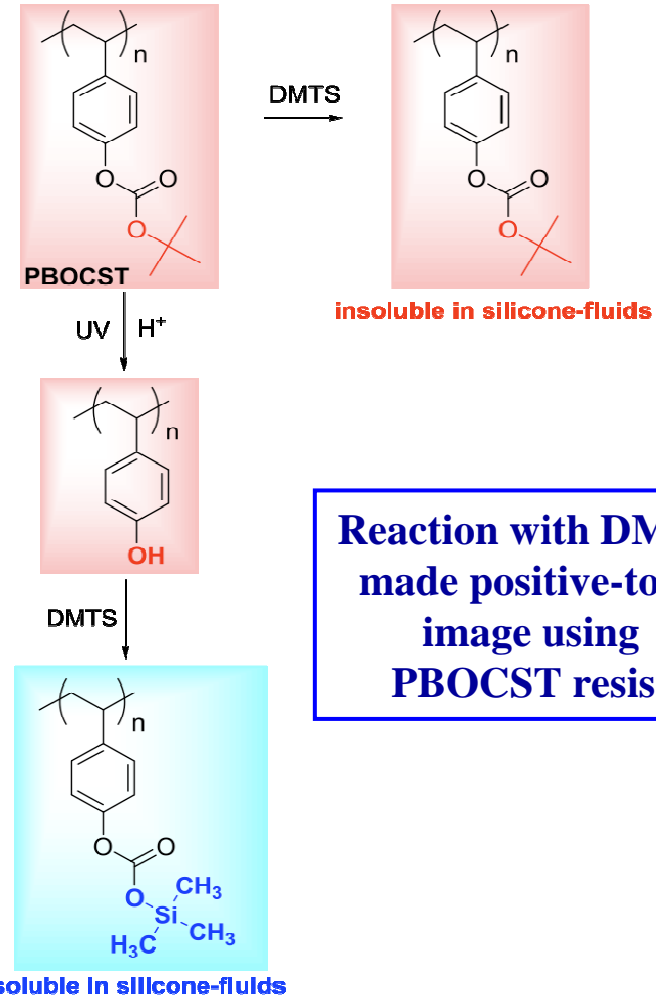
Photoresist: PBOCST

Chemical modifier: DMTS

Solvent: Octamethyldisiloxane

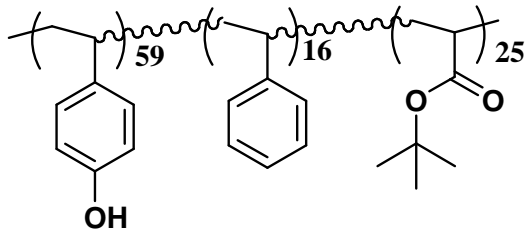
E-beam dose = $\mu\text{C}/\text{cm}^2$

PEB: 90 °C, 60 sec

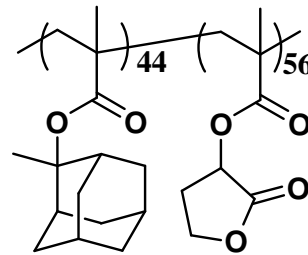


Systems of Interest

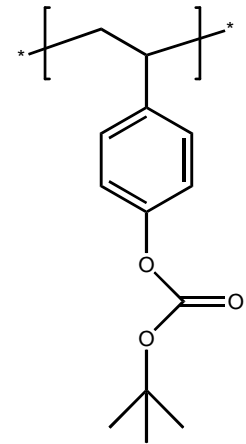
- Model photoresists in their protected forms



ESCAP



193nm-resist

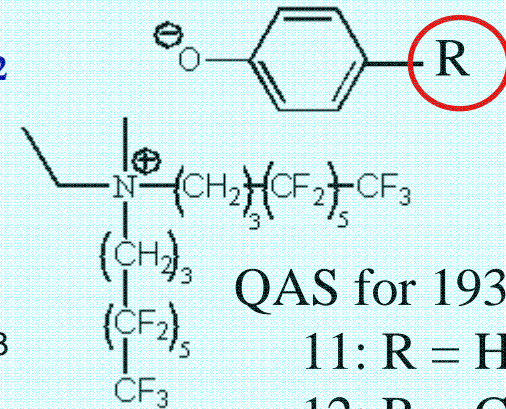
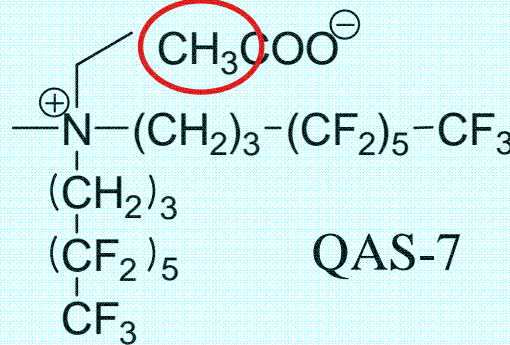
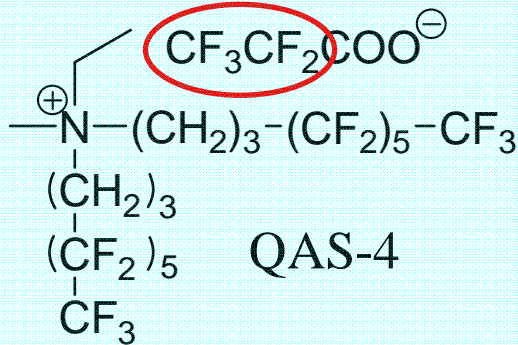


PHOST

- QAS Additives

- Previously shown to be soluble in CO₂

QAS for ESCAP & PHOST

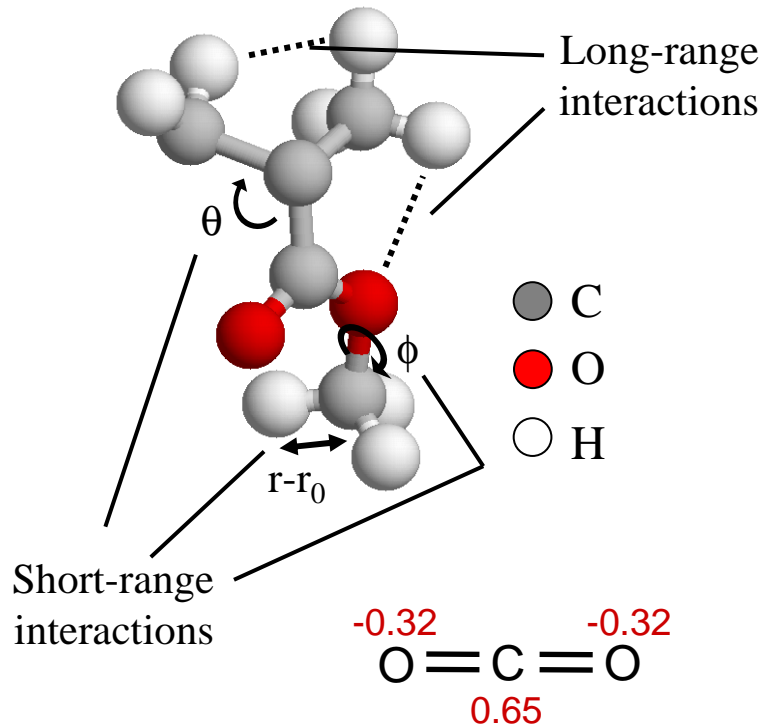


QAS for 193nm-resist

- 11: R = H
- 12: R = CH₃
- 13: R = CF₃
- 14: R = NO₂

Model

- Simulation allows screening of large numbers of systems and enables direct observation of molecular behavior



charges important: scCO₂ has a large quadrupole moment

OPLS Model:

$$V_{\text{tot}} = \underbrace{V_{\text{LJ}} + V_{\text{coul}}}_{\text{Intramolecular}} + \underbrace{V_{\text{bon}} + V_{\text{ang}} + V_{\text{tors}}}_{\text{Intermolecular}}$$

$$V_{\text{LJ}} = 4 \cdot \epsilon \cdot \left[\left(\frac{\sigma}{r} \right)^{12} - \left(\frac{\sigma}{r} \right)^6 \right]$$

$$V_{\text{coul}} = \frac{q_i \cdot q_j}{4 \cdot \epsilon_0 \cdot \epsilon \cdot r}$$

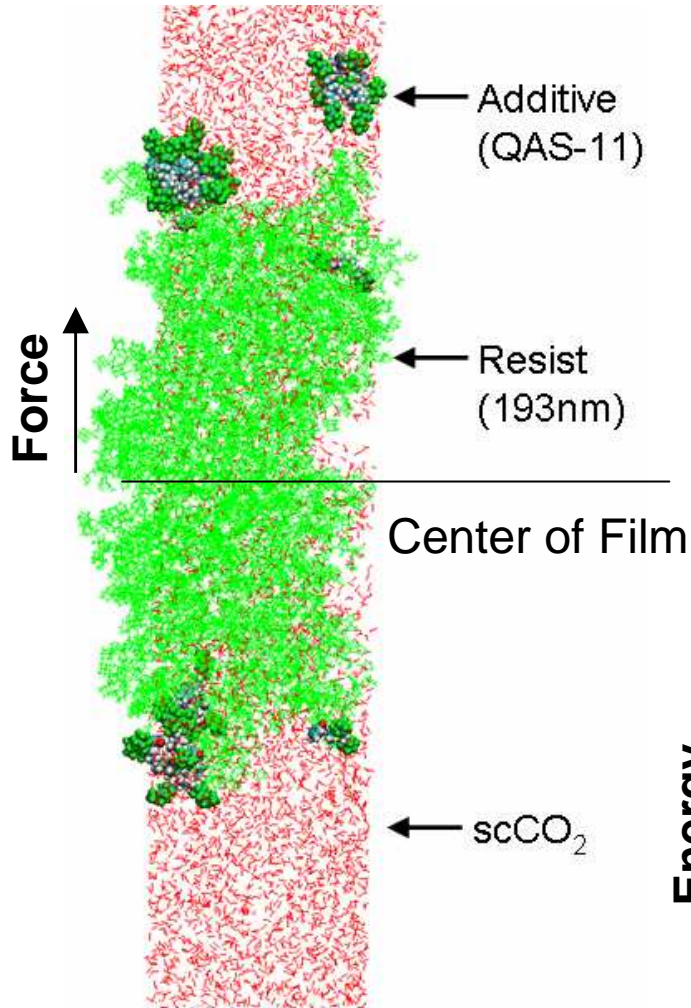
$$V_{\text{bon}} = \frac{1}{2} \cdot k_{\text{bon}} \cdot (r - r_0)^2$$

$$V_{\text{ang}} = \frac{1}{2} \cdot k_{\text{ang}} \cdot (\theta - \theta_0)^2$$

$$V_{\text{tors}} = \sum_n k_n \cdot (1 + \cos(n \cdot \phi - \phi_0))$$

- OPLS force field employed for most parameters
- We calculated charges (q_i) using quantum mechanics
- Process Conditions: $T = 340\text{K}$ ($\sim 67^\circ\text{C}$)
 $P = 345$ bar

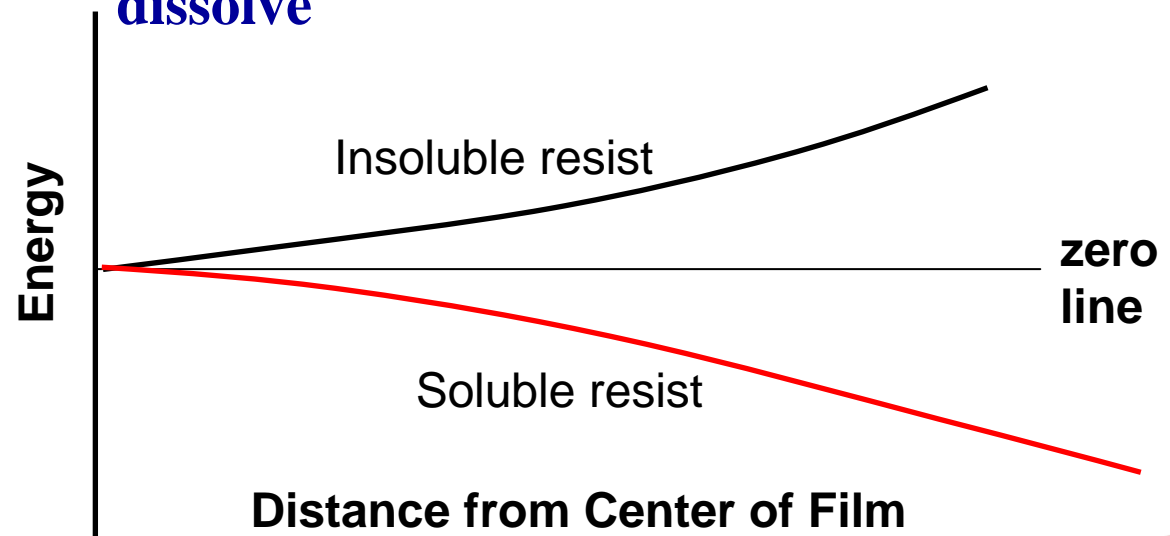
Free Energy Calculation



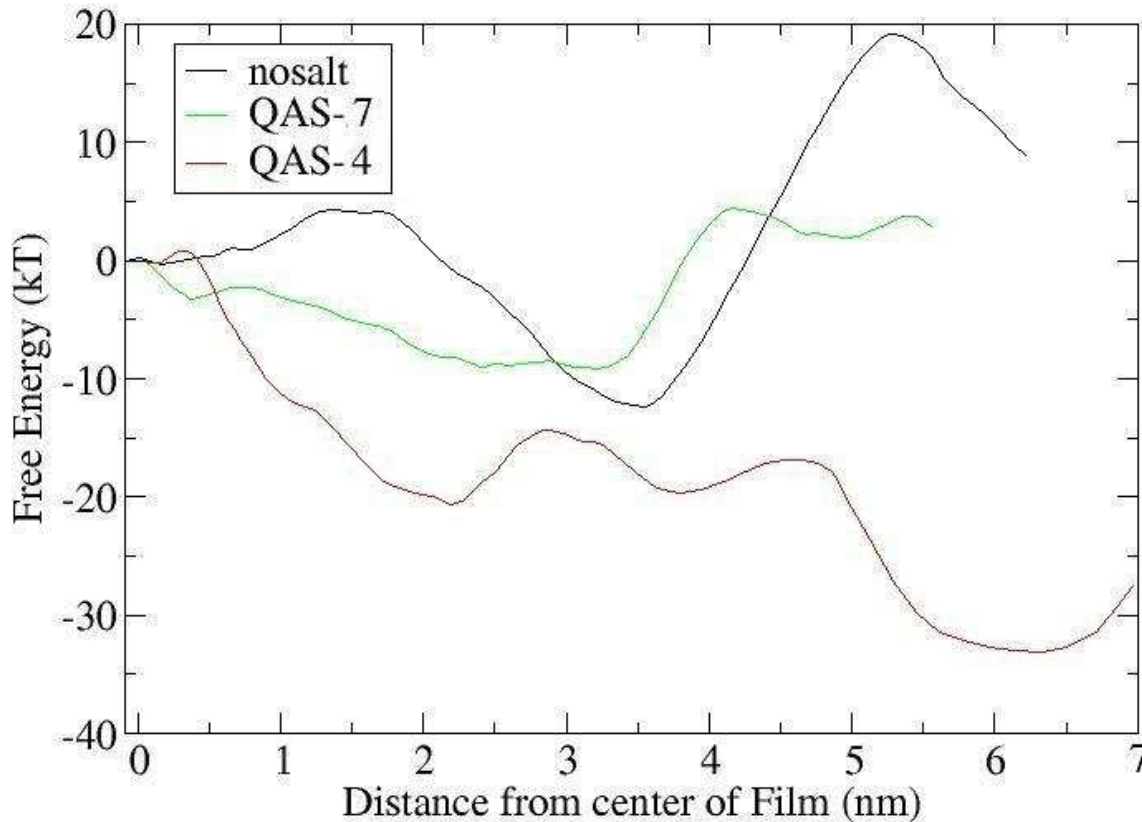
- Thin films of resist are equilibrated in scCO₂ via MD simulation
- Integrating the force on each chain as a function of position provides free energy

$$F(z) = \int_z^{z_\infty} \langle f(z') \rangle dz' + F(z_0)$$

- If the energy is lower at the surface than the center, the film is unstable and will dissolve



Sample Result: ESCAP Energy Curve

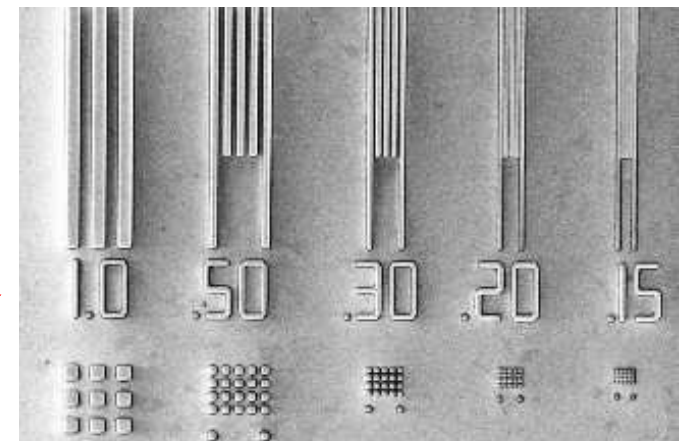
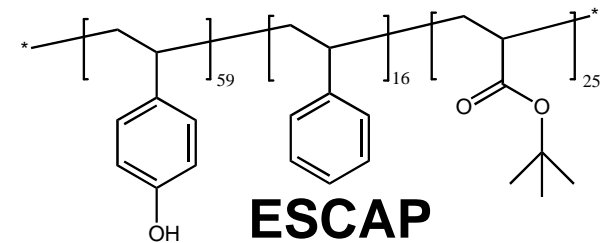


Experimental Results:

No salt – 0 nm/sec

QAS-7 – 0 nm/sec

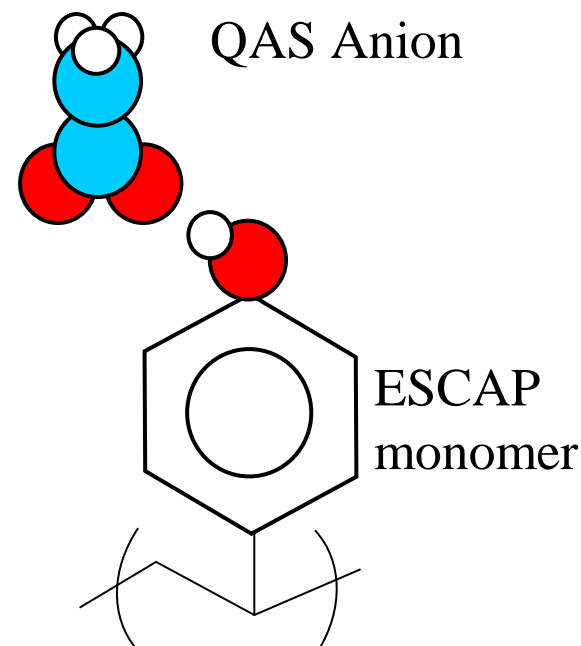
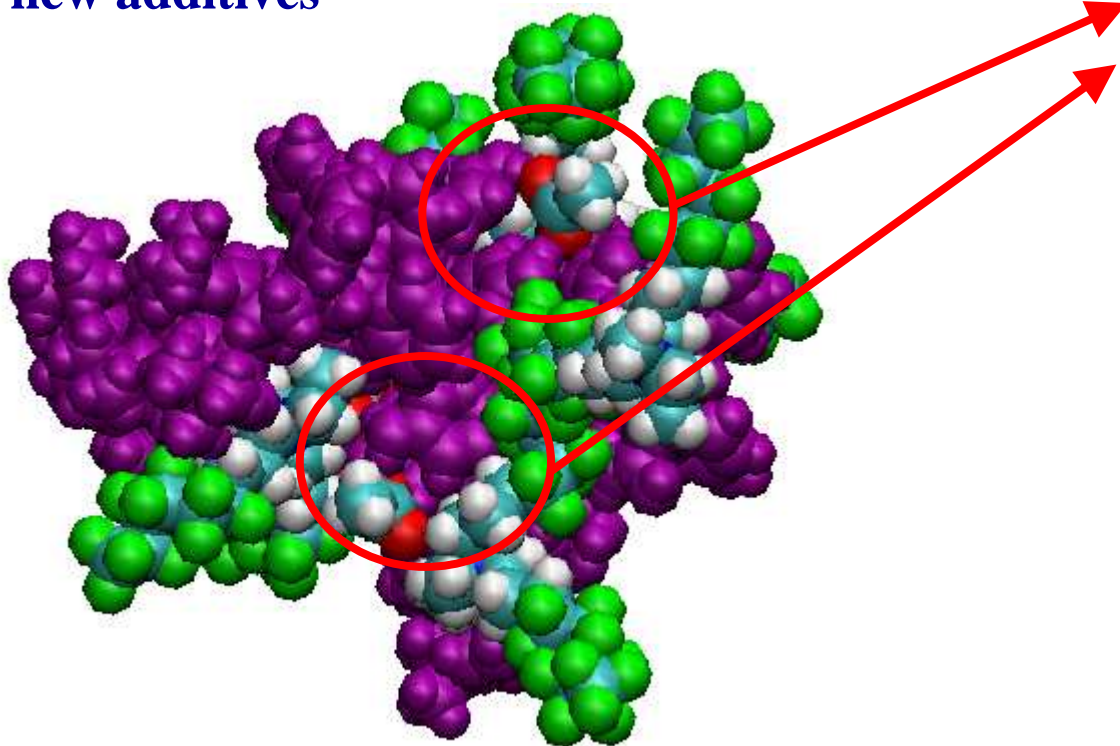
QAS-4 – 20 nm/sec



- Only addition of QAS4 to ESCAP results in reduced energy at surface of film (right of plot), indicating eventual dissolution
- Viability confirmed experimentally

ESCAP Mechanism with QAS4

- The $-OH$ group of ESCAP associates with the anions; contacts last >500 ps.
- Reducing available polar regions increasing solubility in $scCO_2$
- Will use understanding to mechanism to develop new additives

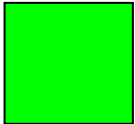
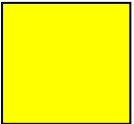
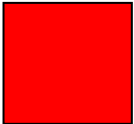



- $scCO_2$ not shown for clarity
- **Purple** – ESCAP
- **Green** – Fluorine (QAS-A2)
- **Cyan** – Carbon (QAS-A2)
- **Red** – Oxygen (QAS-A2)
- **White** – Hydrogen (QAS-A2)

Summary of Fluorinated Additive Results

- We have applied these methods to a range of additive-resist combinations to screen for promising systems
- Excellent agreement with experiment

Possible

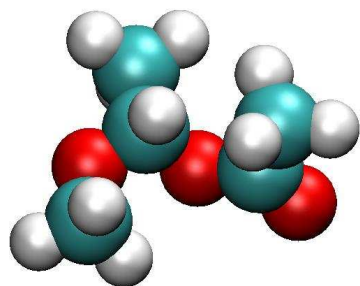
PASS	Pass	FAIL	Untested
			

Photoresist	Additive										
	QAS4	QAS6	QAS7	QAS11	QAS12	QAS13	QAS14	Isocyanate	TMDS	HMDS	none
ESCAP											
193nm											
PHOST											
Molecular Glass I											

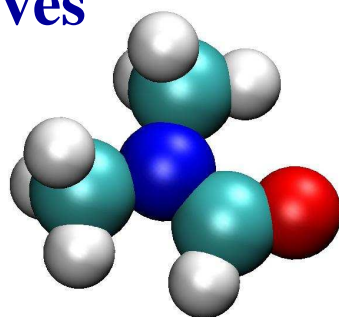
Reactive Additives Not Discussed Today

Non-Fluorinated Systems

- Potential Additives

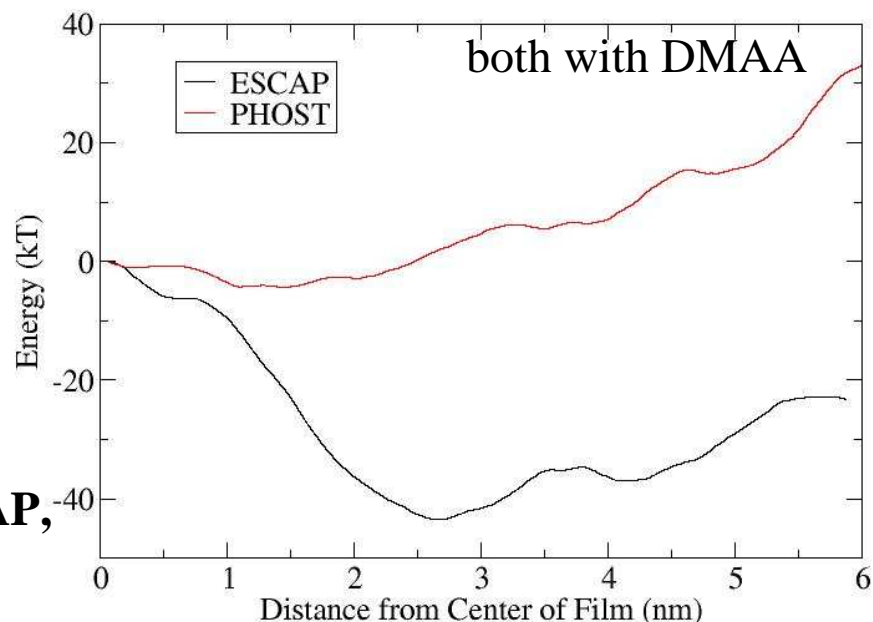


PGMEA

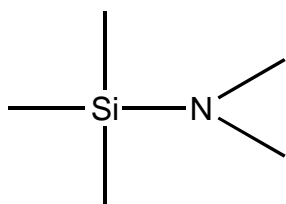


DMAA

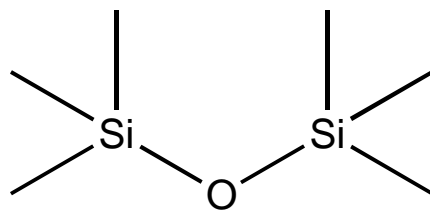
Effective with ESCAP,
but not PHOST



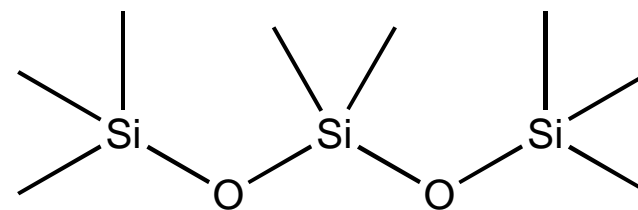
- Alternative solvents not needing fluorinated additives



DMTsilane



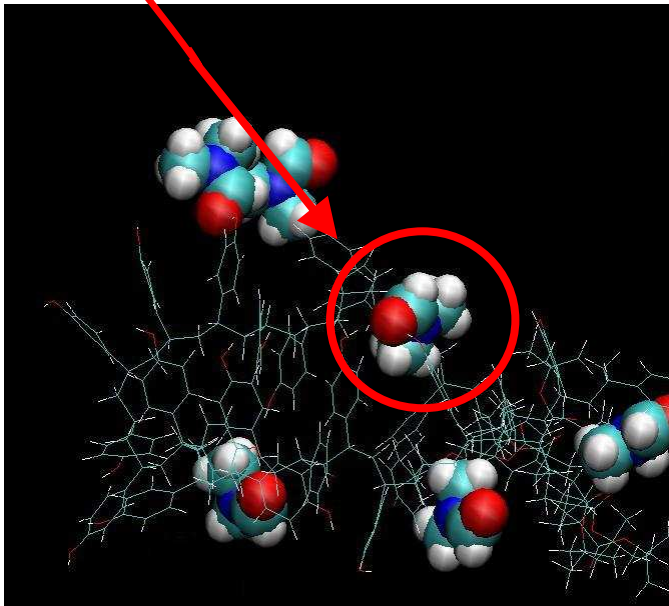
HMDsilane



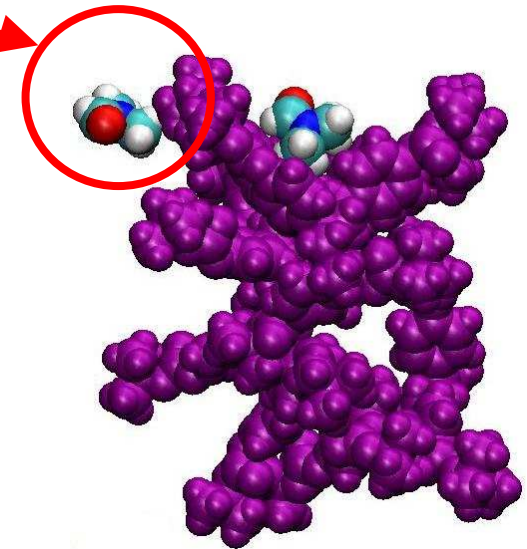
OMTsilane

DMAA Mechanism

- Additive was based on applying our understanding of QAS4 effectiveness on ESCAP
- DMAA demonstrates similar hydrogen bonding
- Ineffective with PHOST; obstructs terminal t-butyl group, instead exposing polar region, reducing scCO₂ solubility

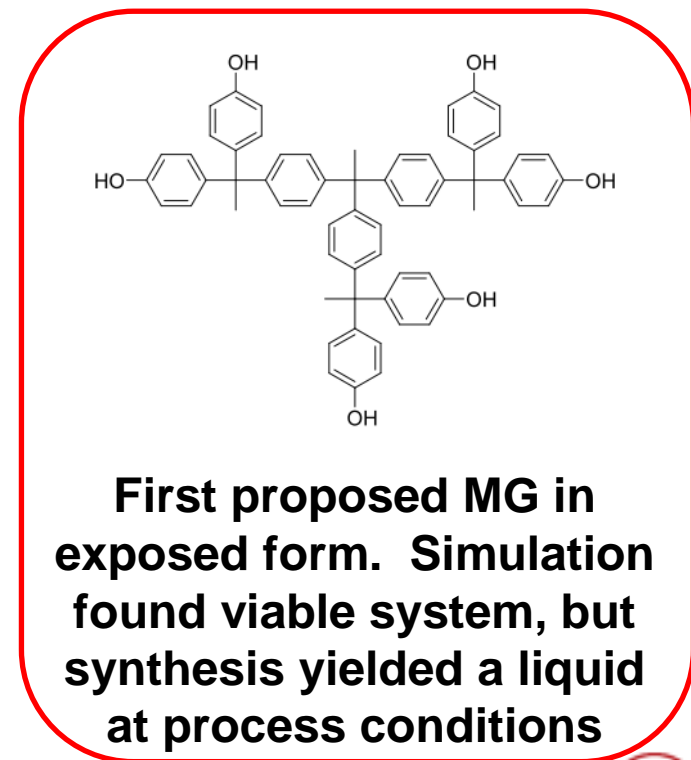
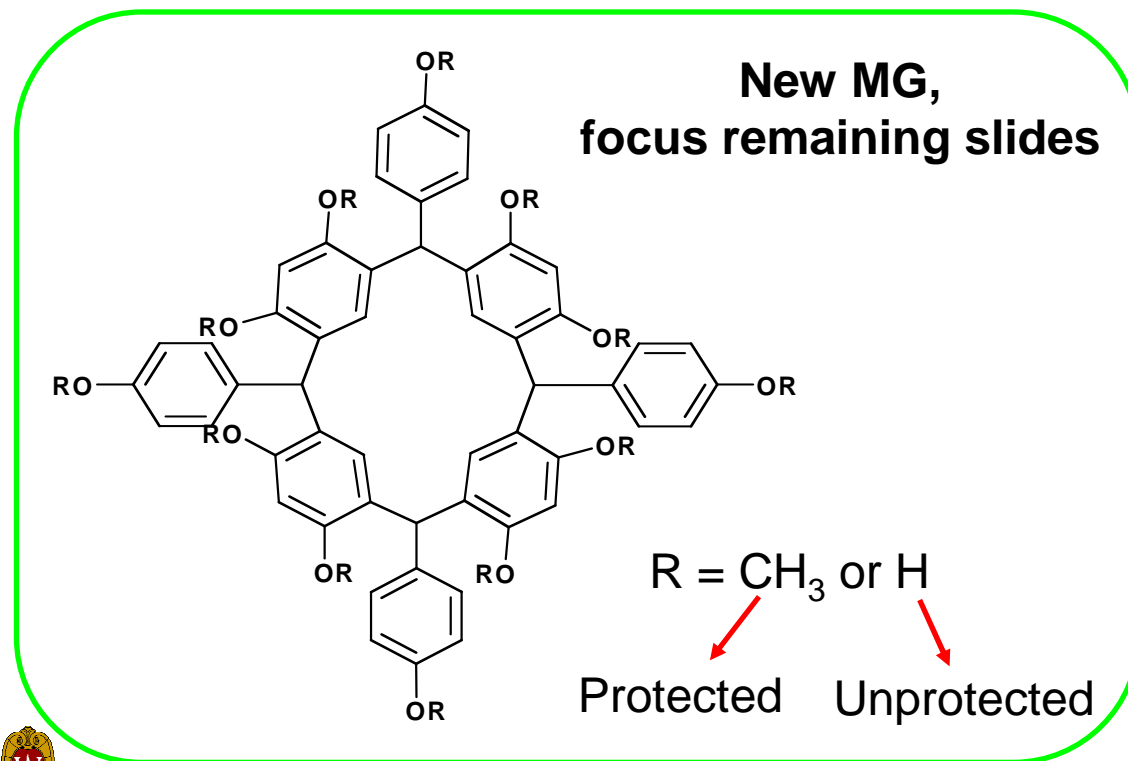


Can develop non-fluorinated additives, but they are more resist-specific



Molecular Glass (MG) Resists

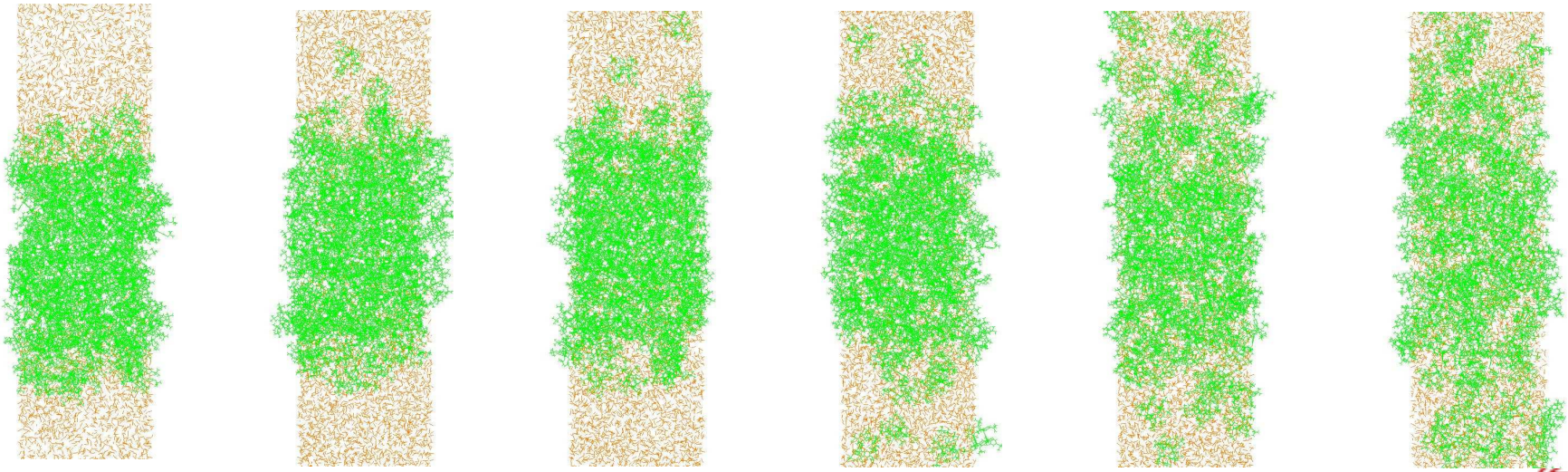
- Molecular Glass have low LER due to small size
- Experimental synthesis and testing is expensive and does not guarantee results; screening via simulation saves resources



Molecular Glass in scCO₂

- Protected MG dissolved in scCO₂ without additive; unprotected form insoluble
- No testing with additives necessary, system shows most robust dissolution to date; no free-energy curve needed
- Highly promising results to be confirmed experimentally

Time (1-2ns between images)



Future Plans

Next Year Plans (seed effort)

- To explore more organosilanes and non-fluorinated quaternary ammonium salts (QAS) for faster dissolution of photoresists in silicone fluids and scCO₂
- To continue synthesis efforts for scCO₂ processable molecular glass resists with environmentally benign, naturally occurring cores for next generation high-resolution lithography
- Verification of new materials of new molecular glass resists and silicone-based solvents
- Additional screening of new non-fluorinated additives for use with traditional photoresists

Long-Term Plans

- To expand use of additives for scCO₂ and environmentally friendly silicone fluids to develop positive tone resists
- To create new chemistries for patterning and functionalizing small, non-polar molecules in scCO₂



SRC/SEMATECH Engineering Research Center for Environmentally Benign Semiconductor Manufacturing



Industrial Interactions and Technology Transfer

- Regular discussions with Intel via Richard Schenker
- Interactions with Dario Goldfarb from IBM
- Interactions with Kenji Yoshimoto from Global Foundry
- Former student (N. Felix) hired by IBM Fishkill Research Center
- Jing Sha moved to Intel grant and interned at NIST
- Interactions with Intel on this topic have been successful
- Collaboration with Albany Nanotech for EUV exposures



Publications, Presentations, and Recognitions/Awards

Publications

- M. Tanaka, A. Rastogi, N. M. Felix, C. K. Ober, “*Supercritical Carbon Dioxide Compatible Salts: Synthesis and Application to Next Generation Lithography*”, *J. Photopolym. Sci. Technol.* (2008), 21(3), 393-396.
- J. Sha and C. K. Ober, “*Fluorine- and Siloxane-Containing Polymers for Supercritical Carbon Dioxide Lithography*”, *Polymer International* (2009), 58(3), 302-306.
- A. Rastogi, M. Tanaka, G. N. Toepperwein, R. A. Riggleman, J. J. dePablo, C. K. Ober, “*Fluorinated Quaternary Ammonium Salts as Dissolution Aids for Polar Polymers in Environmentally Benign Supercritical Carbon Dioxide*”, *Chem. Mater.* (2009), 21(14), 3121-3135.
- J. Sha, J-K Lee, C. K. Ober, “*Molecular Glass Resists Developable in Supercritical CO₂ for 193-nm Lithography*”, *Proceedings of SPIE* (2009), 7273, 72732T.

Presentations

- 25th International Conference of Photopolymer Science & Technology (June 2008). “*Supercritical Carbon Dioxide Compatible Salts: Synthesis and Application to Next Generation Lithography*”
- US-Japan Polymat 2008 Symposium (Aug 2008). “*Environmentally Benign Development of Polymer Photoresists Using Supercritical Carbon Dioxide*”
- ERC Teleseminar (Oct 2008). “*Environmentally Benign Development of Standard Resists in Supercritical Carbon Dioxide Using CO₂ Compatible Salts*”
- Advances in Resist Materials and Processing Technology XXVI conference (part of the SPIE Symposium on Advanced Lithography) (Feb 2009). “*Environmentally Benign Development of Photoresists in Supercritical Carbon Dioxide Using CO₂ Compatible Additives*”

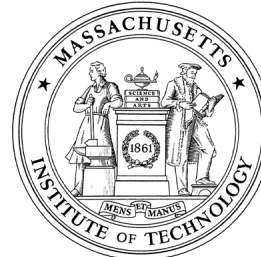


SRC/SEMATECH Engineering Research Center for Environmentally Benign Semiconductor Manufacturing



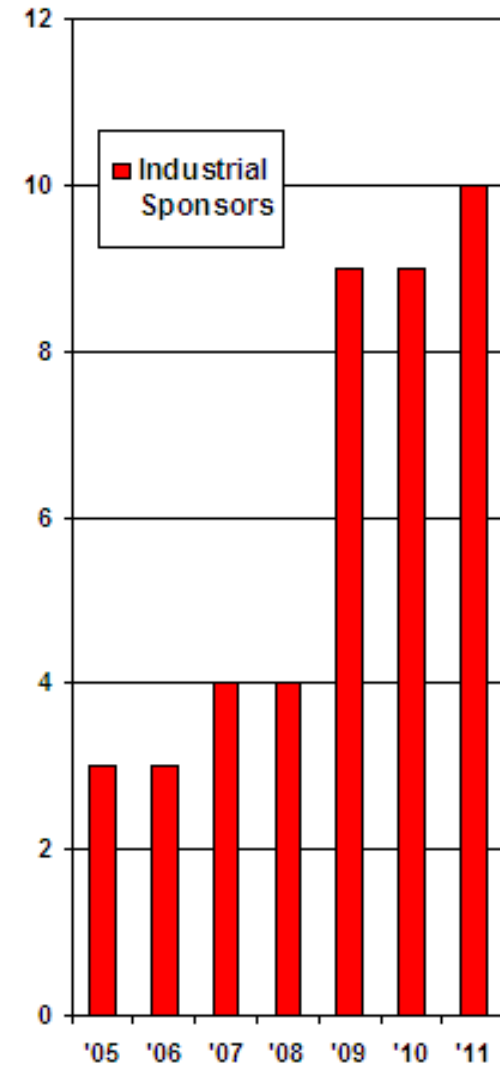
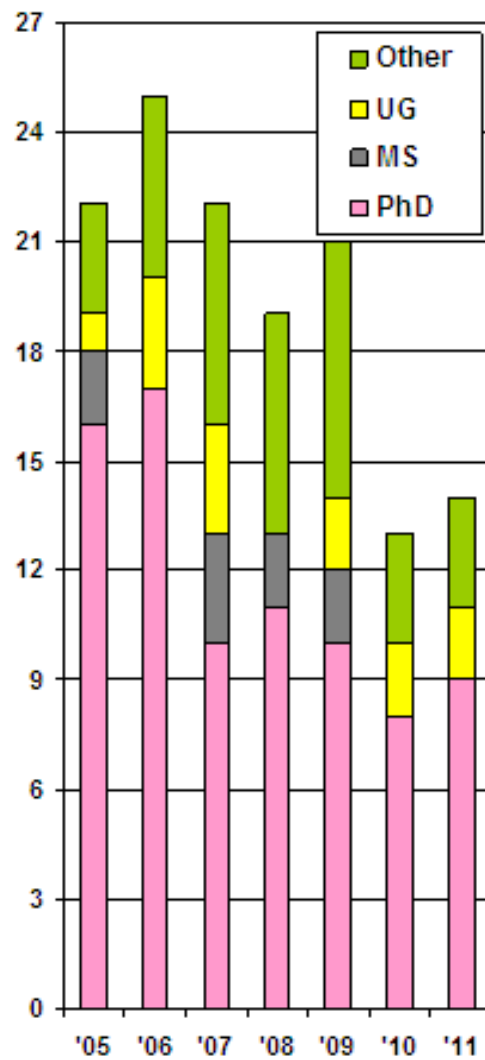
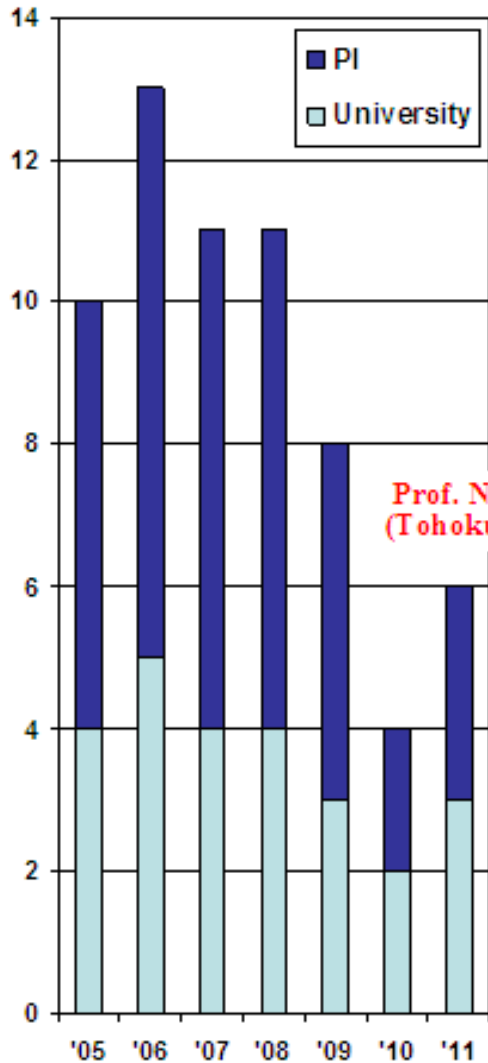
Planarization Long Range Plan

February 2010



SRC/SEMATECH Engineering Research Center for Environmentally Benign Semiconductor Manufacturing

Trends in the Planarization Thrust Team



Next Five Years

- Landscape:

- Research, fundamental yet industrially relevant, addressing the **technological, economic and environmental** challenges of copper and barrier planarization and **post-planarization cleaning**

ALWAYS KEEP THE BIG PICTURE IN MIND

! ... YIELD IS EVERYTHING ... !

Environmental and Economic Losses Resulting from Lower Yields are Orders of Magnitude Greater than any Gains Realized through Consumables Reduction and Incremental Process Tweaks

Advanced Processes and Consumables for Planarization

- Objectives

- Wear phenomena and their effect on process performance
 - Isolate and quantify interactions among **nanoparticles, pads, diamond discs and retaining rings** in representative systems (i.e. 200 and 300 mm processes with mainstream consumables)
 - Understand how these interactions evolve with extended use
- Metrology
 - Deploy and develop tools for measuring **pad asperity-level forces** (more relevant to defectivity and in-situ process monitoring than global forces)
 - Develop methods to visualize slurry flow and measure local wafer-pad-slurry mechanical interactions (i.e. contact area, near-contact area, summit density and wafer topography) using **UV-enhanced fluorescence** and **laser confocal microscopy**

Advanced Processes and Consumables for Planarization

- Objectives (continued)

- Wafer-level and die-level CMP modeling

- Develop new models of **pad macro-texture, micro-texture and slurry flow** to study interactions between wafer-level effects, retaining ring design and chip-scale planarization performance
- Extend **die-level** models to include key pad micro-texture dependencies to better **predict dishing and erosion**
- **Integrate** die-level and wafer-level models to **enable overall uniformity and performance optimization**

- ULK structure collapse

- Determine and quantify main factors affecting advanced ULK structural damage and develop novel process & consumable solutions

Advanced Processes and Consumables for Post-Planarization Cleaning

- Objectives

- Metrology

- Develop **high-speed imaging methods** to validate observed brush-wafer stick-slip effects

- Wear phenomena and their effect on process performance

- Isolate and quantify **chemical** and **mechanical** interactions among **brush rollers, cleaning chemicals and wafers** in representative systems (i.e. 200 and 300 mm processes with mainstream consumables including various ULK candidates)
- Understand how these interactions evolve with extended use

Fundamentals of Advanced Planarization: Pad Micro-Texture, Pad Conditioning, Slurry Flow, and Retaining Ring Geometry

(Task 425.032)

Subtask 1: Effect of Retaining Ring Geometry on Slurry Flow and Pad Micro-Texture

PI:

- Ara Philipossian, Chemical and Environment Engineering, UA

Graduate Student:

- Xiaomin Wei, PhD candidate, Chemical and Environment Engineering, UA

Undergraduate Student:

- Adam Rice, Chemical and Environment Engineering, UA

Other Researcher:

- Yasa Sampurno, Postdoctoral Fellow, Chemical and Environment Engineering, UA

Cost Share (other than core ERC funding):

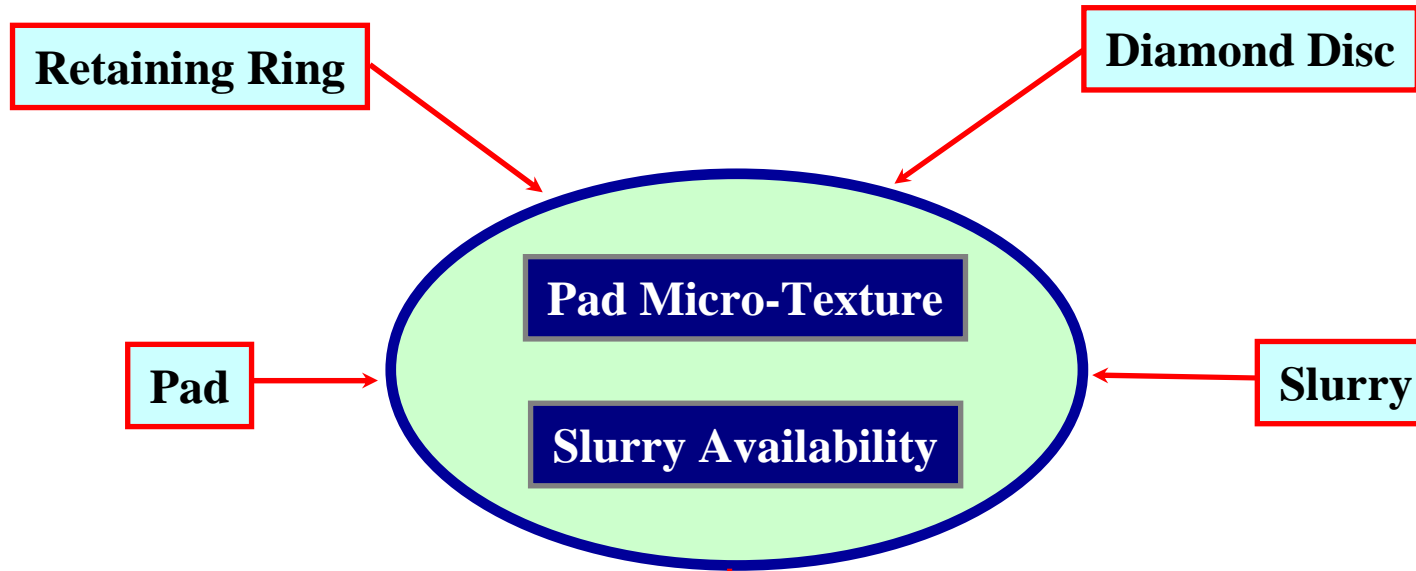
- In-kind donation (pads) from Cabot Microelectronics Corporation
- In-kind donation (retaining rings) from Entegris, Inc.

SRC/SEMATECH Engineering Research Center for Environmentally Benign Semiconductor Manufacturing

Primary Anticipated Result

- **Understand how pad micro-texture and slurry availability are fundamentally affected by:**
 - **Pad type (i.e. porous vs. non-porous, and various degrees of hardness)**
 - **Diamond disc type (i.e. grain size, and morphology)**
 - **Retaining ring slot designs**
 - **Slurry flow rate and injection schemes**
- **Via die-scale and wafer-scale empirical, theoretical and numerical methods, gain a deeper understanding of how the above:**
 - **Interact with one another**
 - **Affect polishing outcomes (on 200 and 300 mm rotary platforms)**
 - **Extendible to 450 mm rotary processes (theoretically)**
- **Ultimately, our goal is for this work to lead to new designs of polishing protocols and consumables with superior performance (i.e. wafer-level topography, uniformity, consumable durability, throughput ...) and more environmentally benign consequences.**

Overall Scope



Empirical, Numerical and Theoretical Characterization (Die-Scale & Wafer-Scale)

**Polishing protocols and consumables with superior performance
(throughput, wafer-level topography, uniformity, durability ...)
with more environmentally benign consequences**

Specific Objectives and EHS Impact

- **Develop UV enhanced fluorescence system and quantify the extent of fluorescent light emitted by the slurry**
- **Employ the fluorescent light data to rapidly assess slurry flow patterns as a function of retaining ring designs, slurry flow rates, pad groove designs, and tool kinematics**

Reduce slurry consumption by 40 percent

General Approach

- **Tag slurry with a special set of fluorescent dyes**
- **Use UV – LED as light sources to excite the dyes in the slurry causing them to emit fluorescent light**
- **Employ a high resolution CCD camera to record the emission of fluorescent light**
- **Develop software and quantitatively assess the flow pattern using the movie from CCD camera**

UV – LED and CCD Camera Set up



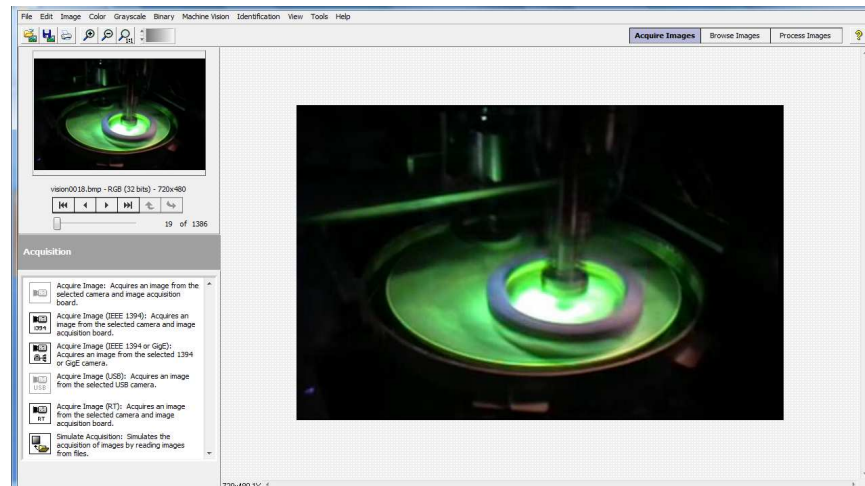
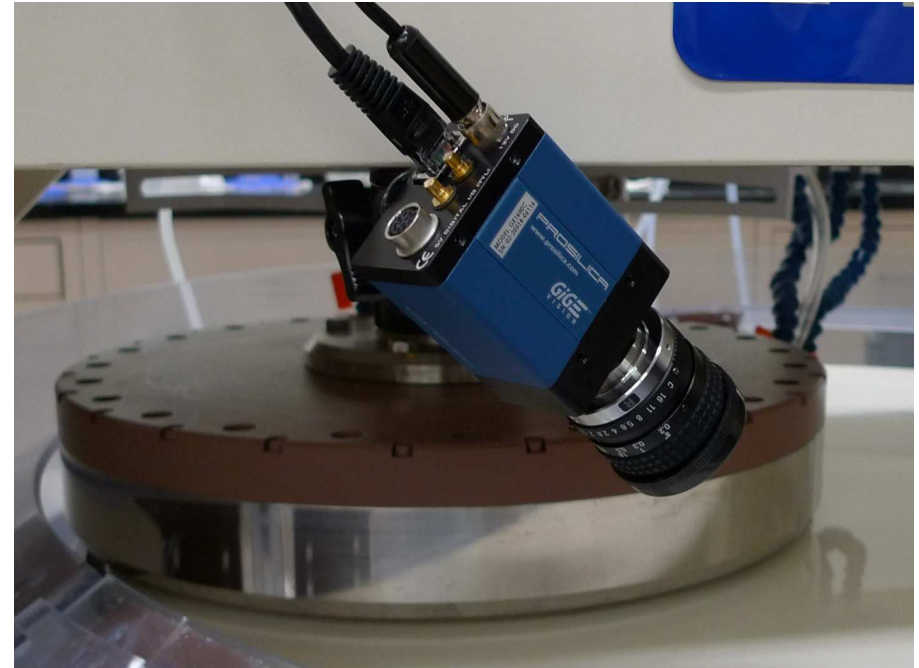
UV – LED



UV – LED Cover



High Resolution CCD Camera



Software Interface for Image Browsing

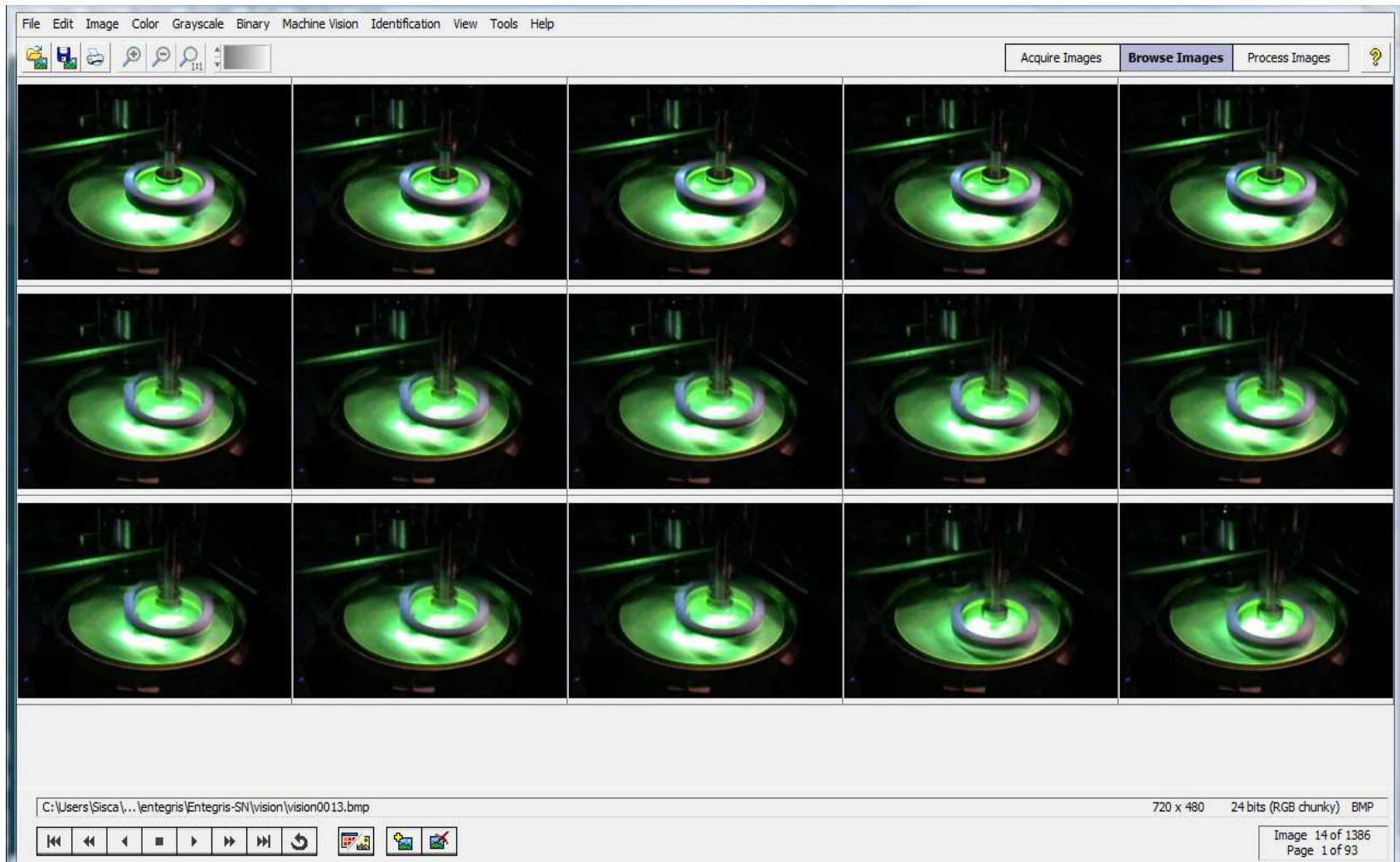
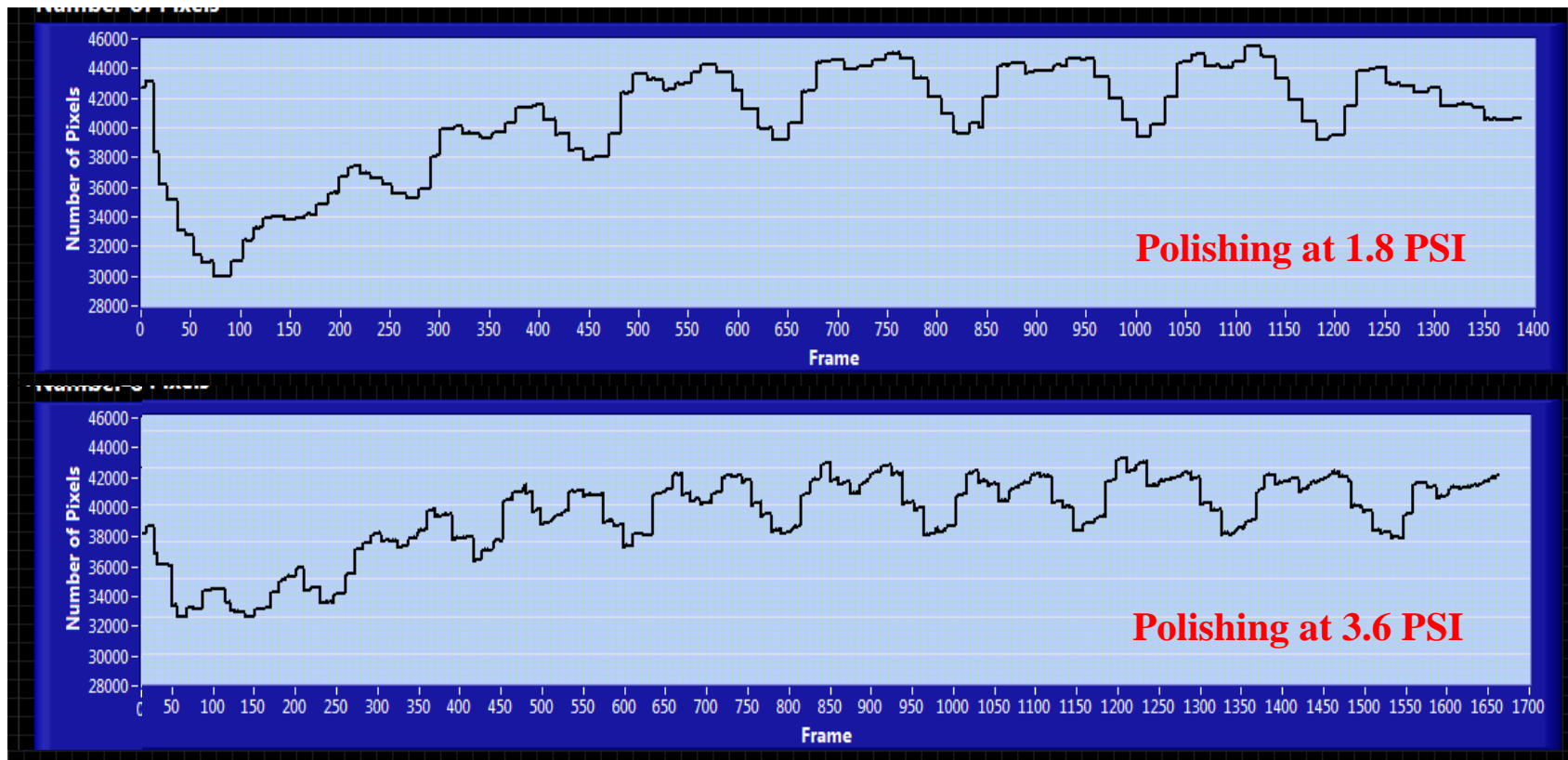


Image Analysis – Effect of Pressure



The UV enhanced fluorescence system can assess differences in slurry flow characteristics at two different polishing pressures.

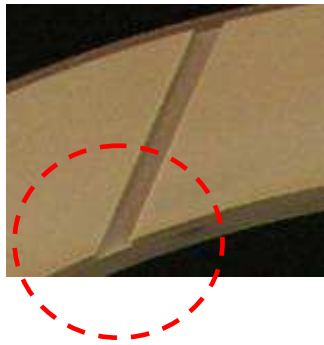
Industrial Interactions and Technology Transfer

Industrial mentors and contacts:

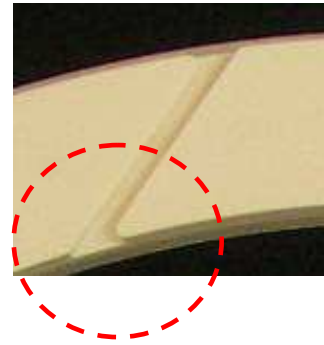
- **Christopher Wargo (Entegris)**
- **Cliff Spiro (Cabot Microelectronics)**

Future Plans

- **Next year plan: investigate the effect of retaining ring geometry on bow wave characteristics, slurry availability and pad micro-texture**



Slot Design No. 1



Slot Design No. 2

- **Long-term plan: develop fundamental understanding of retaining ring's effects on slurry flow and polishing performance to overcome difficult challenges in environmental and manufacturing efficiency.**

Fundamentals of Advanced Planarization: Pad Micro-Texture, Pad Conditioning, Slurry Flow, and Retaining Ring Geometry

(Task 425.032)

Subtask 2: Effect of Pad Conditioning on Pad Micro-Texture and Polishing Performance

PI:

- Ara Philipossian, Chemical and Environment Engineering, UA
- Duane Boning, Electrical Engineering and Computer Science, MIT

Graduate Students:

- Ting Sun, Chemical and Environmental Engineering, UA, graduated with Ph. D. degree in May 2009
- Xiaoyan Liao, Ph. D. candidate, Chemical and Environment Engineering, UA
- Yubo Jiao, Ph. D. candidate, Chemical and Environment Engineering, UA
- Zhenxing Han, Ph. D. candidate, Chemical and Environment Engineering, UA
- Anand Meled, Ph. D. candidate, Chemical and Environment Engineering, UA
- Wei Fan, Ph. D. candidate, Electrical Engineering and Computer Science, MIT

Fundamentals of Advanced Planarization: Pad Micro-Texture, Pad Conditioning, Slurry Flow, and Retaining Ring Geometry

(Task 425.032)

Subtask 2: Effect of Pad Conditioning on Pad Micro-Texture and Polishing Performance

Other Researchers:

- Yun Zhuang, Postdoctoral Fellow, Chemical and Environment Engineering, UA
- Yasa Sampurno, Postdoctoral Fellow, Chemical and Environment Engineering, UA
- Jiang Cheng, Visiting Scholar, Chemical and Environment Engineering, UA

Cost Share (other than core ERC funding):

- In-kind donation (slurry) from Hitachi Chemical
- In-kind support from Araca, Inc.

Specific Objectives and EHS Impact

- Investigate the effect of pad conditioning on pad surface micro-texture, frictional force, removal rate and wafer topography (dishing/erosion) during ILD/STI CMP processes
- Investigate the origin of pad surface contact in CMP processes
- Characterize pad asperity height using stylus micro profilometry

Reduce use of all CMP consumables by increasing yield through reduction of dishing and erosion

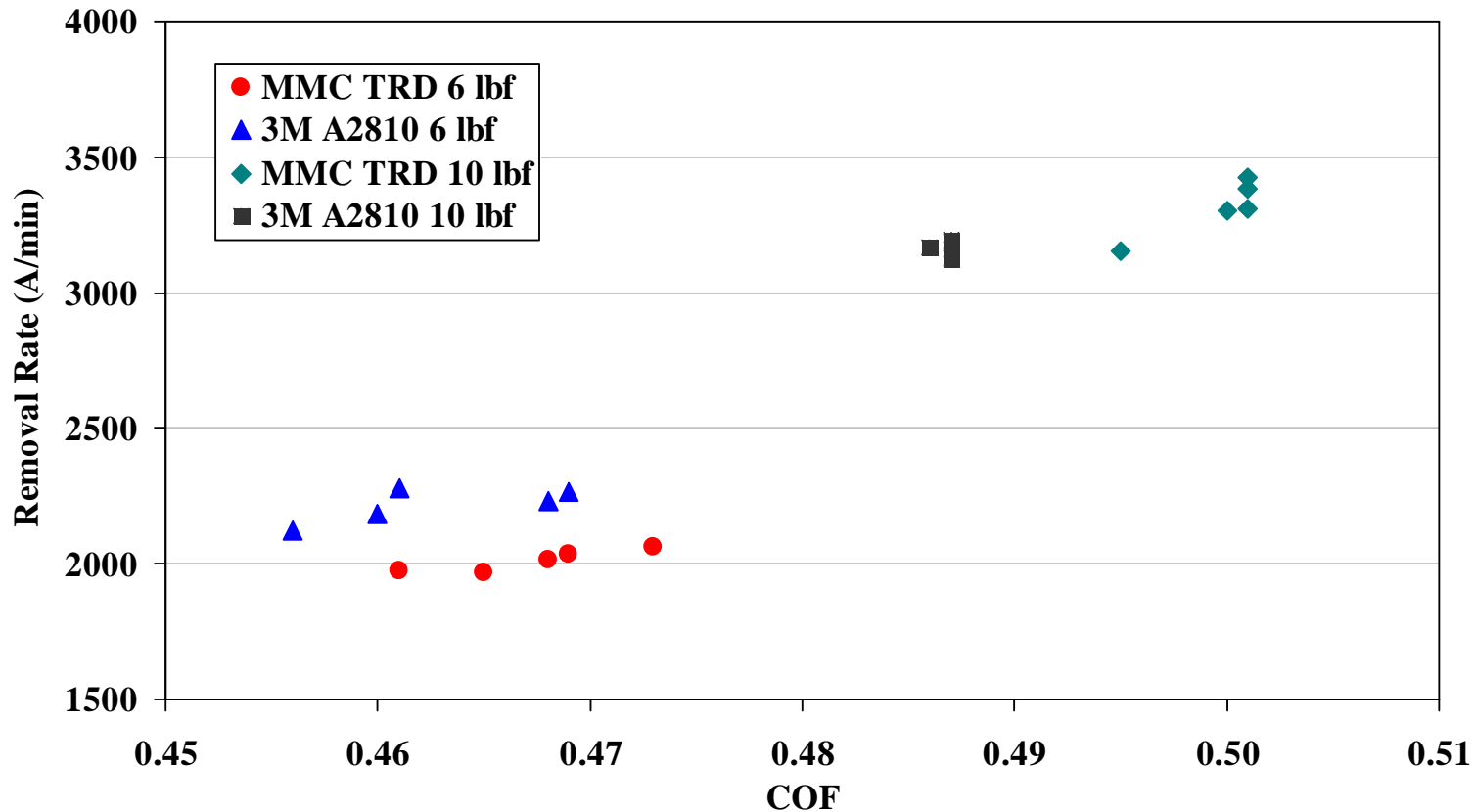
General Approach

Polish 200-mm blanket TEOS and SKW3-2 STI wafers under 6 and 10 lb conditioning forces with a 3M A2810 disc and a Mitsubishi Materials Corporation 100-grit TRD disc

Analyze pad micro-texture through laser confocal microscopy:

- Blanket wafer polishing: frictional force and removal rate**
- Patterned wafer polishing: dishing and erosion**
- Pad micro-texture analyses: contact area, surface abruptness and summit curvature**

Removal Rate vs. COF



The removal rate increased much more significantly with the conditioning force (65% for the MMC TRD disc and 43% for the 3M A2810 disc) than the COF (7% for the MMC TRD disc and 5% for the 3M A2810 disc).

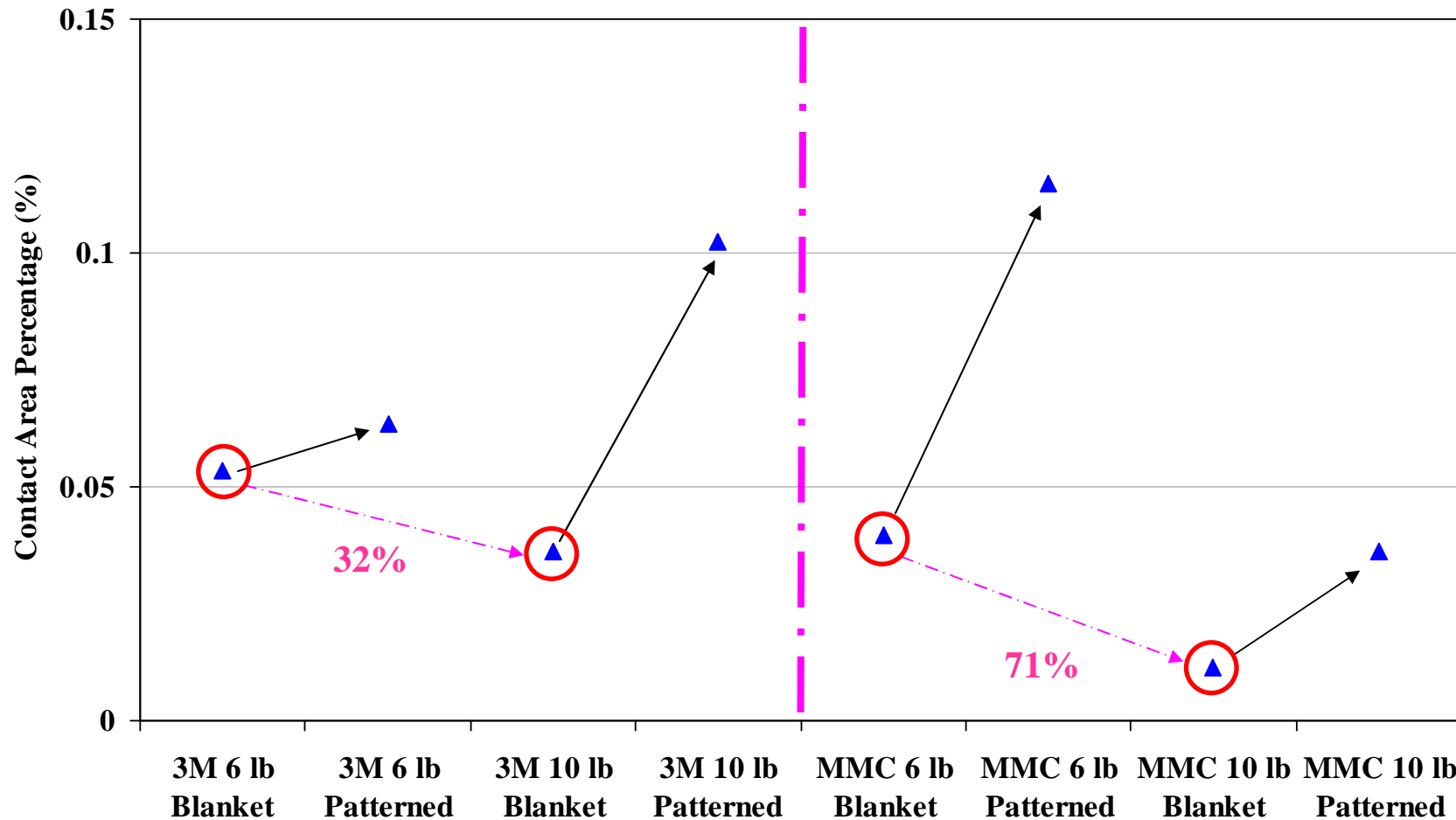
Dishing and Erosion Analysis

Center Die, 100 Micron Pitch

Conditioning Force (lb)	Diamond Disc	Dishing (A)					Erosion (A)				
		Pattern Density					Pattern Density				
		10%	30%	50%	70%	90%	10%	30%	50%	70%	90%
6	3M A2810	125	1200	300	300	275	110	134	125	113	117
	MMC TRD	325	2800	500	500	325	330	215	406	129	172
10	3M A2810	275	600	200	125	175	34	22	49	11	4
	MMC TRD	750	1400	300	225	275	103	23	86	24	18

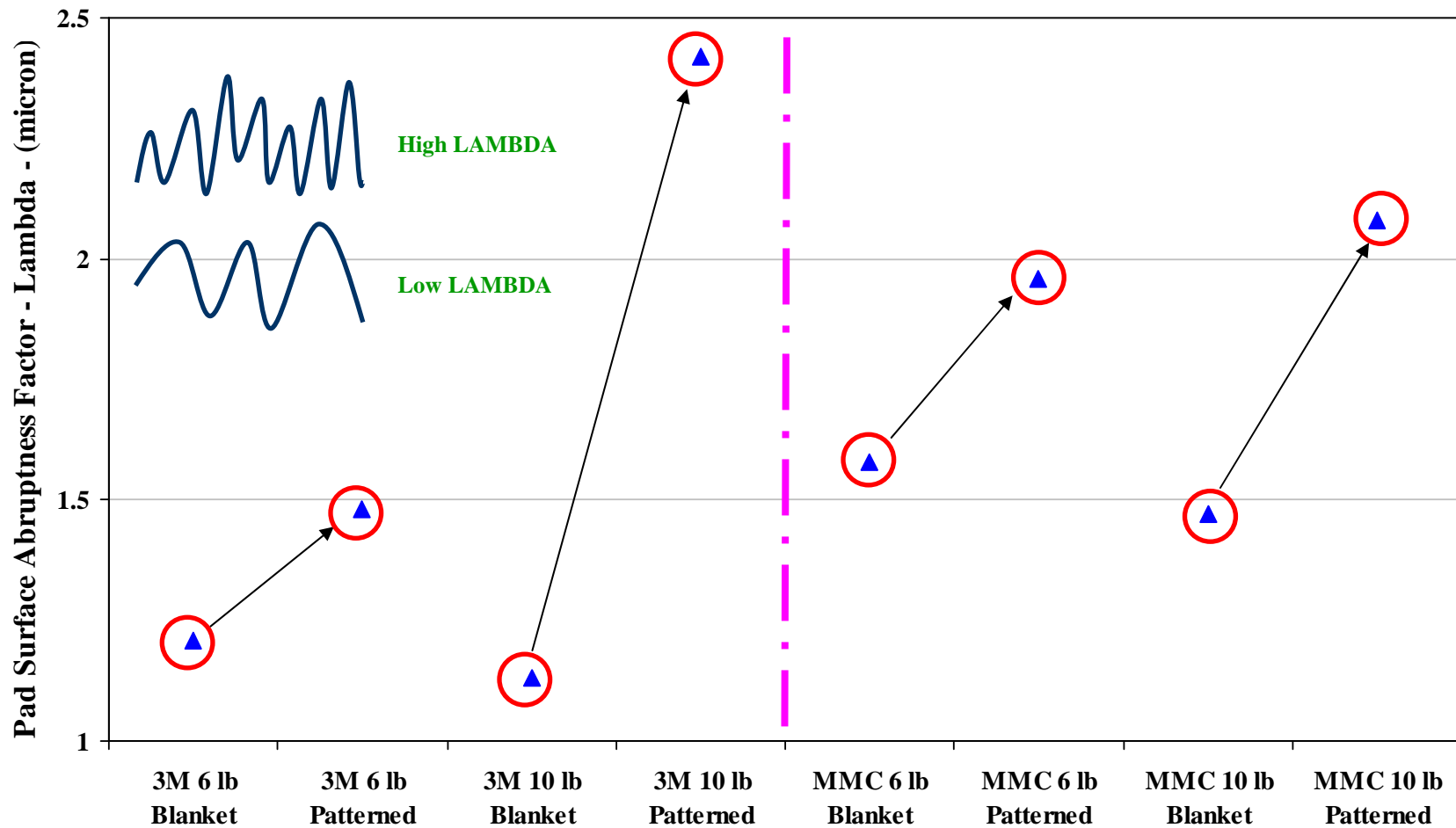
At both conditioning forces, **Dishing/Erosion**_{3M A2810 disc} < **Dishing/Erosion**_{MMC TRD disc}

Contact Area Percentage



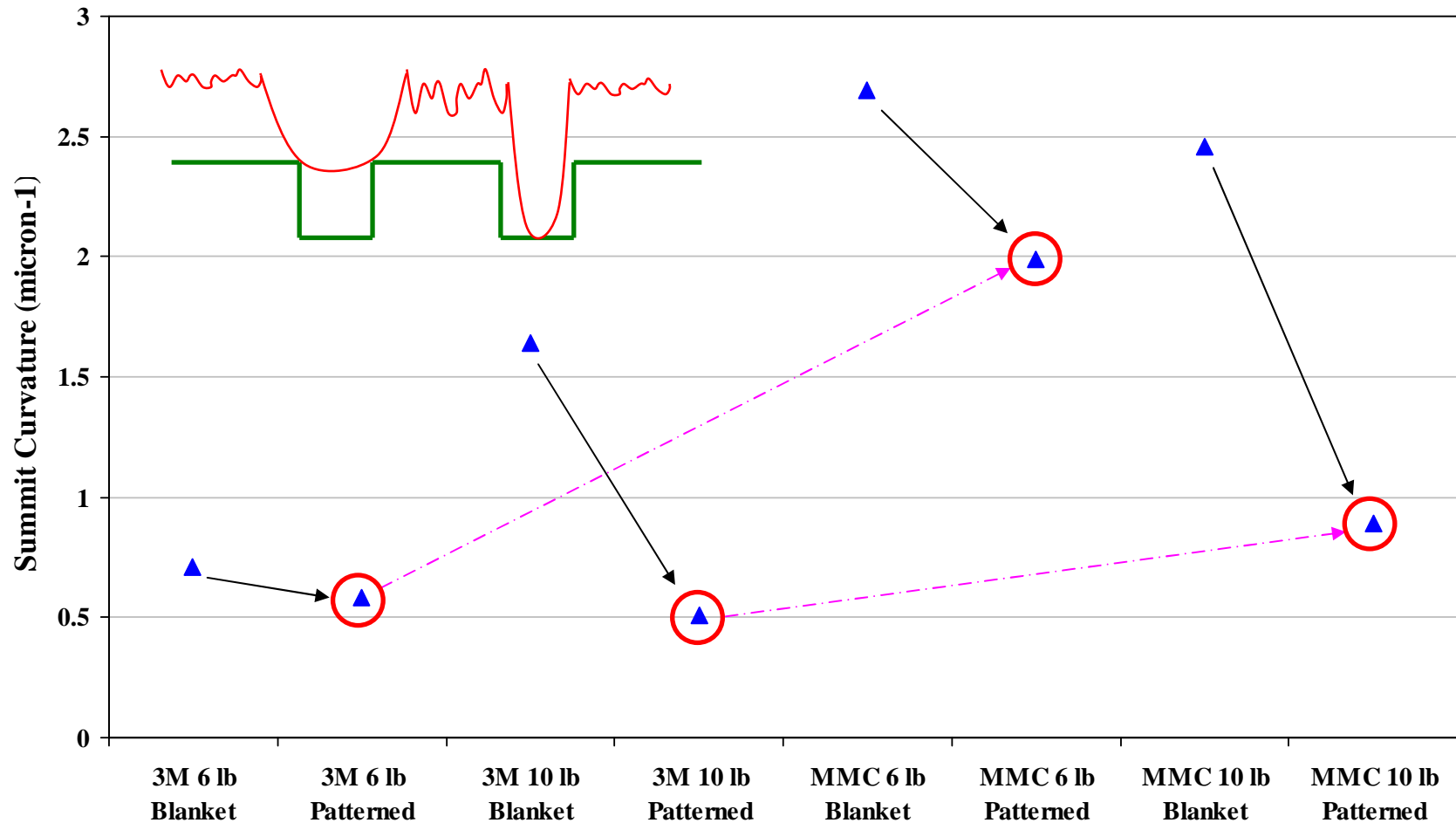
Contact area percentage **decreased** significantly as conditioning force **increased** from 6 to 10 lb for both discs during **blanket wafer polishing**
Smaller contact area → Larger mean contact pressure → Higher RR

Pad Surface Abruptness Factor



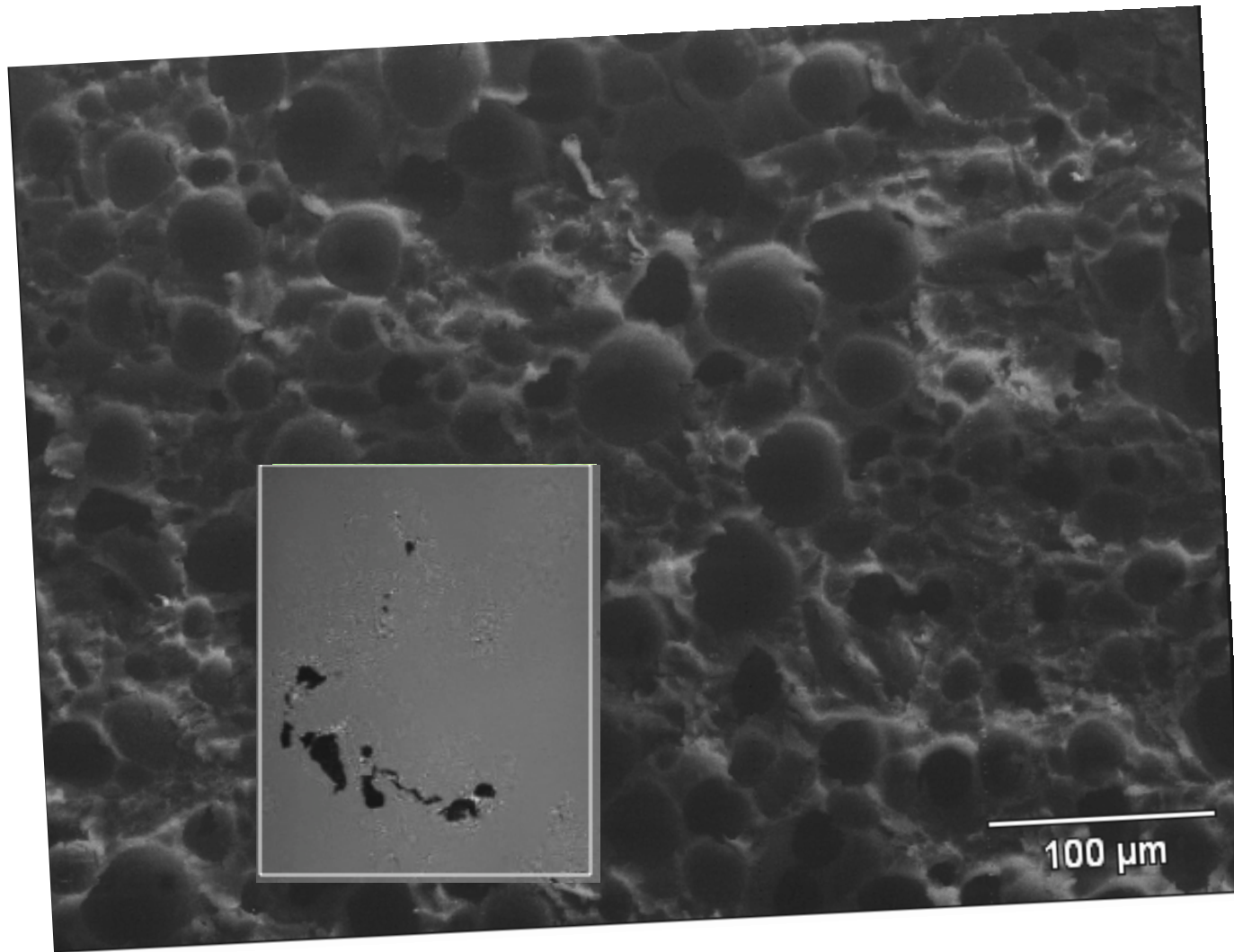
Topography of patterned wafers caused **additional collisions** with pad summits, resulting in **larger values of LAMBDA** compared to blanket wafer polishing.

Mean Summit Curvature



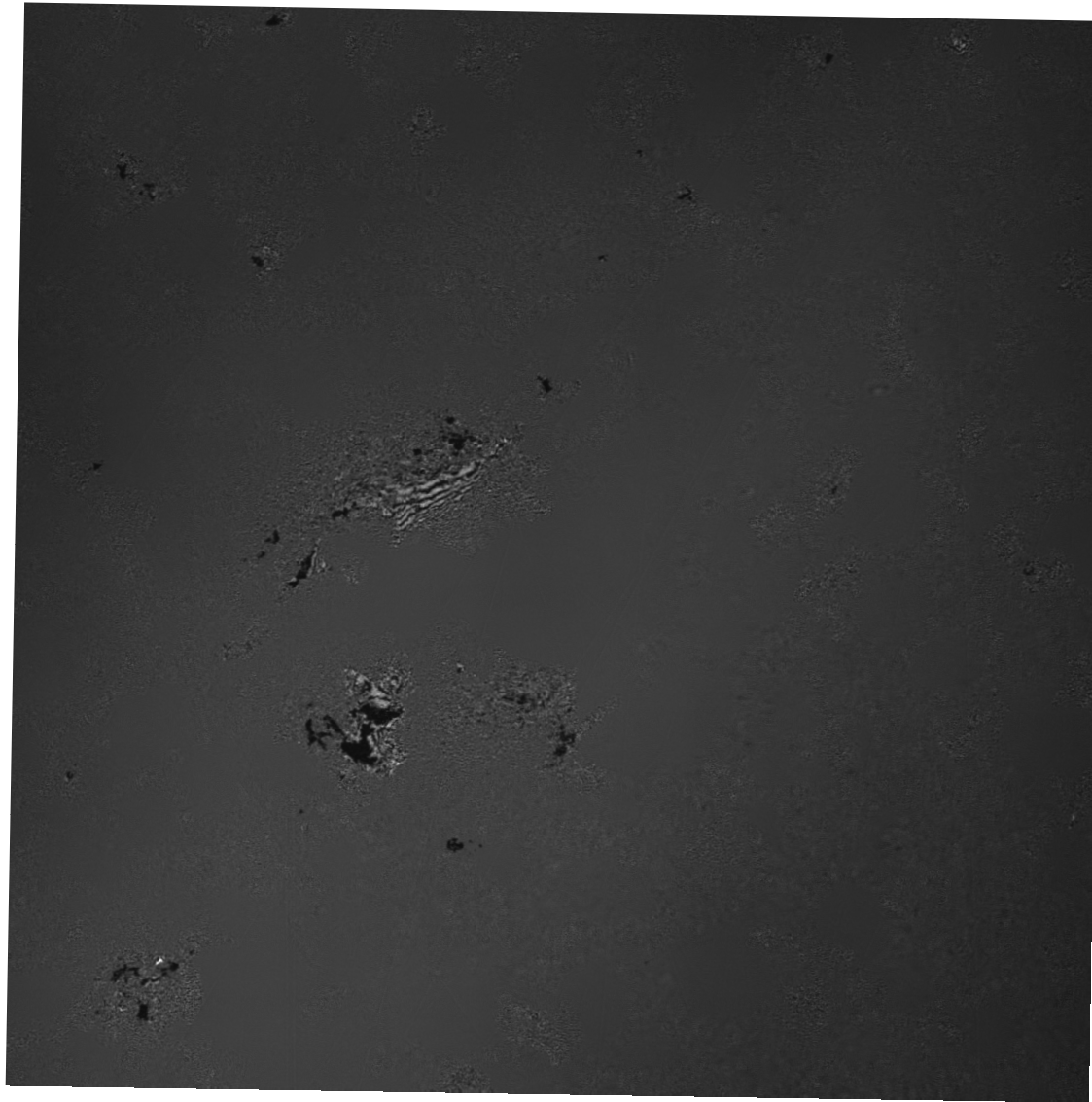
Sharper pad summits (larger summit curvature) contributed to higher dishing and erosion.

SEM, Topography and Contact Image

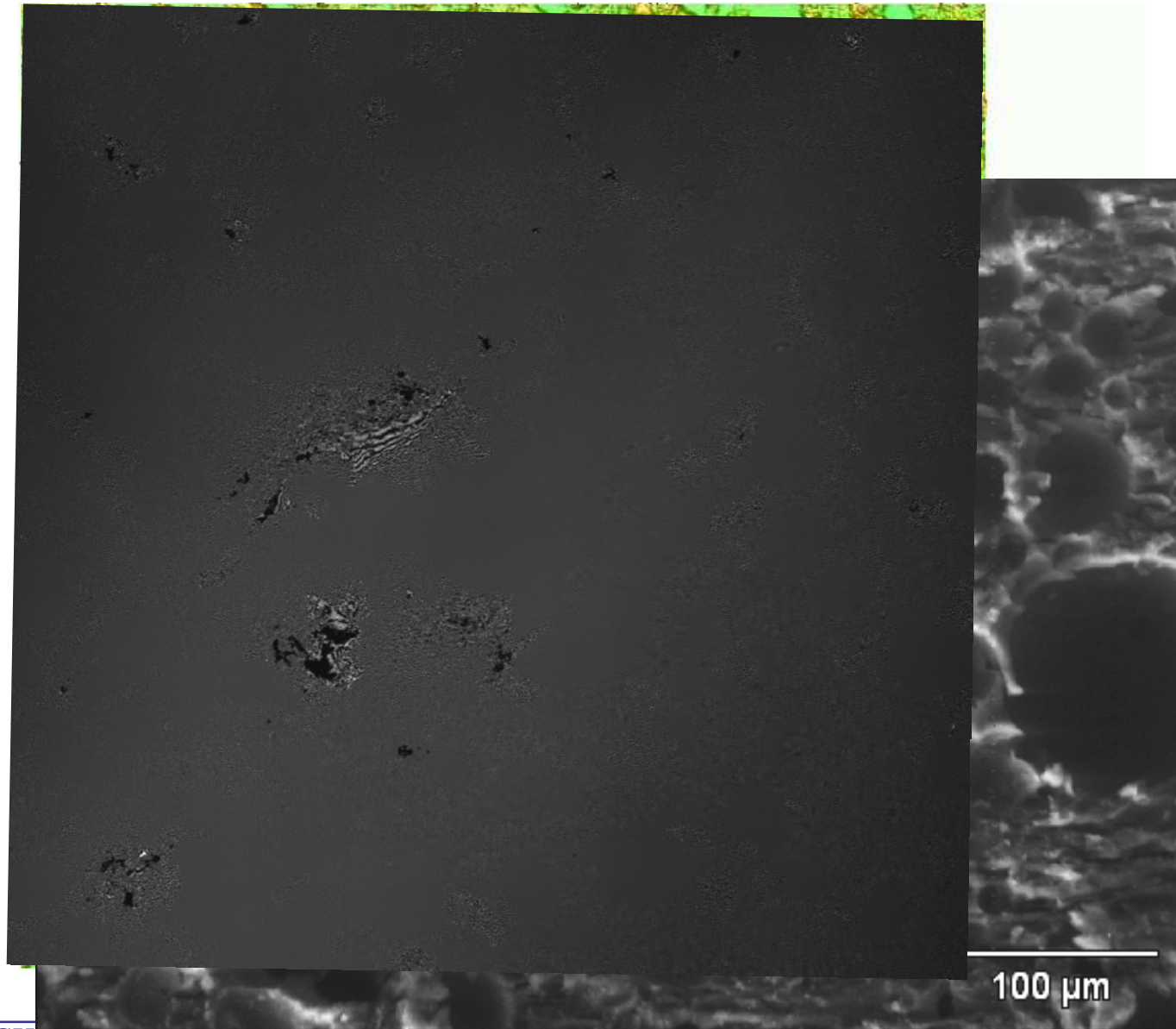


Large Contacts with Fringed Areas

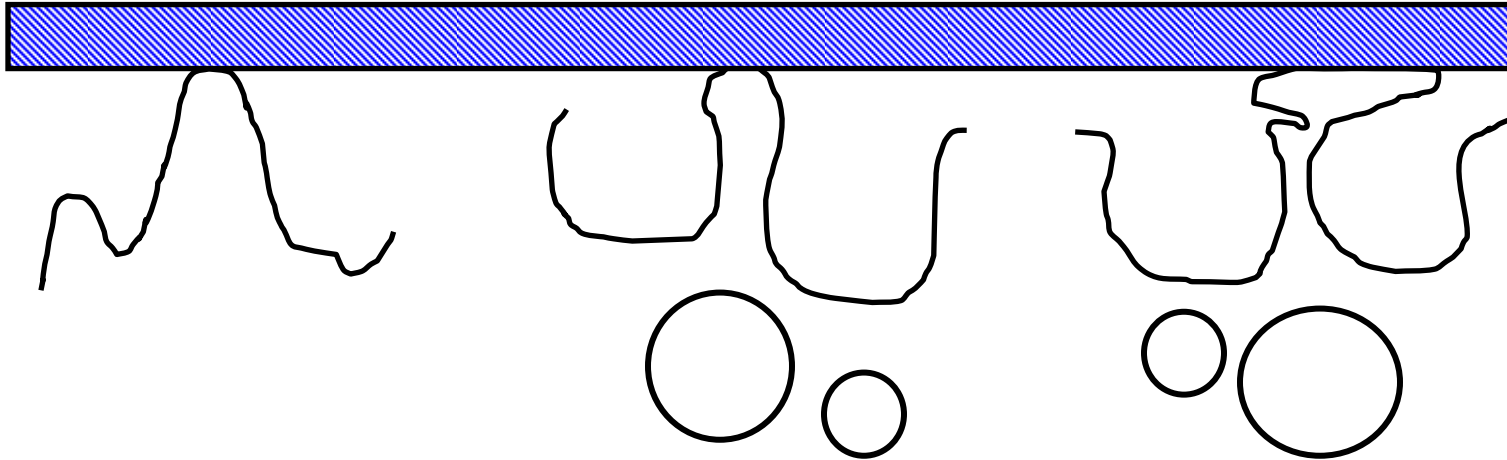
50 μm



Topography and SEM Comparison



Contacting Summit Types



Fully supported contacting summit, solid underlying pad material.

Applied force produces a small deflection and a small contact area.

Assumed in most rough surface contact theories.

May be rare in CMP

Less well-supported contacting summit, pore-filled bulk.

Applied force produces a larger deflection but a small contact area.

Fractured, poorly supported contacting summit.

Applied force produces a large, low pressure contact area.

Contact behaves like a compliant, flexible plate.

Very common in CMP

Industrial Interactions and Technology Transfer

Industrial mentors and contacts:

- **Lenoard Borucki (Araca)**
- **Mansour Moinpour (Intel)**
- **Don Hooper (Intel)**

Future Plans

- **Next year's plan:** Investigate the effect of pad conditioning on pad surface micro-texture, as well as frictional force, removal rate, and wafer topography (dishing/erosion) during copper CMP processes.
- **Long-term plan:** Develop fundamental understanding of the effect of pad conditioning and pad-wafer contact in CMP processes.

Publications

- **Theoretical and Experimental Investigation of Conditioner Design Factors on Tribology and Removal Rate in Copper Chemical Mechanical Planarization. L. Borucki, H. Lee, Y. Zhuang, N. Nikita, R. Kikuma and A. Philipossian. Japanese Journal of Applied Physics, 48(11), 115502 (2009).**
- **Investigating the effect of diamond size and conditioning force on chemical mechanical planarization pad topography. T. Sun, L. Borucki, Y. Zhuang and A. Philipossian. Microelectronic Engineering, in press.**
- **Investigating the Effect of Conditioner Aggressiveness on Removal Rate during Inter-Layer Dielectric CMP through Confocal Microscopy and Dual Emission UV Enhanced Fluorescence Imaging. T. Sun, L. Borucki, Y. Zhuang, Y. Sampurno, F. Sudargho, X. Wei, S. Anjur and A. Philipossian. Japanese Journal of Applied Physics, in press.**
- **Effect of Pad Micro-Texture on Frictional Force, Removal Rate, and Wafer Topography during ILD/STI CMP Processes. Y. Zhuang, X. Liao, L. Borucki, J. Cheng, S. Theng, T. Ashizawa and A. Philipossian. International Conference on Planarization/CMP Technology Proceedings, 85-90 (2009).**
- **Pad Topography, Contact Area and Hydrodynamic Lubrication in Chemical-Mechanical Polishing. L. Borucki, T. Sun, Y. Zhuang, D. Slutz and A. Philipossian. Materials Research Society Symposium Proceedings, Vol. 1157, E01-02 (2009).**

Presentations

- **Effect of Pad Micro-Texture on Frictional Force, Removal Rate, and Wafer Topography during ILD/STI CMP Processes.** Y. Zhuang, X. Liao, L. Borucki, J. Cheng, S. Theng, T. Ashizawa and A. Philipossian. International Conference on Planarization/CMP Technology, Fukuoka, Japan, November 19-21 (2009).
- **The Origin and Mechanics of Large Pad-Wafer Contact Areas.** L. Borucki, Y. Sampurno, Y. Zhuang and A. Philipossian. The Fourteenth International Symposium on Chemical-mechanical Planarization, Lake Placid, New York, August 9-12 (2009).
- **Pad Topography, Contact Area and Hydrodynamic Lubrication in Chemical Mechanical Polishing.** L. Borucki, T. Sun, Y. Zhuang, D. Slutz and A. Philipossian. Materials Research Society Spring Meeting, San Francisco, California, April 13-17 (2009).

Fundamentals of Advanced Planarization: Pad Micro-Texture, Pad Conditioning, Slurry Flow, and Retaining Ring Geometry

(Task 425.032)

Subtask 3: Implementation of an Extended Die-Level and Wafer-Level CMP Model

PI:

- Duane Boning, Electrical Engineering and Computer Science, MIT

Graduate Students:

- Wei Fan, Ph.D. candidate, EECS, MIT
- Joy Johnson, Ph.D. candidate, EECS, MIT

Cost Share (other than core ERC funding):

- Experimental data, Intel
- Experimental support, National Semiconductor Corporation

Objectives

Goal: Improve fundamental understanding of CMP to

- Reduce use of high-cost engineered consumables
- Reduce generation of by-product wastes
- Save processing times requiring significant energy

1. Retaining ring/wafer-level CMP modeling:

- Evaluate within-wafer nonuniformity as function of process and tool design
- Retaining ring geometry: affect on edge polish uniformity

2. Slurry agglomeration/wafer-level CMP modeling:

- Understand how slurry abrasive particles, pad debris, and wafer debris affect agglomeration
- Understand how agglomeration relates to the *planarization* capability of CMP processes as well as defectivity

ESH Metrics and Impact

Driving principle and goals: Joint improvement in CMP performance and ESH performance

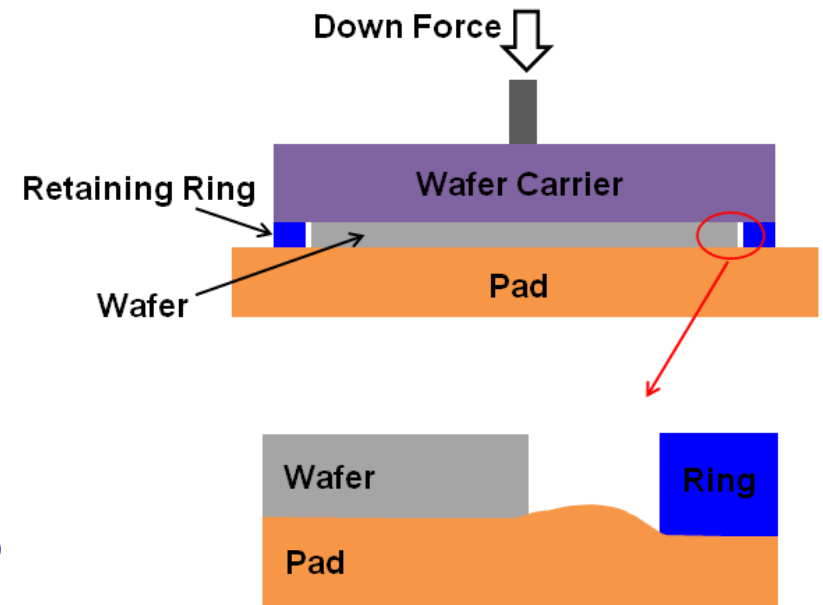
- 1. Reduction in the use or replacement of ESH-problematic materials***
- 2. Reduction in emission of ESH-problematic material to environment***
 - Reduce slurry particle use and Cu solid waste by 20-50%**
- 3. Reduction in the use of natural resources (water and energy)***
 - Shorten CMP polish times (copper, barrier) by 20-50%**
 - Improve yield (multiplication over all inputs/outputs) by 1-2%**
- 4. Reduction in the use of chemicals***
 - Reduce slurry usage by 20%**
 - Improve pad lifetime by 20-50%**

1. Retaining Ring/Wafer-Level CMP Model

- **Evaluate Within-Wafer Polish Non-Uniformity**
 - Pressure distribution is highly non-uniform near the wafer edge
 - The non-uniform removal rate causes a roll-off profile at wafer edge
- **Investigate the Impact of CMP Tool System**
 - Retaining ring geometry and design
 - Relative velocity affected by wafer speed, pad speed and polishing head position

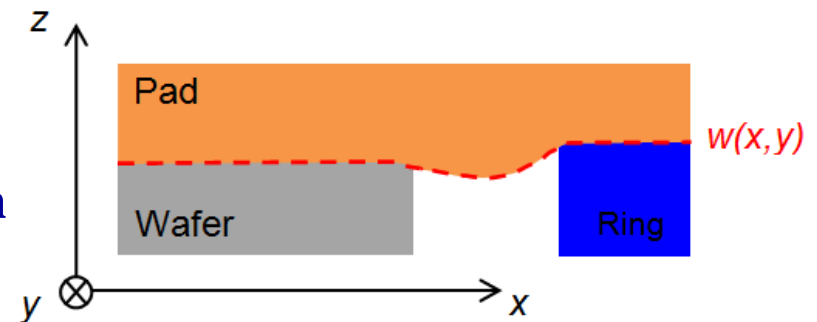
Modeling of Pressure Distribution

- **Non-uniform pressure distribution results from the discontinuities of the process tool geometry at the wafer edge**
- **The retaining ring is usually under higher pressure to prevent the wafer from slipping out**
- **The pad bends around the wafer edge due to the existence of the gap and retaining ring**
- **Wafer edge pressure can be tuned by the ring pressure**



Modeling of Pressure Distribution Cont'd

- The pad can be treated as an elastic body
- Wafer and retaining are both rigid
- The relationship between pad deformation and wafer/ring surface topography can be calculated using a contact wear model



Pad Surface Displacement

$$w(x, y) - w_0 = F(x, y) \otimes P(x, y)$$

Point Pressure Response

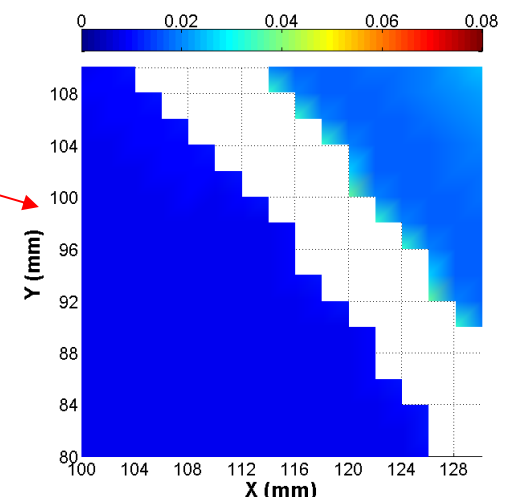
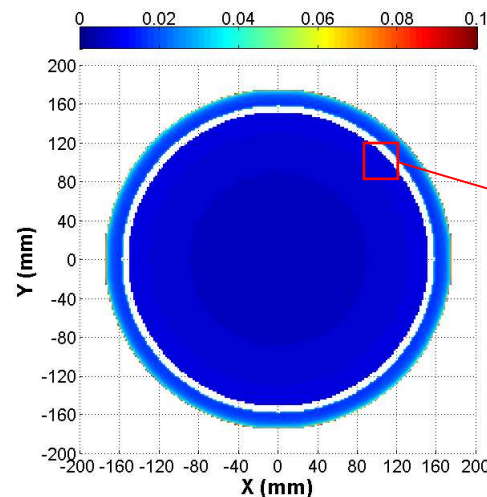
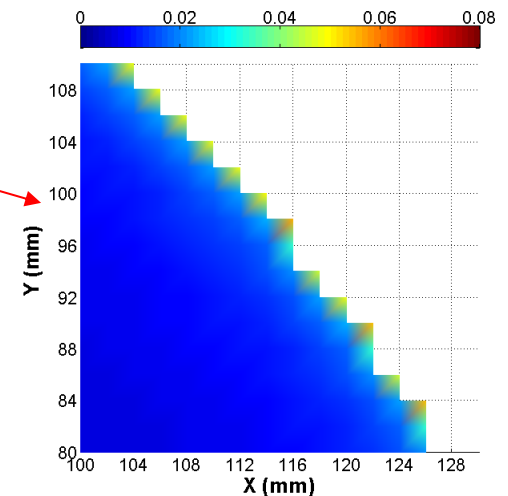
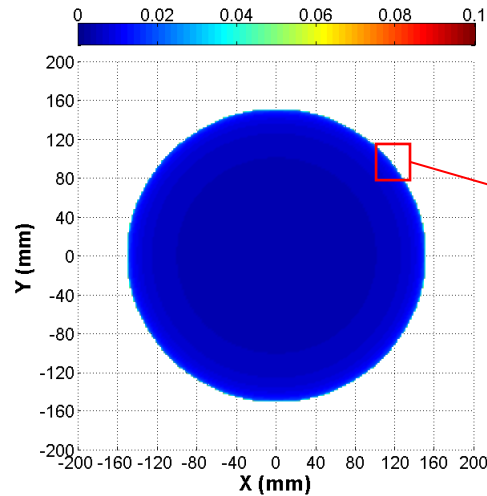
$$F(x, y) = \frac{1}{\pi E} \int d\xi \int d\eta \frac{1}{\sqrt{(x-\xi)^2 + (y-\eta)^2}} \quad E: \text{pad effective modulus}$$

Boundary Conditions

$$\left\{ \begin{array}{l} P(x, y) \geq 0 \\ \frac{1}{S_0} \int_{\text{wafer}} P(x, y) \cdot dx \cdot dy = P_0 \\ \frac{1}{S_r} \int_{\text{ring}} P(x, y) \cdot dx \cdot dy = P_r \\ w(x, y) \geq z(x, y) \end{array} \right. \quad \begin{array}{l} \text{Pressure can not be negative} \\ \text{Average wafer pressure equals to} \\ \text{wafer reference pressure} \\ \text{Average ring pressure equals to} \\ \text{ring reference pressure} \\ z(x, y): \text{ surface of wafer and ring structure} \end{array}$$

Retaining Ring Effect on Wafer Edge Pressure

- 300mm flat wafer surface pressure (MPa) without and with retaining ring
- Assumptions of the simulation:
 - Pad effective modulus: 100MPa
 - Wafer reference pressure: 1psi
 - Ring reference pressure: 4psi
 - Ring width: 20mm
 - Gap between ring and wafer: 4mm
- Wafer edge pressure is tuned by the retaining ring
 - No pressure concentration at wafer edge when retaining ring is applied



Modeling of Relative Velocity

- The instantaneous velocity distribution is a function of the configuration of the CMP machine

$$\vec{V}(p) = -\omega_p (\vec{k} \times \vec{r}_0) + (\omega_w - \omega_p) (\vec{k} \times \vec{r}_w)$$

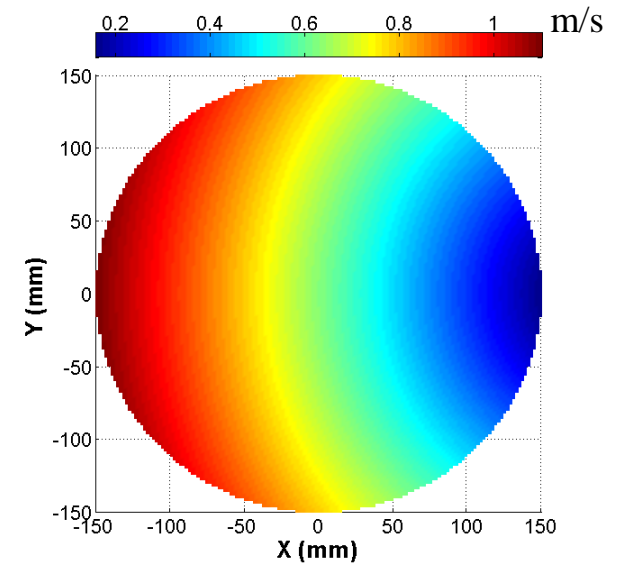
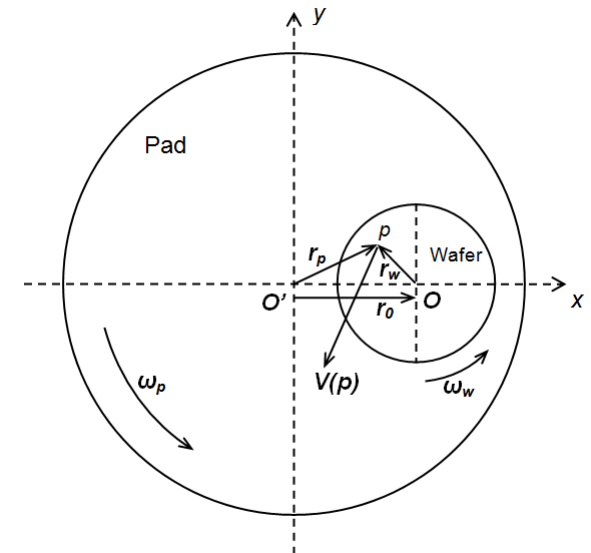
ω_w : wafer angular velocity

ω_p : pad angular velocity

\vec{k} : unit vector perpendicular to the rotation plane

- Assumptions of the simulation:

- 300mm wafer
- Pad rotation speed: 30rpm
- Wafer rotation speed: 60rpm
- Offset distance between pad and wafer centers: 200mm



Next Steps – Wafer-level CMP Model

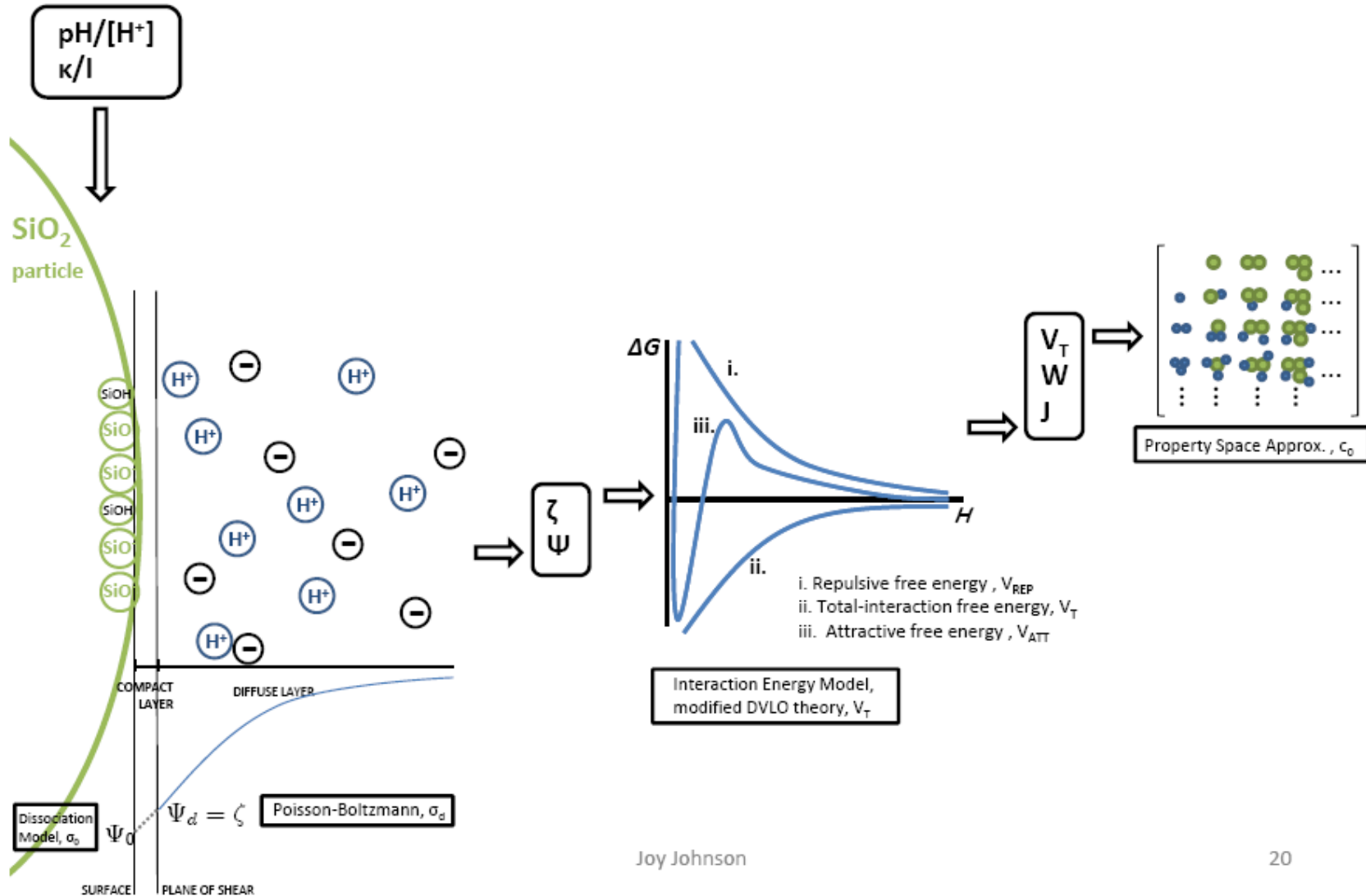
- **Integrate wafer-level model for conditioning**
 - Geometric dependencies in pad surface microtexture generation/modification based on conditioning kinematics
- **Model slurry dynamics**
 - Based on wafer edge and across-wafer pressure profiles, relative velocity kinetics, and pad microtexture
- **Integrate wafer-level with die-level CMP model**
 - Understand and capture wafer level polish rate and slurry/pad-surface nonuniformity impacts on chip uniformity and feature planarization
 - Optimization studies: pad/process/tool to reduce consumables, time, cost and improve performance

2. Slurry Agglomeration/Wafer-Level CMP Modeling:

Issue: Slurry chemistry, process conditions, and tool design affect slurry particle size and agglomeration

- **Model how/when slurry abrasive particles form agglomerates**
- **Understand how agglomeration relates to the *planarization* capability of CMP processes as well as defectivity**
 - agglomerate (particle) size distribution, slurry stability
 - dependency of wafer-scale uniformity (pattern density)
- **Integrate with *wafer- and die-scale* models:**
 - Pressure/velocity (shear) impact on slurry
 - Pad microstructure and slurry interactions

Initial Agglomeration Model



Joy Johnson

20

Next Steps – Slurry Agglomeration Model

- **Agglomeration model verification/improvement:**
 - Account for slurry particles, pad and wafer debris in the creation of agglomerates (respective of size and composition)
 - Account for slurry stability based on agglomerates, chemical composition, and shear forces during CMP
 - Calculate probability of agglomerate size distribution and corresponding stability
- **CMP model/experimental investigations:**
 - Slurry particle size distribution and stability
- **CMP wafer-scale model application**
 - Studies of planarization and defectivity as a function of slurry agglomerates
 - Possible integration of agglomeration model metrics in planarization model on wafer scale

Industrial Interactions and Technology Transfer

- **Intel**
 - **Conducting experiments for agglomeration model metrics and verification**

- **National Semiconductor**
 - **Experimental support for die-level CMP model improvements**

Publications, Presentations, and Recognitions/Awards

1. **Fan, W., D. Boning, L. Charns, H. Miyauchi, H. Tano, and S. Tsuji, “Study on Hardness and Conditioning Effects of CMP Pad Based on Physical Die-level CMP Model,” accepted in Journal of the Electrochemical Society, Dec. 2009.**
2. **D. Boning and J. Johnson, “Slurry Particle Agglomeration Model for Chemical Mechanical Planarization (CMP),” to be presented, CMP Symposium, MRS Spring Meeting, April 2010.**

Students on Task 425.032

- **Graduated Students and Current Affiliation**
- **Current Students and Anticipated Grad Date**
 - Wei Fan (Ph.D.), June 2011
 - Joy Johnson (Ph.D.), June 2012
- **Internships**
 - Joy Johnson, summer 2009, Intel Corporation (Hillsboro, Oregon)

Development of an All-Wet Benign Process for Stripping of Implanted State-of-the-Art Deep UV Resists

(Task number: 425.033)

Experimental Investigation of Catalyzed Hydrogen Peroxide(CHP) System For HDIS

PI:

- **Srini Raghavan, Department of Materials Science and Engineering, UA**

Graduate Student:

- **R. Govindarajan, PhD candidate,
Department of Materials Science and Engineering, UA**

Cost Share (other than core ERC funding):

- **In-kind donation of ion-implanted resist wafers by *Sematech*(~ \$ 5,000)**
- **Donation of amorphous carbon wafers by *Applied Materials* (~ \$ 2,000)**

Objectives

- Investigate the use of Catalyzed Hydrogen Peroxide (CHP) chemical system for disrupting crust formed on deep UV resist layers exposed to high dose of ions ($\geq 10^{15}$ /cm²)
- Identify the effectiveness of CHP system using amorphous carbon as model compound

OXIDATION OF ORGANIC COMPOUNDS BY CATALYZED HYDROGEN PEROXIDE REACTIONS

Classic Fenton's Reaction:

- **Iron catalyzed hydrogen peroxide decomposition (1 part of iron to 5-25 parts of H₂O₂; Fe level < 20 ppm)**



Radicals strong oxidant

Catalyzed H₂O₂ Propagation (CHP):

- **Modified Fenton's reagent : higher concentrations of H₂O₂ (~ 2–25%)**



➤ ***Generation of non-hydroxyl radical reactive species, in addition to OH[•] provides wide reactivity range***

- **Perhydroxyl radical (HO₂[•] – weak oxidant); Superoxide radical anion(O₂^{•-} – nucleophile) ; Hydroperoxide anion (HO₂⁻ – strong nucleophile)**

ESH Metrics and Impact

➤ SPM solution

- Requires high temperature ($\sim 180^{\circ}\text{C}$) for stripping high dose implanted resists

➤ Comparison of toxicity of ingredients in CHP and SPM

Compound	LD ₅₀ (mouse)	Carcinogenic
Ferrous sulfate	1520mg/kg	NO
Peroxide	2000 mg/kg	NO
Sulfuric acid	90 ml/kg (rat)	Yes

➤ ESH Impact

- By using low temperature ($< 100^{\circ}\text{C}$) SPM as a secondary chemical, *energy and safety issues related to the use of very hot SPM can be significantly reduced*

Current Year Activities

- Explored the use of Catalyzed Hydrogen Peroxide (CHP) system for disrupting crust that typically forms on high dose implanted resists using amorphous carbon films as model compound
- Tested CHP system on ion-implanted resists
- Investigated bulk resist removal after CHP exposure using SPM solutions at 80 deg. C

Experimental Approach

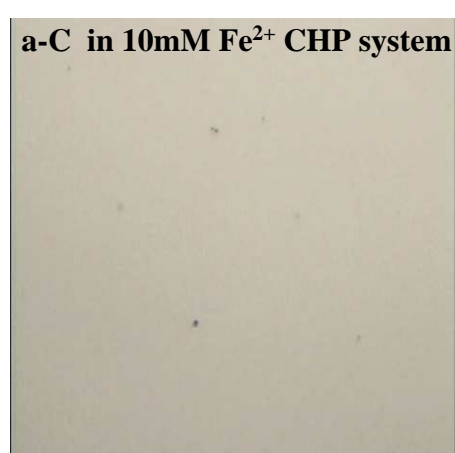
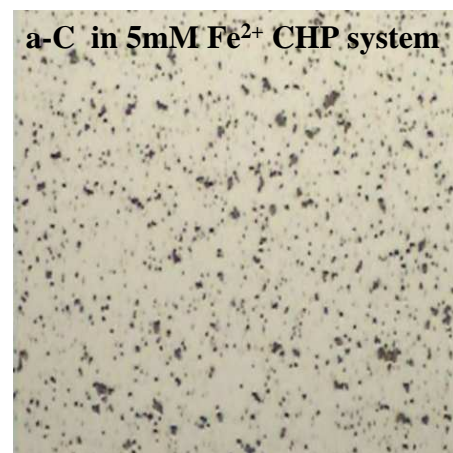
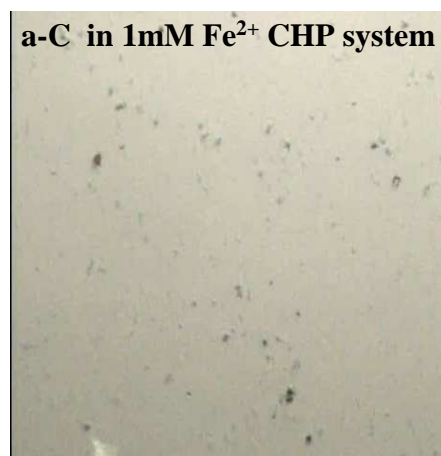
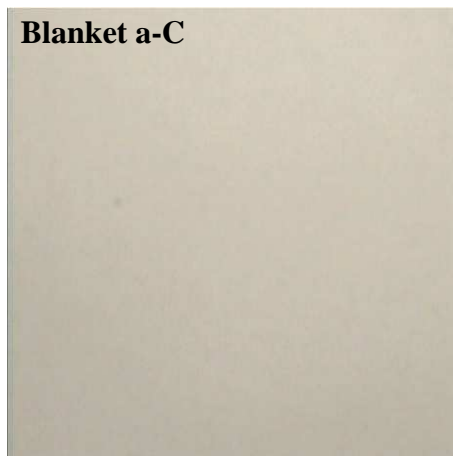
➤ **Methods**

- **Morphological changes after CHP treatment were characterized using Leica DM4000B microscope operated using QCapture Pro 5.0 software, Leeds Confocal microscope, AFM and FESEM**

➤ **Materials**

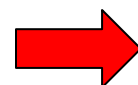
- **Amorphous carbon films ($\sim 900 \text{ \AA}$) donated by Applied Materials, Implanted resist films ($1\text{E}16 \text{ As /cm}^2$; $\sim 1.5 \text{ \mu m}$) donated by Sematech**
- **Ferrous Sulfate ($\text{FeSO}_4 \cdot 6\text{H}_2\text{O}$) , 99.998% pure**
- **Hydrogen Peroxide (30%)**

Attack of Amorphous Carbon (a-C) Films



Optical Microscope : 1000x

Imaged area : ~ 67 x 87 μm



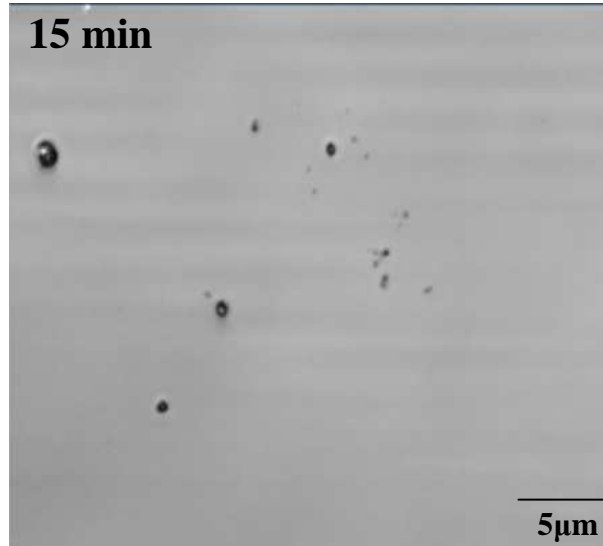
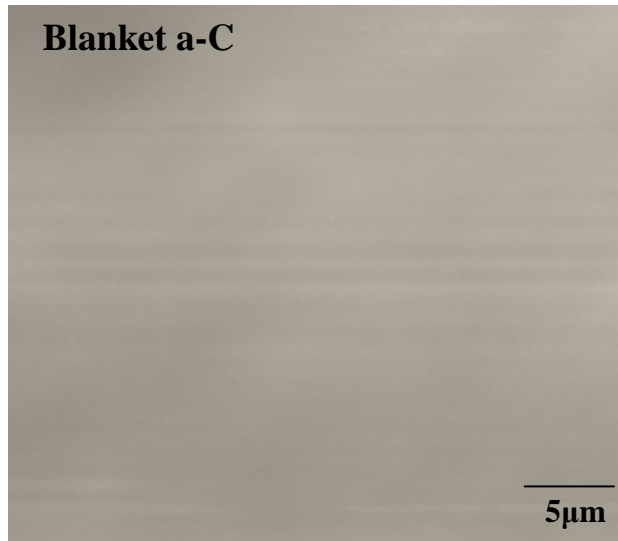
CHP system: 20% H₂O₂ plus variable Fe²⁺ level (pH: 2.8); room temperature; Exposure time: 30 minutes

Cleaning: HCl (1 M) for 2 minutes to remove residual iron

- **Localized attack a function of Fe²⁺ level**
- **Too much Fe²⁺ is a detriment--decomposition of H₂O₂ ?**
- **Higher disruption observed at 5mM Fe²⁺ and 20% H₂O₂**

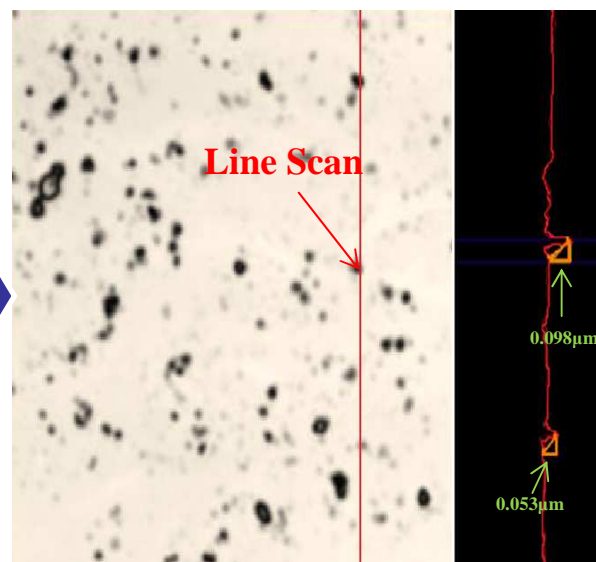
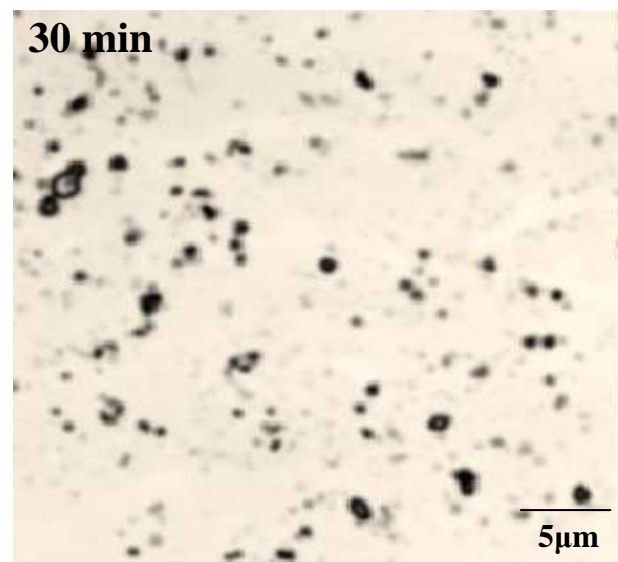
Confocal Images of a-C Exposed to CHP

Confocal mode: 14Kx Magnification (35 X 35 μm)



➤ CHP: 5mM Fe^{2+} ,
20% H_2O_2 (pH: 2.8),
room temperature

➤ CHP exposure time
upto 30 minutes,
post-treatment with
HCl (1 M) for 2 minutes

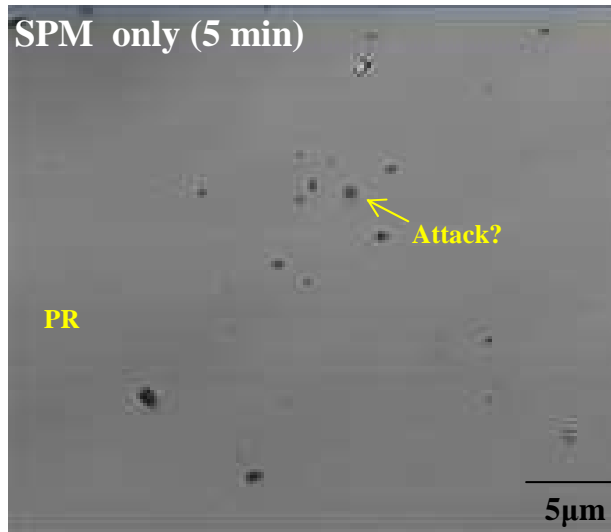


➤ Disruption improves
with CHP exposure time

➤ 30 minutes CHP
treatment creates pores
all over the sample (Pore
size: 28 nm to ~ film
thickness)

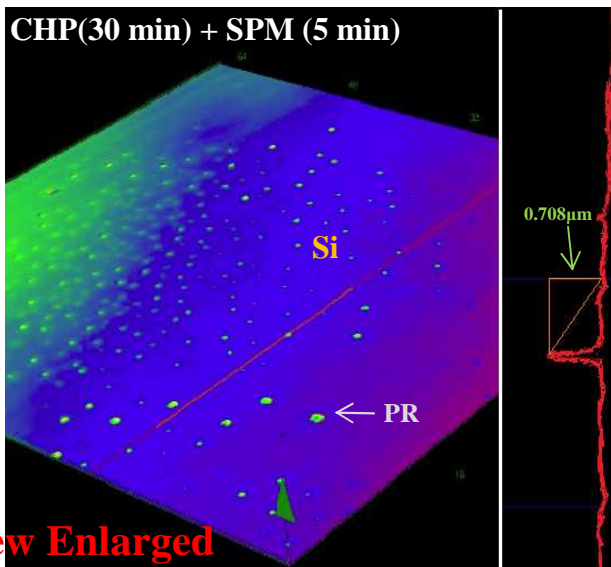
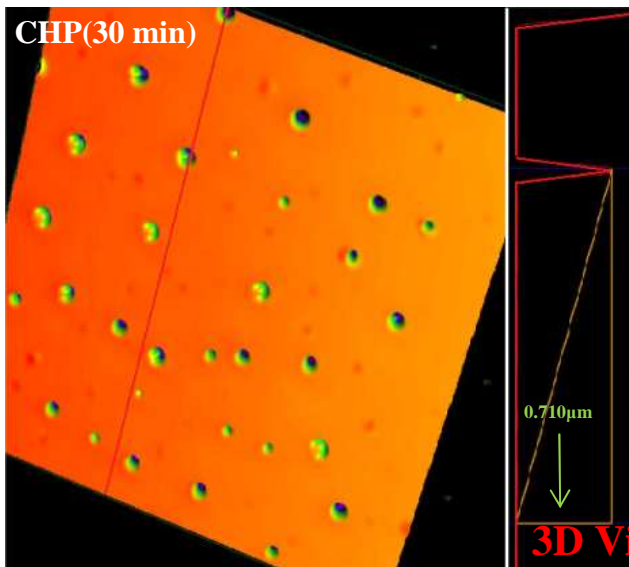
Confocal Images of PR(Dose: 1E16) After CHP & SPM Exposure

Confocal mode: 14Kx Magnification (35 X 35 μm)



➤ CHP: 5mM Fe²⁺,
20% H₂O₂ (pH:2.8),
room temperature

➤ Effect of CHP &
SPM (2:1 for 5
minutes @ 80°C) on PR
films studied

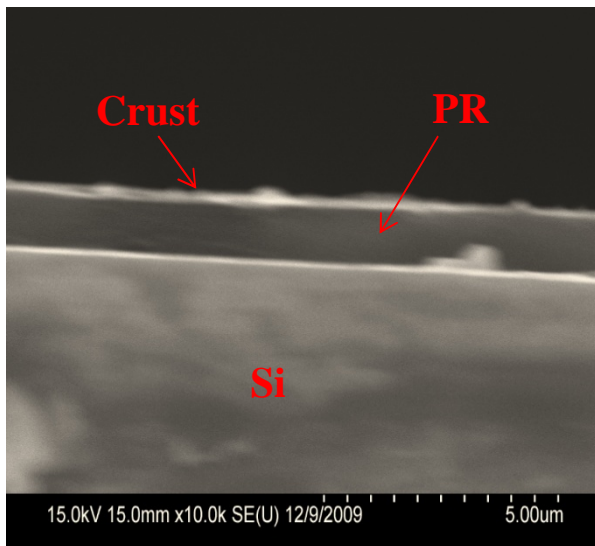


➤ CHP treatment creates
pore of depth ~ 700 nm

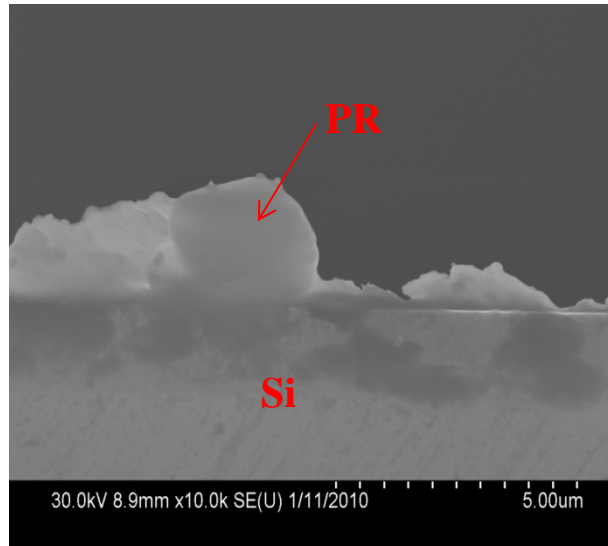
➤ 30 minutes CHP
(room T) + 5 minutes
2:1 SPM @ 80°C
treatment shows good
PR removal (PR remain
at some spots)

Effect of CHP on High Dose Implanted PR film

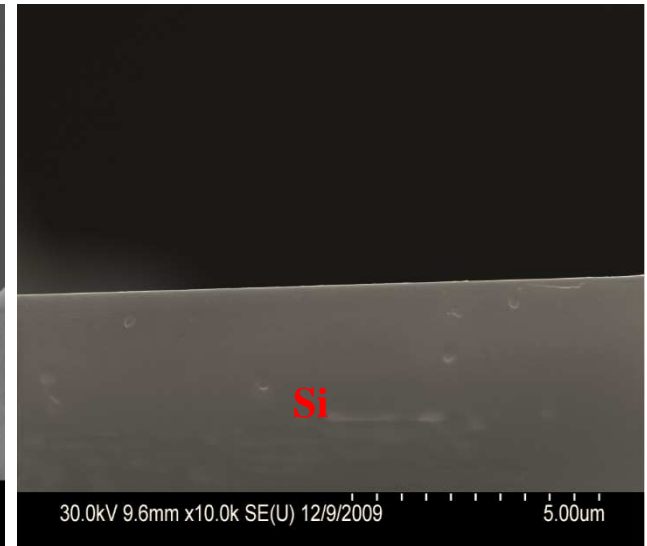
FESEM Images



Blanket PR



PR in 2:1 SPM



PR in CHP + SPM

- **1E16 As/cm² implanted PR shows crust layer**
- **Discontinuous PR residue film observed after 2:1 SPM treatment for 5 minutes at 80°C**
- **CHP (5mM Fe²⁺, 20% H₂O₂; Time: 30min; room temperature) treated PR shows good removal in 2:1 SPM @ 80°C in 5minutes**

Summary

- Effectiveness of Catalyzed Hydrogen Peroxide system in disrupting crust layer was investigated using a-C film as model compound
- CHP system containing 5mM Fe²⁺ , 20% H₂O₂ at room temperature creates surface defects on a-C film and high dose implanted PR; this is confirmed by confocal microscopy
- a- C disruption and PR removal increase with CHP exposure time and CHP followed by 2:1 SPM treatment, respectively
- *Good removal of high dose implanted PR is possible by first exposing the resist in CHP solution for 30 minutes and then in 2:1 SPM at 80°C for 5minutes*

Deliverables Status

Promised Deliverables	Y/N/IP
Analysis of amorphous carbon and graphitic films used as model compounds	Yes for amorphous carbon films
Evaluation of the potential of CHP chemical system to attack amorphous carbon and graphitic materials	Yes for amorphous carbon films
Evaluation of two step (CHP followed by conventional SPM) process to strip films	Yes

Future Plans

Next Year Plans

- Optimization of CHP system to decrease the exposure time prior to conventional SPM treatment
 - Variables: H_2O_2 /catalyst level, Time, Temperature, pH
 - Explore the use of *non-metal catalysts* such as borates, while at the same time determine residual metal levels after current process sequence
- Work with a tool maker to test the chemical system on full wafers

Long Term Plans

- Development of CHP system with minimal use of SPM

Industrial Interactions and Technology Transfer

- Technical discussions with Joel Barnett of **Sematech** on choice of samples and experimental direction
- Discussions with Hsi-An Kwong of Freescale
- Interactions with Renhe Jia and Chiu Chan of **Applied Materials** on a-C films
- Discussions with Jeff Butterbaugh on testing the process in FSI tools
- Assistance of Bob Morris of **Oclaro** on Confocal microscopy

**Improvement of ESH Impact of
Back End of Line (BEOL) Cleaning Formulations
Using Ionic Liquids to Replace Traditional Solvents**
(Task Number: 425.034)

PI:

- **Srini Raghavan, Materials Science and Engineering, University of Arizona**

Graduate Student:

- **Dinesh P R Thanu, PhD candidate, Materials Science and Engineering, University of Arizona**

Objectives

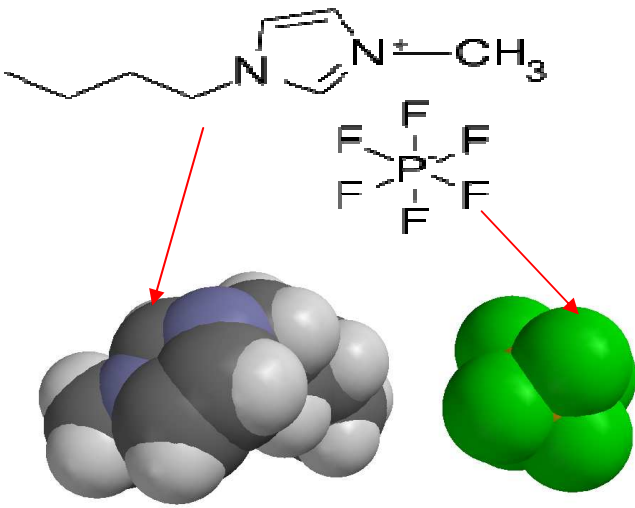
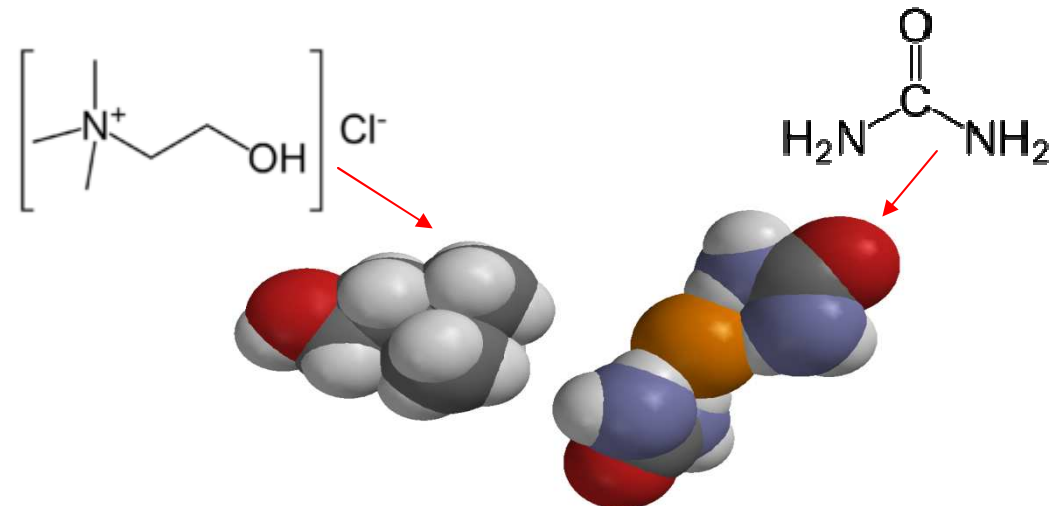
OVERALL OBJECTIVE

- **Develop cleaning formulations based on ionic liquids to replace traditional organic solvent based formulations for BEOL cleaning**

SPECIFIC OBJECTIVES FOR THE CURRENT CONTRACT YEAR

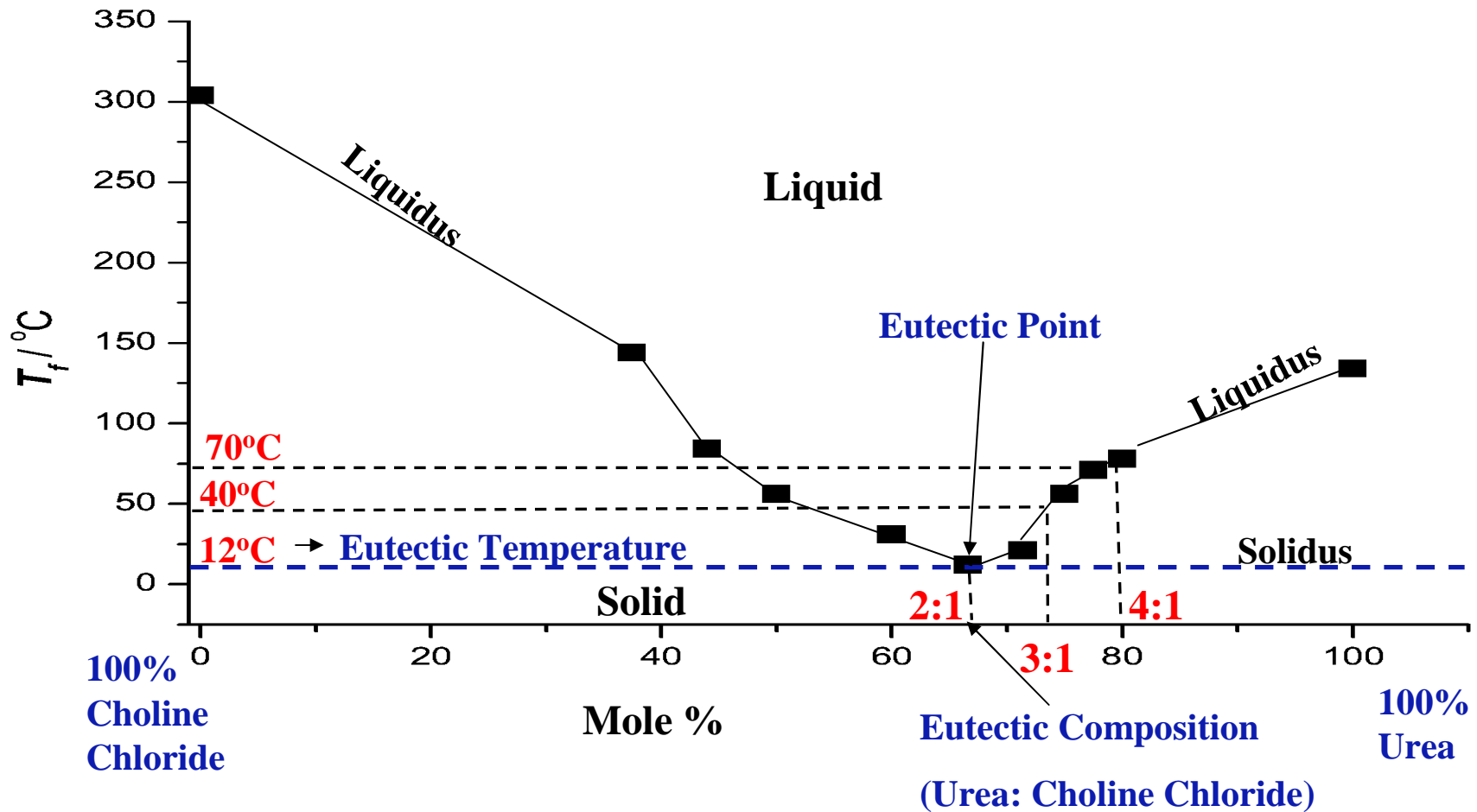
- **Investigate the feasibility of using deep eutectic solvents (DES) based on choline chloride and urea for the removal of post etch residues**
- **Optimize cleaning conditions (DES concentration and temperature) for the selective removal of residues**
- **Determine the etch rate of low-k dielectric in DES formulations**

Ionic Liquids Vs Deep Eutectic Solvents

<i>Ionic Liquids</i>	<i>Deep Eutectic Solvents</i>
<ul style="list-style-type: none"> • Low melting point ionic compounds • Environmental friendly • Solution conductivity-moderate to high • Expensive- Recycling is critical • Highly viscous <p>Applications: Batteries, metal plating etc</p> <p><i>Eg: 1-butyl-3-methylimidazolium hexafluorophosphate</i></p> 	<ul style="list-style-type: none"> • Low melting eutectic mixture of compounds • <i>Highly conductive</i> • <i>Cheaper</i> than ionic liquids • Viscosity can be lowered by mixing with suitable ionic solvents • <i>Low metal corrosion rate and high copper oxide solubility</i> <p><i>Eg: Eutectic mixture of choline chloride and urea</i></p> 

Deep Eutectic Solvents (DES)

(e.g.) Urea-Choline Chloride Binary Phase Diagram

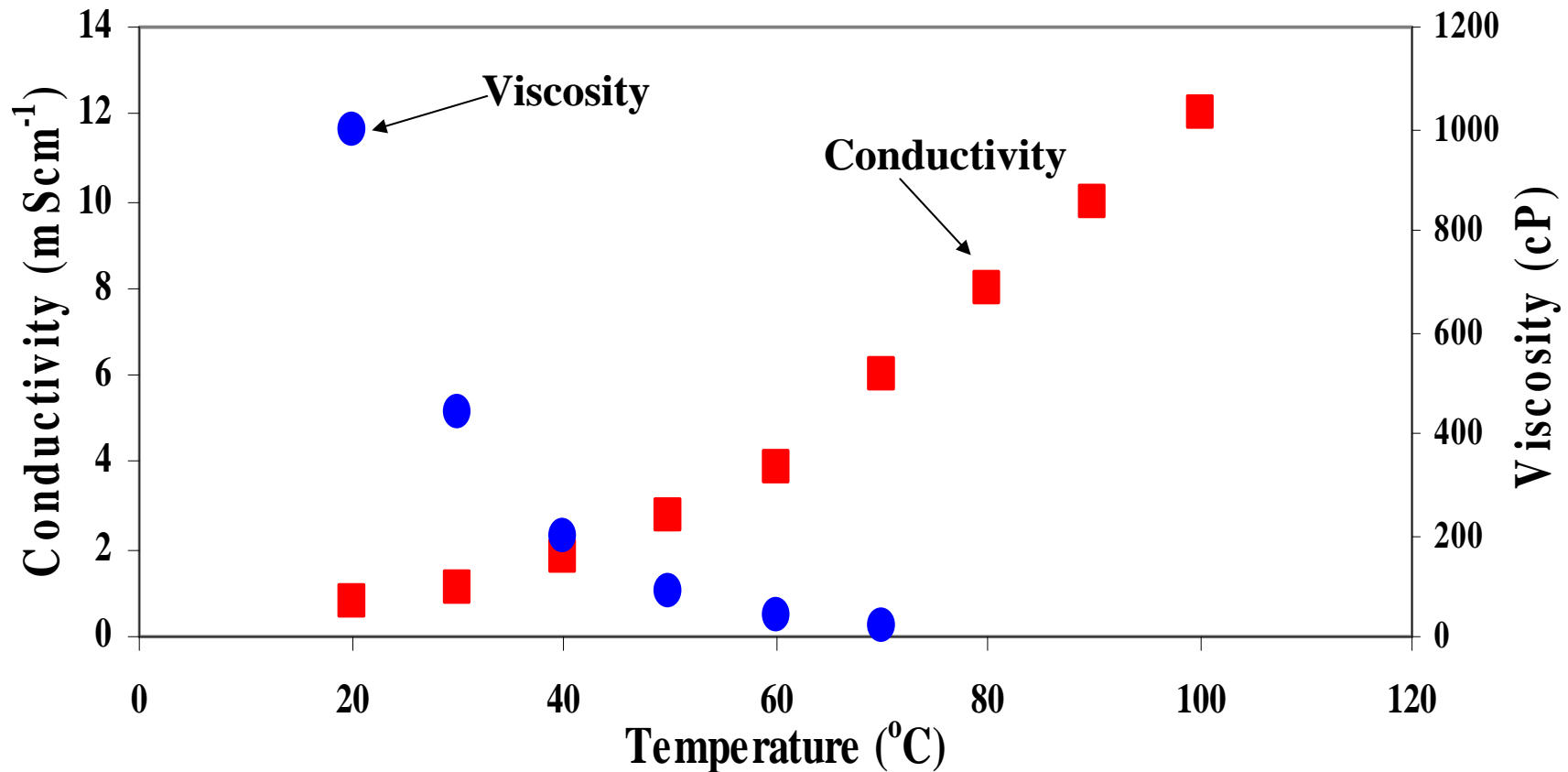


- 2:1, 3:1 and 4:1 (urea:choline chloride) chosen for investigation

A.P. Abbott, et al., *Chemical Communications*, p. 70-71 (2003)

2009 – 2010 Contract Year Research Highlights

Conductivity and Viscosity of Urea:Choline Chloride (2:1) at Different Temperatures



- **Good conductivity (1 mScm⁻¹ @ 20°C)- comparable to 0.005 M KCl**
- **Conductivity increases with temperature (2 mScm⁻¹ @ 40°C, 6 mScm⁻¹ @ 70°C)**
- **High viscosity at room temperature and it decreases with increase in temperature**

Experimental Approach

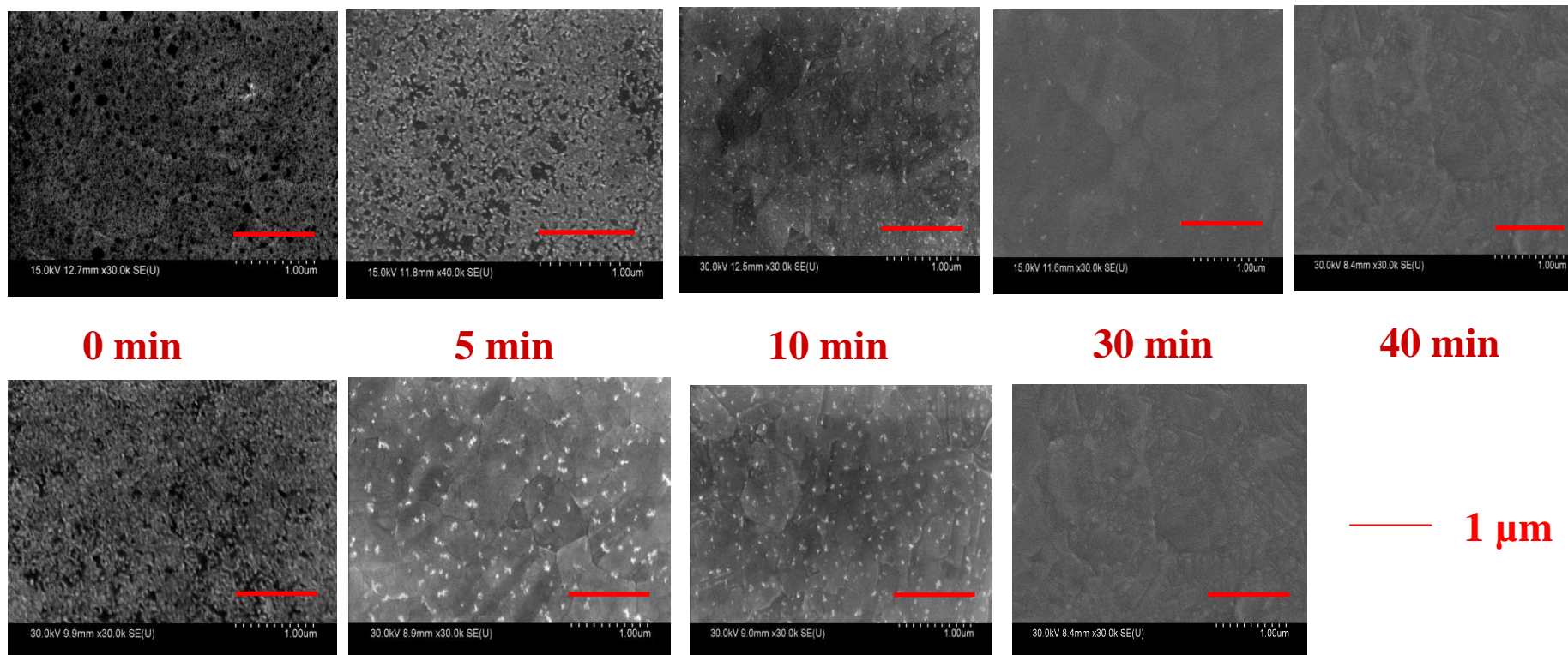
Materials and Methods

- Residue prepared from *g line* and *Deep UV (DUV)* photoresists
- Photoresists spin coated on copper wafers
 - Thickness: *1.5 μm gline* and *0.5 μm DUV*
- Photoresist ashed in Reactive Ion Etcher (RIE) using *CF₄/O₂ plasma*
- Thickness of residue film measured by Atomic Force Microscope step height measurements
 - *~30 nm (gline)* and *~3 nm (DUV)*
- *g line* and *DUV* contains mixture of *CuF₂* and *CuO* as determined from X-ray Photoelectron Spectroscopy (XPS) analysis

- Residue removal investigated using *Scanning Electron Microscopy (SEM)* and confirmed using *XPS* and *open circuit potential* measurements
- Low-k dielectric (Black Diamond[®]) etch rate measured using ellipsometry

Residue Removal using 2:1 DES (Urea:Choline Chloride) at 40°C

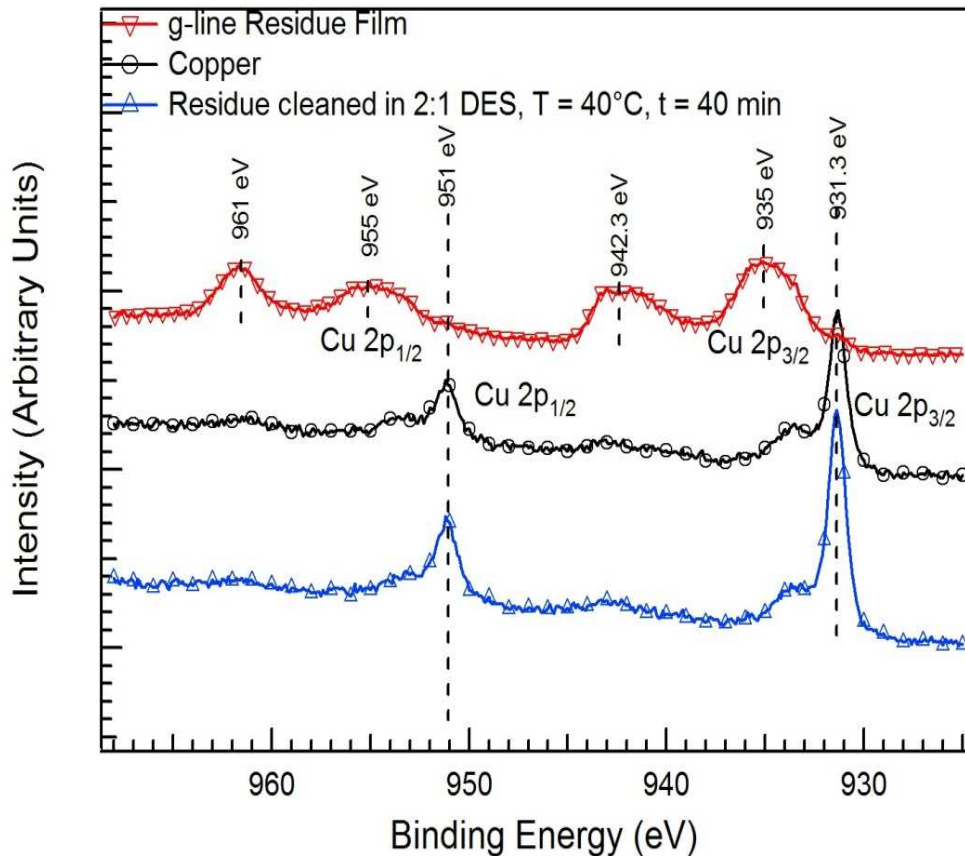
G LINE Residue (~30 nm)



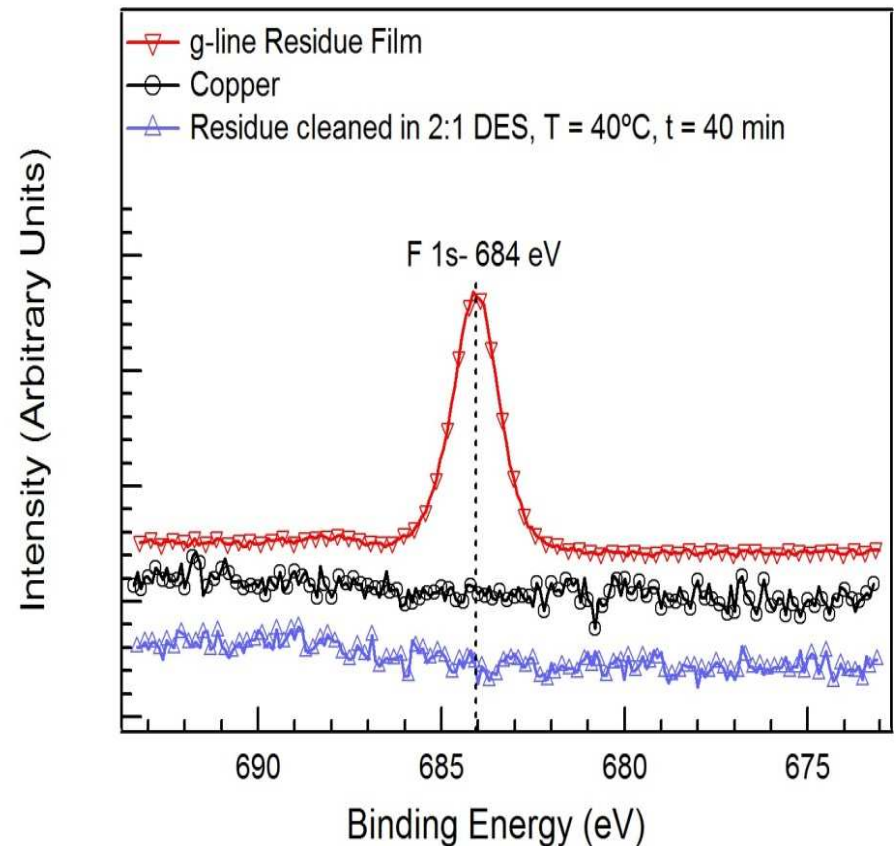
DUV Residue (~3 nm)

- Residue removal monitored using SEM imaging
- Complete removal observed in *~30- 40 minutes* for gline residue and *~30 minutes* for DUV residue

Confirmation of g-line Residue Removal in 2:1 DES @40°C using XPS Analysis



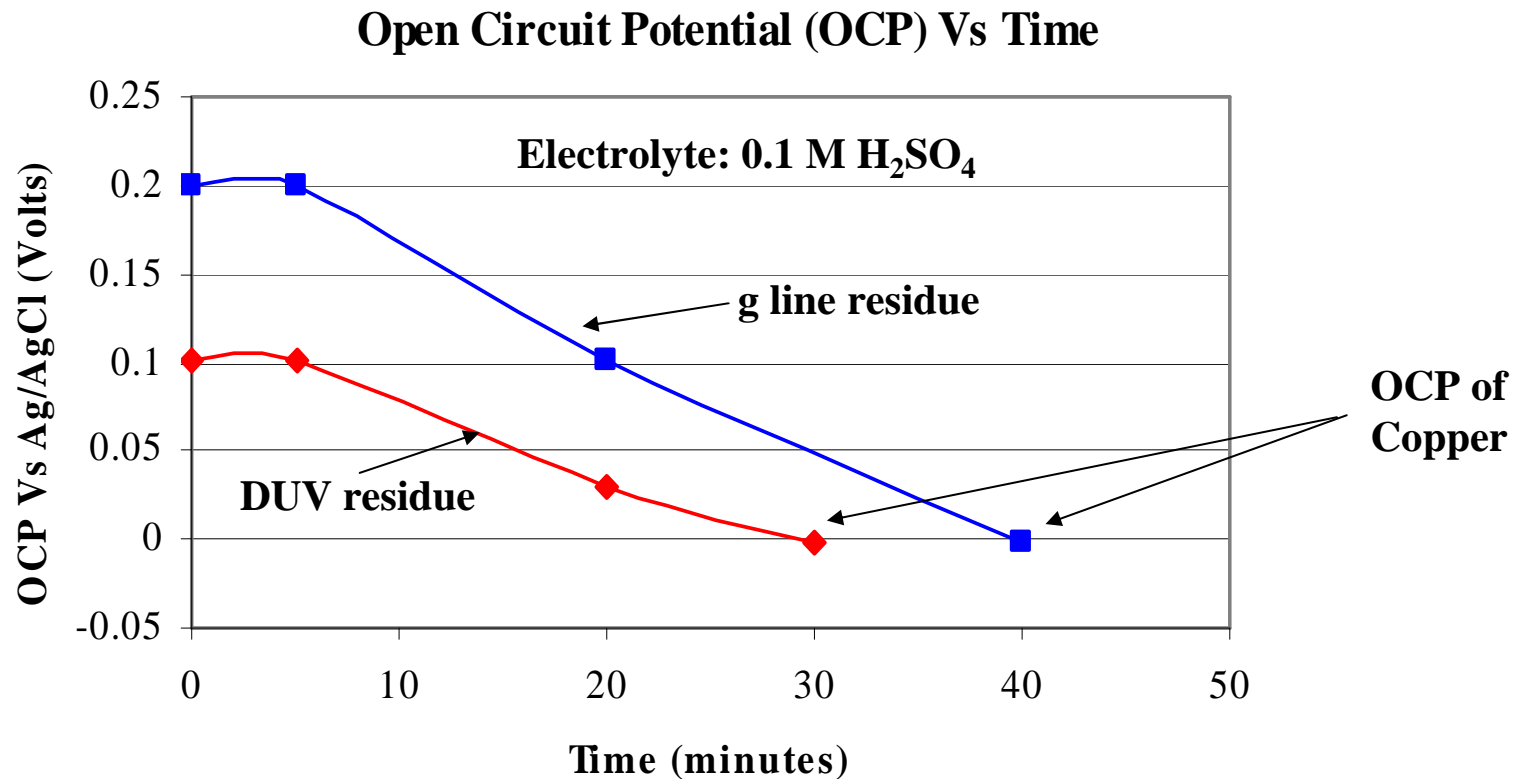
Cu 2p spectrum



F 1s spectrum

- Residue removal exposes bare copper surface after cleaning
- Cu 2p Spectrum-Binding energies in cleaned samples identical to *bare Cu*
- F 1s Spectrum- *Absence of fluorine peak* in cleaned sample indicates good cleaning

Confirmation of Residue Removal in 2:1 @40°C DES using Electrochemical Studies



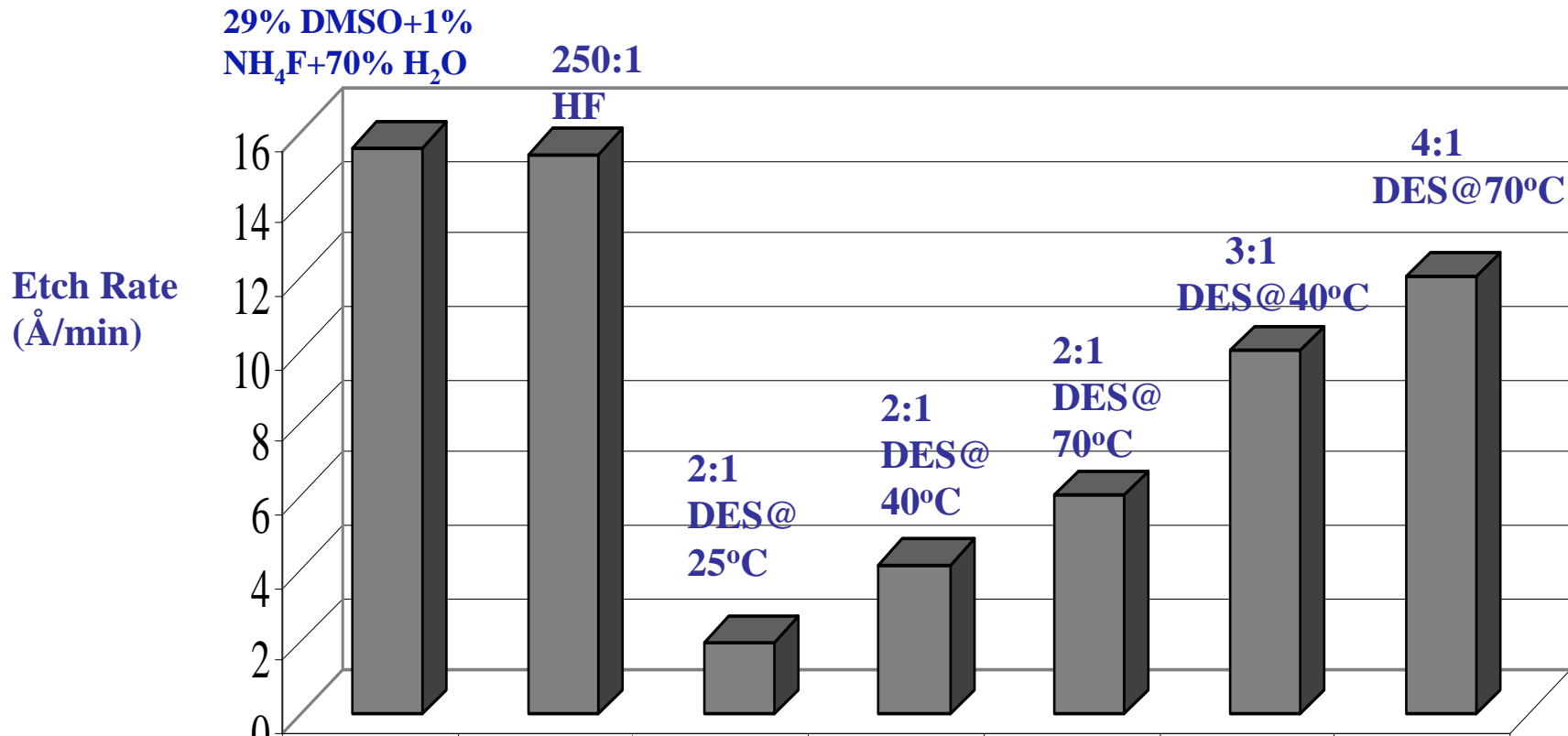
- G line and DUV residue samples cleaned for 40 min and 30 min respectively have OCP of *bare Cu*- Complete Removal
- G line and DUV residues cleaned for 5 min have OCP of *residue*- indicating incomplete film removal

Removal Rate of *Residues* in DES Formulations

Cleaning Formulation	Removal Rate (Å/min)	
	G line Residue	DUV Residue
2:1 DES @40°C	7.5	1
2:1 DES @70°C	10	1.5
3:1 DES @40°C	7.5	1
4:1 DES @70°C	10	1.5
29% DMSO+1% NH₄F+70% H₂O	15	1.5
250:1 HF	10	1.5

- **Dissolution time monitored using SEM**
- **DES formulations effectively removed both g line and DUV residue films**

Etch Rate of Blanket *low-k Dielectric (Black Diamond®)* in Different Cleaning Formulations



- DES provides *lower dielectric etch rate* compared to conventional cleaning formulations

Highlight of Results

- *Choline chloride and urea based DES* shows promise as a BEOL cleaning formulation
 - *2:1 DES at 40°C and 70°C* effectively removed post etch residues on copper
 - Removal of post etch residues confirmed using X-ray Photoelectron Spectroscopy (XPS) and electrochemical techniques
 - DES formulations etched low-k dielectric (Black Diamond[®]) at a *rate much smaller* than conventional cleaning formulations

Future Plans

Next Year Plans

- Reduction of *viscosity, cleaning time, DES carry over and operating temperature*
 - Addition of ethylene glycol or water to DES reduces viscosity without affecting the dissolution properties
 - Reduction of cleaning time using *spin cleaning method*
- Rinsing of cleaned substrates—address any *corrosion issues* during rinsing
- Investigate cleaning of *patterned test structures* and determine the end point removal using electrochemical techniques

Long-term Plans

- Systematic analysis of another DES system as a cleaning formulation for post etch residue removal e.g. *choline chloride/malonic acid*
 - Eutectic mixture of choline chloride with malonic acid has a high solubility for copper oxides

Industrial Interactions

- Discussions with Dr. Robert Small, *R.S. Associates, Tucson*
- Teleconference with Dr. Mansour Moinpour, Paul Fischer and Shan Clark of *Intel*, to discuss results and seek advice on future direction
- Teleconference with John DeGenova, *Texas Instruments Inc.*

Acknowledgements

- Manish Keswani, Assistant Research Professor, Materials Science and Engineering, University of Arizona
- Shariq Siddiqui, PhD student, Materials Science and Engineering, University of Arizona
- Dr. Nandini Venkataraman, Materials Science and Engineering, University of Arizona (Currently with Intel)

High-Throughput Cellular-Based Toxicity Assays for Manufactured Nanoparticles and Nanostructure-Toxicity Relationship Models

(Task Number: 425.035)

Subtask 1: “High Throughput Screening”

Subtask 2: “Computational Models”

PIs:

- **Subtask 1 Leader: Dr. Russell J. Mumper, Center for Nanotechnology in Drug Delivery, UNC Eshelman School of Pharmacy, UNC-Chapel Hill**
- **Subtask 2 Leader: Dr. Alexander Tropsha, Division of Medicinal Chemistry and Natural Products, UNC Eshelman School of Pharmacy, UNC-Chapel Hill**

Graduate Students and Postdoctoral Fellows:

- **Shalini Minocha, PhD Candidate, Center for Nanotechnology in Drug Delivery, UNC Eshelman School of Pharmacy, UNC-Chapel Hill**
- **John Pu, PhD Candidate, Laboratory for Molecular Modeling, UNC Eshelman School of Pharmacy, UNC-Chapel Hill**
- **Denis Fourches, Postdoctoral Fellow, Laboratory for Molecular Modeling, UNC Eshelman School of Pharmacy, UNC-Chapel Hill**

SRC/SEMATECH Engineering Research Center for Environmentally Benign Semiconductor Manufacturing

Objectives

Subtask 1:

- **Validation of high-throughput cellular-based toxicity assays for MNP assessment.**
- **Test QNTR (Quantitative Nanostructure Toxicity Relationship) model using the predictive models developed in subtask 2.**

Subtask 2:

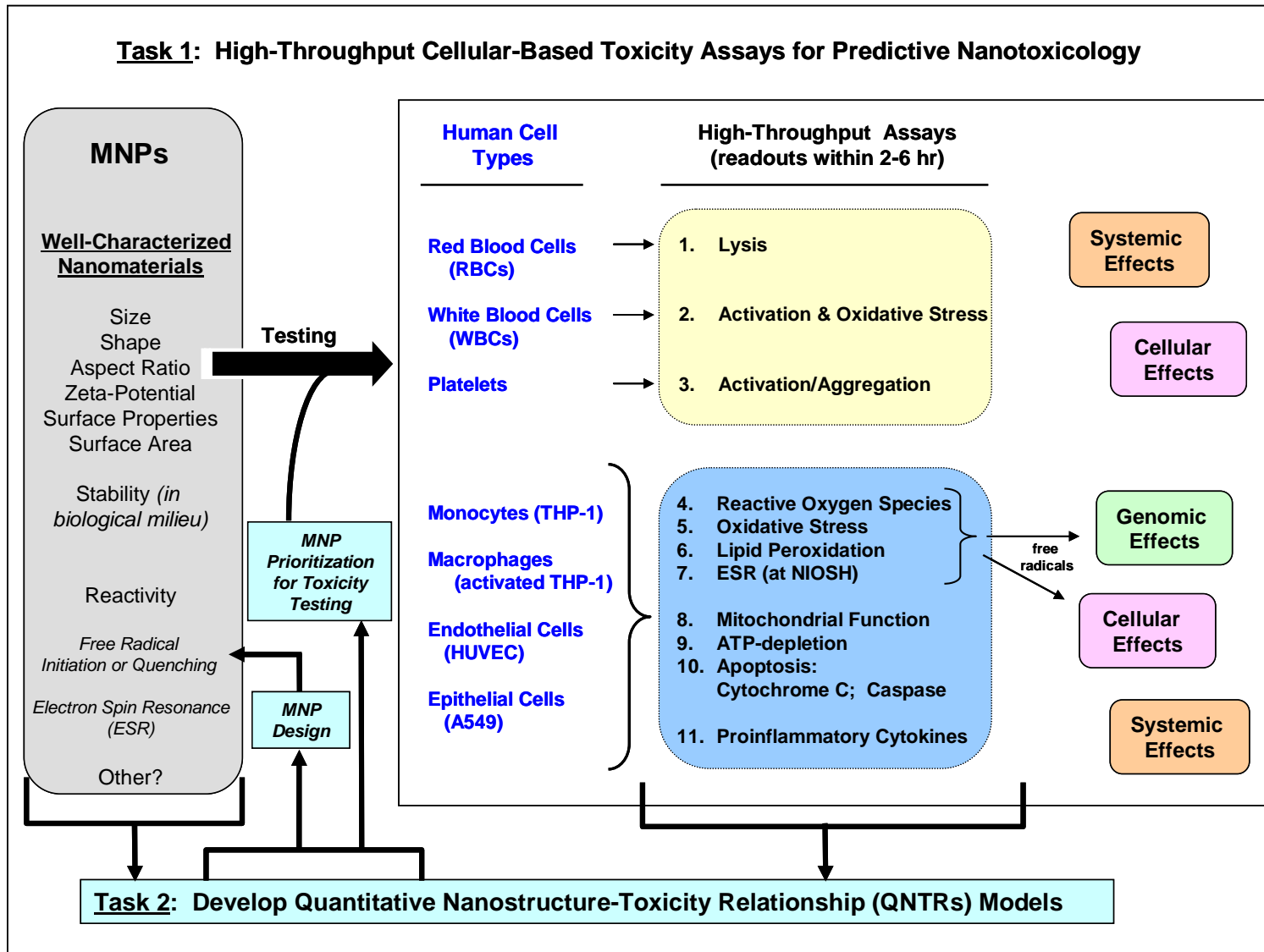
- **Develop QNTR models that correlate the compositional/physical/chemical/geometrical and biological descriptors of MNPs with known toxicological endpoints.**
- **Improve the prediction performance of QNTR models with the availability of new experimental data from subtask 1.**

ESH Metrics and Impact

- 1. Obtain predictive knowledge of the physical and chemical properties of manufactured nanoparticles.*
- 2. Develop relevant in-vitro assays utilizing human cells to predict the toxicity of manufactured nanoparticles.*
- 3. Develop predictive computational models that correlate physical-chemical descriptors of MNPs with their toxic effects.*

Impact: Utilize the knowledge gained through above three metrics for improved MNP experimental design and prioritized toxicity testing toward the manufacturing of safe nanomaterials.

General Framework of the Proposed Approach

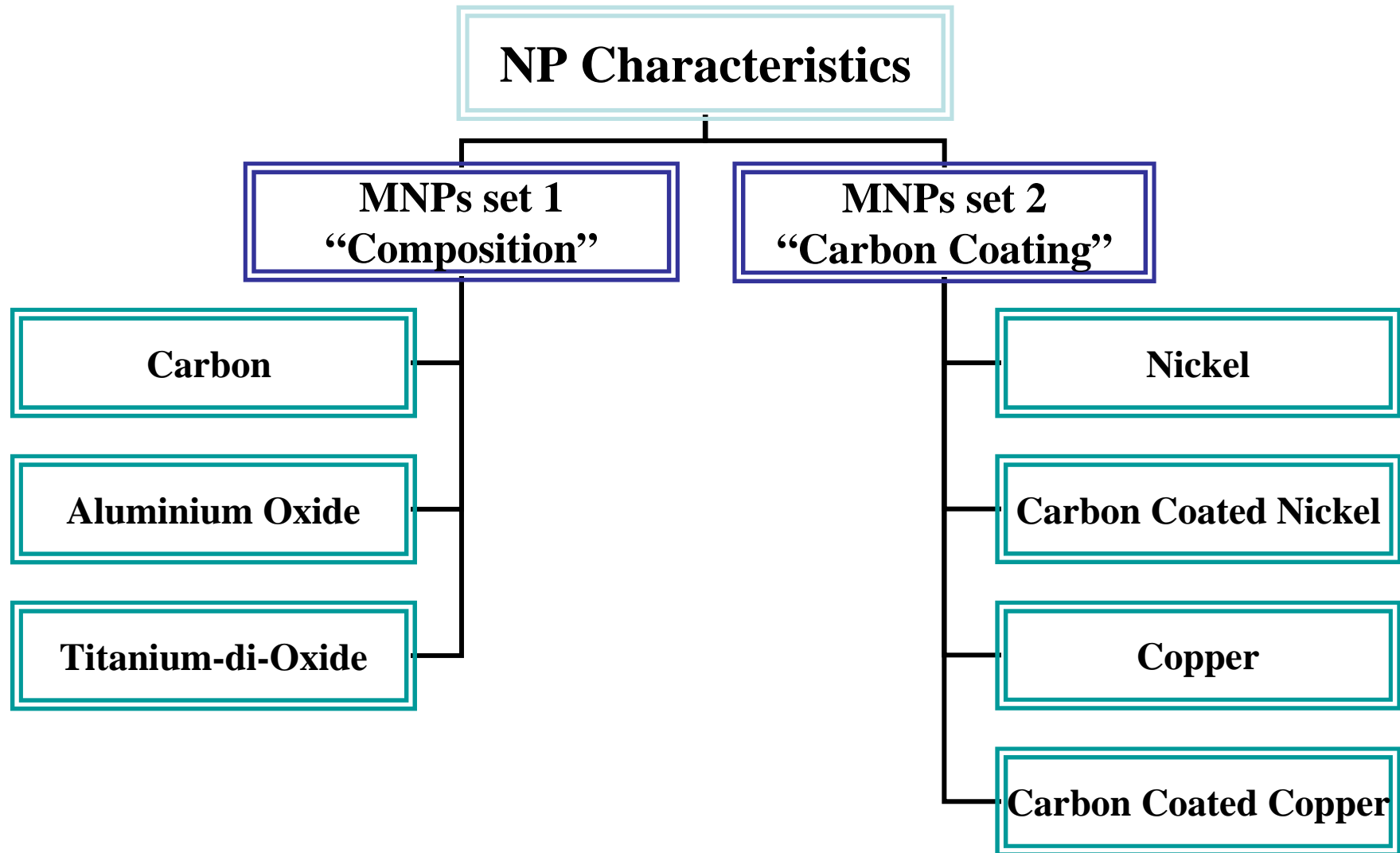


Subtask 1: Potential Cellular-based Assays

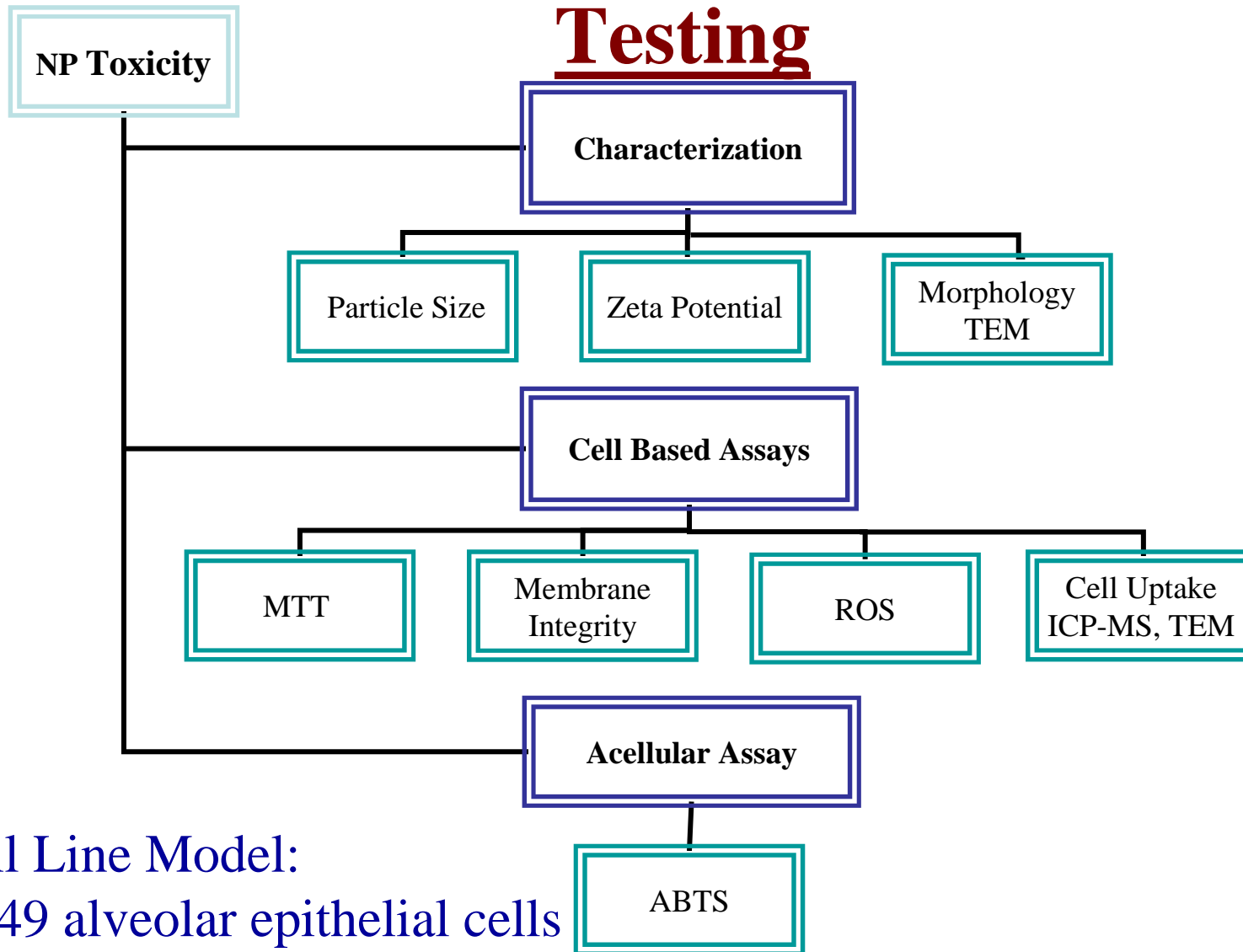
Human Cells	Assay	Description
Red Blood Cells (RBCs)	Lysis	Measure oxyhemoglobin at 540 nm
White Blood Cells (WBCs)	Activation	Measure reduction of ferricytochrome c caused by produced superoxide anions
	Oxidative Stress	Measure intracellular GSSG/GSH ratio; where GSSG is oxidized glutathione and GSH is reduced glutathione
Platelets	Activation	Flow cytometry to measure PAC-1-FITC binding to activated platelets
	Aggregation	Whole Blood Impedance Aggregometry

Human Cells	Assay	Description
Monocytes (THP-1) Macrophages (activated THP-1) Endothelial Cells (HUVEC) Epithelial Cells (A549)	Reactive Oxygen Species	1) Measure intracellular fluorescence produced with H ₂ DCFDA or carboxy-H ₂ DCFDA loaded cells; 2) Measure (a) cellular ESR
	Oxidative Stress	Measure intracellular GSSG/GSH ratio; where GSSG is oxidized glutathione and GSH is reduced glutathione
	Lipid Peroxidation	Lipid Hydroperoxide (LPO) Assay
	Mitochondrial Function	MTT assay & JC-1 assay
	ATP-depletion	ATPlite 1step® Assay Kit (PerkinElmer)
	Apoptosis:	
	Cytochrome C	Cytochrome C immunoassay
	Caspase-3	Caspase-3 Fluorometric Assay (R&D Systems); Quantify caspase-3 activation by cleavage of DEVD-AFC substrate
	Proinflammatory Cytokines	Cytokine assays by ELISA; NFκB, IL-1β, TNF-α, IFN-γ, IL-8

Subtask 1: Current Method Approach



Subtask 1: Current Scheme for Toxicity



Cell Line Model:
A549 alveolar epithelial cells

Characterization: MNPs Set 1 and 2

NP Type	Manufacturer	Particle Size* Range (nm)	Particle Size in DI water (nm)	Zeta Potential (mV)
Carbon	American Elements	55-100	611.7 ± 510.5	-21.1 ± 4.6
Aluminum oxide	Alfa-Aesar	40-50	488.8 ± 318.7	-17.7 ± 7.4
Titanium-di-oxide	NanoAmor	30-40	511.7 ± 336.7	-25.3 ± 5.2
Nickel	NanoAmor	20	834.6 ± 495.1	2.76 ± 0.7
Carbon coated Nickel	NanoAmor	20	466.6 ± 179.6	-16.4 ± 1.8
Copper	NanoAmor	25	662.2 ± 139.3	-9.0 ± 2.4
Carbon coated Copper	NanoAmor	25	412.1 ± 210.9	-6.21 ± 0.7

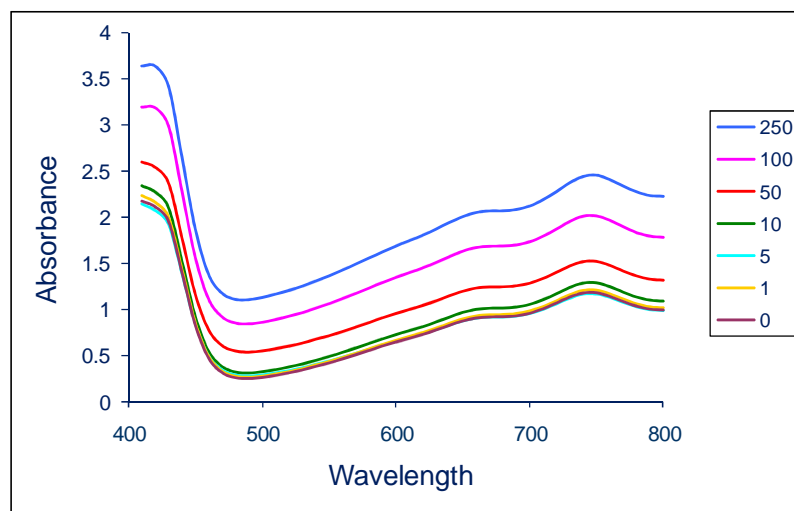
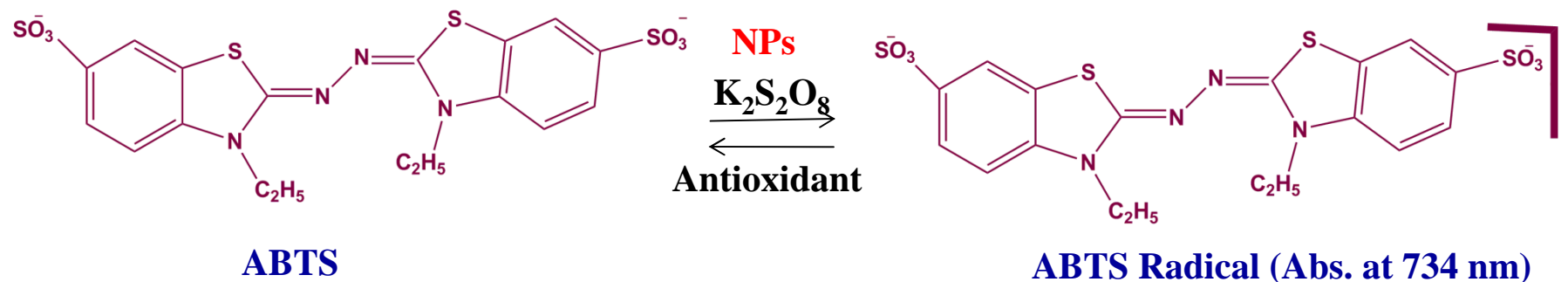
* Provided by Manufacturer

Sample preparation: 1 mg/ml suspensions in DI water; bath sonicated for 6 x30 sec

SRC/SEMATECH Engineering Research Center for Environmentally Benign Semiconductor Manufacturing

MNPs Set 1

ABTS Assay



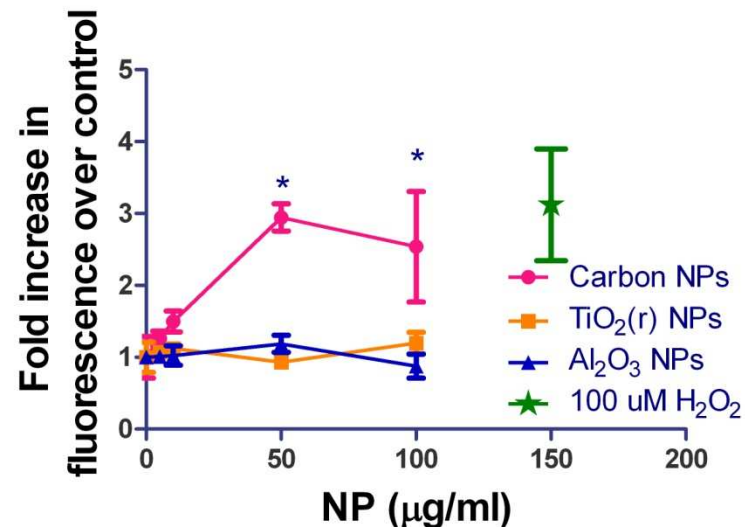
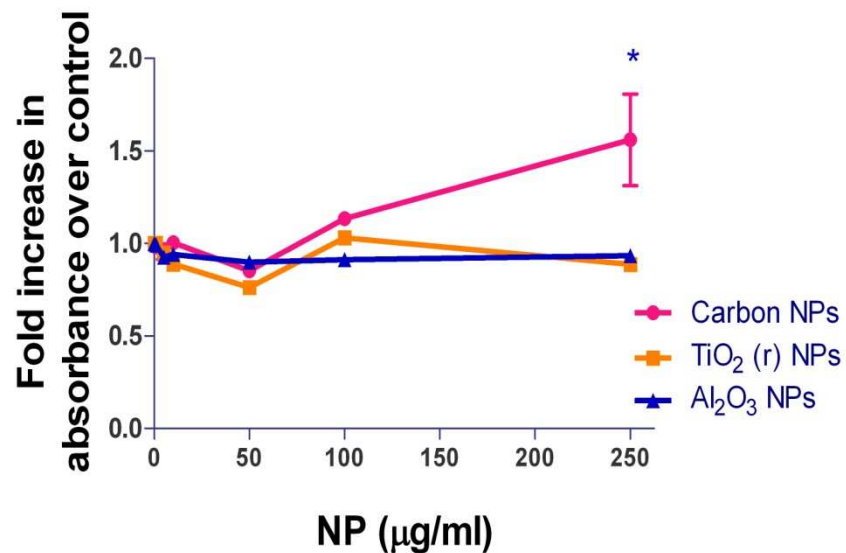
Wavelength vs. Absorbance for Carbon NP induced ABTS radical (not corrected for blank NPs)

ABTS = 2,2'-Azinobis (3-ethylbenzothiazoline-6-sulfonic acid diammonium salt)

SRC/SEMATECH Engineering Research Center for Environmentally Benign Semiconductor Manufacturing

MNPs Set 1

ABTS and ROS Assay



- Assay in 96 well plate, ABTS 60 mM.
- Incubation with NPs for 24 hr.
- Data corrected for absorbance from blank NPs.

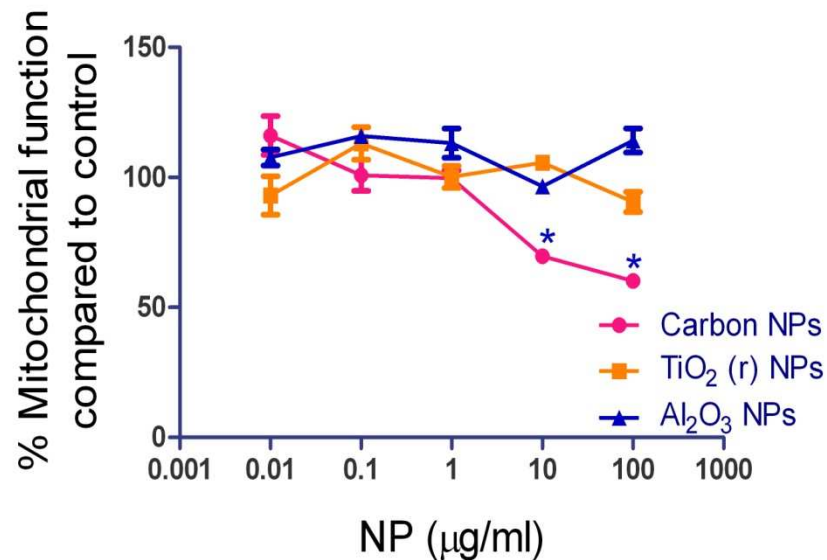
- A549 cells (25,000 per well).
- Incubation with NPs for 4 hr.
- Data corrected for fluorescence from blank NPs.
- H₂O₂ as positive control.

ABTS = 2,2'-Azinobis (3-ethylbenzothiazoline-6-sulfonic acid diammonium salt), (* p < 0.05 as compared to control)

SRC/SEMATECH Engineering Research Center for Environmentally Benign Semiconductor Manufacturing

MNPs Set 1

Mitochondrial Function



Analysis	%
Si	0.1
Al	0.005
Na	0.0008
Cr	0.06
Ni	0.05
Ca	0.01
Fe	0.08
F	0.03

- A549 cells (25,000 per well).
 - Incubation with NPs for 24 hr.
 - Data corrected for absorbance from blank NPs.
- (* p < 0.05 as compared to control)

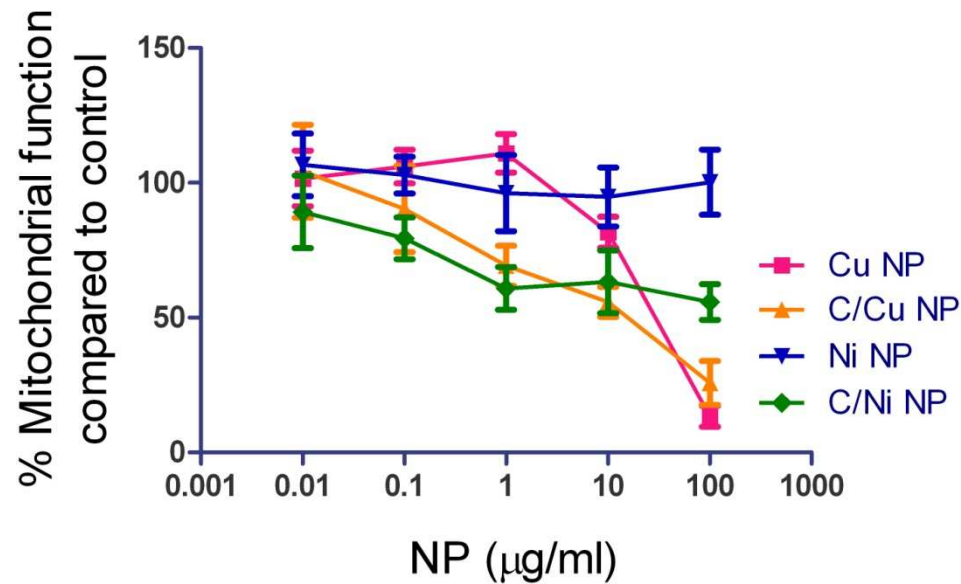
Impurities in Carbon NPs from certificate of analysis provided by the manufacturer.

Conclusions:MNPs Set 1

- Particle size measurement by dynamic light scattering shows that NP sizes are different from those provided by the manufacturer.
- ABTS assay was successfully developed as an *in-vitro* acellular assay to assess the free radical forming potential of NPs. The assay is simple, adaptable to 96 well plate and cost effective.
- Carbon NPs appear to be more toxic as compared to other NPs as shown by *in-vitro* MTT and ROS data.
- Carbon nanoparticles probably act as a vehicle to carry iron/nickel in cells. This is a very plausible scenario as hydrophobicity provided by carbon NPs facilitate iron entry in cells.
- Results from ABTS assay correlates well with ROS and MTT cytotoxicity data.

MNPs Set 2

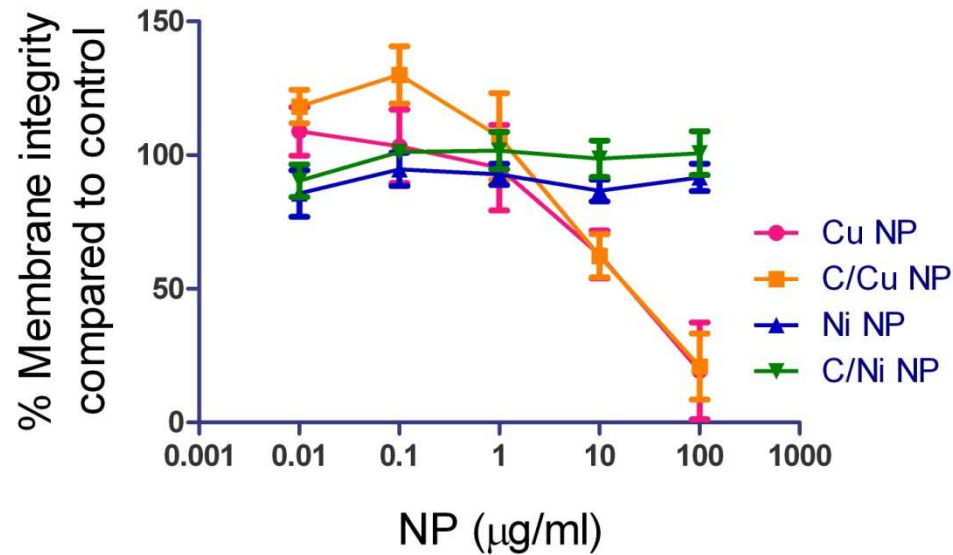
Mitochondrial Function



- A549 cells (25,000 per well), incubation with NPs for 24 hr.
 - Data corrected for absorbance from blank NPs.
 - Ni NPs significantly differ from C/Ni NPs at all doses.
 - Cu NPs significantly differ from C/Cu NPs at 0.1, 1 and 10 µg/ml.
- ($p < 0.05$ as compared to control)

MNPs Set 2

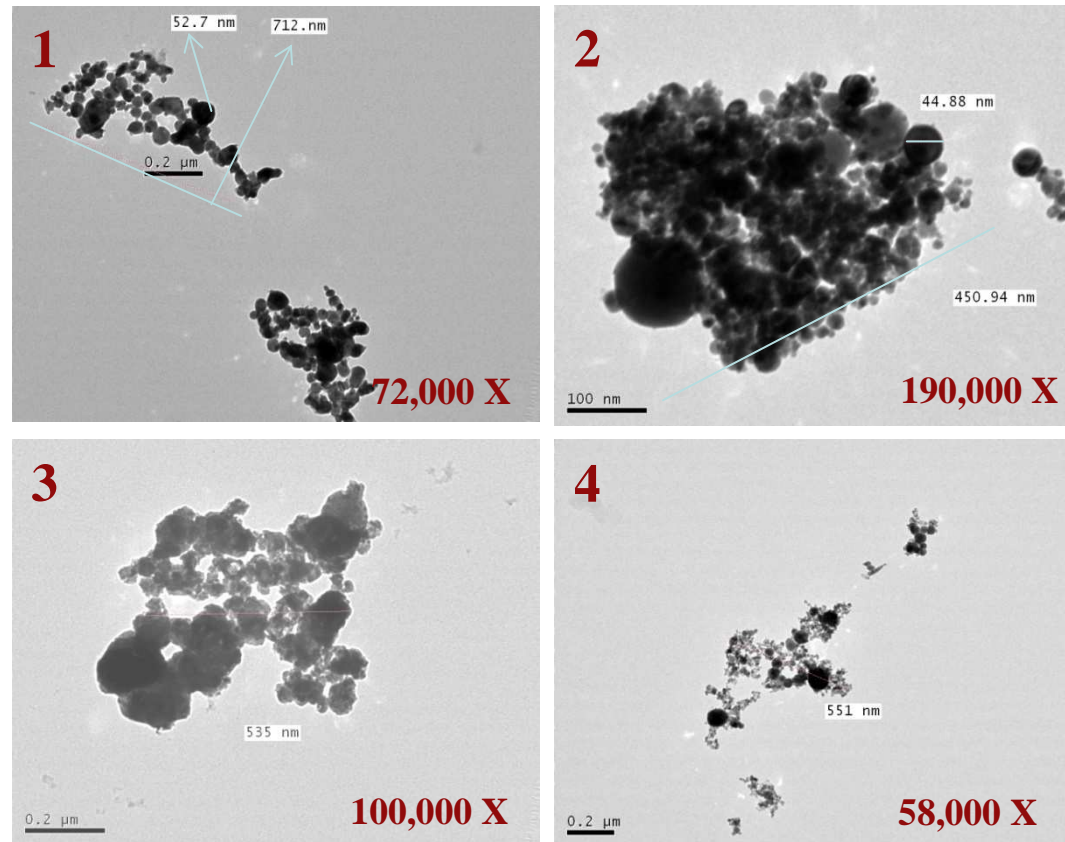
Membrane Integrity Assay



- A549 cells (25,000 per well), incubation with NPs for 24 hr.
- Data corrected for absorbance from blank NPs.
- Ni NPs and C/Ni NPs do not alter membrane integrity.
- Cu NPs and C/Cu NPs are equally toxic.

MNPs Set 2

TEM Characterization of MNPs

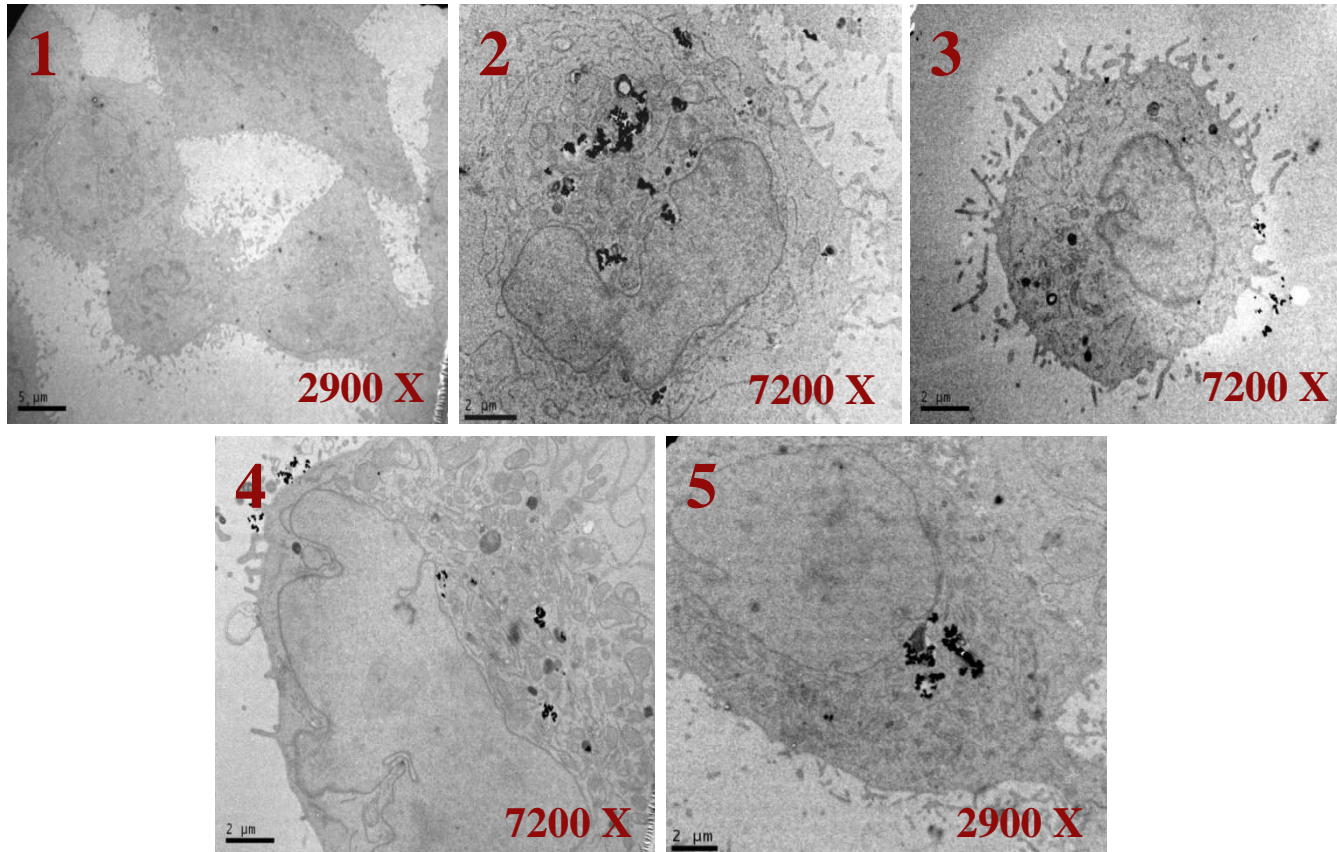


1. Ni , 2. C/Ni, 3. Cu and 4. C/Cu MNPs. Nanoparticles were suspended at concentration of 10 μg/ml in DI water for this analysis. The average particle sizes measured by TEM correlates with the dynamic light scattering data.

SRC/SEMATECH Engineering Research Center for Environmentally Benign Semiconductor Manufacturing

MNPs Set 2

Cell Uptake Analysis by TEM

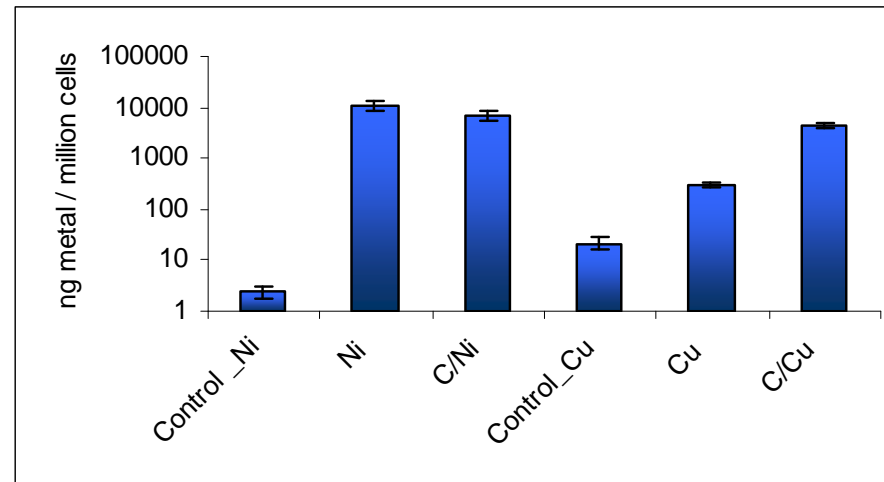


1. Control A549 cells , 2. Cu treated , 3. C/Cu treated , 4. Ni treated and 5. C/Ni treated A549 cells. Cells were treated with nanoparticles at concentration of 10 μ g/ml for 8hr.

SRC/SEMATECH Engineering Research Center for Environmentally Benign Semiconductor Manufacturing

MNPs Set 2

Cell Uptake Analysis by ICP-MS



- Control_Ni and Control_Cu signify the amount of respective metal content in untreated control A549 cells.
- Nanoparticles were tested at concentrations of 10 μ g/ml for 8 hr in A549 cells.
- Ni uptake from Ni and C/Ni NPs is comparable.
- Cu uptake from C/Cu NPs is an order of magnitude higher than uptake from Cu NPs.

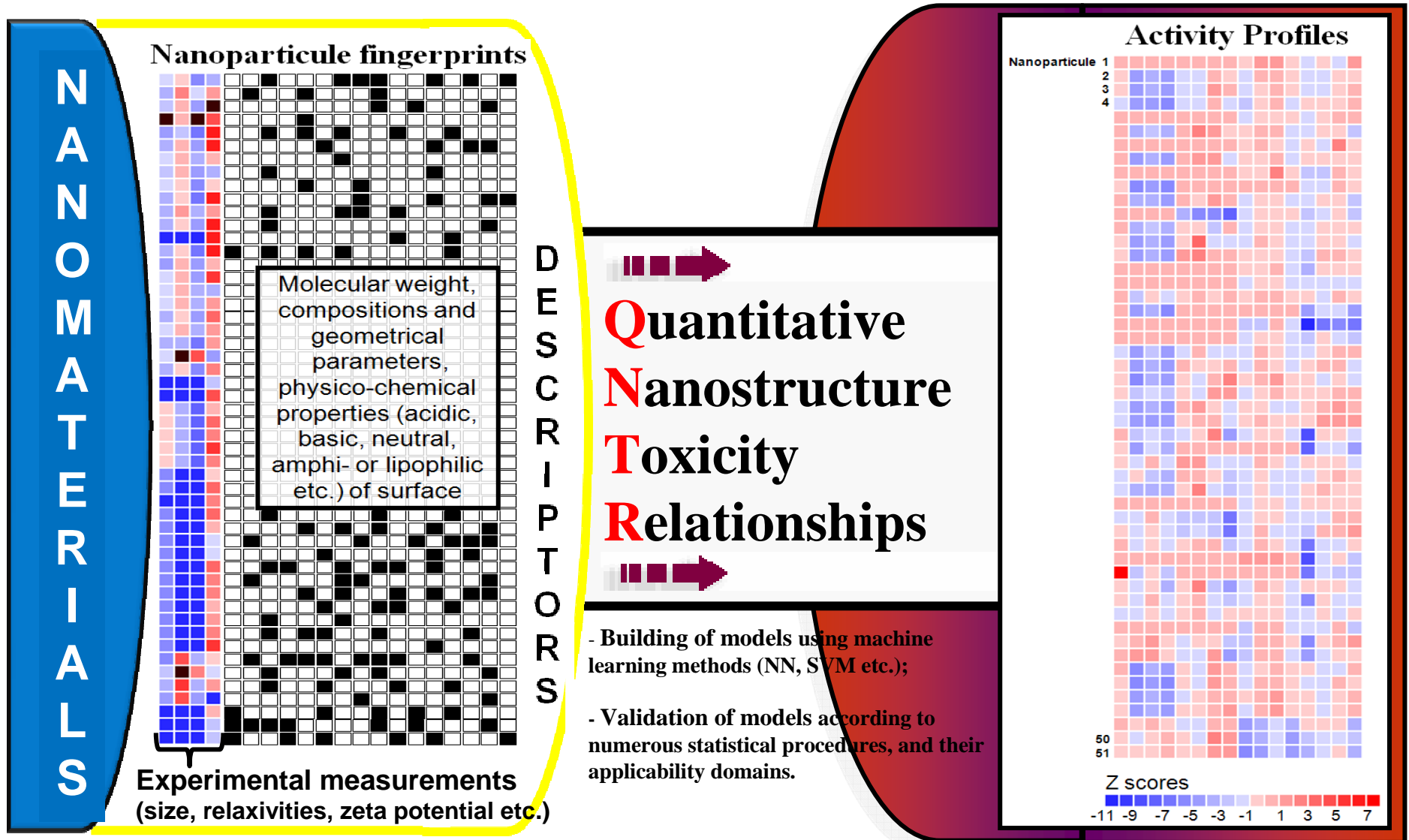
Conclusions: MNPs Set 2

- Average particle size measured by DLS of all MNPs in Set 2 are on an average 20-fold higher than provided by the manufacturers.
- Ni NPs do not alter mitochondrial function and membrane integrity although their uptake by cells is comparable to C/Ni NPs.
- C/Ni NPs alter the mitochondrial function but not membrane integrity.
- Cu NPs alter mitochondrial function at 100 $\mu\text{g/ml}$ but can alter membrane integrity even at 10 $\mu\text{g/ml}$ dose.
- Rounded morphology of Cu NP treated cells and results from membrane integrity and ICP-MS suggest that Cu NPs might act on cell surface at lower dose, possibility of alterations with cell adhesion.
- C/Cu NPs alter mitochondrial function and membrane integrity to the same extent.
- Cu and C/Cu NPs appear to be more toxic than Ni and C/Ni NPs.
- Correlation of uptake data with observed toxicity in cell based assays awaits data on detailed physico-chemical characterization.

Subtask 2: Research Hypothesis

- The effects of MNPs on different types of human cells depend on the compositional/physical/chemical/geometrical properties of the MNPs.
- High-throughput cellular-based assays with endpoints within 2-6 hr provide useful and predictive information about long-term biological properties of NPs.
- Toxicological data obtained from *in-vitro* cellular-based toxicity assays will correlate reasonably with *in-vivo* findings.
- Using physical/chemical characterization and toxicological screens for an ensemble of MNPs, it will be possible to develop **predictive Quantitative Nanostructure – Toxicity (QNTR) models**.

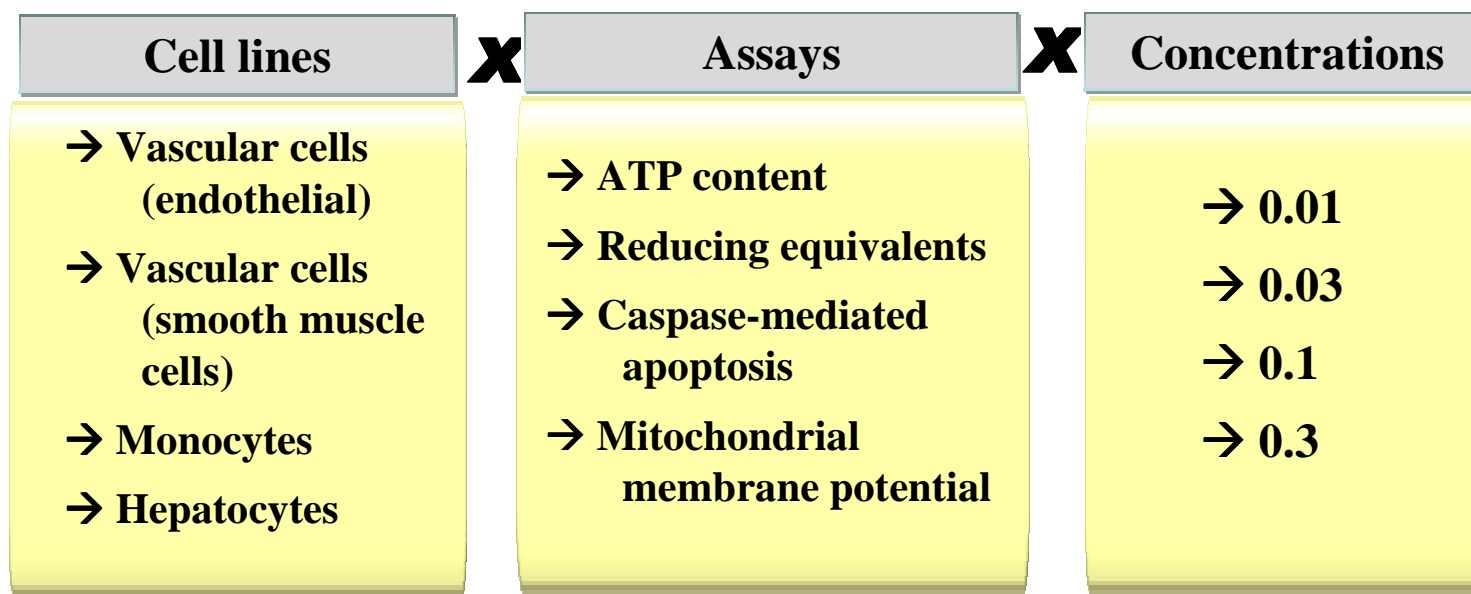
Subtask 2: QNTR Scheme



Case Study 1: QNTR of Whole NPs

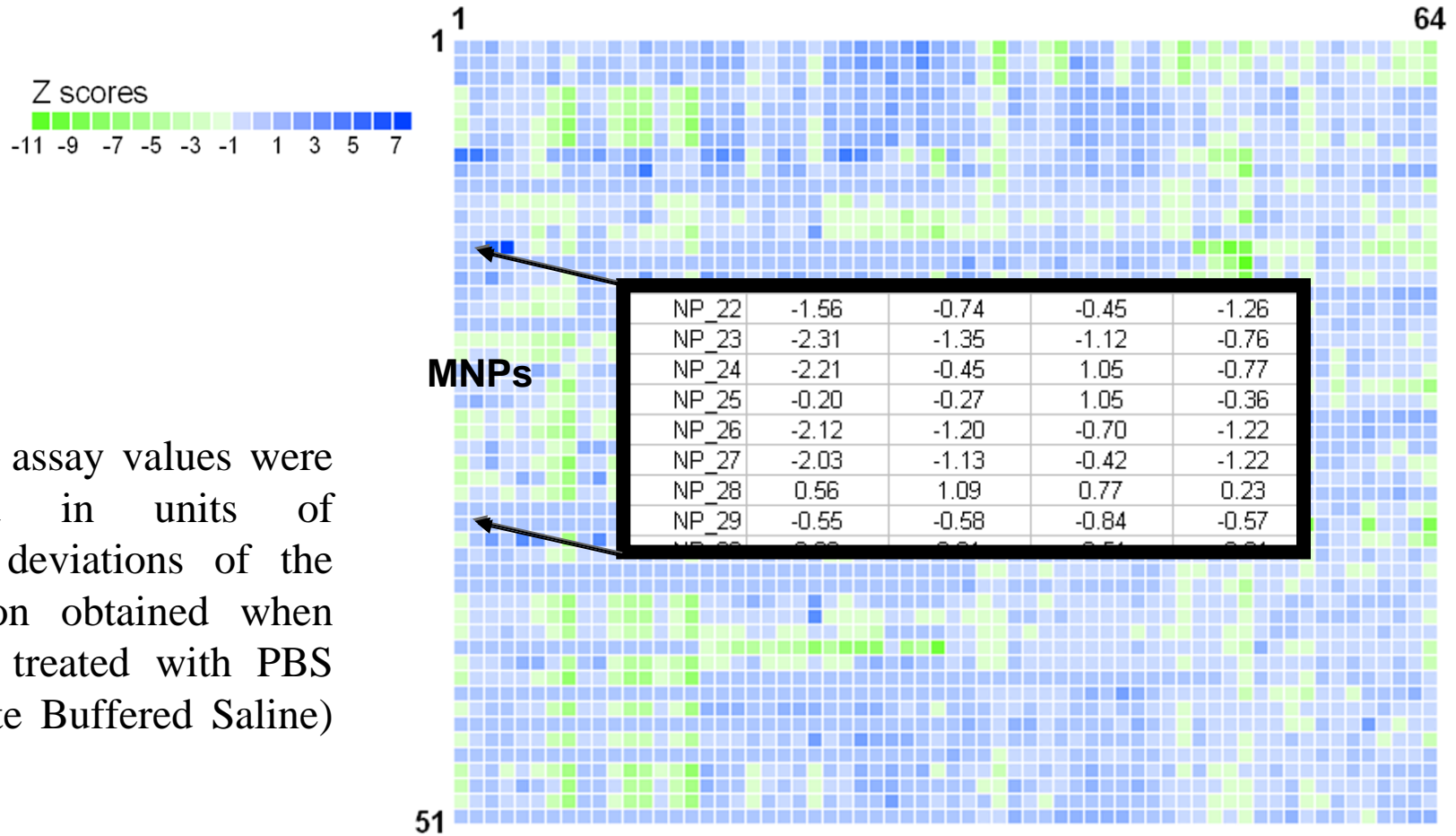
In a recent study¹, 51 diverse NPs were tested *in-vitro* against 4 cell lines in 4 different assays at 4 different concentrations (→ **51x64 data matrix**).

MNP	CLIO	PNP	MION	QD	Feridex IV	Ferrum Hausmann
#. particle	23	19	4	3	1	1



¹ Shaw et al. *Perturbational profiling of nanomaterial biologic activity. PNAS, 2008, 105, 7387-7392*

Case Study 1: Initial Activity Matrix



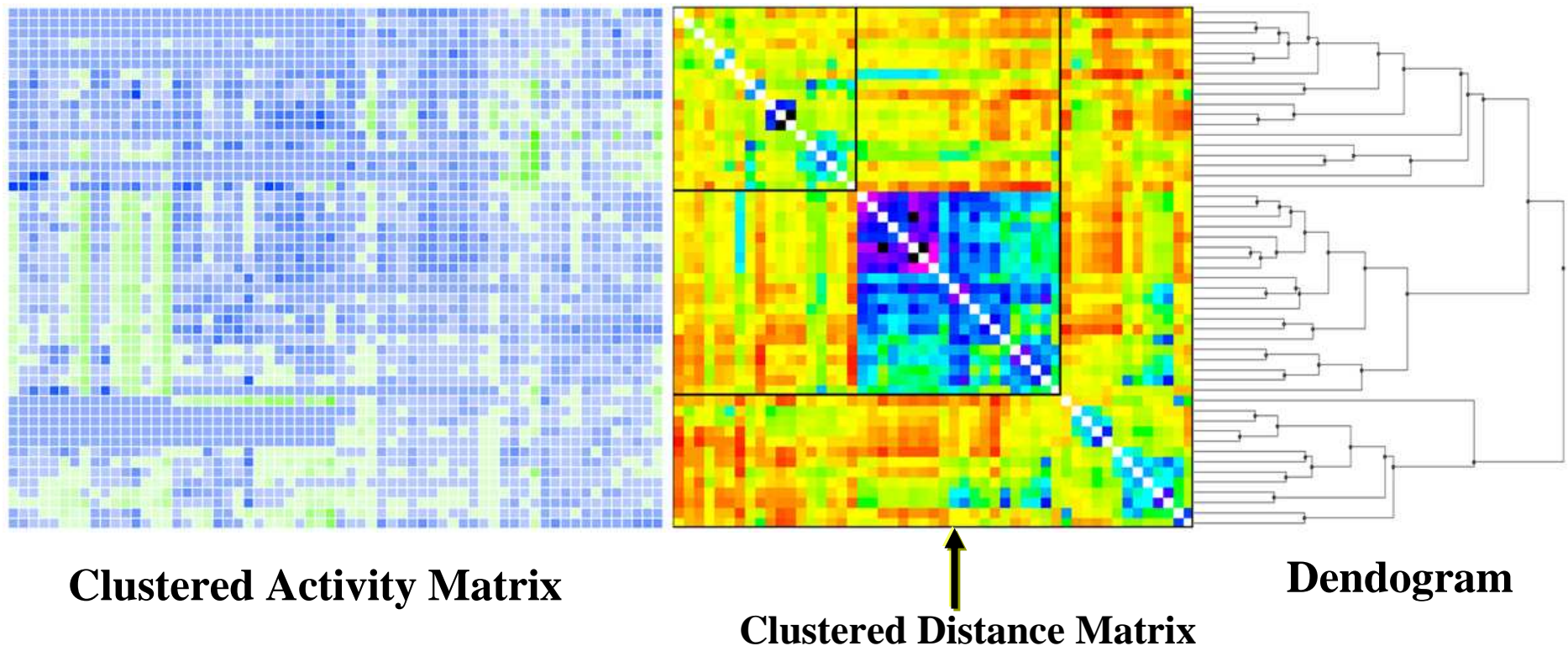
Z scores: assay values were expressed in units of standard deviations of the distribution obtained when cells are treated with PBS (Phosphate Buffered Saline) alone.

$$Z_{NP} = (\mu_{NP} - \mu_{PBS}) / \sigma_{PBS}$$

μ_{NP} : mean of control tests with PBS

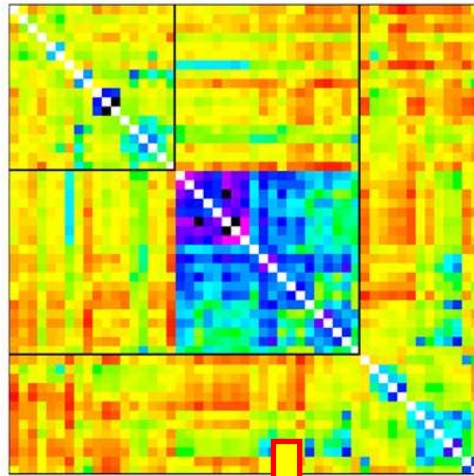
σ_{NP} : standard deviation of control tests with tests

Case Study 1: Hierarchical Clustering of The Activity Matrix



After the normalization of data, ISIDA/Cluster program* was used to cluster the activity matrix (51 * 64), using Johnson's hierarchical method, Euclidean metrics and complete linkage.

Case Study 1: Analysis of Clusters




NP type	CLUSTER 1	CLUSTER 2	CLUSTER 3	Total
CLIO	7	13	3	23
PNP	7	2	10	19
MION	0	4	0	4
Qt-dot	3	0	0	3
Feridex	0	1	0	1
Ferrum Hausmann	1	0	0	1
Total	18	20	13	51


NP Core	CLUST 1	CLUST 2	CLUST 3	Total
Fe ₂ O ₃	5	0	9	14
Fe ₃ O ₄	9	20	4	33
Cd-Se	3	0	0	3
Fe(III)	1	0	0	1
Total	18	20	13	51

A given metal core (i.e, Fe₃O₄) or NP category (i.e, Qt-dot), will induce similar biological effects in most cases, independent of the surface modifications.

Case Study 1: QNTR Matrix and Modeling Results

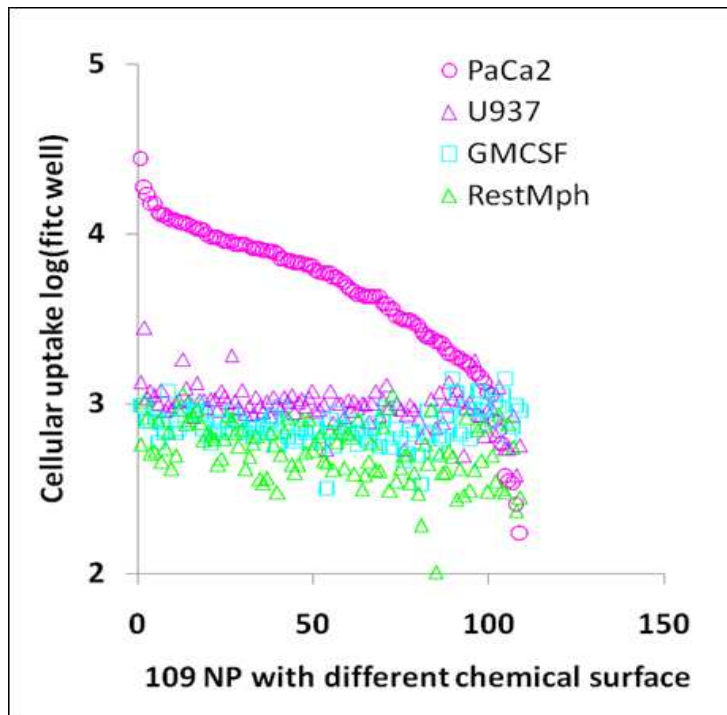
QNTR Matrix 

	Effect	Size	Zeta pot.	Relaxivities	
NP-01	High	0.4865	0.5278	0.2941	0.3986
NP-02	Low	0.4054	0.7222	0.4837	0.6476
NP-03	High	0.4324	0.5833	0.3529	1.0000
NP-04	Low	1.0000	0.5833	1.0000	0.7991
NP-05	High	0.3649	0.4722	0.2353	0.9403
NP-06	High	0.3919	0.6111	0.3333	0.9079
NP-07	High	0.5135	0.5833	0.4052	0.6270

Modeling Results 

Fold	MODELING SETS				EXTERNAL SETS				
	<i>n</i>	# models	% accuracy internal 5-fold CV	% accuracy	<i>n</i>	% accuracy	% CCR ^a	% Sensitivity (SE)	% Specificity (SP)
1	35	11	51.4 – 60.0	71.4 – 82.9	9	78	83	67	100
2	35	13	51.4 – 60.0	71.4 – 77.1	9	78	75	50	100
3	35	16	57.1 – 62.9	74.3 – 82.9	9	78	78	80	75
4	35	11	60.0 – 62.9	77.1 – 88.6	9	56	55	50	60
5	36	4	66.7	83.3 – 86.1	8	75	67	33	100
^a CCR – Correct Classification Rate; CCC = ½ (SE + SP)					44	73	73	60	86

Case Study 2: QNTR Study of NPs Uptake in PaCa2 Cells



PaCa2: Pancreatic cancer cells

U937: Macrophage cell line

GMCSF: Activated primary human macrophages

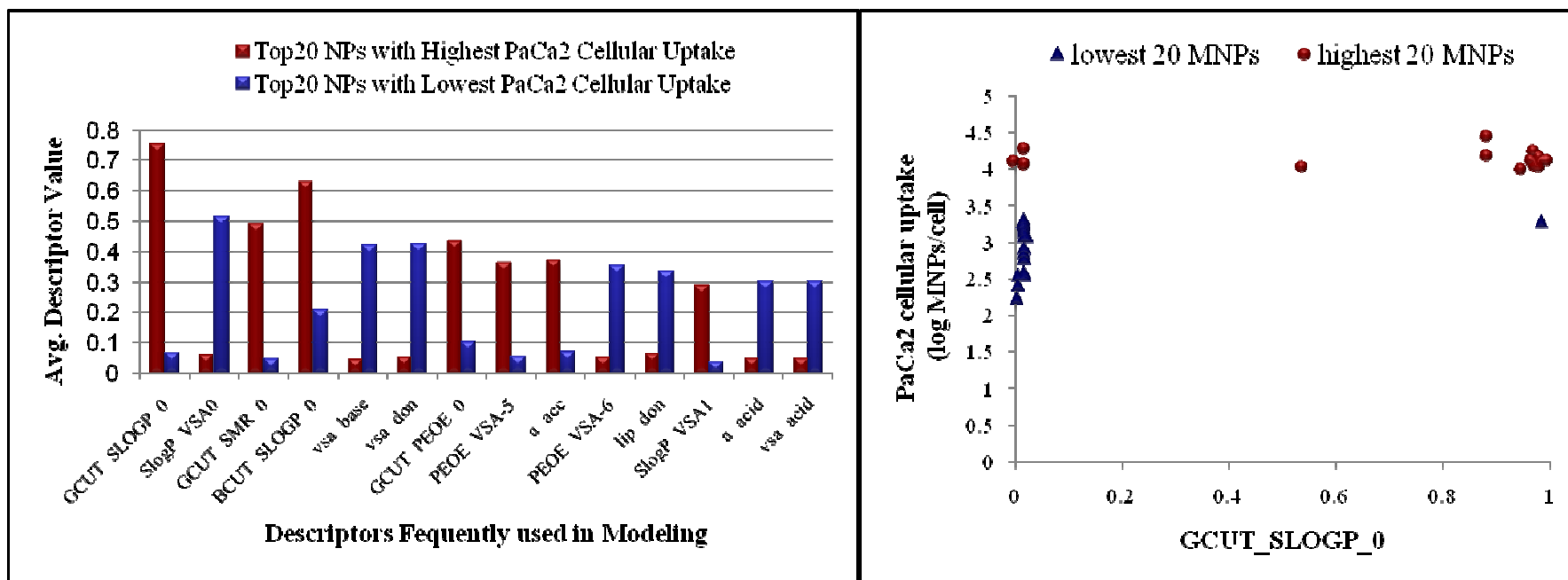
RestMph: Resting primary human macrophages

In 2005, Weissleder et al.* investigated whether the multivalent attachment of small organic molecules on a same NP can modify its binding affinity to certain cells. 109 NPs possessing the same core (CLIO) were attached with different organic compounds on their surfaces

* Weissleder et al. *Nat. Biotechnol.*, 2005, 23 (11), 1418-1423

Case Study 2: Modeling Results and Descriptor Analysis

Fold	# comp. model	# comp. external	w/o AD		w/ AD		
			R _o ²	MAE	R _o ²	MAE	% cov
1	87	22	0.65	0.18	0.67	0.18	86
2	87	22	0.67	0.14	0.73	0.13	91
3	87	22	0.72	0.22	0.75	0.21	82
4	87	22	0.75	0.19	0.90	0.14	64
5	88	21	0.80	0.16	0.78	0.17	76
Average	87	22	0.72	0.18	0.77	0.17	80



Case Study 3: Modeling of NPs for Protein Binding

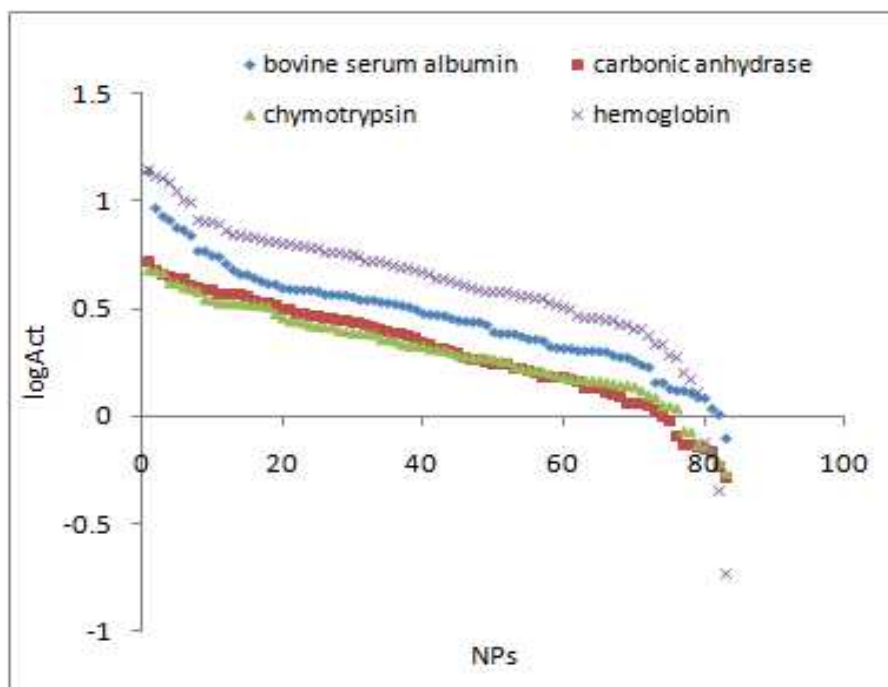
In 2008, Zhou et al* published in vitro protein binding assays for ~80 carbon nanotubes with different surface modifiers.

	R ₁ R ₁ 'N-							
	AM001	AM002	AM003	AM004	AM005	AM006	AM007	AM008
	5	6	7	8	9	10	11	12
H-	13	14	15	16	17	18	19	20
De-Fmoc	21	29	37	45	53	61	69	77
AC001	22	30	38	46	54	62	70	78
AC002	23	31	39	47	55	63	71	79
AC003	24	32	40	48	56	64	72	80
R2- AC004	25	33	41	49	57	65	73	81
AC005	26	34	42	50	58	66	74	82
AC006	27	35	43	51	59	67	75	83
AC007	28	36	44	52	60	68	76	84
AC008								

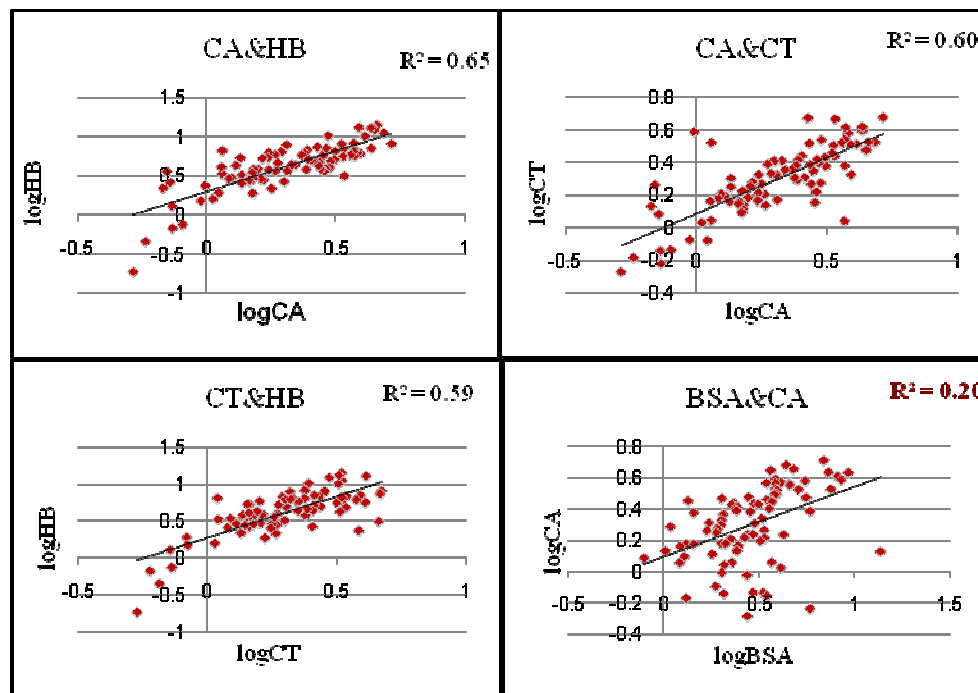
Different surface modifiers were introduced at the R₁, R₁' and R₂ position

*Zhou et al. *Nano Lett.*, Vol. 8, No. 3, 2008

Case Study 3: Protein Binding Profile of Tested NPs

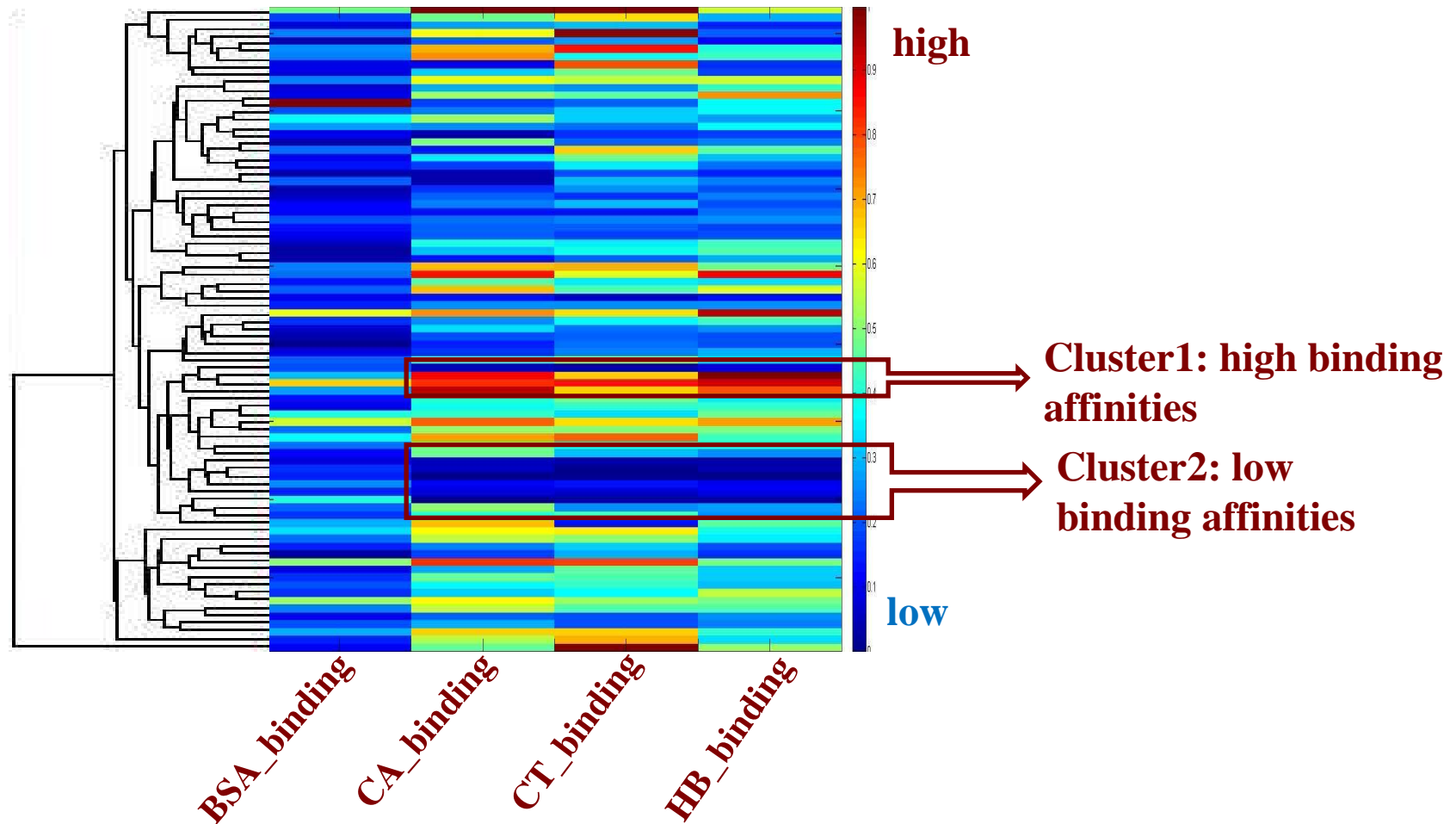


Distribution of binding affinities for 84 NPs



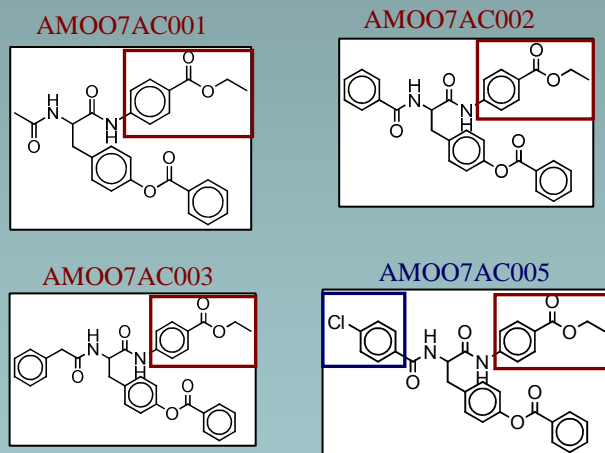
Pairwise correlation between protein binding affinities in different assays.

Case Study 3: Binding profiles sorted according to non-supervised hierarchical clustering of 84 NPs using chemical descriptors

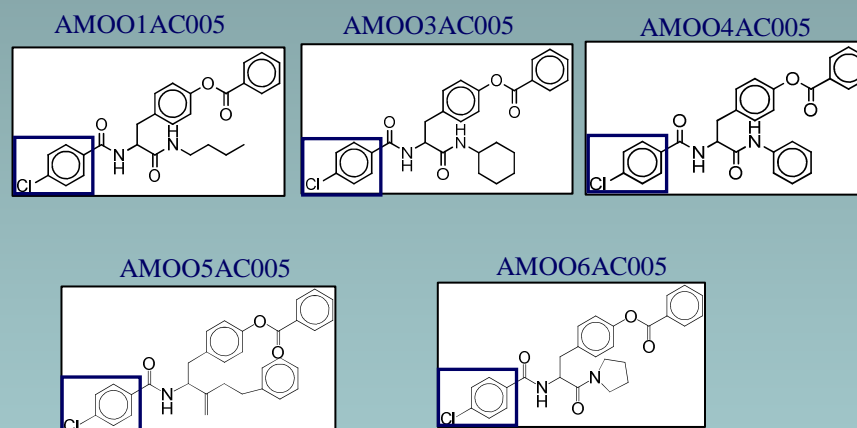


Case Study 3: Clustering Uncovers Common Fragments with Distinct Protein Binding Profile

Cluster 1 (high affinities)



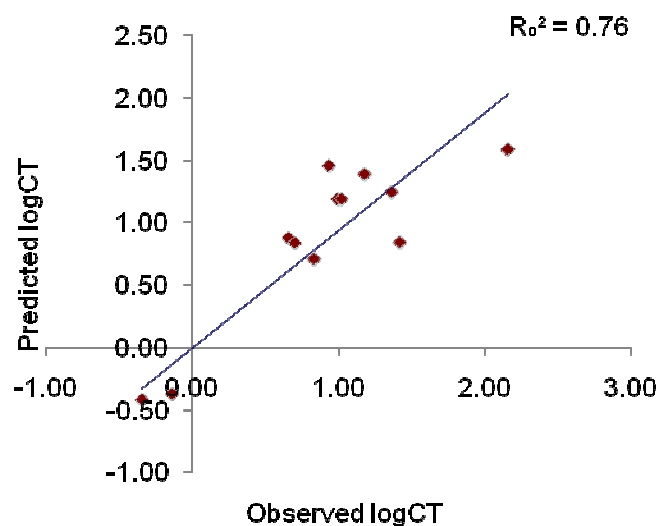
Cluster 2 (low affinities)



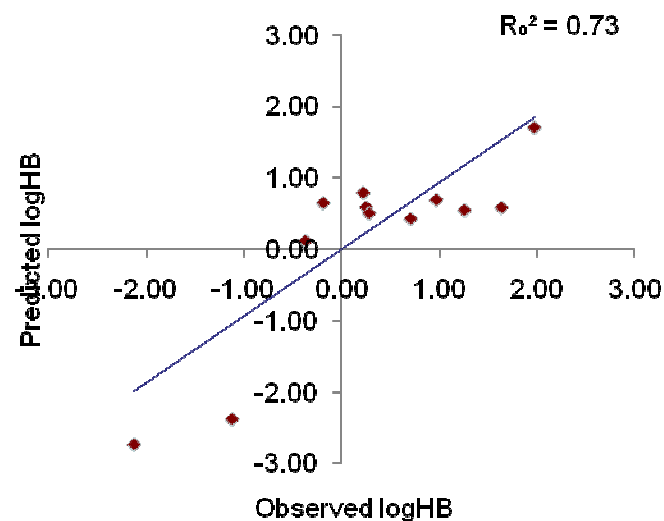
NP ID	BSA Binding	CA Binding	CT Binding	HB Binding
AMOO7AC001	4.0302	4.9276	3.5868	3.3936
AMOO7AC002	4.4012	4.6517	3.5818	4.2787
AMOO7AC003	8.5565	4.4131	4.4598	3.9182
AMOO7AC005	3.0478	0.7487	0.7748	0.3953

NP_ID	BSA Binding	CA Binding	CT Binding	HB Binding
AMOO1AC005	3.7747	1.0774	1.1543	0.4860
AMOO3AC005	1.7175	0.8216	0.7864	0.2294
AMOO4AC005	2.5168	0.5299	0.5772	0.0572
AMOO5AC005	2.7064	0.7509	0.6474	0.2055
AMOO6AC005	2.5128	0.9683	0.9064	0.4592

Case Study 3: QNTR Modeling Using kNN Regression Method



chymotrypsin binding



hemoglobin binding

- Each NP was represented by its surface modifier
- Dragon descriptors were calculated.

Subtask 2: Conclusions

- Preliminary results demonstrate that QNTR models can successfully predict the biological effects of NPs from their descriptors either experimentally measured (e.g., case 1 study), or calculated (case 2, 3 study).
- To increase the accuracy and impact of models on the experiments, we need additional systematic experimental data (structural and biological).
- QNTR approach may allow rational design or prioritization of novel NPs with desired target (physical and biological) properties.

Industrial Interactions and Technology Transfer Wish List

- **Potentially seamless interaction between the ESH Research Center and SRC member companies.**
- **Send nanomaterials to UNC (and other ESH laboratories) for characterization.**
- **Analyze experimental data and build predictive QNTR models.**
- **Prioritize MNP design and toxicity testing.**
- **Provide continuous feedback to ESH and SRC member companies.**

Future Plans

Next Year Plans

- Subtask 1:
 - Complete the standard outlined assays for MNPs Set 1 and 2.
 - Carry out detailed physico-chemical characterization and additional biological assays to identify the cause of differential toxicity profile manifested by MNPs in Set 2.
- Subtask 2:
 - Establish a database of experimental nanotoxicity data
 - Develop extended QNTR models of all available nanotoxicity data

Long-Term Plans

- Obtain predictive knowledge of physical and chemical properties of MNPs that affect human cells and utilize this knowledge for improved MNP experimental design and prioritized toxicity testing.

Publications, Presentations, and Recognitions/Awards

- **Shalini Minocha and Russell J. Mumper, “In-vitro Assays to Assess the Toxic Potential of Manufactured Nanoparticles”, 2009 AAPS Annual Meeting and Exposition, Los Angeles CA, November 8-12, 2009.**
- **Shalini Minocha and Russell J. Mumper, “Characterization and in-vitro Evaluation of Potential Toxicity of Commercially available nanoparticles”, Chapel Hill Drug Conference, May 13-14, 2009, Chapel Hill, NC, USA.**
- **Denis Fourches, Lin Ye, Russell J. Mumper and Alexander Tropsha. Assessing the Biological Effects of Nanoparticles Using Quantitative Nanostructure – Activity Relationships. Spring 2009 ACS Meeting and Exposition, Salt Lake City, UT, March 22-26, 2009.**
- **Denis Fourches, Dongqiuye Pu, Russell J. Mumper and Alexander Tropsha. Quantitative Nanostructure-Toxicity Relationship (QNTR) Modeling. Nanotoxicology, manuscript in preparation.**
- **Shalini Minocha, Dongqiuye Pu, Alexander Tropsha and Russell J. Mumper, “Systematic Evaluation of Toxicity of Metal Based Nanoparticles”, Nanotoxicology, manuscript in preparation.**

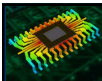
'2010 Annual ERC Meeting'

Green Manufacturing Technology in Semiconductor industry

Feb. 18, 2010

Seung-Ki Chae, Ph.D.

Vice President
Manufacturing Technology Team
Semiconductor Business
Samsung Electronics



Sustainability

✓ Apartment Complex around the World-class Semiconductor Fab.



Samsung Fabs in Giheung & Hwasung

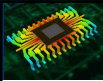
To be a Good Neighbor :

Air Pollution Free

Odor Free

Noise Free

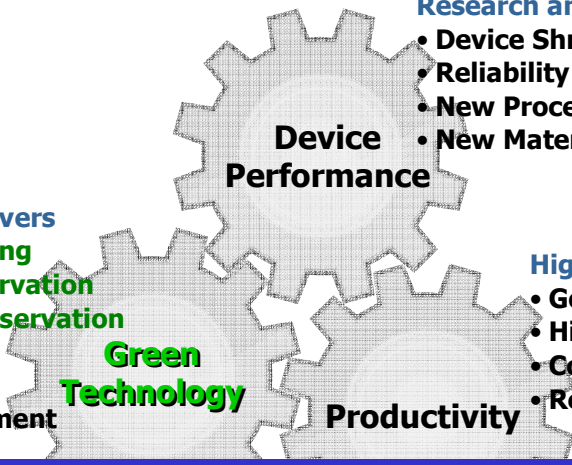




Green Technology

Technology Drivers

- Global Warming
- Energy Conservation
- Resource Conservation
- New Material
- Nanoparticle
- Risk Management



Green Technology

Research and Development

- Device Shrinkage
- Reliability & Quality
- New Process Development
- New Material & Equipment


High Volume Fabs.

- Golden Yield
- Higher Throughput
- Cost-Down
- Reduced Waste

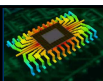
Device Performance

Productivity

Green Technology must be an integral part of productivity enhancement and new process development.



3



Global Warming (PFC Emission Reduction)


✓ **Major Technology and Business Changes in the Fab.**

CF ₄ , C ₂ F ₆ , C ₃ F ₈	CVD Chamber Cleaning Gas	NF ₃	Lower GWP
In Situ Plasma	CVD Equipment Modification	Remote Plasma	95-99% DRE
Heat (Electrical)-Wet	PFC Abatement System	Burn (LNG) -Wet	90-95% DRE

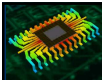
✓ **New Technology Direction and Responsibility**

- NF₃ Gas Reduction and Alternative Gas, such as, F₂
- Reduce Resources for Dry Chamber Cleaning at Higher Productivity
- Energy Saving of PFC Abatement System and Developing Next Generation Tool

WSC voluntary agreement has led to worldwide collaboration .



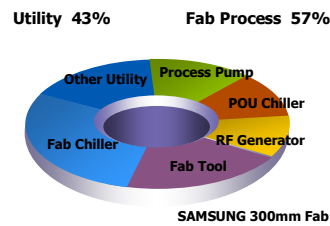
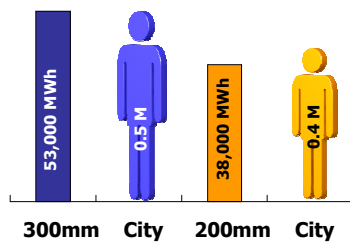
4



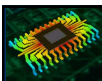
Energy Saving Strategy (Green Fab.)

✓ Electrical Energy Consumption

- One 300mm Fab with 100K per Month \approx Tucson, AZ, with 0.5 Million Population
- 300mm Fab. Saves 38% Energy per Wafer Area Compared with 200mm Fab.
- Samsung's Goal ;
5% Annual Reduction per Wafer Production from 2004 Baseline until 2010.
- **Power Consumption Analysis**



5



Energy Saving Strategy

✓ Green Fab. Design

- Worldwide Benchmarking Fab. to Enhance Energy Efficiency and Saving.
- Electrical Energy also Contribute to Global Warming
- Energy Regeneration and Material Recycling
- Water Conservation and Waste Minimization to be Considered

✓ Responsibility

- Electrical Energy Saving Design for Process Equipment
- Stand-by Mode, Idle Mode
- Electrical Energy Saving Technology Development for Sub-Equipment, such as, Vacuum Pump, Chiller and RF Generator

Electrical energy saving is essential for the green Fab .

6



Resource Conservation

Recycle

- H2SO4, H3PO4, Photoresist...
- Efficient Separation
- Cost Effective Purification

Reuse

- RCA(SC1), SPM (H2SO4+H2O2)
- Monitoring the Bath
- Filtration & Process Control


Chemical Management

Reduction

- Ceria Slurry, Spin-on-Hardmask
- Performance Improvement
- Surfactant, Solvent Optimization

Refuse

- ArF immersion Topcoat-less PR, Process Skip by Photo-Sensitive PI
- Innovative Process Design
- Functional Material Develop



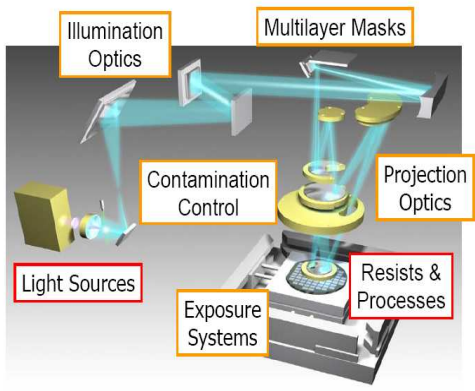
7

New Material and Process Development (EUV)


✓ **New Lithography Tool for sub 30nm Device**

Technological Challenges in EUV

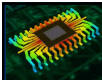
- Vacuum Chamber Lithography
- P/C Free System Treatment
- Power Consumption Reduction
- Monitoring and Measurement
- Volatility Free Photoresist Develop
- Mirror Haze Problem Solution



New lithography has various technical issues and has to be improved for the viewpoints of ESH considerations for mass production



8



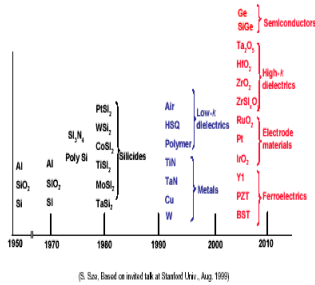
New Material and Process Development

✓ High k Materials for Next Generation Capacitors

Capacitor Material

Al₂O₃, HfO₂, ZrO₂

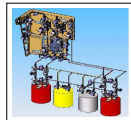
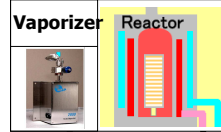
Ref.) Univ. of Arizona



(S. Seo, Based on invited talk at Stanford Univ., Aug. 1999)

Process Equipment

Atomic Layer Deposition



Precursor Delivery Sys.

Liquid Precursor Source
TMA, BTBAS, TEMAZr

Material Delivery System
Auto-refill system, vaporizer



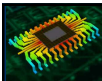
Exhaust Trap



Vacuum Pump Scrubber



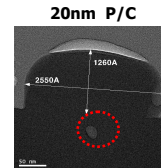
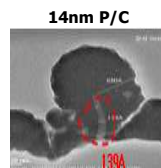
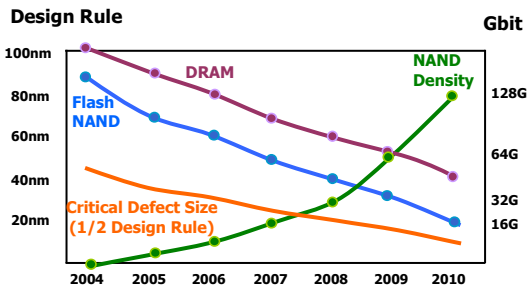
Vacuum Pump, Scrubber
Exhaust Management

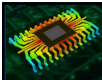


Nanoparticle Control for Manufacturing

✓ Nano-scale Semiconductor Device Manufacturing

- Design Rule for Device Shrink to Nano-scale
- Nanoparticle Control during Manufacturing Process
- Prevention of Particle Generation in Process Equipments

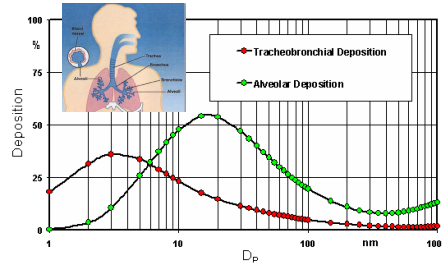




Occupational Health and Safety

✓ Nanoparticle Toxicity for Human Health

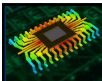
- Nanoparticle Control Technology
- Filtration Technology
- Process Equipment PM
- Powder Treatment
- Monitoring and Measurement



Lung Deposition Curves (ACGIH)

Ref.) Univ. of Minnesota

Nanoparticle control is important not only in wafer production yield, but also in human health and safety.



Conclusions

Device Manufacturer

- Device Road Map
- Develop Common Sense for Cost Implications

Material Supplier

- ESH Guaranteed Materials
- Intensive Studies on Delivery/Exhaust/Cleaning



Equipment Supplier

- ESH Conformed Exhaust Management
- Better Utilization of New Materials

Engineering Research Center

- Novel Solutions to Existing ESH Problems
- ESH-Friendly Novel Materials and Processes
- ESH Aspects of Future Nano-Scale Manufacturing



Energy Conservation in High Volume Semiconductor Manufacturing

Ann Kelleher Fab 12 Plant Mgr
Carl Geisert Sr. Principal Engineer
Skip Benjes Principal Engineer
Intel Corp. Chandler, Az



Agenda

- Intel Factories
- Manufacturing Environmental Footprint
- Recent Corporate Initiatives
- Energy Consumption & Process Tools
- Intel Fab Initiatives & Focus
- A Challenge

Fab and Assembly Test Sites



10 fabs operating in the United States, Ireland, and Israel with 1 more under construction in China

Manufacturing Footprint

Air Pollution (VOC, HAP)

Global Warming Gases

Energy



Water



Wastewater



Chemicals



Chemical Waste



Solid Waste

Intel Plans Eight New Solar Installations in Four States Increases Renewable Energy Credit Purchase by Ten Percent

- Intel has contracted new solar electric installations targeted at eight U.S. locations in four states, generating approximately 2.5 megawatts of clean solar energy.
- Intel increased its renewable energy credit purchases by 10 percent – powering more than 51 percent of Intel's estimated U.S. electricity use – and was again named the largest voluntary purchaser of green power by the EPA.
- These new investments are part of Intel's already established commitment to energy efficiency and footprint reduction programs, with worldwide savings of more than 650 million kilowatt hours since conservation program inception in 2001.

Santa Clara, CA



Solar Plans at Intel Santa Clara RNB

Rio Rancho, N.M.



Solar Plans at Intel Rio Rancho, N.M.

Chandler, AZ



Solar Plans at Intel Chandler, Ariz.

Hillsboro, OR.



Solar Plans at Intel Hillsboro, Ore.

Folsom, CA

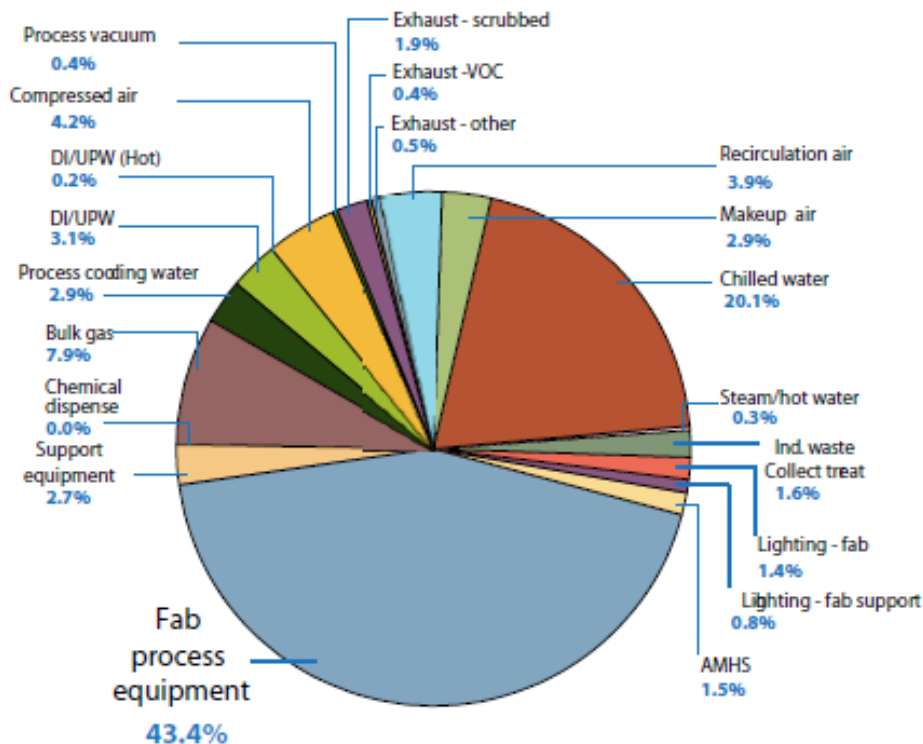


Solar Plans at Intel Folsom

Fab Energy Consumption Survey

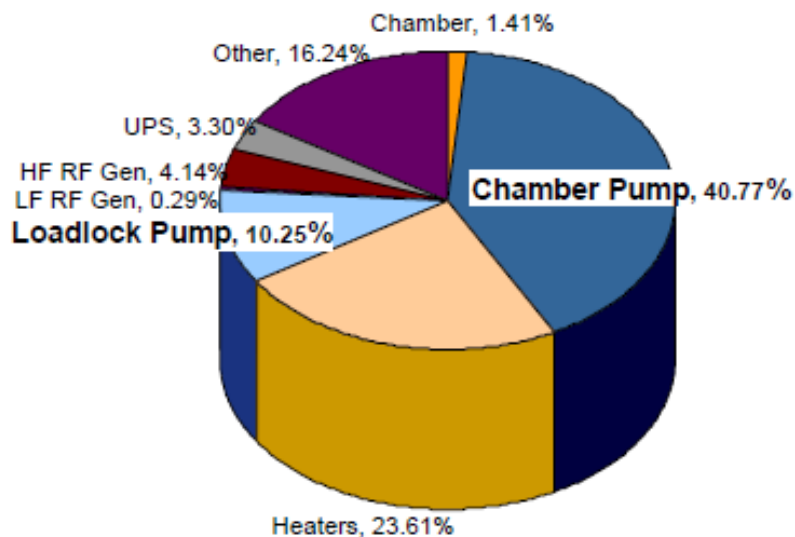
Fab wide energy studies highlight process tool energy reduction opportunities

2007 300mm Fab Energy



Case Study: Vacuum pumps consume the most power on etch/CVD processes

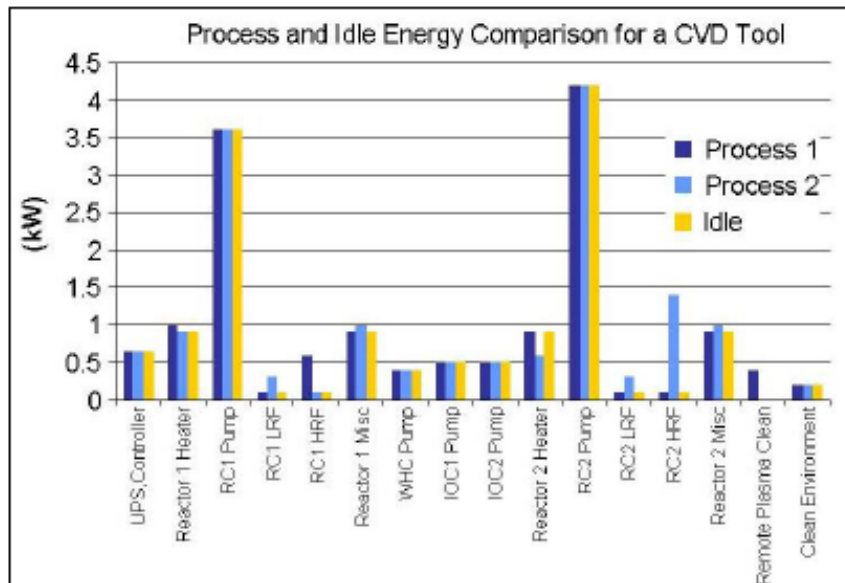
Energy Consumption for 300mm CVD by Component



Energy and Resource Conservation

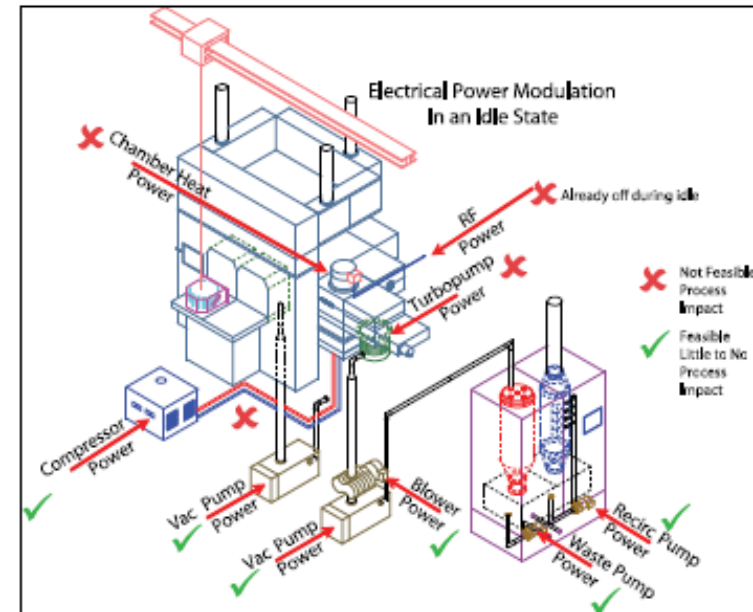
Survey

For nearly all process tool subcomponents, energy consumption is the same whether the tool is processing or idle

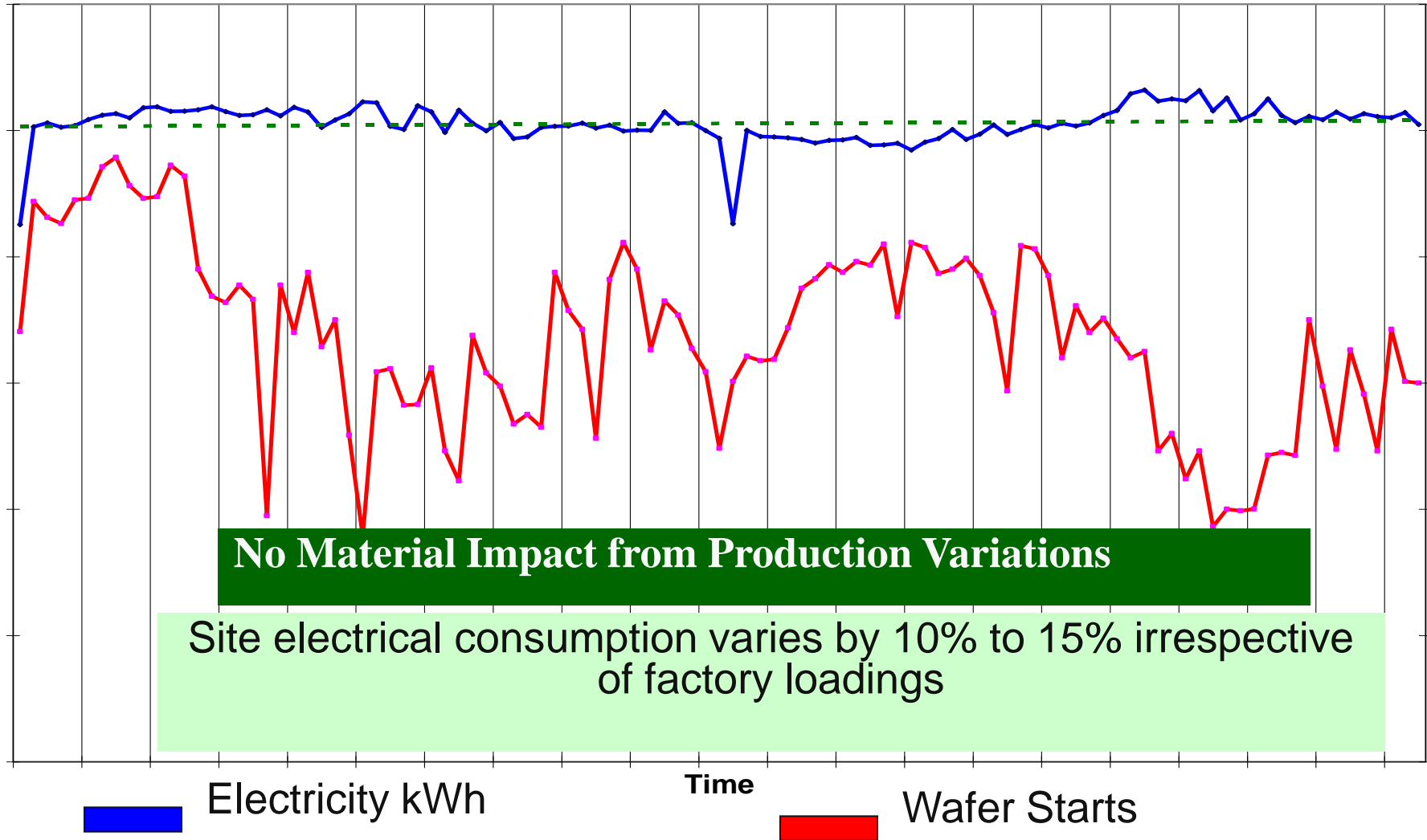


Component Improvements

Reduced utility consumption - idle mode



Electrical Consumption 2004-2007 (typical 300mm fab)



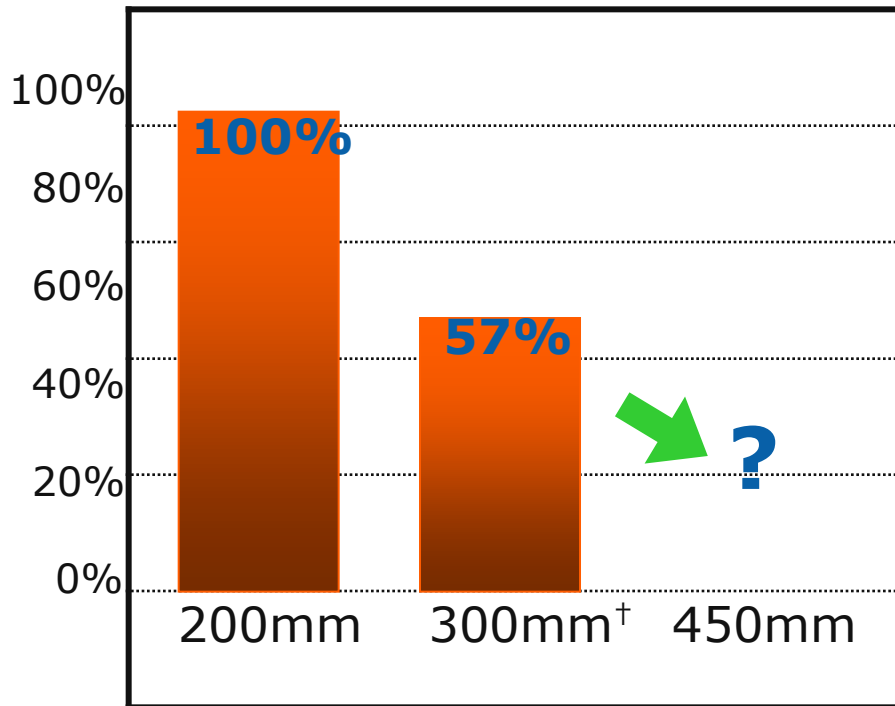
Ireland Site Process Tool Energy Savings



- Detailed review of energy use in every tool state
 - Processing, Idle, “Bagged”
 - Lowering temperatures, gas flows, chemical purges, etc..
- Warm, “Cool”, Cold bagging options to reduce energy & materials cost while allowing flexibility for rapid restart
- More effective energy consumption monitoring to track progress and fine tune the approach
- Several million dollars in savings the first year of implementation across several factories
- Research centre *I2E2 (Innovation for Irelands Energy Efficiency)*. The industry led centre is focused on strategic research and development for the benefit of industry based on common research interests in partnership with academia.

Bigger Wafers, Greener Factories

Aggregate Environmental Impact



- Conversion to 300mm reduced aggregate emissions of air pollution, global warming gases and water by 43%
- Note: Need to validate 450mm model to confirm environmental impact

450mm is an opportunity to significantly reduce our environmental impact

[†] Intel data

Intel Future Energy Conservation Focus

- Equipment Idle
- 450mm Conversion
- Continuous Improvement of utility systems
- Smart Grid research (with Government, Utility Companies)
- S23 enforcement to reduce manufacturing tool utility demands



A Challenge

- Process Tools

- In-process efficiencies with chamber designs, etc
- PCW temperature requirements, flow restrictions
- Efficient standby, idle, warm bagged, “cool” bagged modes
- Cost effective technology for efficient pumps, motors, RF
- Self monitoring energy, gas/chemical consumption
- 450mm redesign for tools provides an opportunity
- *Without impacting the process quality, cycle time,....*

- New Process Technology

- EUV
- Single Spray Tools



Thank You